INTRODUCTION

1.1. COURSE HISTORY AND OBJECTIVES

The origin of this course is based on the perception that each petroleum engineer should be able to recognise reservoir rock and its pore content from well logging information. For this reason at the start of the eighties ir. J.P. van Baaren started his introduction to Petrophysics; a lecture course and two weeks practice in interpretation. This course was based on a Shell training. Over the years the course debased from a fourth year petroleum course to a second year basic course with the objective of a general introduction in physical rock properties including some log interpretation . Subsequently prof. ir. M. Peeters started to revise the course to a general introduction, which also includes aspects relevant for groundwater surveys, coal and mineral exploration. Here the UK based company BPB Wireline Services provided training material for coal logging. The technical information provided by Welenco in their Water & Environmental Geophysical Well Log Volume, and the documentation from TNO-NITG, formed the basis for ground-water logging. For mineral logging papers of the 6th international symposium on borehole geophysics (Santa Fé - New Mexico October 1995) have been of value. In this 1999 version of the course the main objective is the integration of theory and practical work**. Lectures are mixed up with some mental exercises and laboratory experiments.** Each student will have the opportunity to realise several rock physical experiments. For this reason teamwork will be essential; the students are divided in groups with tasks and responsibilities for each of them.

Why is this course relevant?
Each of the students will meet in his geotechnical career situations in which the physical properties of natural or artificial rocks have to be defined or are to be used in project decisions. For example:
Running instruments in boreholes at the end of a wireline, called well logging, is applied in many industries. A log is the continuous record of a physical property of the subsurface as a function of depth. For wireline logging the registration equipment on the surface is connected by a steel armoured electrical cable to the instrument.

- The oil industry is the most important user of physical rock properties to identify hydrocarbon bearing layers, and to quantify the amount of producable oil or gas.
- Applications are also found in conventional mining operations. Examples are quantification of the ash & moisture content of coal, roof and floor strength of galleries and the mineral grade of ore deposits.
- The engineering geologist and hydro-geological engineer use rock physical measurements, or depth records obtained with soil penetrating probes, to measure soil friction, mechanical strength, gas content, water conductivity, etc.
- Physical measurements on rocks gradually are more and more in the detection of soil and aquifer pollution, normally with respect to chemicals and radioactive waste.

In a major part of this course the aspects of petrophysics or, more specific, the utilisation's in log evaluations are providing the exercises for applications of the theory. If one applies empirical relationships, it is essential to use as many checks as available from information and interpretations from other disciplines, to guarantee a meaningful rock physical evaluation. For example; the environment of deposition provided by geologists; stratigraphy extracted from seismic by geophysicists; fluid types provided by production technologists; and reservoir distribution data provided by reservoir engineers, should all be respected to escape from incorrect interpretations. This exchange of data and interpretations is a cyclic process and only the synergy of different disciplines can create an "image" of the subsurface, and "characterise" a water or (hydro-) carbon reservoir or mineral deposit with sufficient accuracy to make a reliable and economic development plan. For example; when a well is considered the first thing to know will be the types of rock that have been perforated and whether some strata contain economic zones. This first information on the lithology and fluid content of the penetrated layers available is contributed by the drill cuttings

LOCATION:	reservoir / coal / mineral - layers
DETECTION:	fluid content water / oil / gas / pollutant coal / ore body
EVALUATION: (for all applications)	lithology mechanical properties gross / net thickness
ROCK PROPERTIES	
hydrocarbon & water reservoirs	porosity / permeability capillary properties salinity / hardness of the water original hydrocarbon saturation movable hydrocarbon sat. residual hydrocarbon sat. % oil/gas/water reservoir pressure
coal	moisture content ash content fixed carbon content
minerals / soil mechanics	ore content and grade fluid/gas content

Table 1. 1: Objectives of a petrophysical interpretation.

and traces of oil and/or gas in the mud. The objectives for a more extensive rock physical evaluation are in table 1.1.

In addition to the direct well information measured rock physical data also are used for the estimation of the desired rock properties. The first group of data give direct "physical" information by means of rock and reservoir fluid samples, and will be discussed in the first part of this course.

DIRECT INFORMATION	***ROCK FRAGMENTS & FLUIDS*** - drill cuttings, mud shows - sidewall samples, cores or core slices - production tests, formation wireline samplers drill-stem tests	
INDIRECT	***WIRELINE LOGS***	
INFORMATION:	**PHYSICAL PHENOMENON**	**MEASURED PARAMETER**
	acoustic - waves	sonic velocities acoustic impedance
	gamma / gamma scattering	electron density photoelectric cross section
	thermal neutron density	hydrogen density
	thermal neutron decay	thermal neutron cross section
	neutron activation	elemental concentrations
	natural gamma radiation	Curie / Bequerel / API / REM
	spontaneous potential	membrane potential
	electromagnetic waves 35 Hz -20 kHz 100 Mhz-2 GHz	electric resistivity / conductivity dielectric permitivity
	nuclear magnetic proton resonance	free hydrogen index spin lattice relaxation time

Table 1. 2: Petrophysical evaluation data sources.

The second group of data consist of logging measurements. The theory behind these applications and some methods of interpretation will cover the major part of this course. Further the interpretation of log and core data for hydrocarbons, coal, minerals , groundwater and environmental applications come up in theory and in the mentioned laboratory experiments.

1.2. HISTORICAL DEVELOPMENT

Petrophysics as its name indicates, has to do with the physics of rock. Mining and the search for rock products, such as metals date from the earliest times. The flintstone caves in Limburg and the exploitation of bog iron deposits in Drente are early examples. Scientific recording of rock properties commenced with the publication in 1556 of the famed disquisition **De re metallica** by Georgius Agricola (1556). For many decades it was the leading work on exploitation of mineral bearing rock. In the following centuries Gilbert discovered and described the earth as a enormous and irregular magnet. In addition Newton's theory of gravitation also contributed to the first notions regarding the physics of rocks. The publication of Thalen's book; **" On the Examination of Iron Ore Deposits by Magnetic Methods."** in 1879, and the construction of his magnetometer for the determination of depth, dip, strike of magnetic dikes, appear to be the first utilisation based on physical rock properties. From the 19th century on the continuous increase in the need for minerals, water and (hydro-) carbons raised a need to develop rock physical techniques of increasing sensitivity for the detection and inventory of invisible deposits and structures. Their detection depends upon those characteristics which differentiate them from the surrounding media. Methods for the detection of variation in electrical conductivity and in natural currents in the earth, the rates of decay of artificial potential differences introduced into the ground, local changes in gravity, magnetism and radioactivity, provide information to the geo-engineer about the nature of sub-surface structures to determine the most advantageous spot for locating the source or determining the quality of the source. The development of new electronic devices for field equipment and the widespread application of the digital computer in the interpretation of data improved the development of technical equipment; especially in Geophysics and Petrophysics. Many of the methods now used were developed for military purposes during the two World Wars. For example; when petrophysics is concerned, the application of rock physics into well measurements (both hydro-carbons and water) and data interpretation, show in the last eight decades the following evolution.

- 1910, introduction of rotary drilling.
- 1927, introduction of electric well logging by the Schlumberger brothers.
- late 1930's, introduction of natural gamma-ray logging and the dipmeter.
- 1940's, development neutron-gamma logging.
- 1941 first electric survey run in a Dutch water well (J.H. Beltman)
- 1950's, introduction neutron-neutron logging.
- 1950's, development of sonic logging.
- late 1950's, introduction of induction, lateral and formation density logging.
- 1960's introduction of wellsite tape recording and digitisation of logs
- 1965 introduction of pulsed neutron logging tools
- late 1960's introduction of first nuclear magnetism, and dielectric tools
- 1970's introduction of micro-resistivity and acoustic (BHTV) imaging tools,
- 1980's introduction of array-induction and azimuthal resistivity imaging tools
- late 1980's development of nuclear magnetic resonance tools with permanent magnets.

Besides applications in war, one should not forget that many applications already were in use for the exploration and exploitation of coal fields and minerals, originally from petrology, mineralogy, geochemistry, geomechanics and geophysics. Further space technology can be regarded as the new provider of knowledge for interpretation.

1.3. ROCK PHYSICAL DATA PLACED AGAINST PROFIT

As the roman business people already stated “pecunia non olet”, is certainly of valid in any geo-engineering project. Managers and investors want to dig in rock, want to build on rock and want to produce from rock with the main target: long term or short term profit! Initially all activities regarding research or analysis are too expensive. The costs “wasted” on rock physical information, or in our cases:

- petrophysical data logs,
- the evaluation of the logs,
- the acquisition of cores and outcrop samples, and
- the analysis of core and rock samples,

often depend on the total cost of the exploration or appraisal phase.

The significance of the gathered data, i.e.:

- contingency on repeated sampling,
- the risks involved in obtaining the data, i.e. well damage/loss, and
- the time needed for,

are also important to be considered when exploitation has to be interrupted or slowed down.

As an example; for wells the evaluation cost are in general between 6 and 12 % of the total expenditure. For shallow ground water wells and mineral/coal exploration wells the risks and total cost are usually relatively small (<< $ 100.000,-). As a result the evaluation cost will be in the order of a few thousand dollars. For an offshore oil exploration well, drilled with a floating rig in deep water, the total well cost can be 20 million dollars. Optimising the direct, derived and deduced knowledge gathered from this “unique” exertion will be necessary. Evaluation of the cost for such a venture can be amount to several millions of dollars.

1.4. A FOREWORD TO THE EXERCISES

1.4.1. PRACTICAL COURSE RELEVANCE FOR THE STUDY

Since this practical work is a part of the second year programme, the subjects are related to a wide field of interests. Petrophysics is an applied discipline, with connections and roots in many fields of exploration. Both geophysics and ore/coal exploitation are valuable sources for many petrophysical interpretation techniques. Examples of well log interpretations for various disciplines are:

- **Petroleum Engineering**

From logs the following information:

- Reservoir thickness, gross/net.
- Reservoir properties, such as; porosities, permeability, rock strength, wettability, etc.
- Fluid content and properties; water, %, salinity, gas, oil.
- Environment of deposition.
- Source rock potential.

- **Geophysics**

From logs the following information:

- Impedance as a product of Density and Sonic.
  Proper editing is needed, such as checks on calliper (washout sections useless to apply)

environmental corrections such as; borehole size, mud type, invasion. In a gas bearing formation, the sonic shows erroneous velocities.

- With other logs the sonic-density can be made artificial.

- **Engineering Geology**

Objectives of well logging surveys:

- Geological; thickness, depth to engineering rock bed, establishing weathering profiles, location of buried channels etc.
- Resource assessment; location of aquifers, determination water quality, exploration of sand, gravel and clay deposits.
- Engineering parameters; dynamic elastic module, rock quality.

- **Mining; exploration and exploitation.**

Objectives of well logging surveys:

- Detection of ore bodies or other productive seams.
- Non recovered sections of cores can be correlated with logs

- **Coal logging**

Lithology interpretations from:

- Sonic, density and neutron readings.
- 100% matrix responses of the minerals; coal consists of: carbon (Vcarb, Dcarb, dTcarb), ash (Vash, Dash, dTash) and moisture (porosity) (Vmois, Dfl, dTfl).

  dT = dTfl.Vmois + dTash.Vash + dTcarb.Vcarb

  D_{bu} = Dfl .Vmois + Dash.Vash + Dcarb.Vcarb

  1 = Vmois + Vash + Vcarb

  Three equations, three unknowns: Vash, Vcarb, Vmois

- **Gold or ore Exploration**

Gold associated with pyrite (high conductivities)

- **Other**

Many other purposes can be mentioned, especially regarding drinking water resources, environmental aspects such as groundwater contamination, the use of brine, nitrogen injection, sub-surface (nuclear) waste storage, underground coal gasification, etc.

1.4.2. INFORMATION ON THE EXERCISES

This course is primarily an introduction to the basic elements of rocks and related physics and secondly an introduction to some useful aspects of borehole log interpretation. The emphasis lies on the application of theoretical work, supported by log interpretations.

During the first meeting relevant rock and fluid characteristics are introduced. Thereafter the world of pores is discussed, i.e. the relation between textures, porosity, permeability, capillary pressures, etc.. Subsequent sessions show more complex interpretation techniques, and by that the most important logs are used; calliper, gamma ray, spontaneous potential, induction, neutron, density, sonics. The number of interpretation techniques is kept to a minimum. The most important relations are dealing with:

- The resistivity of rock, pore fluid, mud (-filtrate), Archie, and by that porosity and Sw.
- Bulk density and porosity and by that shale volume determination.
- Lithology determination
- Calculation of gross/net volumes of specified strata and/or formation fluids/gases.

- **The exercise are presented within the lectures. So, attendance will be essential.**

After each session, the participants are urged to study the related course notes, as provided.

- **The practical work also consist of some laboratory work at the Dietz-laboratory.** This work includes the measurements on one solid core and two porous cores:
  - Measured are bulk volume and bulk weight and the related matrix volume and matrix density.
  - Calculation of the porosity on the two porous samples, with a dry method and the wet/dry method.
  - Calculation of the gas-permeability of the two porous samples.
  - Estimation of the measurement errors and calculation of the accuracies of the measurements.

This work is done in groups of five students in the Dietz laboratory and a technical report is hand in by each group. The report will be credited for 1/3 of the final mark.

Appointments for the practical work are made with B. Meyer and R. Ephraim

2. CONSTITUTION OF ROCKS AND ROCK FLUID BEHAVIOUR

2.1 Rocks in general

2.2 Matrix minerals and geochemistry
- 2.2.2 The presence Elements
- 2.2.2 The presence of minerals, coal and hydro-carbons

2.3 Geological classification

2.4 Geo-temperatures, geo-Pressures, Time-effects
- 2.4.1. In-situ temperatures and related salinities
- - Geothermal gradient
- - Chemical reactions
- - Fluid salinity and water resistivity
- 2.4.2 In-situ pressures
- - Pressure gradients
- - Overpressures
- - Pressure gradients with variable fluid and gas densities.
- 2.4.3 Effects of time

2.5 Rock bulk densities and matrix densities
- 2.5.1 Density definitions
- 2.5.2. Laboratory measurement methods

2.6 Exercises

2.1. ROCKS IN GENERAL

Rock material and rock mass can be classified, from microscopic to scenic scale through its heterogeneity and anisotropy. Conventional concepts of physical behaviour of materials are, with precision, occasionally applicable on rocks. Normally, within the volume of rock being studied and regardless of the scale, the properties vary from point to point (heterogeneity) and with direction (anisotropy). The rock material, or rock substance/intact rock/rock element, is the - to all appearances - continuous substance on which laboratory property tests are run, and to which rigid body continuum mechanics can be practised. The rock material volume element is large regarding grains, pores, and cracks and small when discontinuities like fracs, cleats and layering are considered. The rock mass, or in-situ rock, include a larger mass than does the resembling rock material. In the sense of physics rock mass means mass of rock. However, in nature it consists of heterogeneous material and discontinuities such as pores and fracs. Hence the difference in physical properties between rock material and rock mass justify the distinction between the two.

In general rock consists of minerals, grouped in certain shapes, with openings that can be filled with fluids or gases.

- Minerals are the structure elements of rocks. The structure of the network normally is heterogeneous. Ordinary rock-forming minerals are anisotropic with impurities of other mineral matter. The minerals are connected at grain surfaces, by cements and cohesive aggregates.
- Groups of grains or minerals can be arranged in layers, lenses, etc. and represent in a certain way a part of its geological history, such as grain-size differences due to sediment transport by water or air, or from parallelism of platy grains recrystallized in equilibrium with a stress field.
- At small scale (< 10 cm) rock already is filled with cracks and pores. At larger scales it is cut by discontinuities like fractures (joints) and divisions between layers. The pores and fractures and their orientations are rarely distributed uniformly through rock.
- Pores and cracks can be filled, partly or completely, with water. Water and rock affect each other chemically and physically. Dissolution and precipitation strengthens or weakens rocks. Moreover, a dry rock is a different material from water-saturated rock. In general rock that has been exposed to percolation or weathering normally differs considerably from its unweathered equivalent.
- Although residual stresses are not a part of the composition of rock, stress impact can affect its characteristics. For example, residual stresses affect the amount of load needed to reach failure and may influence the orientation of failure surfaces. Fractured rock behaves differently from its unfractured equivalent. Further fracture properties such as spacing, orientation, size, and roughness are covering the rock heterogeneously. The stronger the rock material, the more important are the discontinuities in determining the behaviour of the rock mass.

In all considerations of the composition of rocks, it is essential to keep in mind the effects of scale. This is particularly important with regard to heterogeneity and anisotropy. Rock material viewed at one scale might be homogeneous and isotropic, but viewed at larger or smaller scales it could be neither homogeneous nor isotropic.

2.2. MATRIX MINERALS AND GEOCHEMISTRY

A small amount of elements form the bulk of the earth's crust. Moreover, an even less number of elements in minerals make up the major parts of rocks. Chemical content and crystal shape determine the properties of minerals and mineral composition and matrix textures define the rock characteristic features. Mineral content and textures are used to explain the bulk physical characteristics of rocks. The crust's mass is about 2.5×10^{22} kg (≈ 0.4% of the earth mass, Turekian, 1972).

2.2.1. THE PRESENCE OF ELEMENTS

Eight elements make up over 98 wt.% of the oceanic and continental crusts. Even more, Si and O account for 65 % to 75 % of the Earth's crust. The difference in presence of elements projects the variety in differences in geological settings of the crust, to wit:

- More potassium, sodium and silicon in "granitic" continental crust.
- More iron, calcium and magnesium in "basaltic" oceanic crust.

TABLE 2.1: Main elements in the Earth's Crust (from [1]Tan et al., 1970 & [2]Tiab et al., 1996)					
ELEMENTS in wt.%	**Crust**			**Rocks**	
	Ocean[1]	**Continental[1]**	**Earth's crust[2]**	**Igneous & metamorphic[1]**	**Sedimentary[2]**
O	45	46	46.40	46	50
Si	23	29	28.15	27	21
Al	8.4	8.3	8.23	8.6	5.6
Fe	7.5	4.8	5.63	6.0	3.3
Ca	7.1	4.1	4.15	4.8	10.0
Na	2.0	2.5	2.36	2.5	0.9
K	1.1	2.0	2.09	1.6	1.9
Mg	3.9	2.1	2.33	2.8	2.0

Table 2. 1 Main elements in the Earth's Crust (from [1]Tan et al., 1970 & [2]Tiab et al., 1996)

The volume percentage of elements gives a different view. Oxygen, normally bound with Si and Al, and the largest of the mentioned elements, justifies ≈ 95 vol.% of the earth's crust.
In addition, many elements are dissolved in water (table 2.2.). Chlorine, sodium, sulphur, and calcium are the five most abundant dissolved elements in both sea water and fresh water. In this respect one also can imagine the idea of brine that is stored in pores and vugs in a major part of the sediments and to a large extent in igneous and metamorphic rock. Oxygen is the most abundant element in water and by

Main elements dissolved in (mainly from Turekian, 1972)		
	Sea water in mg/l	***Fresh water mg/l***
Cl	$1.94 * 10^7$	7800
Na	$1.08 * 10^7$	6300
Mg	$1.29 * 10^6$	4100
S	$9.04 * 10^5$	5600
Ca	$4.11 * 10^5$	15000
K	$3.92 * 10^5$	2300
Br	67300	20
C (inorganic)	28000	11500
N	15000	n.a.
Sr	8100	70
O	6000	n.a.
B	4450	10
Si	2900	6100
F	1300	100

weight almost twice that in rocks.

Table 2. 2: Main elements dissolved in (mainly from Turekian, 1972)

The composition of rocks, water, and air, in and on the crust change in time and are interacting with each other chemically and physically.

2.2.2. THE PRESENCE OF MINERALS, COAL AND HYDRO-CARBONS

A rock forming mineral normally is defined a naturally occurring inorganic crystalline synthesis. According to this definition coal and hydro-carbons are no minerals, but in this course they are included as a division of the rock components. Mineral compositions can be categorised in:

- silicates
- oxides and hydroxides
- sulphides and sulphates
- carbonates
- sulphates
- phosphates
- halides,
- and in our case coal + hydrocarbons.

Silicates as a total are the most present minerals in the earth's crust. In addition, feldspars constitute over half and when quartz is included nearly two third of the total.

Principal minerals in the Earth's Crust (after Ronov and Yaroshevskiy, 1967)	
Mineral	**Presence in %, based on the actual mineral composition**
Quartz	12
Potash feldspars	12
Plagioclase feldspars	39
Micas	5
Amphiboles	5
Pyroxenes	11
Olivines	3.6
Clay minerals and Chlorite	4.6
Calcite and Aragonite	1.5
Dolomite	0.5
Magnetite and Titanomagnetite	1.5
Other minerals like Garnet, Kyanite, etc.	4.9
Coal and hydro-carbons	accessory
	-------+
Total	100

Table 2. 3: Principal minerals in the Earth's Crust (after Ronov and Yaroshevskiy, 1967)

In order to get acquainted with the most occurring matrix minerals, their composition and densities, they are listed in table 2.4. The mentioned minerals are predominantly present in sediments and to a lesser extent in igneous and metamorphic rocks. Some ore minerals are tabled due to their general presence in many rock categories. However as parts of ore bodies they will not be discussed in this lecture and therefore the major part of these mineral will be neglected in the overview. All tabled minerals are also classified on their occurrences. Igneous and volcanic rocks are formed from solidification of molten crust/mantle substance. Sedimentary rocks are fragmented clastic matter or precipitated chemical substance formed at the surface. Diagenetic/Metamorphic products are developed by the presence of pressure, heat, or both to already existing rocks. In other words, diagenesis/metamorphism is a rock-to-rock transformation.

The matrix minerals form a fabric, which is the sum of all the structural and textural features, including the correlative physical properties, of a group of arranged minerals. Fabric data can be separated into:

- scalar data, which include non-directional characteristics like; grain shapes, grain-size distribution, density, porosity and permeability.
- vectorial data, which are based on characteristics like orientation of grains, fractures/pore shapes, etc. Diagenesis/metamorphism, mineral growth and clastic deposition are mainly responsible for vectorial fabrics.

The mineral composition and fabrics or textures are the major criteria for the geological classification of the various rock types. Fabric analysis is normally used as a classification tool to value rock engineering parameters that are used for, among others, (directional) drilling, bore hole stability, excavations, large (sub-surface) constructions, off-shore installations, etc.

Most relevant minerals, composition, density and main occurrence (from Carmichael, 1985 and Schlumberger 1989)				
Name	**Composition**	**Density kg/m^3 x 10^3**	**Occurrence ***	
Silicates				
Olivine	$(Mg,Fe)_2.SiO_4$	3.2 - 4.14	i, v	
Garnet	$(Fe,Mg,Ca)_3.(Fe,Al)_2.(SiO)_3$	3.75 - 4.25	i, m	
Pyroxenes	$(Ca,Mg,Fe,Al).[(Al,Si)O_3]_2$	3.2 - 3.5	i, m	
Amphiboles	$Ca_{0-2}.(Mg,Fe,Al)_{5-6}.[(Al,Si)_4O_{11}]_2.(OH)_2$	3 - 3.2	i, m	
Quartz	SiO_2	2.65	i, (v), m, s-cl/ch, d	
Feldspar	$(Na,K,Ca).Al.(Al,Si)_3.O_8$	257 - 2.76	i, m, v, d, s-cl	
Micas	$K_{0-1}.(Mg,Fe,Al)_3.(Al,Si)_3.O_{10}.(OH)_2$	2.7 - 3.2	i, m, (d)	
Clay minerals	$(K,Na,Ca,Mg)_{0-2}.[(Al,Si)_8.O_{20}].(OH)_{2-4}.n(H_2O)$	2.5 - 2.65	s-cl/ch, m, d	
Carbonates				
Calcite	$Ca.CO_3$	2.72	s-ch/cl, d (i)	
Dolomite	$(Ca,Mg).CO_3$	2.85	s-ch/cl, d (i)	
Siderite	$Fe.CO_3$	3.96	s-ch/cl, d	
Sulphides & sulphates				
Pyrite	FeS	5.02	i, m, d, s-cl	
Galena	PbS	7.6	i, m, d, s-cl	
Sphalerite	ZnS	4.1	i, m, d, s-cl	
Gypsum	$CaSO_4.n(H_2O)$	2.31	d	
Anhydrite	$CaSO_4$	2.96	s-ch, d	
Oxides				
Haematite	Fe_2O_3	5.28	i, m, (v), d, s-ch/cl	
Magnetite	Fe_3O_4	5.20	i, m, (v), d, s-cl	
(Hydro)-Carbons				
Coal	C:H:O - Antracite; 93:3:4, Bituminous; 82:5:13	1.8 - 1.2	s-cl/ch, d	
Oil	$n(CH)_2$	0.85	d	
Natural Gas	$C_{1.1}H_{4.2}$	$0.83 * 10^{-3}$	d	
i - igneous; v - volcanic; m - metamorphic; d - diagenetic; s - sedimentary; cl - clastic; ch - chemical				

Table 2. 4: Most relevant minerals, composition, density and main occurrence (from Carmichael, 1985 and Schlumberger 1989)

2.3. GEOLOGICAL CLASSIFICATION

Rocks are normally classified in three main categories:

- igneous and volcanic,
- sedimentary, and,
- diagenetic to metamorphic.

The classification within those groups is based on a mixture of genetic and visual illustrative factors, e.g. mineral composition and texture in a hand specimen. Based on the mineral composition an chemical composition can be estimated and rocks can be classified. However minerals are grown in an environment with specific physical and chemical conditions, thus knowledge of the mineral composition affords information on the history of the rock and its constituents; especially igneous rocks. If minerals are difficult to determine physical appearances like colour and lamination are used. (e.g. pink granite, black shales, red sands, etc.). Textures normally are connected with particle size, shape and arrangement. The three categories, as mentioned above are related as shown in figure 2.1.

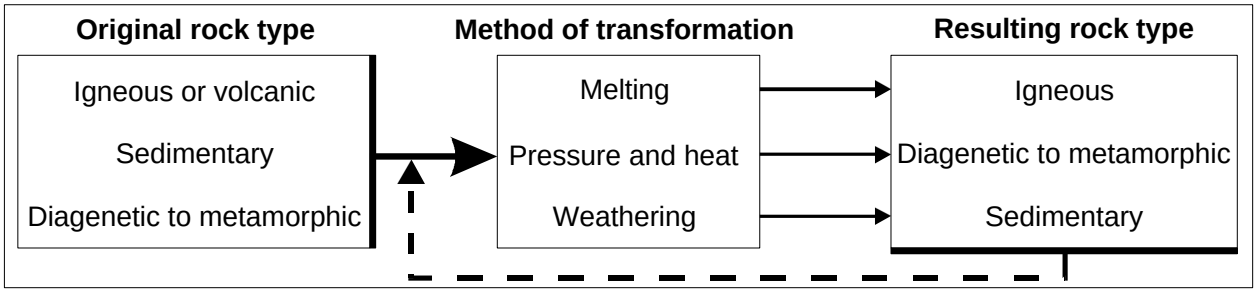

Figure 2. 1: The generic relationship of rocks (revised after Ho et al., 1989)

In this course the emphasis is placed on sedimentary rock. Mining engineers, engineering geologists and petroleum engineers are mainly interested in the physical and geological interpretations. Geologic classification and mapping greatly enhance the reliability of interpolated property data used in engineering classifications. Moreover, a major part of their engineering activities are related to sediments or diagenetically altered sediments. In the coming tables 2.5 a, b and c, for normal sedimentary rocks principal mineral constituents, clastic grain sizes, chemical variety and (bio) organic particles are classified and grouped. Here the most striking particle feature is used to classify the rock. Often sediments are classified in more than one of the main categories, e.g. Oolites, cemented sandstone, fossil bearing limestones.

A general classification of sedimentary rocks, based on composition and texture.

A: Classification based on clastic fragments

Texture; grain size	**Group name**	**Composition**
Cobbles, pebbles, granules	Blocks to gravel	Rounded & angular fragments
Coarse; > 2 mm	Breccia	Large angular fragments
	Conglomerate	Large rounded fragments
Medium; 2-0.0265 mm	Sandstone	Quartz, feldspar, clay Quartz, feldspar, micas Quartz (feldspar)
Fine; 0.0265-0.0039 mm	Silt	Mainly quartz and clay Quartz, carbonate cement
Very fine; < 0.0039 mm	Clay	Compacted clay Clay, organic matter and some sulphides

Table 2. 5: A general classification of sedimentary rocks, based on composition and texture.

Note that table 2.5 can be regarded as an introduction to rock classification systems and not as a complete reference.

Besides the geological rock classification systems the potential engineering use of the rock or of space in the rock is an engineering classification of rocks. These classifications normally apply to rock material and to rock mass. The related rock properties or material parameters are measured, in a usual way, in a laboratory, and called index properties. Some examples are; porosity, permeability, unconfined compressive strength and specific gravity. The characteristics of a rock mass determined in situ often

has an identical name as the laboratory-measured property of rock material. Be aware that the tow measurements cannot be regarded as equivalent measurement results. Compilation of data and application of classification criteria must take into account the way in which each data point has been obtained. Depending upon the needs of the user, classification may be based on one criterion or on a combination of several criteria. The majority of subjects in this course, with respect to rock measurements, are based on these viewpoint.

B: Classification based on chemical components		
Group name	**Example**	**Composition**
Limestone	Chalk	Micro fossils, micro parts of shells etc., clay
	Boundstone	Fossil components bound together by organic growth
	Crystalline limestone	Crystal grains of calcite with relics of ghost structures.
Dolomite	Dolomitic limestone	Dolomite
Chert	Chert	Micro-grains of hydrated silica, light coloured
Flint	Flintstone	Micro-grains of hydrated silica, dark coloured
Evaporites	Gypsum	Gypsum
	Rock salt	Halite, sylvite, aragonite

C: Classification based on bio-organic components		
Group name	**Example**	**Composition**
Coal	Peat	Decaying wood embedded in disintegrated plant debris
	Brown coal or Lignite,	Humic (<40 % water) coal with vegetal structures
	Bituminous to Antracite	Organic sediment (< 40% ash) composed of polymers of cyclic hydrocarbons and low water content
Asphalt	Tar	Migrated and solidified immature petroleum. Black to dark brown.
Limestone	Coquina	Fossil fragments, loosely cemented like sand.

Table 2.5.<u>continued:</u> Classification based on chemical components (B) and on bio-organic components (C)

2.4. GEO-TEMPERATURES, GEO-PRESSURES, TIME-EFFECTS

Many sub-surface activities in rocks and its pore space are depending on:

- In-situ temperatures, which normally depend on the geothermal gradient and in that relation the rock type and burial history.
- In-situ pressures, which depend directly on the thickness and density of the overlying rock. Indirectly the stress is depending on the tectonic history, e.g. regional compression zones, shear zones, extension zones and local fault and folding activities. In relation in-situ pore pressures are depending on the height and density of the fluid column. In addition, the presence of sealing layers can develop areas with over pressures.
- Time. All chemical and physical activities in rock need time to proceed. Some effects, like compaction and pressure solution are relatively long term phenomena. Dissolution of carbonates and precipitation of cement or clays could be short term phenomena.

2.4.1. IN-SITU TEMPERATURES AND RELATED SALINITIES

Many processes, related to the in-situ temperature, are constantly changing the rock characteristics through time. Three thermal relevant processes of major importance will be discussed.

Geothermal gradient

Geo-temperatures in-situ depend on the geothermal gradient (G_t) and in that relation the rock type and burial history. In western Europe, in the predominantly Palaeozoic and younger rocks, G_t is about 30°C/km. In shields of Cambrian and older rocks, G_t can be much lower, i.e. 10°C/km. In a crust of approximately 35 km thickness the temperature can reach to some 1000 °C. In the oceanic crusts G_t

ranges from circa 40°C/km at the margins to > 200°C/km at the spreading axis or other active plate margins. The normal thermal gradient measured all over the world has an average of G_t = 18.2°C/km. In this course sedimentary basins are the main type of rock in our topics. If from a certain area the mean surface temperature; T_s, the formation temperature; T_f (boreholes, mines) and depth; D, are known, then one easily estimates the geothermal gradient (G_t):

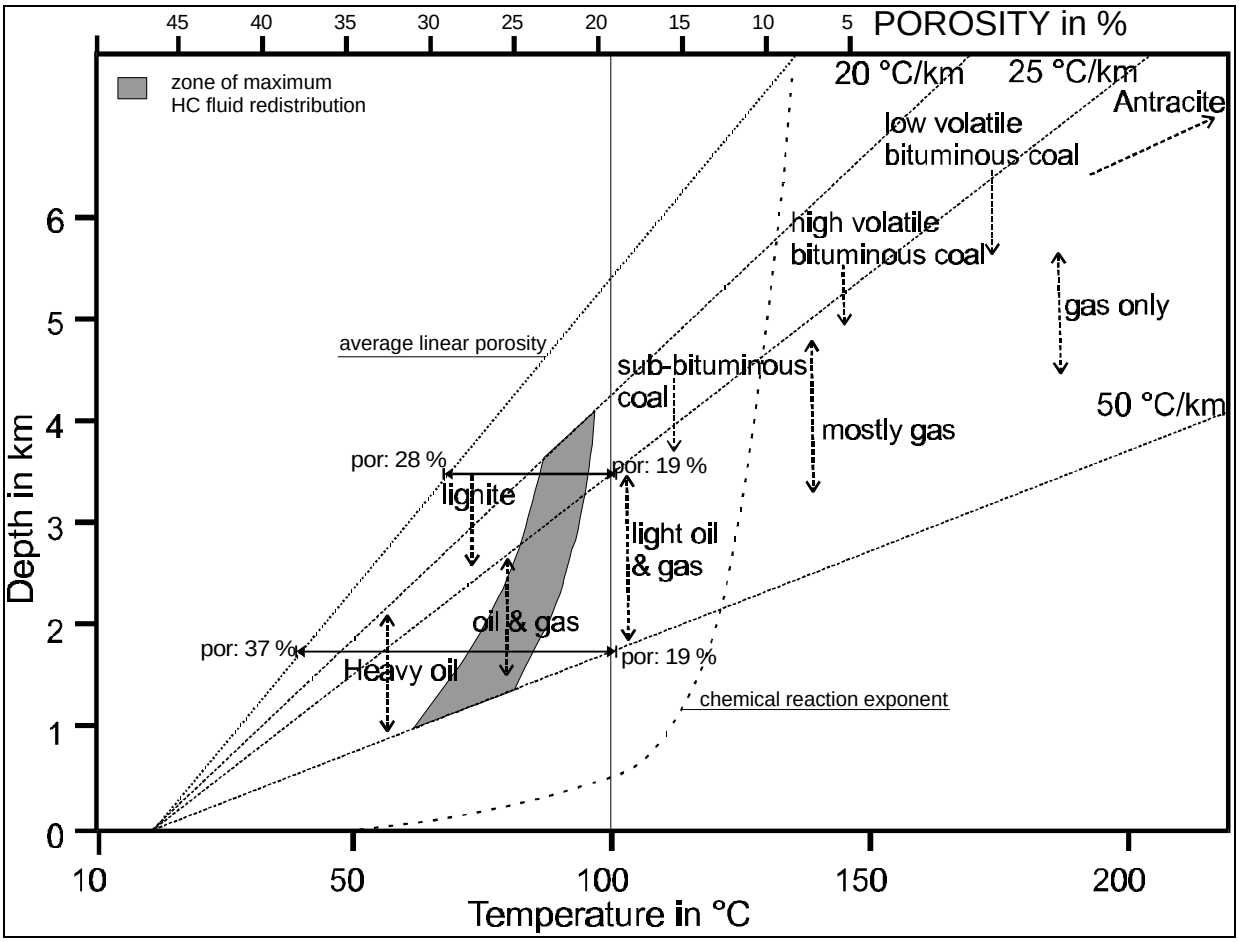

Figure 2. 2 Relation between the depth, temperature, formation of coal, hydrocarbons and the development of porosity.

$$G_t = \frac{T_f - T_s}{D} \qquad \text{(eq. 2.1)}$$

Chemical reactions

In figure 2.1. the effects of temperatures are related to the maturity of coal and the generation of hydro-carbons. Important are the thermal behaviour of fluids like water and the chemical reaction of minerals and organic matter with or without fluids. These chemical reactions often are depending on temperatures, which can be expressed in the Arrenius equation:

$$k = Ae^{-\left(\frac{E_a}{RT}\right)} \quad \text{or} \quad \ln k = \ln A - \frac{E_a}{RT} \qquad \text{(eq.2.2)}$$

where:

k : the rate constant
A : pre-exponential factor, depending on environment and mineral types
E_a : the activation energy of the reaction *(J)*
R : gas constant *(J/K)*
T : Temperature (*K*)

The equation shows that the rate of reaction more or less doubles with every 10 °C in rise of temperature.

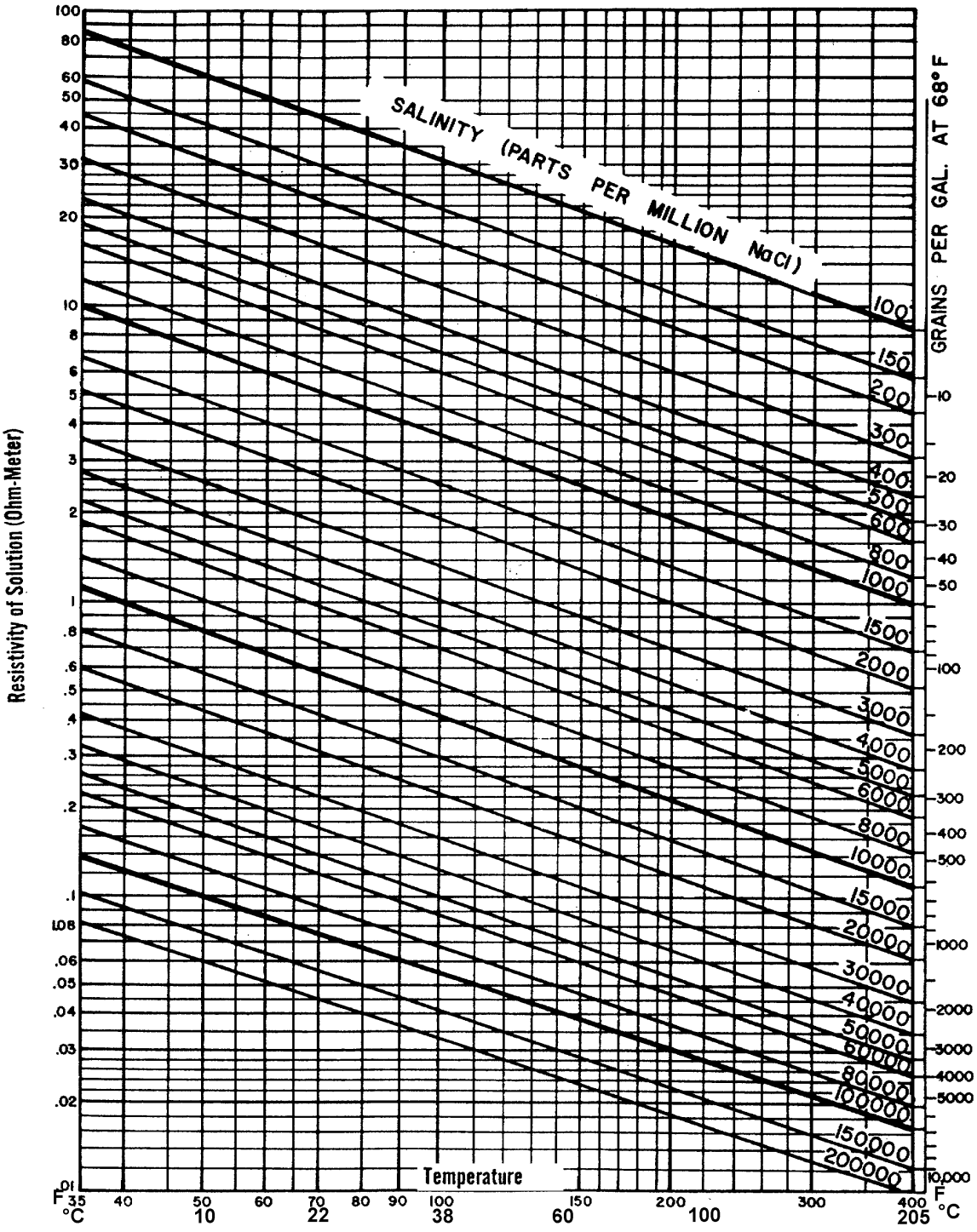

Figure 2. 3: Water resistivity as a function of temperature and salinity (from the Schlumberger log interpretation chart books)

Fluid salinity and water resistivity

For water, normally present as a brine and sometimes as fresh water (table 2.2), the temperature, salinity and related water resistivity are important. They have to be determined for environmental corrections in bore hole measurements, for example, when the water salinity at surface conditions has to

be estimated. The resistivity (ohm.m) or conductivity (mmho)[1] of water; R_w can be estimated on the basis of fluid salinity. The solutions are expressed in ppm NaCl-equivalents. Parts per millions (or ppm) is the ratio of weights, e.g. expressed as g/l or µg/g, and related as:

$$S_1 = \frac{S_2}{\rho_{sol}} * 1000 \qquad \text{(eq.2.3)}$$

with: S_1: salinity in ppm, S2: salinity in g/l and ρ_{sol}: solution density in g/l. Figure 2.3 shows the graphic relation between the dependency of Rw from salinity and temperature. It shows that water resistivities decrease with increasing temperature. Here Arp's empirical relation gives for Rw an estimation of the temperature dependency:

$$R_{wT2} = R_{wT1}\left(\frac{T_1 + 6.77}{T_2 + 6.77}\right) \qquad \text{(eq.2.4)}$$

where, $T_{1,2}$ are the temperatures at specific depths (**in °F**) and $R_{wT1,2}$ (in ohm.m) the respective water resistivities. For saline water a constant (or correction factor) of 6.77 is inserted. This correction is eliminated when fresh water is dealt with. If the surface temperatures are taken as a standard, T_1 will be 24°C or 75°F and any in-situ R_w -value is estimated for its salinity. Now equation 2.4 can be generalised as:

$$R_{wT2} = R_{w75}\left(\frac{81.77}{T_2 + 6.77}\right) \qquad \text{(eq.2.5)}$$

Normally a brine consists of a complex sum of ions in a solution. In the previous text we mentioned

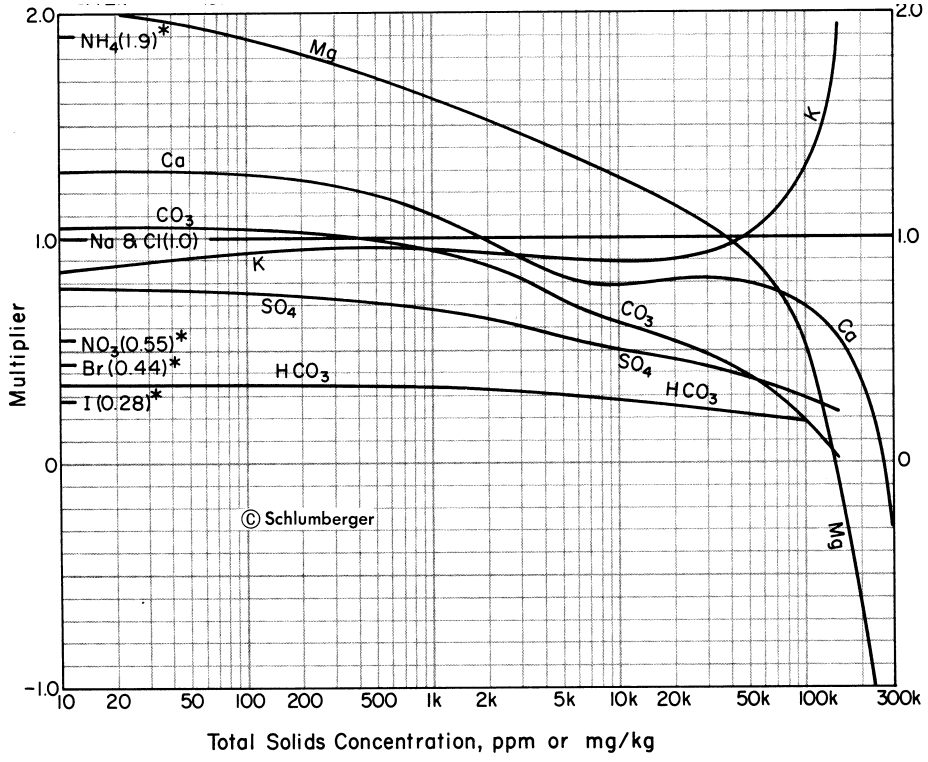

Figure 2. 4: Multipliers for dissolved salt components to equivalents of NaCl concentrations (from the Schlumberger log interpretation chart books)

NaCl-concentration equivalents, or C_{sum}. This concentration is the summation of all ions (n) present in the solution as different ions (C_{ai}), multiplied by their weighting multiplier (M_a), or:

[1] 1 mmho = $(\text{ohm.m})^{-1}$ x10^3

$$C_{sum} = \sum_{a=1}^{n} M_a C_{ai} \qquad \text{(eq. 2.6)}$$

The multipliers are determined experimentally and gathered in figure 2.4. When ion concentrations are known from chemical analysis, it is also possible to estimate the R_w at surface condition (24°C or 75°F) with the surface temperature specific relation:

$$R_{w75} = \left(2.74 \times 10^{-4} C_{sum}\right)^{-1} + 0.0123 \qquad \text{(eq. 2.7)}$$

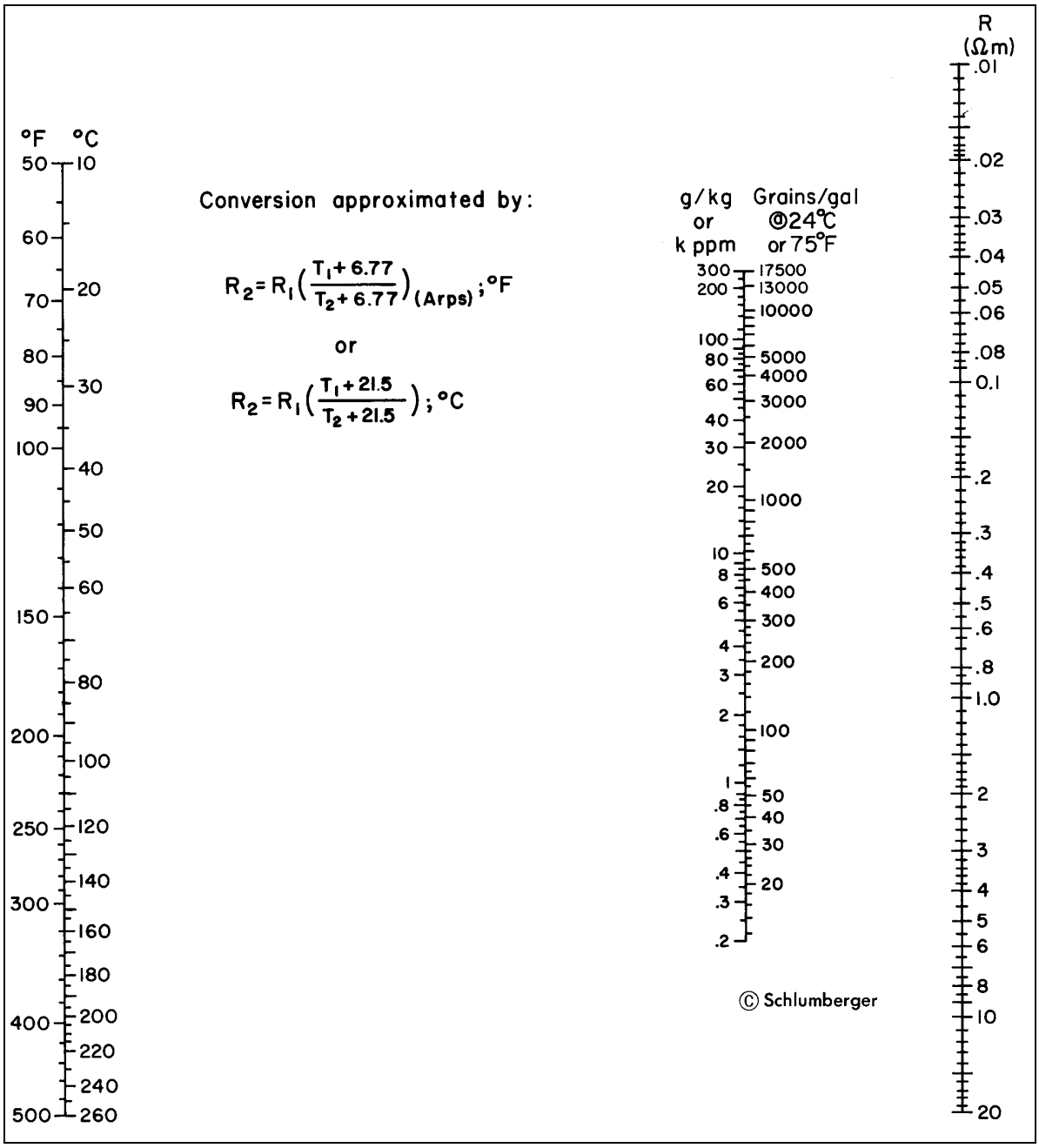

Figure 2. 5: Resistivity nomograph for NaCl solutions. From the Schlumberger log interpretation chart books.

Figure 2.5 gives a second and faster method to relate salinity in NaCl-equivalents with temperature and resistivity. This graphical method shows that each water resistivity at a specific temperature ($T_{1,2...n}$) can

be estimated when a straight line is moved from the temperature line through a point of constant concentration on the salinity line. This method makes it easy to convert surface conditions to in-situ conditions.

2.4.2. IN-SITU PRESSURES

In-situ pressures, directly depend on the thickness and density of the overlying rock. Indirectly the tectonic history also contributes to anomalies in the stress-distribution. Further the omnipresent pore pressures are related to the height and density of the fluid column. In addition, the presence of sealing layers may develop zones with overpressures.

Pressure gradients

The total overburden pressure (P_o) or confining stress in a rock under compaction, at a specified depth, can be expressed as the sum of the lithostatic (grain) pressure (P_r) and the fluid pressure (P_f). In other words, the lithostatic weight is supported by the pore fluids and its potential energy is stored in the fluids.

$$P_o = P_r + P_f \qquad \text{(eq.2.8)}$$

In homogeneous systems pressures increase linear with depth. The lithostatic pressure gradient depends on the rock densities, whereas the geostatic pressure gradient depends on the densities of the rock matrix and pore fluids. Hence, the grain framework provides the effective stress (σ_p) in a rock, which can be expressed as:

$$\boldsymbol{s}_p = P_0 - P_f \qquad \text{(eq. 2.9)}$$

In theory the effective stress (σ_p) is equal to the matrix stress (σ_m) or load on the grain framework. The average overburden pressure gradient (rock) is approximated at 22.6 kPa.m^{-1}, which corresponds with an average bulk density of 2.31*10^3 kg.m^{-3}. A common fluid pressure gradient is in between 9.8 kPa.m^{-1} (fresh water) and 10.5 kPa.m^{-1} (brine). Normal fluid pressures have the ability to equalise pore fluids in rock with the related hydrostatic pressures for a specific depth. Overpressures have a gradient higher than 10.5 kPa.m^{-1}.

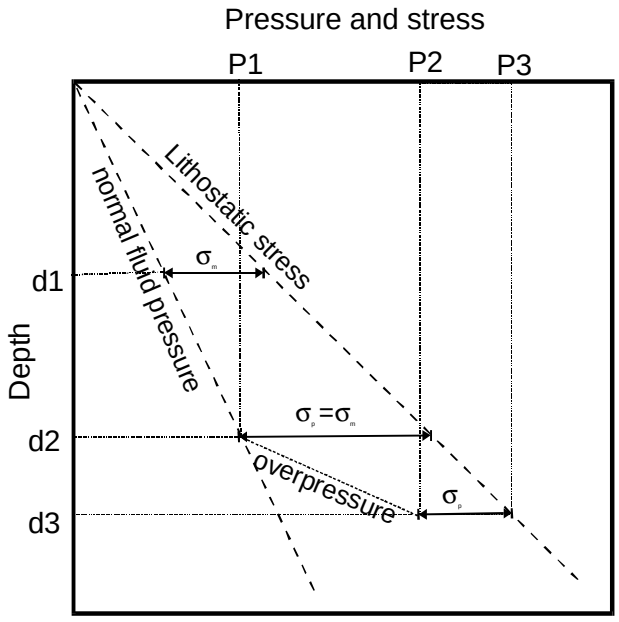

Figure 2. 6: Pressure -depth relation for normal compaction and non-equilibrium.

Overpressures

Overpressures (figure 2.6) are not constrained to depth or age. They need an implicit dynamic fluid system (i.e. porous rocks) enclosed by a sealing rock type. Most overpressured zones are present in young basins which are rapidly filled in a regressive regime. For example; near shore sediments are fast accumulating on off-shore mud rocks. Now the increasing fluid pressure gradient forces fluids to upward or side away.

Decreasing porosity and permeability prevent the fluid to migrate and pore pressure built up starts. The driving force is the load of the water filled overburden.

Several types of geopressures can be named:

- Load pressure due to rapid increase in overburden, without fluid escape.

- Tectonic pressure, by thrust or gravity movements of sediment zones, or folding.
- Inflated pressure, induced by fluid recharge
- Phase pressure, due to the change of matrix minor phases or pore fluids like hydro-carbons.

Pressure gradients with variable fluid and gas densities.
In-situ borehole measurements (Wireline Logging, Formation Testing) give a direct indication of the in-situ pore pressures ($P_{f1,2,3,..}$) and as a result indirect indications on the fluid types that occupy the pore space. Some decades ago a repeat formation tester (RFT) was developed, which consists of a sample chamber and a pad (figure 2.7). The pad is pressed against the borehole wall and a perforating charge is used to get communication between the porous rock and the sample chamber through a flow line. In a second option a nozzle is extended through the mudcake into the rock. Now it is possible to measure the formation pore pressure and to get samples from an open hole. The flow-line that connects the nozzle or probe to the chamber contains a number of valves which give way to multiple settings of the tool and collection of several formation fluid samples. At each setting the pressure of the reservoir fluid can be measured with a strain-gauge or a quartz high resolution pressure gauge. The accuracy of the setting of the test tools at a certain depth is controlled by other borehole measurements tools (i.e. Gamma Ray and SP). The reservoir pressure measurements plotted against the depth gives a gradient that is very steep for gas, much flatter for oil, and a small angle for water. The pressure measurements are used to detect contacts such as fresh water/brine, gas/water, gas/oil or oil/water contacts (fig. 2.8).

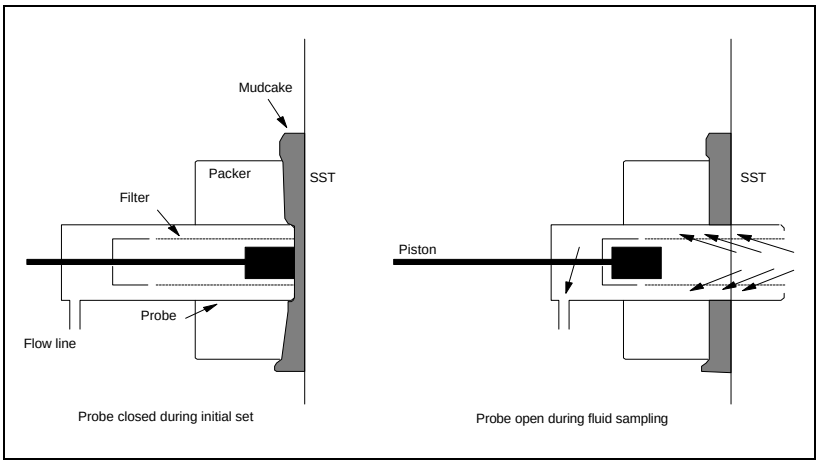

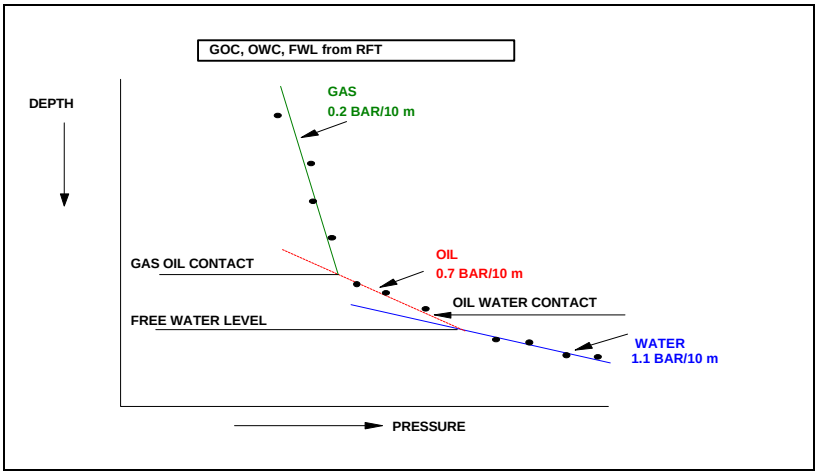

Figure 2. 8: Fluid contacts that can be obtained with fluid pressure measurements.

2.4.3. EFFECTS OF TIME

Time. All chemical and physical activities in rock need time to proceed. Some effects, like compaction and pressure solution are relatively long term phenomena. Dissolution of carbonates and precipitation of cement or clays could be short term phenomena. The relation between temperature and time is essential for the formation/recrystallization of minerals, the maturation of oil and the coalification of plant relics. A simple rock maturity relation, originally by Vassoyevich, included pressure (P in atm) , time (t in million years) and temperature (T in °C). This “geochronothermobar” (G) is defined as:

$$G = \frac{T \times t \times P}{1000} \qquad \text{(eq. 2.10)}$$

Lopatin (1971) developed a time-temperature index (TTI) for the maturity of organic matter. He covered a depth-age plot with a simplified temperature grid. Here the increment in maturity (***D****M*), for a specific depth interval, is related to the exponential relation:

$$\Delta M = \Delta T r^n \qquad \text{(eq. 2.11)}$$

Here *n* is an index value for temperature intervals of 10°C. For 100 -110 °C the value n = 0 was chosen. Therefore, lower intervals had a n < 0 and higher intervals a n > 0. The temperature factor r^n consists of the value r, which is based on the type of organic matter and the previously explained exponent *n*. If the Arrhenius equation is applied (eq. 2.2), with the conclusion that the rate of reaction doubles with every 10°C rise in temperature, then *r* = 2. The time span (***D****T*) is reconstructed from isotope findings or palaeontology.

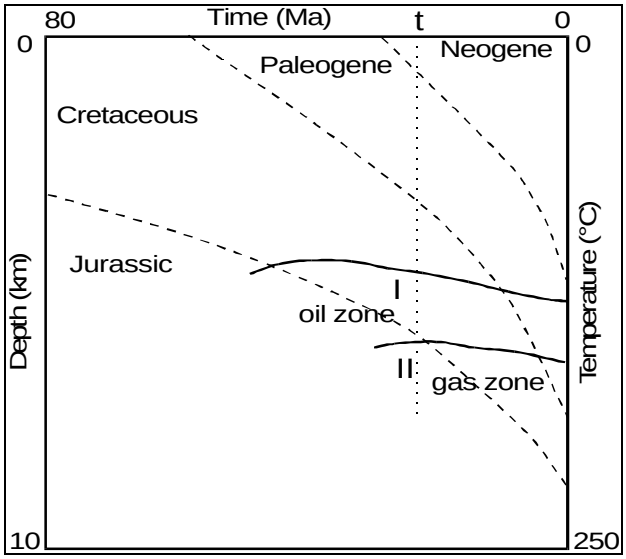

Figure 2. 9: Example of the combined role of time and temperature in the maturation of organic matter. Revised after Lopatin, Int. Geol. Review, 1980)

Figure 2.9 shows, in an example, that porous rocks of "age I" have been in the oil zone for a period of t Ma. In the same time span porous rocks of "age II" have been in the gas zone.

2.5. ROCK BULK DENSITIES AND MATRIX DENSITIES

With the exception of bulk density most of the aspects regarding mineral densities, textures, fluid densities and related in-situ environments have been discussed in this chapter. Density is the specific rock property that represent the coherence between mass and unit volume. It is used as an index property or as an independent variable to predict other rock properties. However, uniformity of density values are difficult to obtain, because of the environmental effects, such as; temperature, pressure, kind of fluid and degree of fluid saturation and mineralogical alterations. Further different methods of density determination can give a variation in density values for what seemed to be similar rock types.

2.5.1. DENSITY DEFINITIONS

The American Society of Testing and Materials Standards provided various descriptions for density and specific gravity. In these formulations the temperatures of the material and fluid that is used in the test has to be specified.

- **True density or matrix density:** The mass of a unit volume of a solid material where the volume of only the impermeable portion is considered, represented as: $\dfrac{mass}{V_{total} - V_{pore}}$ (eq.2.12)
- **True Specific Gravity:** The ratio of the mass of a unit volume of solid material, of the impermeable part, to the mass of the same volume of gas-free distilled water.
- **Apparent Density:** The weight in air of the non-permeable part of the unit volume of rock.
- **Apparent Specific Gravity:** The ratio of the weight in air of a unit volume of material to the weight in air of equal density of an equal volume of gas-free distilled water. Represented as: (dry weight in air)/(dry weight in air - submerged weight).
- **Bulk Density:** Often considered to be equivalent with the apparent density. The weight in air of a unit volume of a permeable material including both permeable and impermeable voids normal to the

material. This is expressed in two ways:
1. (weight)/(volume including all voids) and
2. (weight)/(unit volume, including the fluid).

- **Bulk Specific Gravity:** The ratio of the weight in air of a unit volume of a permeable material (including all voids) to the weight in air of equal density of an equal volume of gas free distilled water. Here represented as:(dry weight in air)/(saturated weight-submerged weight).
- **Grain Density or matrix density:** Often considered to be equivalent with the true density. Defined as the mass of a unit volume of grains. Also represented as (mass of grains)/(volume of grains) or represented by the formula: $\rho_g = \sum_{i=1}^{i=n} \rho_i \cdot v_i$. (eq.2.13)

  n is the number of minerals, ρ_i the grain density of each mineral, v_i the volume of each mineral.

Measurement of grain densities decrease the volume effects of pores and fractures. Frequently from density data it is not known if their "true," "apparent," or "bulk" measurements. If the measurement units (g/cm^3) are not presented than the data presumably represent specific gravity (a ratio). If contrarily, then density is intended to be used. Generally measuring methods that are put to use also deal with a measurement of the pore volume, the bulk volume and in consequence the apparent grain volume (both grains and isolated pores). Note that the distinction between bulk volume and apparent grain volume is equal to the volume of interconnecting pores.

2.5.2. LABORATORY MEASUREMENT METHODS

Bulk densities and matrix densities are calculated using the bulk weight or matrix/grain weight and the related volume.

In a laboratory one can measure three different bulk densities:

1. Dry bulk density: $\rho_b = \frac{W_g}{V_b}$, (eq.2.14)

   in which W_g is the weight of grains or matrix and V_b is the volume of grains and pore space.

2. Natural bulk density: $\rho = \frac{W_g + W_w}{V_b}$, (eq.2.15)

   were W_w is the weight of the available pore fluid.

3. Saturated bulk density: $\rho_s = \frac{W_g + \left(V_p \cdot \rho_w\right)}{V_b}$, (eq.2.16)

   with V_p as the volume of interconnecting pores and ρ_w as the fluid density.

The bulk weight of matrix and pores or grains is easily and accurately measured with a balance. The procedures used to get a matrix density or bulk density involve the determination of any two of either pore volume, bulk volume, or grain volume.

Bulk volumes can be measured with several methods:

- Volumetric dimensioning of symmetrically shaped specimens (cubes or cylinders) with a ruler or sliding gauge.
- Direct measurement of liquid displacement by submersion of the sample in a non-penetrating fluid; normally mercury.
- Direct measurement of liquid displacement by submersion of a waxed or impermeable sample in a fluid.
- The buoyancy method, based on Archimedes' principle. It requires the weight of a sample in air, both dry (W_1)and saturated (W_2), and its weight hanging in a liquid (W_3). The liquid is of known

density (ρ_w). Here the dry bulk density is calculated as: $\rho_b = \frac{W_1}{W_2 - W_3} \cdot \rho_w$ (eq.2.17)

and the grain density as: $\rho_g = \frac{W_1}{W_1 - W_3} \cdot \rho_w$ (eq.2.18)

Methods for the determination of grain volumes are:

- Fluid displacement of submerged pulverised grains. The pulverised minerals are disposed of major part of the pores and fracs.
- The buoyancy method. The method uses the weight of grains and weight of the specimen that is suspended in a liquid of known density.
- Boyle's law; gas volumenometry methods; figure 2.10. Several kinds of porosity-meters, using the pressure-volume relationships of Boyle's law for perfect gases, have been invented. The devices, like the pycnometer, use air or a non-adsorbing gas to get the highest accuracy in analysis. Helium, the best option, invades all void spaces except those that are impermeous. Hence, its results are representative for matrix and grain volumes and they provide the total porosity.

  The working method is as follows:
  A cleaned and dried sample is placed in a sample holder with a gas pressure P_1. When the valve that connects the sample chamber with the reference volume chamber is opened the gas will expand isothermally and equilibrate on a pressure P_2. The volume of the sample chamber is V_0, and that the core sample has a grain volume V_{ma}. For that reason, the sample chamber will contain a gas volume of V-V_{ma}. If this gas pressure changes from the pressure P_1 to P_2 by adding the reference volume dV (normally the same as V_0) we can use Boyle's law and use:

$$(V_0 - V_{ma}) \cdot P_1 = (V_0 - V_{ma} + dV) \cdot P_2 \quad \text{(eq.2.19)}$$

  Now V_{ma} can be calculated, though be aware that isolated pores, common in carbonate rocks, will not be accounted for.

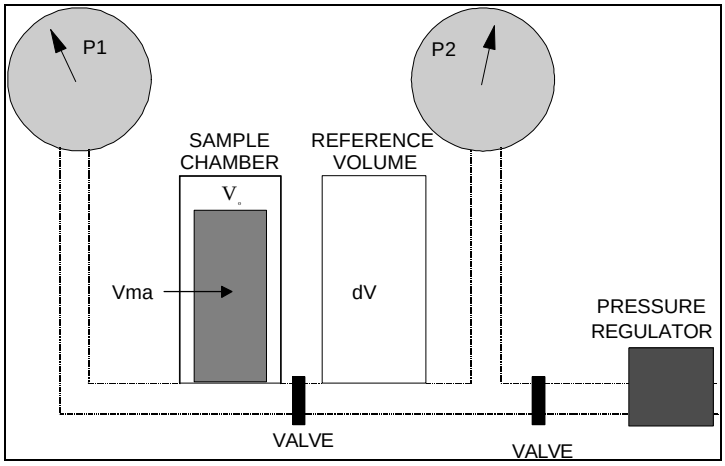

Figure 2. 10: Boyle's law porosimeter, grain-volume determination.

2.6. EXERCISES

Bad Bentheim, accommodates a famous German "Kuhrort" for patients with serious skin diseases. Unfortunately the medical springs are depleting. Nevertheless, newly drilled exploration wells show highly porous sand bodies and fractured carbonate horizons in Jurassic sands and Bundsandstein formations, thus new prospects. The Delft Engineering Geological Group is asked to give an opinion on these findings, with respect to salinity, conductivity and reservoir quality of the drilled wells.

1. For the determination of the water salinities of the different sands, the following salinity results have to be converted to water resistivities at the formation depths e.g. formation temperatures. All resistivities are in ohm.m, FT is the formation temperature in °F or °C, 1 mol Na = 23 gram, 1 mol Cl = 35.5 gram). Use table Ex.1.
2. At the faculty all relevant information on borehole depth and bottom hole pressures have been stored in one computer. Unfortunately, during renovations this specific computer was stolen. Someone found in the literature the regional thermal gradients, with an average estimated gradient of G_t=30.5°C/km. The average surface temperature is 14°C. Calculate the bottom hole depths and put them in table E1.
3. Now it is also good to know the bottom hole pressures for engineering purposes. Here the salinity and depth are needed.
4. In order to get acquainted with the stability of the porous sandstones, one likes to know the effective stress σ_p on the grain framework. An average bulk density (σ_r) of 2.31 g/cm^3 is normal in these areas.

Table Ex.1

Well nr	Bottom hole depth in km	Formation water salinity	ρ_f in g/cm^3	P_f in bar	P_0 in bar	ft	Rw at ft in ohm.m	σ_p in MPa
1		200,000 mg/l NaCl				212 °F		
2		100,000 ppm NaCl				122 °F		
3		50,000 ppm NaCl				130 °F		
4		50,000 mg/l Cl				122 °F		
5		100 g/l NaCl				100 °C		

5. A sixth well was analyzed on the ion-content of the formation water at a surface temperature of 75°F. Further information was vanished. Further information was vanished. The concentrations are: 8.000 ppm Na^+, 10.000 ppm Cl^-, 5.000 ppm Mg^{2+}, 3.000 ppm Ca^{2+}, 7.000 ppm CO_3^{2-}
   - Determine the solid concentration and the equivalent NaCl concentration.
   - Determine the resistivity at reference temperature and resistivity of the brine at 130°F.

3. ROCK & CORE ANALYSIS

3.1 GENERAL INTRODUCTION

This chapter consists of six parts. The section on mud logging describes the information that can be obtained during drilling. The second part on coring discusses the various methods to obtain an intact piece of the rock down hole and bring it to the surface for analysis. In the following section, the sampling and retrieval of reservoir fluids is covered. In part four relevant analysis techniques to define mineral characteristics, texture properties and fluid behaviour are explained. Part five reviews well logging and part six covers measurements with instruments embedded in the drill string.

3.2 ASPECTS OF MUDLOGGING

Important information can be obtained during the process of drilling a well by the analysis of :

- cuttings produced when the drilling bit grinds the rock to small pieces, which are carried to the surface by the mud when it is circulated through the hole.
- oil or gas shows in the mud stream.
- the rate of penetration of the drilling bit.

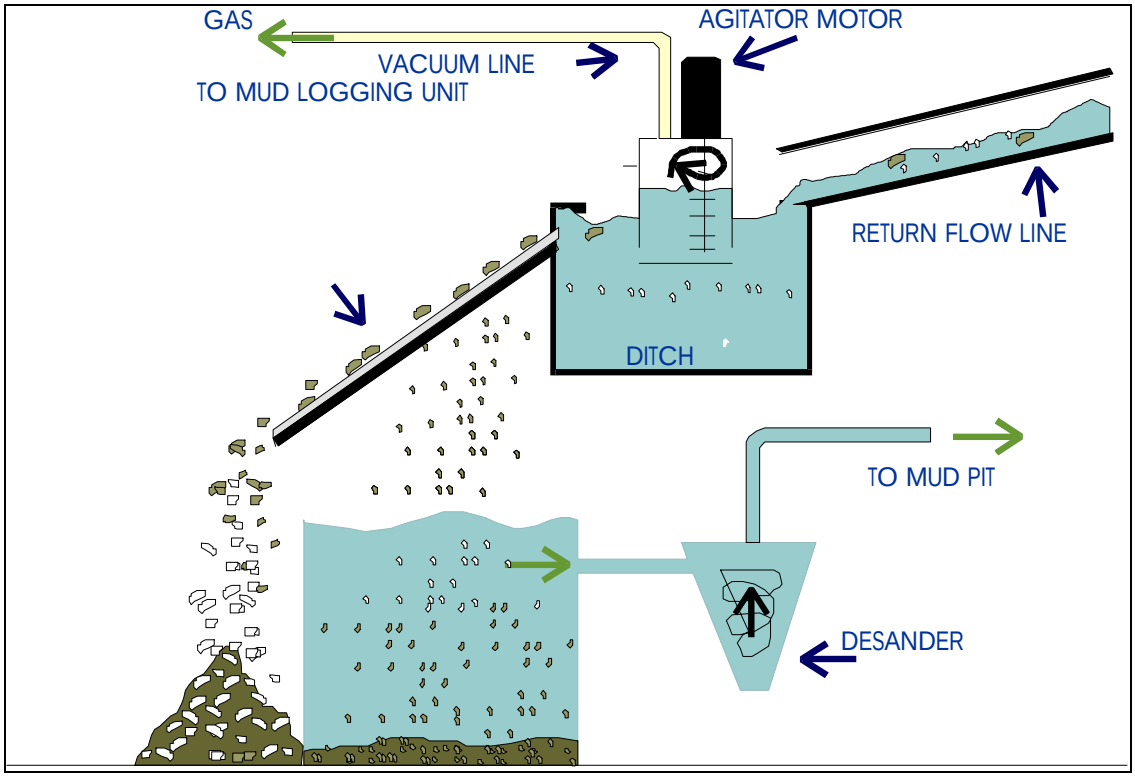

Figure 3. 1: Gas extraction at the ditch. (Revised after Exlog, 1985)

For the interpretation of the mud logging data it is important to know the time when and the place where the cuttings and gas were collected (Figure 3.1).

A mud logging unit on a large drilling rig used for oil exploration has the following facilities:

- Equipment for sieving, washing and drying of cuttings (figure 3.2)
- Laboratory set-up for chemical tests on cuttings and mud.
- Microscope and ultraviolet-light inspection chamber for the identification of oil and description of the lithology of the cuttings.
- Continuous recording of gas with recorders: hot wire analyser/thermal conductivity cell/gas chromatography/infrared analyser.

- Continuous recording of drilling parameters: pump rate, rate of penetration, weight on bit, rotary speed, drilling torque, standpipe and casing pressure.
- Mud properties at the flow-line and in the pit: density, conductivity, temperature, flow rate, mud pit level.

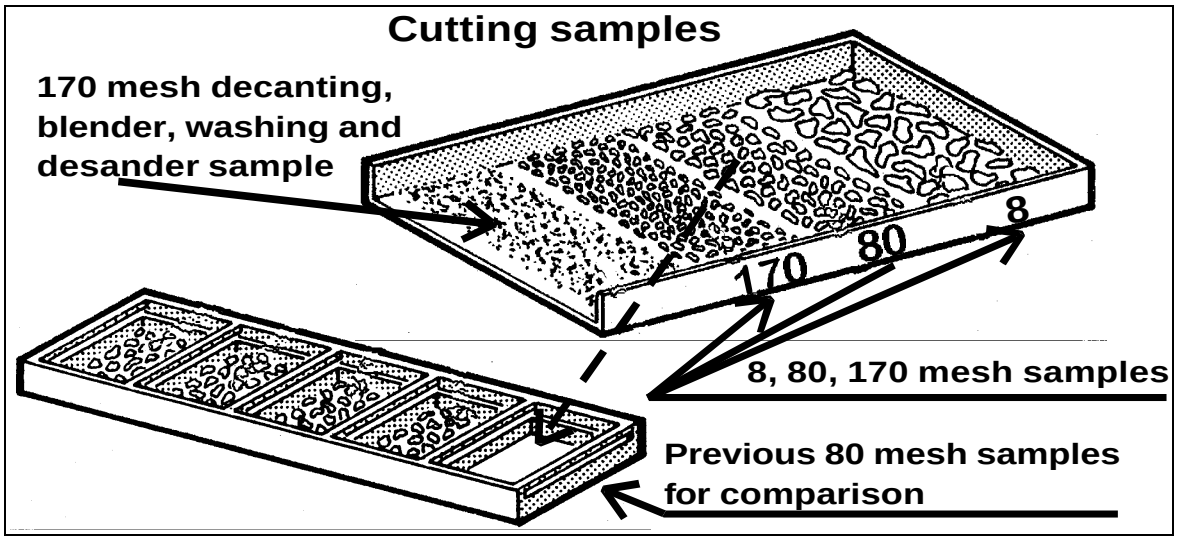

Figure 3. 2: Cutting samples for microscope analysis, X.R.D., X.R.F. and E.M.

3.2.1 CUTTINGS

Investigation of cuttings under the microscope enables the petroleum engineer or the geologist at the well site to describe the various rock types that were penetrated by the bit. Useful information on porosity and permeability may also be obtained. When the cuttings originate from an oil bearing formation they will usually retain only a fraction of the oil that was present in the undisturbed rock. This severe reduction is due to flushing by the mud filtrate, and expansion of gas. This gas was first compressed or was dissolved in the oil, but is released and expands up to 200 times, when the pressure decreases from a few hundred atmospheres downhole to one atmosphere at the surface.

Note: The methods described in this chapter are also applicable to define the quality op asphalt (road-pavement) and coal maceral types.

3.2.2 FLUORESCENCE

Fluorescence occurs when a substance is exposed to ultraviolet radiation (Photo 3.1). Not all materials fluoresce. If the fluorescence caused by ultraviolet excitation is in the ultraviolet region, it cannot be observed by the human eye. Simple organic molecules like paraffin's rarely fluoresce. Fortunately, a sufficient number of aromatics and naphthenes are present in most crude oils, which provide a distinctive fluorescence in the visible region (wavelength 4000-7800 Angstrom). Sometimes crude oil or diesel oil are added to the mud as a lubricant. In addition pipe dope or lubricants are used for connecting the drilling pipes. The presence of these refined rig oils makes the interpretation on hydro-

API	DENSITY(60 F)	COLOUR FLUORESCENCE
< 15	>0.96	brown
15-25	0.9 - 0.96	orange
25-35	0.85 - 0.9	yellow - cream
35-45	0.80 - 0.85	white
>45	<0.80	blue white - violet

Table 3. 1: Colour of fluorescence as a function of oil density.

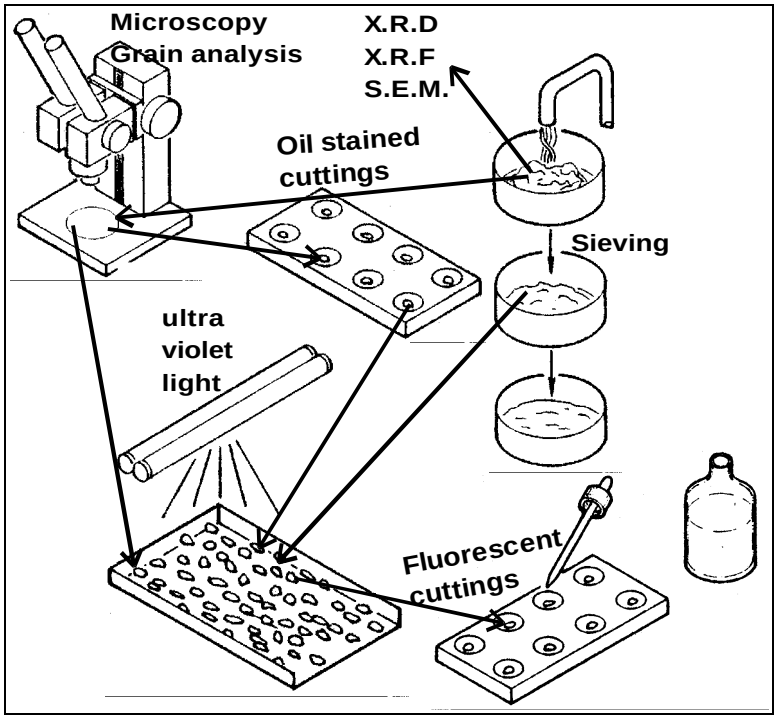

Figure 3. 3: Washed cuttings used for examination on rock type and pore fluid content (i.e. water, oil, drilling fluids)

carbons ambiguous. The colour of fluorescence is, normally characteristic for the gravity of the oil as shown in Table 3.1. Crude oil produces fluorescent light with characteristic colours which fortunately deviates from the fluorescence produced by diesel. In contrast the fluorescence from diesel and from condensates found in gas reservoirs can be very similar.

3.2.3 GAS ANALYSIS

In Figure 3.1 is shown how the agitator motor stirs the mud. The gas that escapes due to the stirring is transported via the vacuum line to the mud logging unit. The gas collected from the ditch is analysed in the mud logging unit. Coal layers can release methane, and trip gas released from the drilling mud when the drill pipes are pulled out of the hole should not be confused with gas from hydrocarbon reservoirs. Analysis of gas can be carried out with a number of methods:

1. **Hot Wire Analyser**
   The heart of the analyser is a Wheatstone bridge of which two resistors are replaced by a pair of matched platinum filaments. One is in a cell that is open to the atmosphere while the other is in a cell through which the sample gas is passed. The filaments are heated to high temperatures by passing a current through the bridge. The recorder reads zero when air is present in both the calibration cell and in the gas sample cell. When the sample contains hydrocarbons, catalytic oxidation of the hydrocarbon gases at the filament occurs. This causes an increase in the temperature of the filament and consequently an increase in its resistance. The recorder is roughly proportional to the amount of hydrocarbon gas in the sample.
2. **Thermal Conductivity Cell**
   This cell is similar to the hot wire analyser, but operates at a lower temperature (lower voltage). As a result there is no combustion of gas, and the temperature and resistance fluctuations of the filament depend solely on the rate of heat conduction. This conductivity depends on the thermal conductivity of the gas in the cell.
3. **Gas Chromatography**
   The two foregoing methods can only indicate the presence of hydrocarbon gases and give a very rough indication of the quantity. The gas chromatography is used to distinguish the various components (methane, ethane, propane) and to obtain a more accurate quantitative analysis. A sweep gas flows continuously through a small column, packed with an inert solid, coated with a non-volatile organic liquid.

At the inlet a small measured volume of the gas sample is injected into the sweep gas stream. The column separates the components by their different absorption characteristics. Methane is relatively insoluble in the column and passes quickly. The various components are identified by the length of time it takes to move through the column. These travel times can be determined for each component. The arrival times of the various components can then be determined by monitoring the passage of the individual components with a thermal conductivity cell at the exit of the separation column. The position of the peak in the time sequence identifies the compound and the area under the peak gives its quantity.

3.3 DRILLING SPEED AND CORING

3.3.1 PENETRATION RATE.

The penetration rate is based on the vertical movement of the Kelly or the swivel on top of the drill string. This movement is plotted as a function of time to produce a penetration log. Progress of the drill bit depends amongst others on the strength of the rock matrix and the porosity these rocks. Slow penetration is indicative for tight and hard rock, while fast penetration is obtained in soft, porous rock. A sonic log (porosity log), which is run later over the same interval, often correlates with the penetration rate. The effect of weight on bit, mud pressure, changing bits have to be taken into account, when the penetration rate is correlated with rock properties. An attempt to normalise the drilling parameters was made by the introduction of the "d" exponent. However like many geo-parameters the correlation often prove to be only valid for one field, one reservoir or even one layer.

3.3.2 CORING

All oil, coal, ground-water, mineral, and soil-mechanic logging activities have in common that log measurements have to be calibrated sooner or later with analyses results on formation samples. These rock samples are obtained by coring. The core is cut using a special hollow bit. The cylindrical core is usually split lengthways in at least two pieces. The first half is photographed in natural light for a detailed lithological description, and in ultra-violet light to detect residual oil. Small cylindrical samples are drilled from the other pieces and used to measure reservoir properties such as porosity, permeability and grain density. For proximate analysis of coal properties such as moisture and ash content larger samples are usually required. For soil mechanics undisturbed cores can often only be obtained in unconsolidated formations with a hollow probe. This probe penetrates the shallow subsurface like an apple bore.

3.3.3 CORING VIA THE DRILLSTRING

Two types of coring techniques are used with the drillstring. In the first, the standard in the oil industry, the hollow tube which receives the core remains in position during the coring operation. In the second the core barrel can be retrieved back to the surface, while the drillstring remains in the hole.

1. **Conventional Coring**
The coring assembly consists of the core head or bit and the core barrel. This technique utilises a hollow core bit which cuts the periphery of the hole while leaving a centre stub of rock. The barrel consists of two parts : the outer barrel for mechanical strength in the string and the inner light weight aluminium or fibreglass barrel to guide the core. This inner barrel does not rotate to avoid breakage and grinding of the core. Most common core diameters are 3 to 5 inch in diameter. The maximum length is 90 feet.

2. **Retrievable core barrel**
A disadvantage of the above coring method is that at least two additional round-trips are required. In the first all drill pipes are removed and unscrewed to get the core barrel to surface, the second to run a new barrel in the hole. The retrievable core barrel is similar to a conventional barrel with the exception that the inner barrel is connected to a wireline and can be run-in and pulled-out of the drillstring without tripping the drill pipes. It allows continuous coring over long intervals. Diameters range from 1½ to 3 inch. This method is particularly attractive for mining companies, because it is economic and provides immediately samples for proximate or ore grade analysis. It has been used by the mineral industry for several decades and was recently adapted to slim-hole drilling for the oil-industry. The risk of blow-out in the oil industry has hampered general acceptance.

3.3.4 SIDEWALL CORING & WIRELINE HARD ROCK CORING TOOLS

The side-wall sampler is an instrument run at the end of a logging cable. It can be positioned accurately by means of Spontaneous potential or Natural gamma-ray logging tools, that are run together with the sidewall sampler (see Chapters 8 and 9) . Hollow bullets (about 2 inches long and 1 inch diameter) are fired individually from the "gun" body by electrically ignited powder charges that are placed behind the bullets. The bullet cuts a cylindrical plug from the formation and remains attached to the gun by two heavy wires. After the sample has been cut, it is detached from the surrounding rock and recovered by an upward pull on the gun body. The standard gun carries 30 bullets.

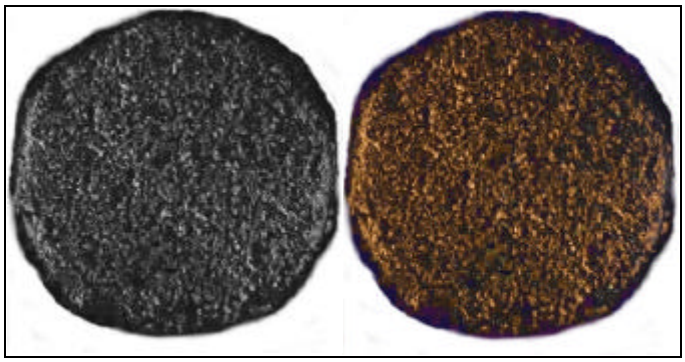

Photo 3. 1: Sidewall sample under microscope: left with plane light, right with fluorescing light (UV), giving a brown colour to the oil.

The method is widely applied to sample clays and shales for palynological analysis. It is also used for positive identification of oil in fresh water sands. A disadvantage when sampling soft formations is that the impact of the bullet tends to compact the formation and thereby distort the porosity and permeability. Rock properties such as grainsize and sorting can still be obtained from disturbed samples. In hard formations the recovery can be very poor, due too lack of penetration and adhesion between sample and bullet. In the late eighties a wireline tool was developed with a small hollow rotary drilling bit, which can take small (2 cm x 2.5 cm) plugs from the borehole wall. After the plug is drilled the bit is retracted and the samples removed from the bit by a punch. Up to 20 plugs can be individually drilled and stored in the tool. The main advantage of this tool is its ability to function well in hard formations where the conventional sidewall sampler often fails. Moreover, the plugs are usually little disturbed and the porosity and permeability analysis performed on these rock samples can be very reliable.

3.3.5 COMPARISON OF CORING METHODS

A rough comparison between the three types of formation samples that is made in Table 3.2. Figures on costs must be used as a guide only, they mostly depend on the drilling location and the well depth. Table 3.3. indicates the capability of the three types of formation sampling techniques to assess the reservoir parameters for the requirements listed in the first column of the table. Here the recovery is one of the important aspects. The core recovery is the percentage of the core that has been recovered. When the recovery is poor the continuous record is poor and the thickness depth control is poor. Most striking is the common inability to provide saturation data as illustrated in Figure 3.4. At the bottom of the well the mudfiltrate can flush a part of the oil and water that was originally present in the pores of the rock. The oil in-situ contains dissolved gas because the pressure is above the bubble point. During pulling of the core barrel to the surface the pressure and temperature decrease and gas will escape from the oil which will expand and finally flush oil and

	Cuttings	Cores	Sidewall samples
Size rock	1-3 mm	70-100 mm	40-25 mm
Length	collected ~ each meter	9-27 m	Up to 72 SWS/trip
Acquisition Cost	none	3000$/m	250$/sample
Accuracy in depth	lagtime, slippage	depends on recovery	good

Table 3. 2 : Comparison methods to obtain formation samples

ITEMS	Cuttings	Cores	Sidewall samples
DEPTH CONTROL	POOR	FAIR (*)	EXCELLENT
CONTINUOUS RECORD	YES	GOOD(*)	NO
THICKNESS	POOR	GOOD(*)	NO
POROSITY	INDICATION	GOOD	POOR
PERMEABILITY	INDICATION	GOOD	POOR
SATURATION	NO	NO	NO
TIME CONSUMED	NO	YES	YES
EXPENSIVE	NO	YES	YES
HOLE RISK	NO	POSSIBLE	POSSIBLE

Table 3. 3: Capabilities of the methods for obtaining formation samples

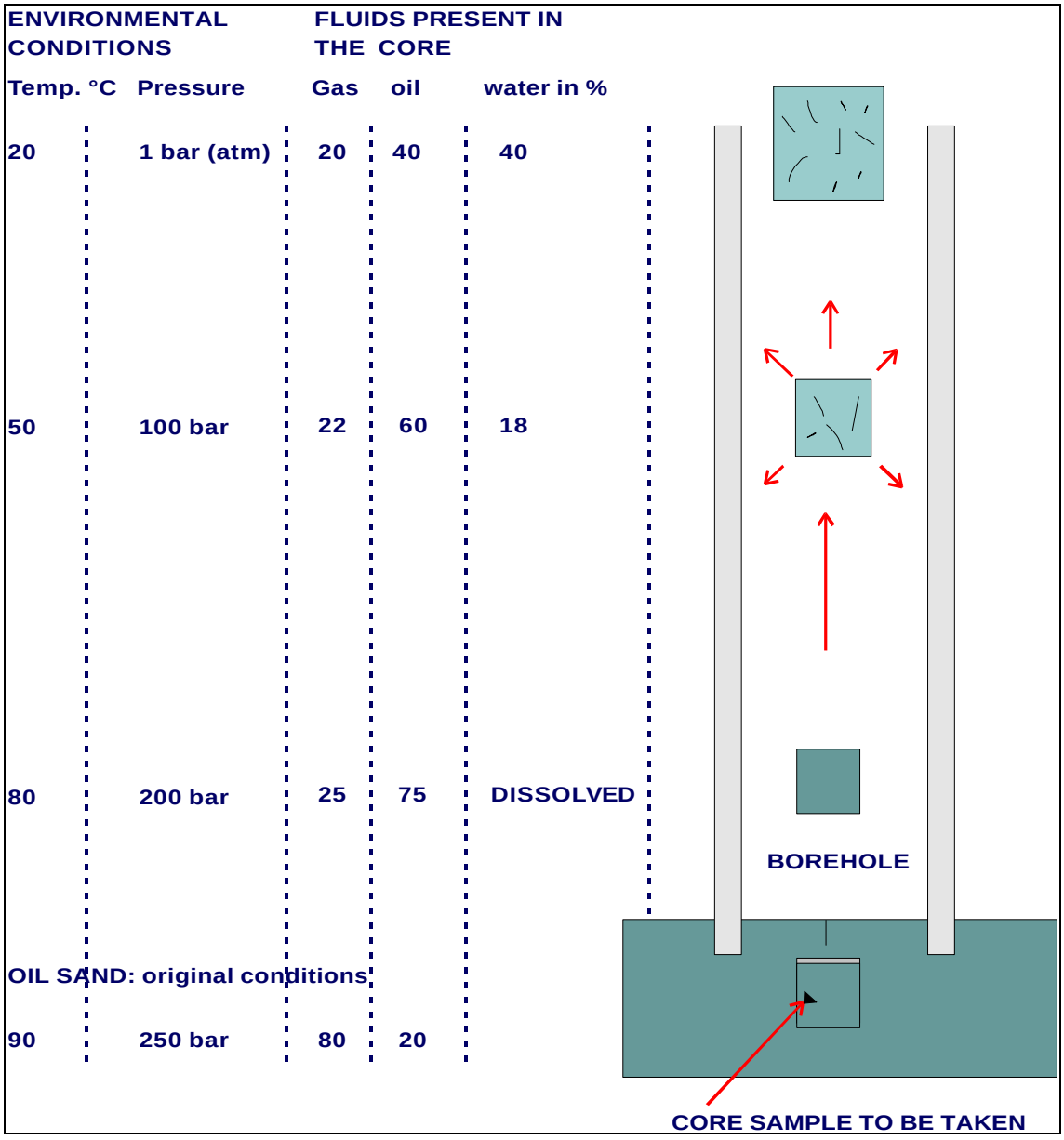

Figure 3. 4: The history of the core from in-situ conditions to atmospheric circumstances.

water from the pores. Hence the oil content at the surface is much lower than it originally was at in-situ conditions in the reservoir.

3.4 FORMATION FLUID TESTING

Information on the presence of hydrocarbons, their composition and ability to flow can be obtained by means of formation fluid testing. Three methods are available :

1. Drillstem testing
2. Production testing
3. Wireline formation testing

3.4.1 DRILLSTEM TESTING

This technique is applied with the drilling string augmented with hydraulic components. A valve, a packer and a length of perforated tail pipe is lowered on the end of drill pipe to the depth of the potential reservoir. The packer is expanded to fill the space between the borehole wall and the drill string, thus separating the test interval from the mud above. The drill string is only partly filled with fluid, hence when the valve is opened, the formation fluid pressure will be sufficient to produce reservoir fluids towards the surface. This technique is basically a temporary completion of the well.

3.4.2 PRODUCTION TESTING

This method is carried out in the cased hole, properly completed with a packer to isolate the reservoir interval that is tested, and with production tubing to conduct the fluid to the surface facilities. The casing opposite the reservoir interval is perforated using shaped explosive charges. If the test is positive, production may continue without any changes to the well design. This method is very reliable and accurate, and most of all safe and is therefore routinely applied in offshore exploration. It is also the most expensive technique from the point of view of elapsed time, material and manpower resources.

3.4.3 WIRELINE FORMATION TESTING

The third method of formation fluid testing is provided by wireline contractors. This technique inserts a nozzle surrounded by a rubber pad into the reservoir. After the pad is firmly pressed against the borehole wall the nozzle is opened and reservoir fluids can flow into a sample chamber in the tool (Fig.3.5). In the late eighties the modular formation tester (MDT) was introduced that contains several fluid sample chambers and up to three fluid entry ports.

- **RFT Capabilities**
  The Repeat Formation Tester tool (RFT) has been designed to measure the formation pressures and t collect reservoir fluid samples
- **MDT Capabilities**
  The modular formation tester can, as indicated by the name, be assembled from several parts. The most extensive version contains 3 sample chambers and three different pads that each contain an extendible nozzle to communicate hydraulically with the reservoir. The pads can be arranged to carry out interference tests, which give indications on vertical permeability. The MDT is equipped with infrared and conductivity cells in the flow lines, which can be used to detect the onset of oil production after the mudfiltrate has

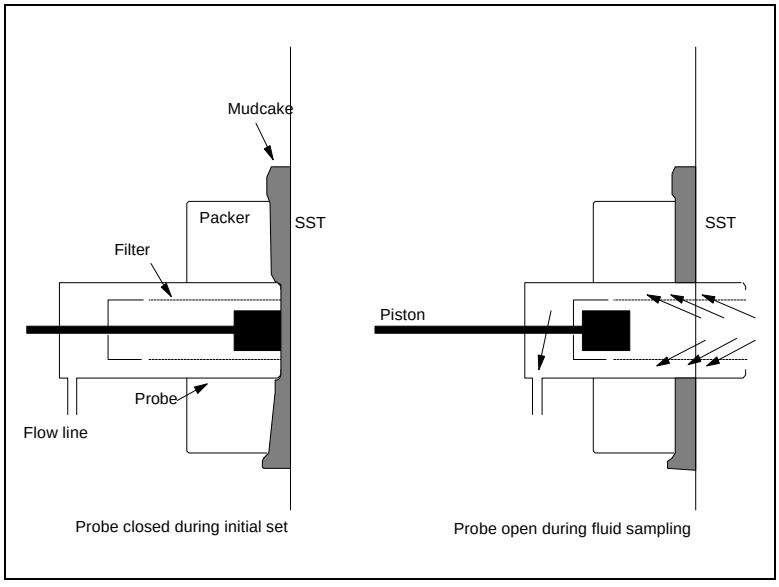

Figure 3. 5 : Operation of the RFT tester probe(revised after Schlumberger, 1984)

been removed. After switching of flow-lines a second chamber can then be filled with a virtually uncontaminated hydrocarbon sample. The contents of the sample chambers can be pumped out into the borehole, which gives the capability to take multiple fluid samples. A strain gauge pressure transducer located in the flow line monitors the pressure during the test. The application of the fluid and pressure data obtained with the wireline formation testers is further discussed during the course.

3.5 LABORATORY ANALYSIS METHODS

3.5.1 INTRODUCTION

Many information is already obtained during the drilling stage, both from the registration at the drill hole and from the cuttings. However, everyone, reservoir engineer, hydro-engineer, mining engineer, geologist and engineering geologist like to know more specific characteristics of profitable horizons on rock strength, porosity, permeability, mineral content, pore type, cementation, mineral weathering, fluid contents, etc. They want to put values obtained by microscope to implement in rock classification systems or to quantify engineering parameters for predictions.
A laboratory study has the following objectives:

- to identify the core damage from drilling and transport to the surface.
- to analyse the rock matrix: mineral content, texture and structure.
- to analyse the formation fluids still present and the penetrated drilling fluids.
- to analyse the basic physical properties, i.e. density, porosity and permeability.
- Indirect information on minerals & texture versus rock strength parameters.

Formation cores, samples of formation fluids and sometimes samples of the damaging material (organic deposit or scale) are required to perform a laboratory study. Various analyses are then performed on these samples to obtain the information necessary for designing a matrix treatment.

3.5.2 CORE ANALYSIS

Core analysis, including various flow tests, is an integral part of the laboratory study used to help design a matrix treatment, The various methods applied in the core analysis for the grain and pore characterisation are summarised in figure 3.6., and can be grouped as follows:

- Petrographic studies, including X-ray diffraction analysis, binocular lens observation, thin section examination under a polarising microscope and Scanning Electron Microscope observation.
- Petrophysics studies to determine the porosity and permeability of the sample.

Some widely used and novel techniques will be discussed in this section:

1. Microscopy,
2. Scanning Electron Microscopy (SEM and EDAX)
3. X-ray diffraction/X-ray fluorescence.
4. Image analysis as a quantitative tool

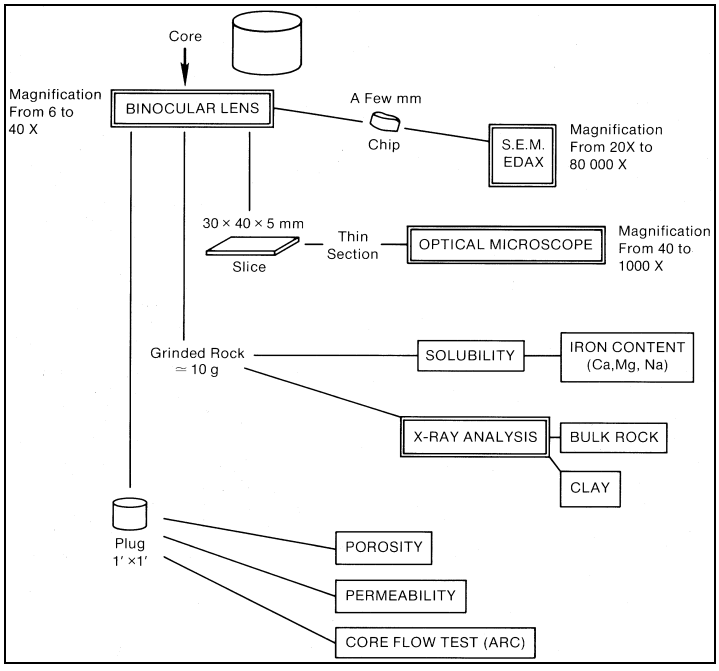

Figure 3. 6: Core analysis program, according to Dowel Schlumberger, 1986.

3.5.3 MICROSCOPY

Much is already explained in the first year and second year courses microscopy. Here we only summarise several methods that are used to define texture characteristics:

1. **Binocular microscope:**

Used for the analysis of cores and cuttings in grain size, sorting, and the larger sedimentary characteristics such as laminae, vugs, fracs, etc. Here geologists and hydrologist get an opportunity to define all textural parameters that are relevant for their specific questions on sedimentological maturity, weathering aspects and rock strength. Here some of the appearances, like grain size, mean, sorting, etc. can be defined in order to estimate a quick permeability, as defined in "de van Baaren-equation". This technique can be considered as a non-destructive technique. The sample is not damaged or prepared before or during the analyses.

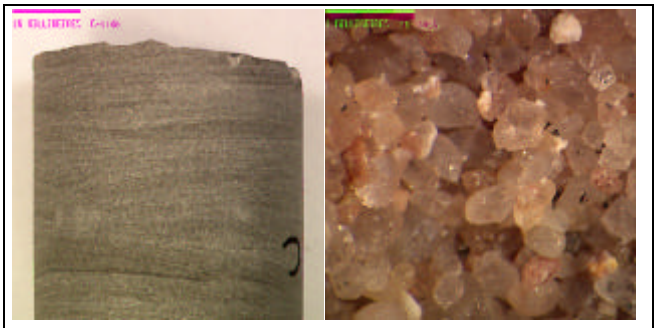

Photo 3. 2: Carboniferous cores and core surface of Bentheimer sandstone that can be described with the use of a binocular microscope.

2. **Polarisation microscopy:**

The original cores have to be damaged to prepare polished planes or thin sections. The rock can be filled with a special dye to define the pore space by straight colours (yellow, red, blue) or by fluorescence (yellow, green, red). Now many micro-textural aspects, such as grain-mineral content, 2-D pore sizes, grain shape, sorting, cementation, pressure solution, weathering, diagenetical features, grain damage, grain/porosity generation, can be studied to describe a rock history or burial history and to define the micro-values for geo-engineering purposes. The photos 3.3 show a good example of the different aspects, as mentioned before, that can be characterised. Note the presence of abundant nitre-particle porosity.

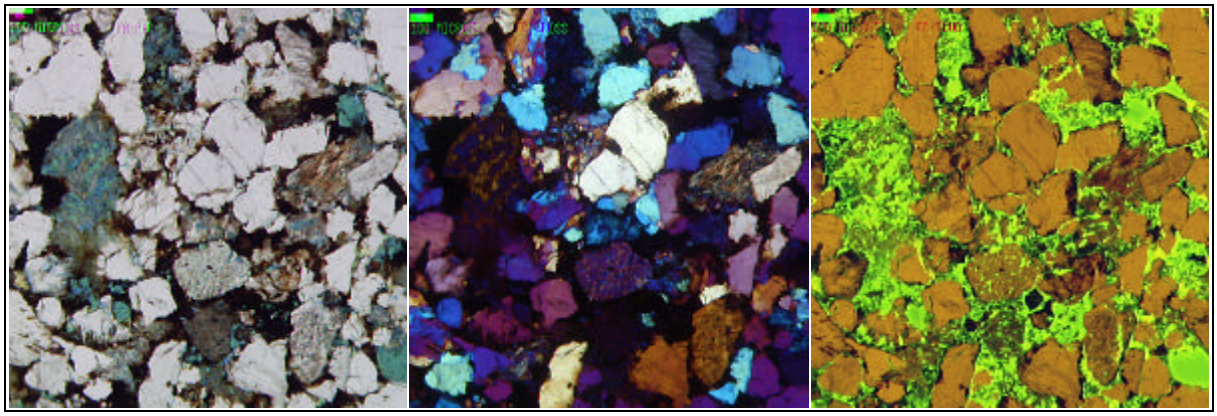

Photo 3. 3: Thin section of Felser sandstone: //-nicols, X-nicols and the fluorescing surface showing weathering (left), mineral content (middle) and pore space distribution (right).

3. **Scanning Electron Microscopy and Micro-probe.**

The basics of Electron Microscopy contain the use of an electron gun which produces a stream of electrons. This stream is accelerated at a voltage up to some 30 kV and bundled by some electromagnetic lenses. Then the bundle hits a rock specimen which reflects electrons; Back Scatter Electrons (BSE) and Low Energy Secondary Electrons (SE). Emission of electromagnetic radiation from the specimen produces visible light (cathode-luminiscensce) and X-rays. The BSE and SE are

caught in a scintillator. Here several main types are used:

A. SEM:

The photographic options, in which a pseudo 3-D image is constructed. At a size of less than 1 micro-meter it is possible to characterise textural aspects. This option only shows shapes and no chemical content (photo 3.4).

B. Micro-probe:

The photographic options, in which a 2-D image is constructed from a polished section. At high accuracies of less than 0.25 micro-meter, a reflecting electron bundle is detecting reflection densities. These densities are translated to grey-tones which give a map with density-differences of the present elements.

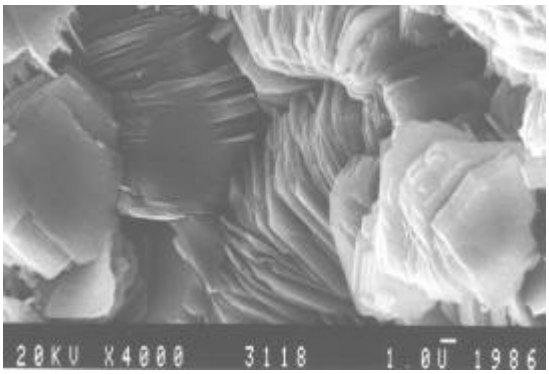

Photo 3. 4: S.E.M.-photograph of kaolinite; Whitby, Jurassic, Dogger hardground.

C: EDS:

An Energy Dispersive X-ray analysis system. Here spot analysis are made of areas of 1 square micrometer. The reflecting waves are giving a product of various wavelengths and amplitudes or intensities, which can be related to element specific wavelengths. In this way it is possible to analyse a certain spot on element distribution and quantity. When combined with option B, one can map large areas on the density of a specific element. For example Si, Al, Fe, Mn, Ti, Mg, Ca, Na, K as the main elements of sedimentary rocks (photo 3.5).

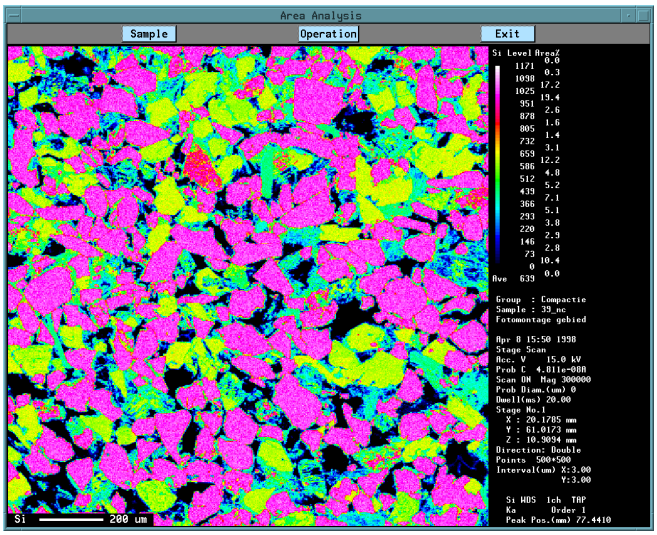

Photo 3. 5: Microprobe scan on the Si-component of a Jurassic reservoir. Dark colours quartz, lighter colours feldspar, clays, etc.

4. **X-ray diffraction** (XRD):

This method is commonly used to get a whole rock analysis of the matrix minerals, as found in regular cores. A Röntgen X-ray tube provides radiation , and preferably monochromatic radiation, that is sent to a sample consisting fine powdered matrix mineral matter. For this radiation preferably Kα,β radiation is used. The X-ray beams meet the powdered sample, creating a reflective radiation due to collision at the different mineral planes. At specific angles a detector counts the reflecting electron, which results in the registration of an angle and the intensity. According to Braggs' law a whole number (n) of wavelengths (λ) represents the distance in a crystal lattice (d), at specific refraction angles (α) or: $n.\lambda = 2d.\sin(\alpha)$. The output from the detector is a film that shows the angles (α) and peeks at a specific wavelength (λ). Now the d can be used to define the different mineral/crystal types. In this destructive way the qualitative and semi-quantitative mineral content of a matrix can be defined. Unfortunately the samples have to be destroyed.

5. **X-ray fluorescence** (XRF):

This method is used to define the bulk element weight percentage of the present elements. It has more or less the same background of operation as the micro-probe. However, this method is very destructive. The sample is powdered and fused with a borate to a homogeneous and isotropic glass pellet. This method gives the best bulk element analysis and is used for igneous rock, metamorphic rock and sedimentary rocks.

3.5.4 AN INTRODUCTION TO IMAGE ANALYSIS AS A QUANTITATIVE TOOL

Preface

Quantitative Image Analysis is a technique used already for many years in:

- astronomy and space travel, for processing and enhancement of satellite and radio telescope images from space
- industry, for control of production processes and quality control of products
- administration, for recognition of handwriting
- science, for visualization and measurements of experiments

The aim of Quantitative Image Analysis is generally spoken the processing and eventually enhancement of images with the use of a computer and the measurement of properties in these images.

The **enhancement** is necessary to suppress or put emphasis on certain properties. It is used to make an image more easily readable or measurable, to recognize patterns or to reconstruct unreadable images.

Measurement of many object parameters are possible, to name: area, length, brightness, shape. Visual properties are in this way changed to numerical values.

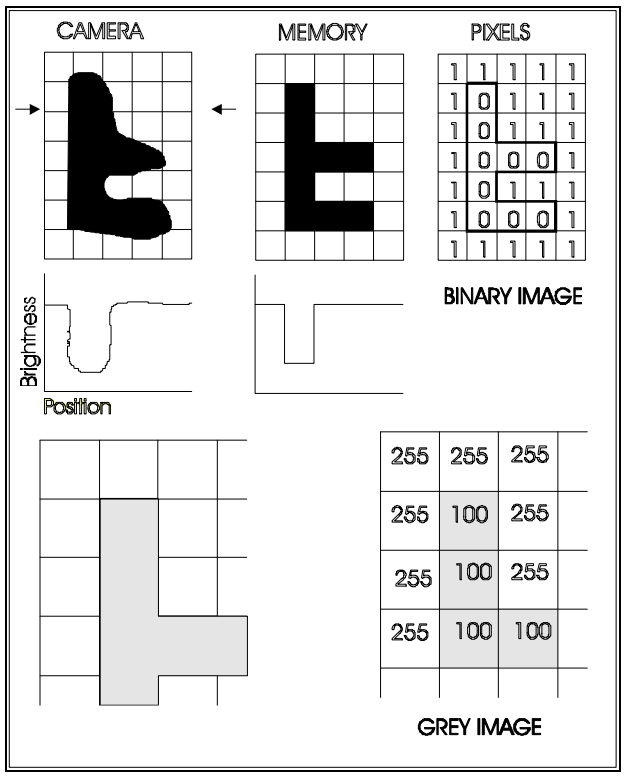

Figure 3. 7: Visualization of the concepts of a binary image and a grey image.

Methods of image acquisition

An image is acquired with the use of a videocamera. In the camera, changes in optical brightness are transformed to analog electrical signal fluctuations. But a computer can only handle two different states: high (5 V) or low (0 V) or - in an other way - 1 and 0 (digits). That is why it is necessary to transform images to a digital format before they can be processed in a computer. This is called *digitizing* - the image is divided into single picture elements (*pixels*). The brightness (*greylevel*) of each pixel is stored as a code of 8 zeros and ones (8 *bits* = 1 *byte*). In one byte of information 256 grey-levels are stored, from

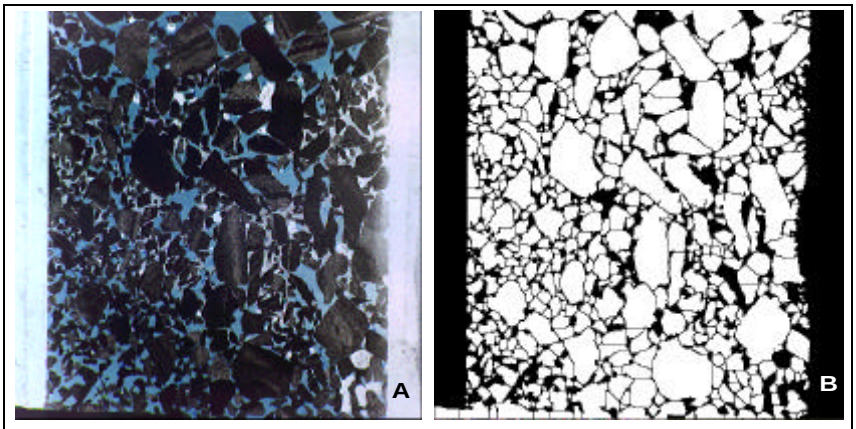

Photo 3. 6: fig.A. shows a color digitized thin section with the black parts as the grains and the remainder as pore space. Figure B. shows a binary image after detection of the grains (white, pixel value 1) and pores (black, pixel value 0). The grains are automatically separated for detection puroses.

00000000 = black, to 11111111 = white. Hence, a digitized image consists of a matrix of pixels each with a code for its individual brightness.

To digitize a colour representation, (photo 3.6) a possibility is to split the picture into three images, each representing the relative amount of red, green and blue (*RGB format*) in the original image. So the colour information of a single pixel is stored in 3x8 = 24 bits. After digitizing, an image is in fact a file that can be processed and stored in a computer. An image analysis system like *Quantimet* (a dedicated computer system) or *Qwin* (a program that can be run on a PC under Windows) can handle the file for processing and measurement. Here, a colour image of 512x512 pixels (each image in the posters) will be stored as a file with a size of 512x512x24 = 6291456 bits or 6291456/8 = 786432 bytes.

Image processsing

Changes in the image can be performed by replacing each pixel value with another, say 2 times the original value = 2 times brighter. This is called *pointprocessing*. An other option is making the new value depending on the values of the surrounding pixels: *neighbourhood processing* (figure 3.8,3.9) This is a very sophisticated and powerful technique used in two important image processing applications:

- *Mathematical Morphology*
  There is a relatively simple mathematical relation between the processed and the surrounding pixels. The processing speed is high and can be controlled well. Basic processes are *erosion* and *dilation*. In erosion the pixel value is decreased and in dilation increased according to that of the neighbors.

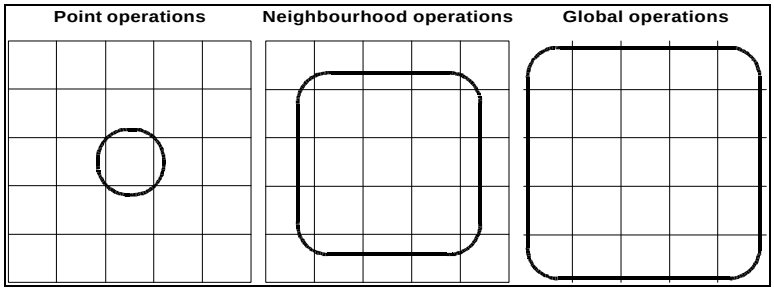

Figure 3. 8: Three kinds of mathematical operations that can be applied to pixelvalues.

- *Convolution*
  There is a more complex mathematical relation between the processed and the surrounding pixels. This technique is often applied in the enhancement of fuzzy (unfocussed) images and in geophysical signal processing methods like Laplace and Gauss filters (figure 3.9)

Also the whole picture can be considered as a set of data. In *Fourier Analysis* this set is processed as a whole, filtered and 'translated' backwards. Using this technique certain signal frequencies in the set can be located and suppressed or intensified (*highpass* and *lowpass* filters). Applications for suppressing image noise and interference jam.

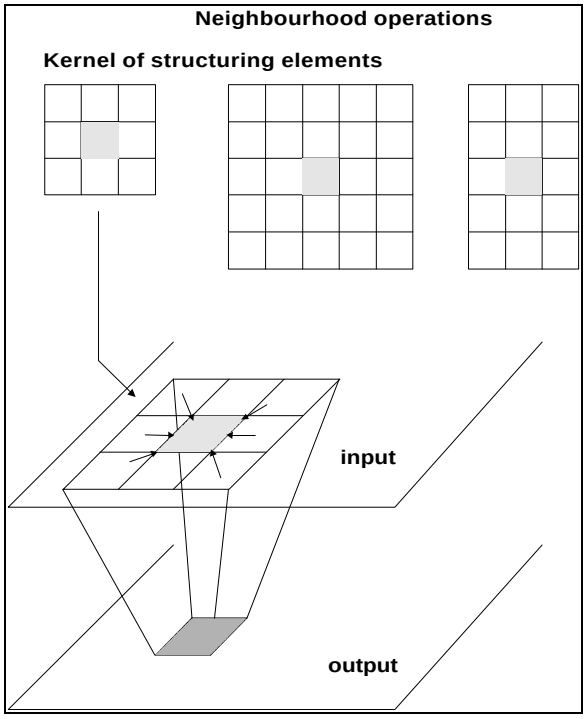

Figure 3. 9: Visualization of an operation on a pixel value and its neigbours, as discussed.

Image Analysis

Image properties can be analyzed at two levels:

- ***Grey level***
  Grey values are measured directly in the original image.
- ***Binary level***
  In the grey image, pixels within a certain

brightness range are '*detected*' and stored in a separate image. This subimage is called *binary* because each pixel in this image satisfies the brightness criterion (=1) or not (=0). So the image consists only of pixels with values 0 or 1. Also this image can be processed in the usual way.

3.5.5 IMAGE ANALYSIS APPLICATIONS FOR STUDENTS DURING THEIR STUDY

- ***Geophysics***: Image improvement in seismics, Ground Penetrating Radar
- ***Engineering Geology***: Satellite images, surface geology, groundwater, rock engineering characteristics
- ***Reservoir Engineering***: porosity/permeability relations, rock engineering characteristics
- ***Raw Material Section***: ore or material distribution, liberation analysis
- ***Mining Engineering***:Coal vitrinite/ore – reflectometry, fracture analysis
- ***Petroleum Geology***: Mineralogy, petrography, reservoir characteristics.

3.6 WELL LOGGING

As discussed in the introductory chapter, well logs are records of physical properties as a function of depth. Many physical phenomena can nowadays be measured in the borehole ranging from simple spontaneous electric potentials, obtained with only one electrode, to gamma-ray spectrometers, which require the equivalent of a Pentium PC to be incorporated in the tools, to cope with the huge amount of data. The electronics is able to operate at temperatures up to 200 °C and pressures as high as 1,500 bar, but still fits into sondes with a diameter of only 3 5/8" or 92 mm. One can measure on the formations after drilling; open hole logging or cased hole logging, or during drilling, called measure while drilling.

3.6.1 OPEN HOLE LOGGING

In the oil industry a standard cable for open hole logging consists of 7 insulated conductors inside flexible steel armour. Its diameter is about 0.5 inch. A mono-conductor is normally used for logging in cased holes, where both the tools and the cables have a smaller diameter (1 11/16"or 43 mm) to pass through the production tubing. The data transmission rate of the cables is limited to 200 - 500 Kbytes, which imposes restrictions on the spectrometer and imaging tools due to the very high data rates. For mineral and ground-water logging both open and cased hole logging is almost exclusively carried out with small diameter, so called slimline tools (1 11/16", 43 mm). The reason is that most exploration wells in these industries have a diameter of less than 5" in which tools with the standard oil industry size of 3 5/8" (92 mm) cannot be run. The same counts for conventional mining. In these cases the tools are used sub-surface in long walls and tunnels for (sub) horizontal laterals exploration. It is clear that in narrow spaces bulky and weighty equipment is preferably avoided.

3.6.2 MEASUREMENTS WHILE DRILLING (LOGGING WHILE DRILLING)

Till the seventies measurements with instruments that were embedded into the drillpipes were limited to weight on the bit with strain-gauges, and directional data with magnetic devices. These two were later augmented with a simple geiger-müller gamma-ray counter. The need to measure resistivity, density and neutron porosity during drilling became acute when highly deviated and horizontal wells were drilled in large numbers. In these wells it is usually very difficult and often impossible to run wireline tools into the hole, due to the lack of the pull of gravity. Running tools at the end of the drillpipe is a costly, time consuming and often unsafe. Measurement while drilling (MWD) was therefore an attractive alternative. During the eighties equivalent MWD versions of the gamma-gamma density; the neutron scattering porosity; and simple lateral resistivity wireline tools were developed, which could be inserted in recesses in the drill pipes. Moreover new tools like the electromagnetic wave propagation resistivity, and bit resistivity tools were developed that have no wireline equivalent. The instruments are either powered by a generator connected to the mud-motor,

or by batteries. The measurements are either stored in a memory downhole or transmitted via pressure pulses in the mud to the surface. The most advanced instruments use sensors placed on or immediately behind the bit, and EM signals are used to bypass the mud motor. The receivers above the mud motor convert the EM signals to mud pulses which are transmitted through the mud to the surface.

4. A: PORE SPACE AND PORE FILLING

GENERAL INTRODUCTION

4.1. POROSITY

- 4.1.1. Historical Aspects
- 4.1.2. Porosity Definition
- 4.1.3. Porosity values and spatial characteristics
  - 4.1.3.1. Spatial conditions of the grain shape and packing
  - 4.1.3.2. Grain size uniformity
  - 4.1.3.3.Consolidation and cementation
  - 4.1.3.4. Pore space reduction during and after deposition
  - 4.1.3.5. Grain size - pore size relation
  - 4.1.3.6.Dual porosity
- 4.1.4. POROSITY CLASSIFICATION OF Carbonates BY Archie, 1952
- 4.1.5. Laboratory analyses of porosity
  - 4.1.5.1. The wet and dry weight method
  - 4.1.5.2. Boyle's law porosimeter
  - 4.1.5.3. The total porosity measurement
- 4.1.6. Core - log correlation

4.2. PERMEABILITY

- 4.2.1. General definition of permeability
- 4.2.2. Flow in a tube (Poiseuille)
- 4.2.3. permeability measured on core samples
- 4.2.4. Correction for a flowing medium in laboratory measurements
- 4.2.5. Correction for gas slippage
- 4.2.6. Correction for turbulence
- 4.2.7. Permeability related to texture properties
- 4.2.8. Relation between pore space and permeability
- 4.2.9. Empirical relations
- 4.2.10. Permeability from logs
  - 4.2.10.1 Introduction
  - 4.2.10.2. Permeability as a function of porosity
  - 4.2.10.3. Permeability by porosity and irreducible water saturation in reservoirs and contaminated sands

GENERAL INTRODUCTION

Porous media as a source of fluids and vapours like water, oil, gas or as a depot for the storage or disposal of fluids or other materials is getting more and more attention. To describe the state of the pore content, it is necessary to specify the spatial characteristics of the pore space and the pressure, the composition and the energy contained in the pore filling material. To estimate the flow in porous media, in time and space, certain parameters must be specified. For flow considerations, the primary parameters are porosity and permeability. For the vertical dimensions of fluid zones the capillary pressures are of importance. The purpose of this chapter is to present data on these factors, combined with geological and reservoir technical relations.

4.1. POROSITY

4.1.1. HISTORICAL ASPECTS

Theoretical points of view of the transit of ground water in porous media went ahead of the developments in reservoir engineering, as needed in the oil industry. Slichter [1899] already showed that the porosity of uniformly sized spheres varied from about 47% for the cubic packing to a minimum of 26% for the rhomboedrical packing. However naturally occurring grain aggregates are heterogeneous and their measured porosities are above and below these limits. Fraser [1935] considered the following factors and their relative importance in determining the porosity of unconsolidated natural deposits:

- Absolute grain size
- Grain size distribution
- Sorting
- Grain shape
- Way of deposition
- Degree of compaction
- Consolidation

His work has been used for many attempts to create porosity relations. Slichter defined porosity simply as *"The percentage of open space to the whole space"* or "*as "that part of the rock where no matrix material is present"*. Later on the effective porosity was defined as *"the amount of interconnected pore space available for fluid transmission, expressed as a percentage of the total volume"*. In our professions can be stated that *"The effective porosity is the fraction of the total rock volume, which is filled with water, gas, or oil"*. The material of a porous rock may range from very loose unconsolidated sand to a very hard, dense sandstone, limestone or dolomite. Sand grains and particles of carbonate materials, that make up sandstone and limestone reservoirs, usually never fit together perfectly due to the high degree of irregularity in shape. The cement that fills the pores and binds the grains together may consist of silica, calcite or clay. This mixture of matrix material, cement, and pore filling clays create a large range of porosity values and porosity types.

4.1.2. POROSITY DEFINITION

The porosity is the amount of pore space expressed as a fraction of the total volume.

$$f = \frac{V_b - V_{ma}}{V_b} \cdots or, \qquad f = \frac{V_p}{V_b} \cdots or, \qquad f = \frac{V_p}{V_{ma} + V_p} \qquad \text{(eq. 4.1,2 and 3)}$$

where: j : porosity V_p : pore volume V_b : bulk volume, V_{ma} : matrix volume

4.1.3. POROSITY VALUES AND SPATIAL CHARACTERISTICS

Porosity may range from 80 % in volcanic tuffs or 60% as found in diatomites in the Monterey formation in California - which do not, or hardly, produce any fluid - to a porosity value of 1% in fractured carbonate formations (Middle East). Here one well occasionally produces more oil than all productive oil wells in The Netherlands (on-shore). The factors governing the magnitude of porosity in clastic sediments are:

1. Spatial conditions of the grain shape and packing,
2. Grain size uniformity,
3. Consolidation and cementation
4. Pore space reduction during and after deposition
5. Grain size – pore size relation
6. Dual porosity.

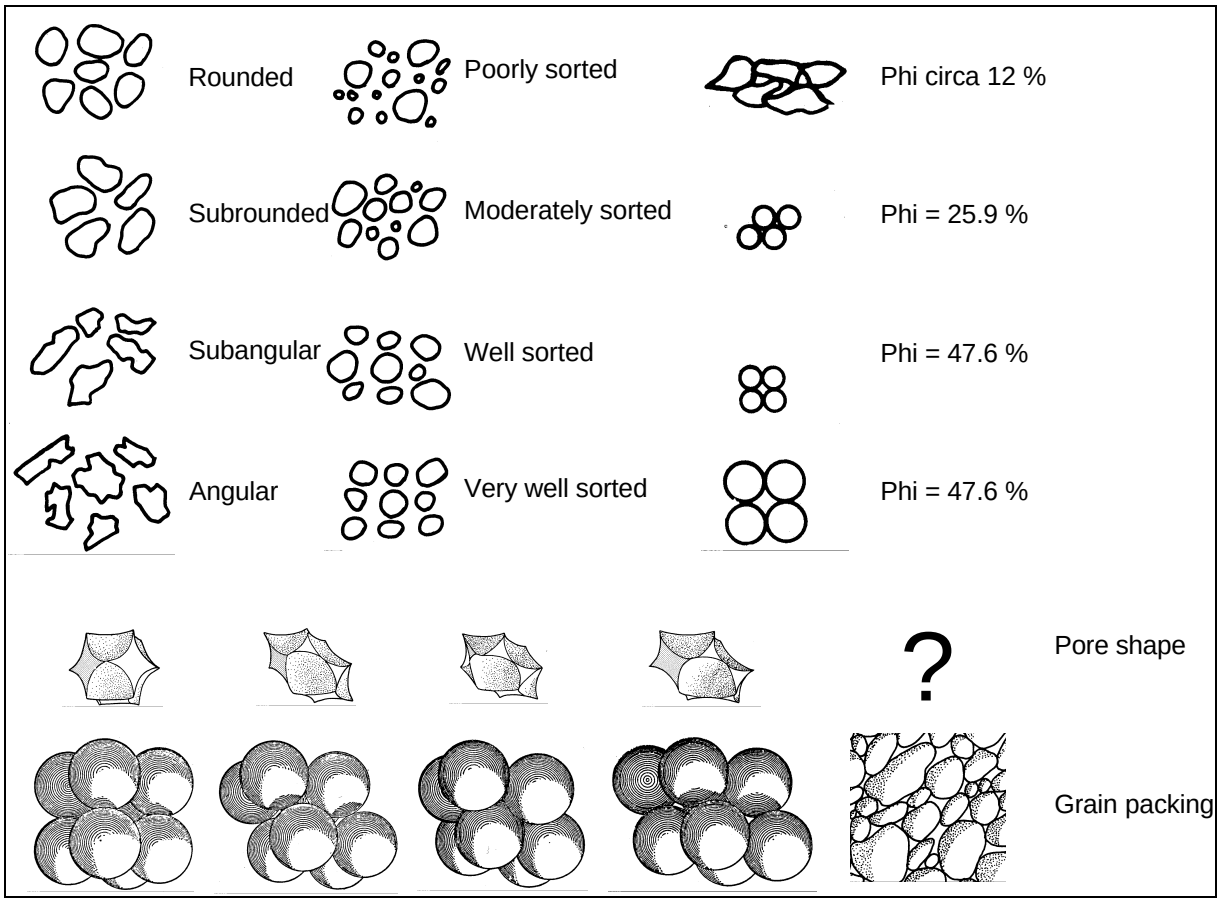

Figure 4.1:Grain shapes and grain packing as major spatial characteristics for the amount of pore space.

4.1.3.1. SPATIAL CONDITIONS OF THE GRAIN SHAPE AND PACKING

The arrangement of uniform spheres already shows that different packing create different porosities. A cubic, or wide-packed system, has a porosity of 47.6%, orthorhombic 39.5% porosity, a rhombohedral, or close-packed system, 25.9% and tetragonal a porosity of 30.2%.

Cubic packing is formed when the centres of spheres in the second square layer projected on the plane of the first layer coincide with the centres of the first layer. Orthorhombic packing is formed when the centres of spheres in the second square layer are in line with those of the first layer but are offset by a distance equal to radius R. Rhombohedral packing is formed when the centres of spheres in the second square layer are offset by half the distance between centres of diagonal spheres in the first layer. Tetragonal packing is formed when the centres of spheres in a second rhombic layer are in line with those of the first rhombic layer but are offset by a distance equal to radius R. When all spheres are

identical the porosity is only a function of the packing and independent of the sphere size. *Note that the porosity for such a system is independent of the sphere diameter*. Though, in case of a mixture of smaller spheres among larger spheres, the ratio of pore space to the solid framework becomes lower and porosity reduces. The porosities of reservoirs range from < 5 % to > 40 %. Normally the porosity values are in between 10 - 20 volume percent.

4.1.3.2. : GRAIN SIZE UNIFORMITY

Uniformity or sorting is the gradation of grain sizes in a collection of grains. For example; when silt or clay particles are mixed with sand, the intercommunicating porosity will be notably reduced (fig. 4.1). Sorting depends on four significant factors:

1. size range of the grains,
2. kind of deposition,
3. nature of the transporting current, and
4. the time span of the sedimentary process.,

There are many definitions for sorting of which the Trask sorting is the most commonly used. This parameter makes use of the cumulative weight percentage in a sieve analysis and is defined as:

$$S_0 = \sqrt{\frac{S_{25}}{S_{75}}} \qquad \text{(eq. 4.4)}$$

S_{25} is the grain size at 25% cumulative weight percentage. This means that 75% of the weight of the rock has larger sizes than this 25% grain size value. S_{75} as the grain size at 75% cumulative weight percent. This is also illustrated in the figures 4.2. and 4.3.

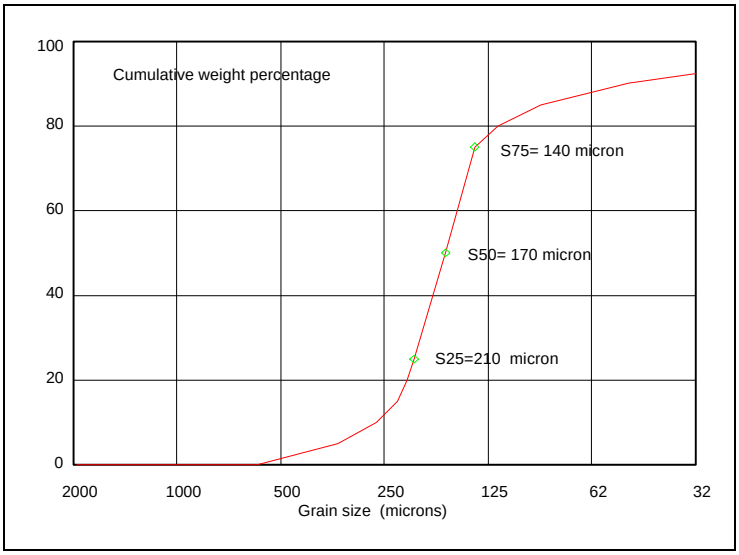

Figure 4.2: Grain size distribution with a Trask sorting of So=1.22

unconsolidated sands	35 - 45 %
more consolidated sandstone	20 - 35 %
tight/well cemented sandstone	10 - 20 %
limestone (e.g. Middle East)	5 - 20 %
dolomite (e.g. Middle East)	5 - 20 %
chalk (e.g. North Sea)	5 - 20 %

Table 4.1: Wentworth system for grain size analysis of siliciclastics

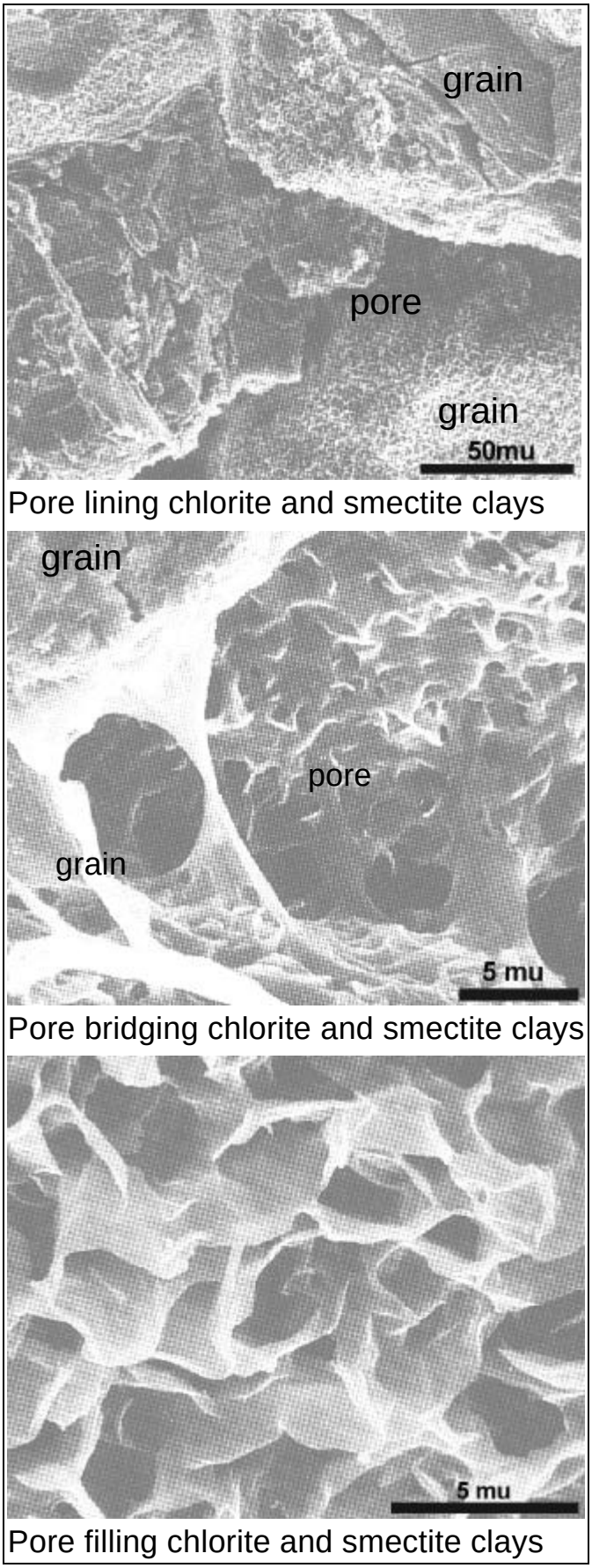

Photo 4.1: Clay minerals filling pore space during diagenesis.

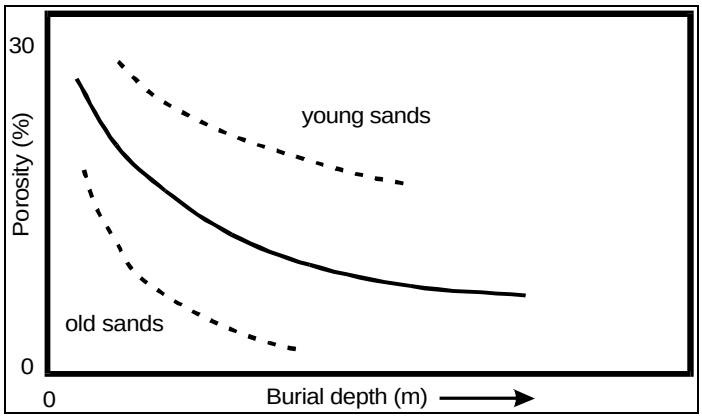

Figure 4.4: Porosity reduction as a function of depth.

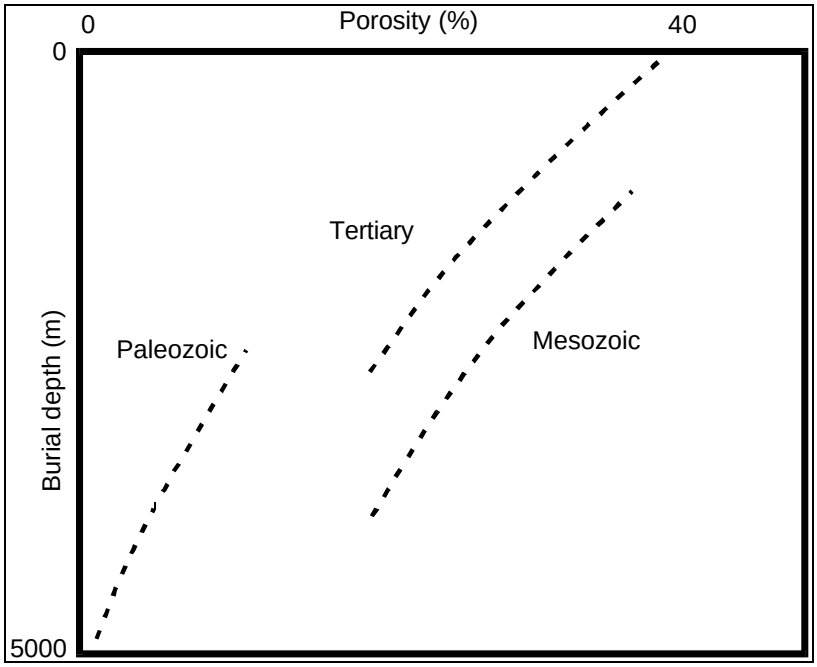

Figure 4.5: Porosity reduction with depth of different generations of porous rock.

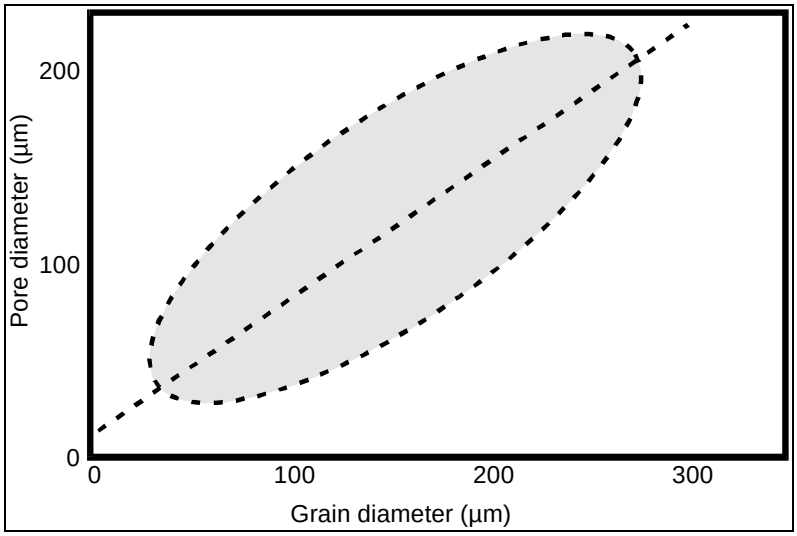

Figure 4.6: Relation between grain size and size of pore diameter.

4.1.3.3. CONSOLIDATION AND CEMENTATION

Unconsolidated rocks or fresh sediments do have high porosities, while cemented sandstones usually do have very low porosities. Cementation occurs during lithification and due to alterations by groundwater. Then pores are filled with minerals. The major present cementing materials are: calcium-, magnesium-, and iron carbonates, iron sulphides, limonite, hematite, dolomite, calcium sulphate and clay minerals. As an example we show Scanning Electron Microphotographs of secondary clays, grown during diagenesis (photo 4.1: a, b and c)

4.1.3.4. PORE SPACE REDUCTION DURING AND AFTER DEPOSITION

Compaction squeezes fluid out of pores and brings the grains closer to each other, closing pore space. In particular the finer-grained sedimentary rocks are subject to this phenomenon. Compaction is a major lithifying process in claystones, shales, and fine-grained carbonate rocks. However, in packed sandstones or conglomerates it is neglectible. As shown in the figures 4.4 and 4.5, porosity is lower in deeper, older rocks, but exceptions to this basic trend are known. With an increasing overburden pressure, poorly sorted angular sand grains show a progressive change from random packing to a closer packing. Some crushing and plastic deformation of the sand particles is a part of the process.

Category	Median grain size in µm
GRAVEL	2000
VERY COARSE	1000
COARSE	500
MEDIUM	250
FINE	125
VERY FINE	62
COARSE SILT	16
FINE SILT	8

Table 4. 2: average porosities of several porous rock types

4.1.3.5. GRAIN SIZE - PORE SIZE RELATION

It is already mentioned that reduction of grain size normally indicates a reduction in pore size. This is shown in figure 4.6: Pore size increases with grain diameter and the grain size appears to be bigger than the pore size. For this reason the grain size distribution for siliclastics, as defined by Wentworth (table 4.1 and 4.2), also gives an indication on the maximum pore sizes.

4.1.3.6. DUAL POROSITY

The heterogeneity of grain compositions also produces heterogeneity in pore sizes. This distribution of pore sizes can be random or uniform. Hence a zonation of different pore size areas is not possible. However, in case of layering/lamination or grouping, different areas with different pore spaces are defined. Here we speak of a dual porosity system. Examples are:

- Turbidites with a stratification of coarse and fine grains.
- Coal with highly large porous cleats and fractures and a very fine porous matrix of coal macerals.

4.1.4. POROSITY CLASSIFICATION OF CARBONATES BY ARCHIE, 1952

In carbonates there are several basic porosity types such as oolitic, vuggy, fracture or intercrystalline porosity. The Archie system divides carbonates in a descriptive way (table 4.3). The classification consists of two parts:

1. The texture of the matrix. This fulfils in part the lithological description and also gives information on the minute pore structure between the crystals, granules or fossils.
2. The character of the visible pore structure. A skeleton classification with symbols is used and co-ordinated with petrophysical data.

Example: A carbonate rock of type III F-B is defined as a finely sucrosic carbonate with matrix porosity Φ_{ma} of 10%, visible porosity about 10% with pores smaller than 0.1 mm, resulting in a total porosity Φ_{total} of 20%.

Class	Crystal size	Top val. size (μ)	Appearance	ϕ_{ma} (%)	*Visible porosity* *Size of pores in (mm)*			ϕ_{total}
				A	B <0.1	C 0.1-2.0	D >2.0	
I	Course	1000	Resinous	2	e.g. 10	e.g.15		27
Compact	Medium	500						
Cryst.	Fine	250						
	Very Fine	125	to					
	XF	62						
	SL	20						
	Li	4	vitreous	5	e.g.10	e.g.15		30
II	SL	20	Chalky	15	e.g.10	e.g.15		40
Chalky	Li	4						
III	C	1000	Coarsely	5				
Sucrosic	M	500	sucrosic to	10	10			20
Granular	F	250	extremely					
	VF	125	fine	10	e.g.10	e.g.15		35

Table 4.3: Modified Archie classification for porosity in carbonate rocks.

Another classification, which includes the aspects of matrix/porosity relations, is the Dunham Classification. It will be discussed during the courses and practical work of applied sedimentology.

4.1.5. LABORATORY ANALYSES OF POROSITY

The laboratory porosity determination on a number of core samples is used as the basis for calibration of all kinds of field porosity measuring tools. Care must be taken to choose representative samples, because the samples have small volumes (10^{-4} m^3) when compared to the volume of a m^3 surveyed by measurement tools (density , neutron, sonic). The investigated volume of a porosity-logging tool is normally circa 1,000 times larger than the volume of a core plug.
Depending on the type of material several porosity measurements are possible. In chapter 2 several measurements are already discussed for the determination of the bulk density and matrix density. The most important measurement methods for porosity are:

1. Water absorption: a number of methods are known to fill the pore space with a liquid of known density.
2. Absorption of an organic liquid in a vacuum
3. Determination of the volume of natural present water, for example by heating and weighting.
4. Injection of mercury at high pressures into sample pores. Here pore size distribution also can be determined.
5. The Buoyancy method, based on Archimedes' principle. It requires the saturated weight of a porous sample in air and the weight of the sample suspended in a liquid of known density.

In this chapter three methods will be reviewed:

1. The wet and dry weight method
2. Boyle's law porosimeter, and
3. The total porosity measurement

4.1.5.1. THE WET AND DRY WEIGHT METHOD

The sample is extracted with a solvent and dried. The bulk volume V_b is then obtained by a direct measurement of the dimensions or by measuring the displaced volume of a non-penetrating fluid such as mercury. The grain volume V_{gr} can be determined by measuring the weight W_1 of the dry core

sample. Thereafter it is saturated with a wetting liquid with density ρ_{fl} and the submersed weight W_2 is measured:

$$V_{pore} = \frac{W_2 - W_1}{r_{fl}} \qquad \text{(eq. 4.5)}$$

Then the porosity φ can be calculated from V_b and V_{gr}.

$$f = \frac{V_b - V_{gr}}{V_b} \qquad \text{(eq.4.6)}$$

4.1.5.2. BOYLE'S LAW POROSIMETER

The porosimeter is already discussed in chapter two. There three figures and relations are extensively explained.

4.1.5.3. THE TOTAL POROSITY MEASUREMENT

The bulk volume V_b is determined by submerging the sample in mercury as previously described. Then the sample is crushed to decompose it into the individual grains. The matrix volume V_{ma} is determined by utilising a compression chamber or by liquid displacement. The advantage of this method is that all pore spaces are taken into account including the isolated pores that are not connected to the pore network.

4.1.6. CORE - LOG CORRELATIONS

For groundwater measurements, the recognition of water, oil and gas and humidity of coal, standard core measurements are performed to get their porosity, permeability and grain density. The porosity can be plotted on a depth scale and correlated with porosity logs, such as the density, neutron or sonic log. In order to obtain a good correlation several criteria can be used :

1. Compare the logger's depth with the driller's depth as indicated on the log heading. When the bottom of the casing is found at the same depth a shift is probably not needed.
2. Observe the core recovery. When 100% core is recovered the core can be shifted as one unit. For smaller recoveries it is often possible to shift each core section separately within a range indicated by the non recovered section.
3. Clear lithology breaks in the core and on the log give often a good depth calibration point.
4. A gas-oil, oil-water or water-air contact observed in the core can be correlated with the log contacts.

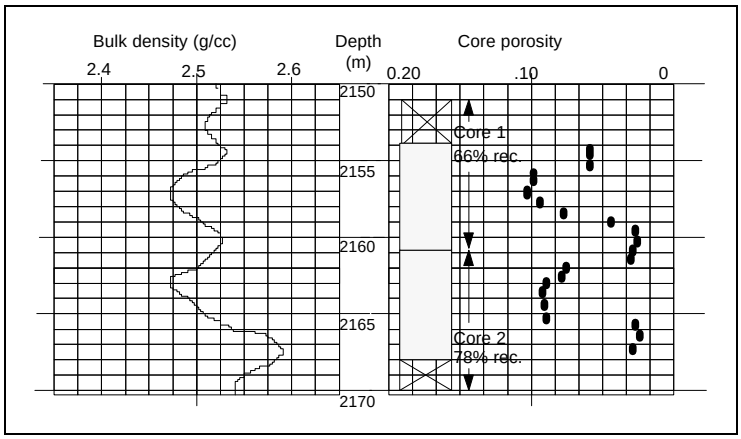

Figure 4.7: Density - core porosity correlation

4.2. PERMEABILITY

4.2.1. GENERAL DEFINITION OF PERMEABILITY

A rock that is used for the injection of production of water, oil or gas needs to have the ability to transport the substance through the connected pores. Or, in general terms, one needs to know the flow rate of flow of a fluid through a system consisting of porous media, tubes, etc.. It is dependent upon two basic properties:

- the fluid potential gradients, and
- the resistance to the flow of that fluid along the pathway traversed.

In terms of electric conductivity of a material it is called the ratio of the electric current and the electric potential. In the hydraulic equivalent the electric potential is replaced by the pressure drop ΔP and the electric current by the fluid flow Q. Ergo the calculable "constant" that integrates the "resistance" factors for porous media is named "permeability". In other words, the permeability is a measure of the relative ease with which a porous medium can transit a liquid or gas under a potential gradient. It is a property of the medium alone and is independent of the nature of the pore filling matter and of the force field (pressure gradient) causing movement. It is also a property of the medium that is dependent upon the shape and size of the pores. Consequently, permeability is influenced by grain size, shape, sorting, packing, degree of consolidation and cementation.

Porous rock can have two types of permeability:

- primary permeability, or the matrix permeability which is created during deposition and lithification of the sediment to rocks.
- secondary permeability is created during the alteration of the rock by compaction, fracturing solution, and cementation.

Compaction and cementation normally reduce the permeability, fracturing and solution normally increase it. When fresh water is present in a clay rich porous rock, several clay minerals like smectites and montmorillonites do swell and may cause a complete close off of pore space.

4.2.2. FLOW IN TUBE (POISEUILLE)

Hagen in 1839 and Poiseuille in 1846 worked on the laws affecting the flow of water through capillary tubes. The latter defined for a flow through a cylindrical tube Poiseuille's law :

$$Q = \frac{p \cdot r^4 \cdot \Delta p}{8 \cdot m \cdot L} \qquad \text{(eq. 4.7)}$$

with:

Q	: volumetric velocity cm^3/s
r	: radius tube in cm
P	: pressure difference $dyne/cm^2$
μ	: dynamic viscosity in poise or (gram/sec.cm)
L	: length tube in cm.

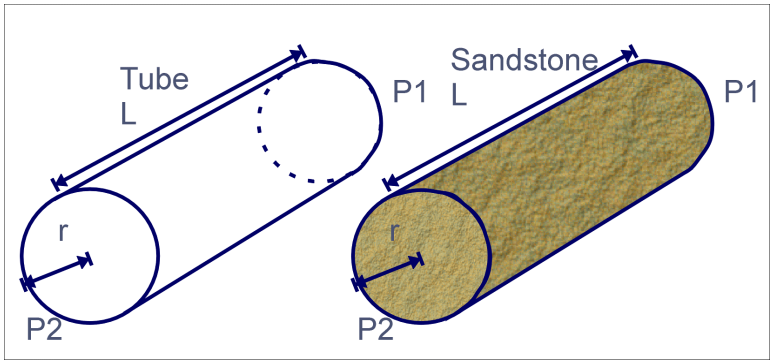

Figure 4.8: Comparison of flow in a tube with flow through sandstone

4.2.3. PERMEABILITY MEASURED ON CORE SAMPLES

In 1856 Darcy determined permeability experimentally by flowing water through sands proposed as filtering material for sanitary purposes, for the town of Dijon, France. His law extended for different fluids originally is written as :

$$Q = \frac{-k(h2 - h1)}{l} \qquad \text{(eq. 4.8)}$$

where:

Q : volumetric fluid velocity in $L^3.t^{-1}$

l : thickness of the sand L.

h_2, h_1 : the elevation above a reference level of water in manometers terminated above and below a vertical column of sand and L

k : a proportionality factor also in $L^3.t^{-1}$, which contains the properties of the fluid and the porous medium.

All relations were associated with a water column (m) and flow capacity ($L^3.t^{-1}$). Viscosity of the fluid was not included. This principle is still in use with permeability estimations in groundwater flow measurements. The generalisation of the Darcy relation includes the viscosity and dimensioning of the porous medium, including the pore energy by surface, length and pressure drop:

$$Q = \frac{k \cdot A \cdot \Delta P}{h \cdot L} \qquad \text{(eq. 4.9)}$$

where:

Q : volumetric fluid velocity in $cm^3.s^{-1}$

A : surface area perpendicular to flow direction in cm^2

ΔP : pressure difference in atm.

h : dynamic viscosity of the fluid in cpoise (kg/sec.cm)

L : length in cm

k : permeability in Darcy (1 D=0.986*10^{-8} cm^2)

4.2.4. CORRECTION FOR A FLOWING MEDIUM IN LABORATORY MEASUREMENTS

Nowadays permeability is, in principle, determined with the same equation Darcy published back in the nineteenth century. The Ruska permeameter is normally used for this measurement, with gas as the flowing medium. We usually want to know the permeability of the reservoir rock for fluids, hence for the determination of water or oil permeability corrections have to be made to the measured gas permeability. Darcy's law is different for gases, because the volume of gas that passes through the sample is not only dependent on the pressure differential but also on the absolute pressure itself. When taking the mass flow into consideration the following equation for gas can be used:

$$Q = \frac{k \cdot A \cdot \Delta P \cdot \overline{P}}{h \cdot L \cdot P_{atm}}, \ldots . at; 20^0 C, 1 \cdot atm \qquad \text{(eq. 4.10)}$$

where $\overline{P}$ is the average pressure over the sample in atm, and P_{atm} the pressure outside the system.

4.2.5. CORRECTION FOR GAS SLIPPAGE

In contrast with liquids that adhere to the pore walls, gases are hardly affected by the same pore walls. Gases flow with an almost piston shaped flow profile, while liquids in the laminar flow regime exhibit a parabolic flow profile with a maximum flow in the center and zero flow velocity at the pore walls. The higher flow of gas compared to liquids is called gas slippage. In 1941 Klinkenberg was able to show that by gas slippage at the gas/solid boundary, measured gas permeability is higher than liquid permeability. He introduced the following correction:

$$k_a = k\left(1+\frac{b}{\overline{P}}\right) \qquad \text{(eq. 4.11)}$$

where:

$\overline{P}$: mean test pressure of the gas in the pores
k_a : apparent or observed permeability with gas
k : liquid permeability
b : Klinkenberg factor

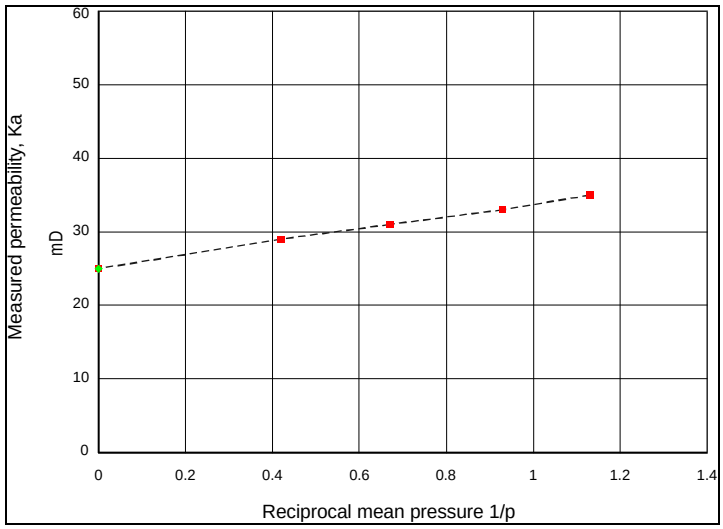

Figure 4. 9: Correcting air permeabilities for slip flow (After Lynch, 1962)

By carrying out measurements at different pressures on one sample, one can extrapolate in a "k_a versus (1/p)" plot the k_a to the point 1/p=0. At this point the pressure is infinite and there is no difference between liquids and gases. Here we find the true liquid permeability as depicted in Fig. 4.9. The Klinkenberg factor is inversely proportional to the radius of the capillaries and therefore also to permeability. Several authors have found slightly different relationships for different permeability fields (Fig.4.10). The slip effect is significantly recognizable below 100 mD.

4.2.6. CORRECTION FOR TURBULENCE

At higher flow velocities the flow regime changes from laminar to turbulent. This means that the liquid particles are not all moving parallel in the same direction but follow irregular vortexes with an overall resultant movement along the pore axis. The flow energy provided by the pressure differential is in this case not only used for the movement of the fluid as a whole but also spent on internal movements, that can be characterised by the kinetic energy of the fluid ($\rho.v^2$). Darcy's law is therefore extended by a term that reflects the flow energy spent on the kinetic energy of the flowing medium itself. Forchheimer adapted Darcy's law as follows :

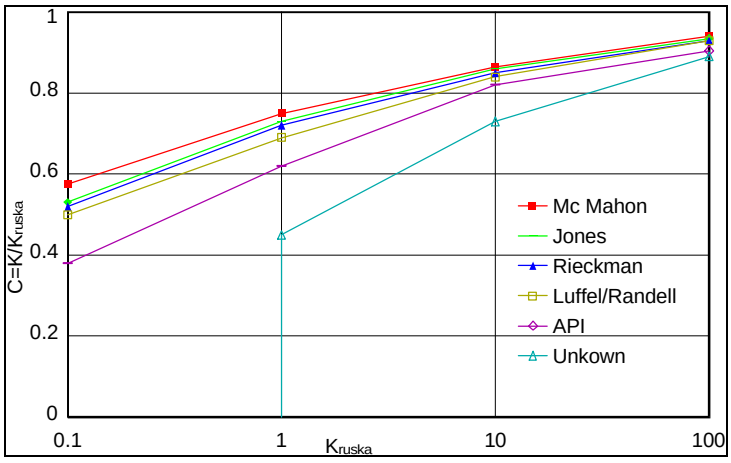

Figure 4.10: Influence of Klinkenberg factor on the liquid permeability K (van Baaren, 1982)

$$\frac{dP}{dL} = h \cdot \frac{v}{k} + b \cdot r \cdot v^2 \qquad \text{(eq. 4.12)}$$

with:

β	: turbulence factor (-)
ρ	: gas density ($kg.m^{-3}$)
v	: gas velocity ($m.s^{-2}$)
dP/dL	: pressure gradient ($Pa.m^{-1}$)
η	: fluid viscosity ($kg.m^{-1}.s^{-1}$)
k	: permeability (m^2)

Some gas producing reservoirs have a high turbulence factor. The result is that the gas permeabilities measured at the well are lower than the liquid permeabilities measured on core samples. The turbulence effect is only important for gas production in reservoirs with a permeability significantly higher than 100 mD.

4.2.7. PERMEABILITY RELATED TO TEXTURE PROPERTIES

As mentioned before, the factors affecting the magnitude of permeability are:

1. **Shape and size of sand grains:**
   If the grains are elongated, or large and flat and regularly placed with the length axis, the horizontal permeability **(k_h)**will be very high when compared to the vertical permeability **(k_v).** The vertical permeability will be medium-to-large (figure 4.11.a). If the rock is composed mostly of large and uniformly rounded grains, its permeability will be considerably high and of the same magnitude in both directions (figure 4.11.b). Further if the grains are small and of irregular shape, permeability quickly reduces to very low values (figure 4.11.c).
2. **Sedimentation, compaction and zonation:**
   The types of porous rocks or reservoirs with directional permeability are called anisotropic. It affects fluid flow characteristics and the permeability that is found parallel and vertical to a bedding plane. During sedimentation grains submerge in water with their longest and flattest sides in a sub-horizontal position. Succeeding compression and compaction improves this arrangement of the grains. Hence very flat minerals, such as phyllo-silicates like biotite and muscovite, and clay/shale laminations, are serious obstructions for a vertical permeability. The ratio of horizontal to vertical permeabilities (or the k_h/k_v -ratio) usually ranges from 1.5 to 3. Fractures etc. may cause a $k_v >> k_h$.
3. **Cementation:**
   Permeability of porous rocks is affected by cementation and the distribution of the cementing material within the pore space.

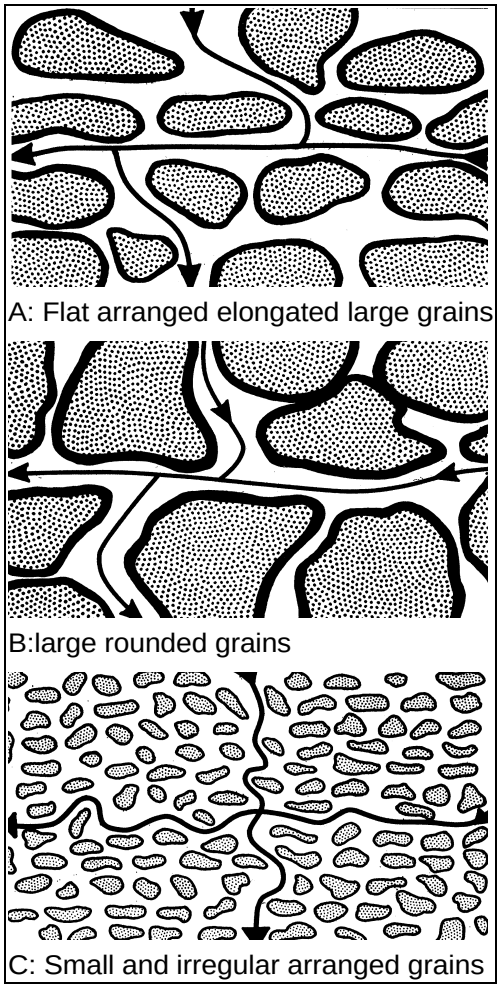

Figure 4. 11: Textures versus differences in permeability (revised after Djebbar 1996)

4. **Fracturing and solution:**
   Fracturing is an additional secondary permeability feature. However, when porous strata alternate with chemical sediments (salt, limestone, etc.), or are connected by fractures, mineral solution by percolating surface and subsurface acidic water, increases and decreases the permeability in the different zones.

4.2.8. RELATION BETWEEN PORE SPACE AND PERMEABILITY

Permeability is depending on the amount of pores, pore shape and thus the complement of the present minerals and their spatial characteristics. Kozeny produced a fundamental correlation which defines permeability as a function of the specific pore surface area and porosity. He consider a porous rock with a cross-section A and length L, consisting of n parallel capillary tubes, all of the same radius r (cm) and length L (cm) and cemented between the tubes. Here he combined the flow rate of Poiseuille's equation with Darcy's law getting the relation:

$$k = \frac{n \cdot p \cdot r^4}{8A_c} \qquad \text{(eq. 4.13)}$$

with A_c as the capillary tube surface. Porosity itself is defined as the ratio of the pore volume and bulk volume or:

$$j = \frac{V_p}{V_b} = \frac{n \cdot p \cdot r^2}{A_c} \qquad \text{(eq. 4.14)}$$

When j is inserted in equation 4.13, the permeability for a series of capillary tubes can be defined as:

$$k = \frac{j \cdot r^2}{8} \qquad \text{(eq. 4.15)}$$

with: k in cm^2 ($\approx 10^8$ D) , j as a fraction. Now the ratio of the internal surface area A_s of the tubes and the pore volume P_v give the internal surface area per unit pore volume (S_{Vp} = 2/r). Now the total area in the pore space per unit of grain volume, (S_{Vgr}) can be defined as:

$$S_{Vgr} = S_{Vp} \cdot \frac{j}{1-j} \qquad \text{(eq. 4.16)}$$

Substituting S_{Vp} = 2/r and combining equation 4.13 with 4.16, gives the relation:

$$k = \left(\frac{1}{2s_{Vgr}^2} \right) \cdot \frac{j^3}{(1-j)^2} \qquad \text{(eq. 4.17)}$$

When the pores are expressed as the complement of grains, the tubes have to be replaced by a winding flow path. Then a new term has to be implemented; the tortuosity (t), which is the actual flow path length (L_a) divided by the minimum length between the two ends of the flow path (L):

$$t = \left(\frac{L_a}{L} \right)^2 \qquad \text{(eq. 4.18)}$$

Now the tortuosity is inserted in equation 4.17, which results into:

$$k = \left(\frac{1}{2t \cdot s_{Vgr}^2} \right) \cdot \frac{j^3}{(1-j)^2} \qquad \text{(eq. 4.19)}$$

$2t$ is replaced by a constant K_z, or K_s which is defined as a shape factor for the spatial pore space characteristics. For the major part of the porous media it appeared to have a value of 5. This results into a general relation of:

$$k = \left(\frac{1}{5 s_{Vgr}^2} \right) \cdot \frac{j^3}{(1-j)^2} \qquad \text{(eq. 4.20)}$$

4.2.9. EMPIRICAL RELATIONS

Permeability is a geometrical property and is therefore depending on rock properties such as composition, texture and fabric. If the composition is assumed to be essentially constant then the texture will be the dominant factor. Many semi-empirical relationships are created between permeability and the textural properties grain size, sorting and porosity. The relation by van Baaren (1979) proved to give useful results for non shaly sandstones :

$$k = 10.D^2{}_{dom} \cdot C^{-3.64} \cdot j^{\,m+3.64} \qquad \text{(eq. 4.21)}$$

Where:

k : one-phase permeability (mD)

D_{dom} : dominant grainsize (micron) from cutting inspection with a microscope.

Consolidation	Cementation factor	
	atmospheric	in-situ [3]
unconsolidated sand	1.4	1.6
unconsolidated to friable sand	1.5	1.7
friable sandstone	1.6	1.8
hard to friable sandstone	1.7	1.9
hard sandstone	1.8	2.0
very hard sandstone	2.0	2.2

Table 4.5: relation of cementation factor (m) and sand

Sorting	C	$D_{dom.max}./D_{dom.min}.$
extremely well to very well sorted	0.70	2.5
very well to well sorted	0.77	
well sorted	0.84	3.5
well to moderately sorted	0.87	
moderately sorted	0.91	8
moderately to poorly sorted	0.95	
poorly sorted	1.00	

Table 4.4: relation of sorting, C, to the spread in dominant grainsize, D_{dom}.

C : a constant derived from the sorting observed with a microscope (Table 4.5)

f : porosity, fraction of bulk volume. Derived from well log evaluation.

m : cementation factor. Estimated by scratching of rock samples (Table 4.4).

This relation enables permeability data to be obtained during initial field development, before a core is cut and analysed in the laboratory, a process that can take several weeks to accomplish. The relation can in principle be applied within hours of logging the well and therefore uses readily available data sources such as cuttings, and/or sidewall samples, together with the porosity derived from well logs.

4.2.10. PERMEABILITY FROM LOGS

4.2.10.1.INTRODUCTION

To derive permeability from logs many methods have been proposed in literature. In this section only the methods that are used on a routine basis are discussed. During exploration or appraisal drilling cores are taken across the reservoir section of interest. Porosities can often be derived with a high degree of accuracy from the wireline logs when a correlation with the porosities measured on core samples is made. In turn permeabilities measured on core samples can usually be related to porosities, provided the relation is restricted to one sedimentological unit. The following symbols are used in the equations that describe these relations :

			dimension
k	=	Permeability in	mD
ϕ	=	Porosity in fraction of bulk volume	%
S_{wirr}	=	Irreducible water saturation as a fraction of the pore volume	%
D_{dom}	=	Dominant grainsize diameter in microns	µm
S_o	=	Sorting expressed as a constant (Trask) see eq. 3.4.	d.l.
m	=	Cementation factor as used in the Archie equation (Chapter 6)	d.l.

4.2.10.2. PERMEABILITY AS A FUNCTION OF POROSITY

Depending on the environment of deposition core permeabilities can often be correlated with the core porosities. These relations have the following kind of layout :

$$k = 10^{\left(C_1 + C_2 \cdot \log(j)\right)} \qquad \text{(eq. 4.22)}$$

and

$$k = 10^{\left(C_1 + C_2 \cdot j\right)} \qquad \text{(eq. 4.23)}$$

C_1,C_2 are constants that are determined by the regression analysis on permeability - porosity data pairs.

A crossplot of permeability versus porosity is used to determine the most appropriate relation, which in turn can then be applied to find permeabilities in uncored intervals from porosity log values.

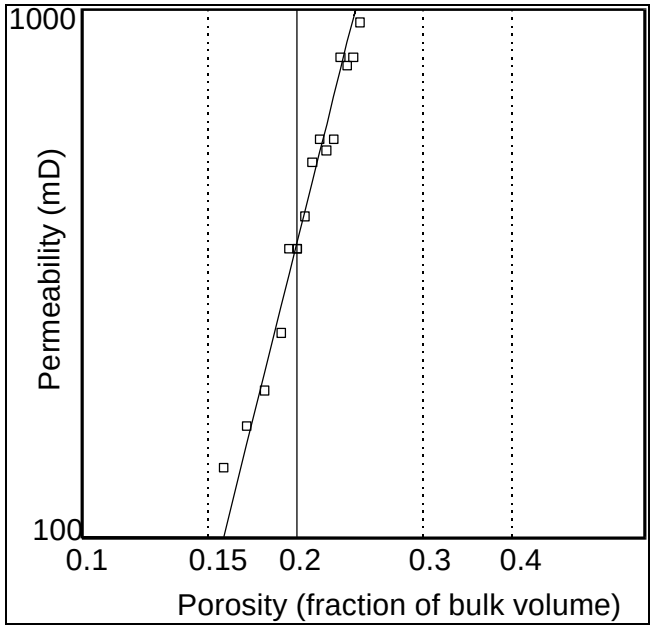

Figure 4.12: Example of the porosity versus permeability of laboratory results from several reservoir sandstones

4.2.10.3. PERMEABILITY BY POROSITY AND IRREDUCIBLE WATER SATURATION IN RESERVOIRS AND CONTAMINATED SANDS

Equations like eq. 4.20, 4.22 and 4.23 only use the porosity of the reservoir. This approach is not unique because rocks with the same porosity can have widely different grainsizes and therefore a wide range of permeabilities. Porous rocks with large grains will have a higher permeability than small grained reservoirs. If the reservoir or contaminated sand contains the maximum amount of oil, the irreducible water volume will cling to the grain surfaces, provided the rock is water wet. For a reservoir that consists of small grains the grain surface area will be much larger than for a reservoir composed of large grains. The irreducible water saturation (S_{wirr}.) is in that case a measure for grainsize, and also an indication for permeability. The following equation is by Wyllie and Rose is one of the many found in literature :

$$k = \left(100 \cdot j^{\,2} \cdot \frac{1 - S_{wirr}}{S_{wirr}}\right)^2 \qquad \text{(eq. 4.24)}$$

When core measurements are available it is worthwhile to determine the constants experimentally.

4.2.11. FIELD EXAMPLES

Laboratory results on cores

When the permeability is plotted versus the porosity on double logarithmic paper a straight line is often retrieved. In these cases the cementation factor (m), grain size and sorting usually are constant. In Figure 4.12 permeabilities measured on core samples are plotted vs. the porosities, and compared with the relation (straight line) derived with equation 4.21 The average grainsize and cementation factor "m" used in the relation for this clean sandstone are 250 microns and 1.8.

Drilling example: Invasion

One of the purposes of the mud column is to maintain an overpressure in the borehole with respect to the fluid pressure in the reservoir rock. As a result, water will filter from the mud into the rock. The invading mud filtrate will displace a part of the oil in the rock around the well bore and create an invaded zone as depicted in figure 4.13. In the figure d_{i1} and d_{i2} are respectively the diameters of invasion of a high and a low porosity sandstone (SST) layer, and d_h is the borehole diameter.

Solid (clay) particles contained in the mud will be deposited along the hole opposite permeable zones, and form a mud-cake with a permeability that is much lower than the permeability of the invaded reservoir rock. The rate of mud filtrate flow into the formation will be controlled by the low permeability of the mud cake, and be in first approximation independent of the permeability of the various layers, except of course when the permeability is close to zero. The distance into the reservoir rock that the invasion will progress in a given time period is therefore governed by the rock porosity and not by the magnitude of the permeability. The depth of invasion in a low porosity rock is as a consequence deeper than in a high porosity (larger storage capacity) rock.

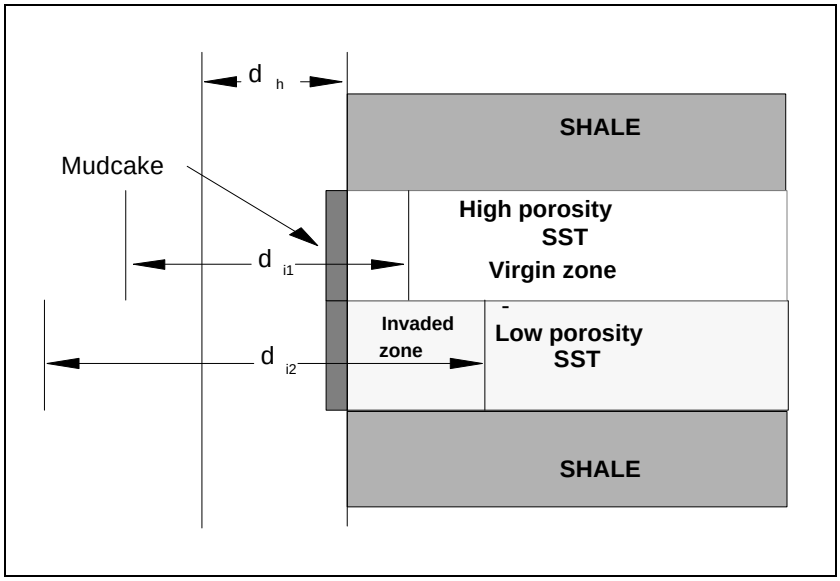

Figure 4. 13: The invasion profile in a reservoir sand

4.3. CAPILLARITY

4.3.1. INTRODUCTION

The accumulation of fluids in a reservoir rock is affected by the interaction of rock and fluids, which in the static situation is dominated by two forces: the gravity and the interfacial tension. To explain the distribution of fluids, and the positions of oil-water and oil-gas contacts knowledge of interfacial tension, wettability and capillary pressure is essential. These concepts will be explained in the following sections.

4.3.2. SURFACE TENSION

Surface energy

Surface tension of a gas-liquid interface has its origin in the fact that at a surface the intermolecular (van der Waals) forces are unbalanced and the surface molecules thus experience a net pull directed into the bulk of the solution (Fig. 4.1.A). Consequently, energy is required to increase the surface area of an interface. This explains why droplets and bubbles spontaneously minimise their surface area by creating a spherical shape. The force per unit length is referred to as the surface tension.

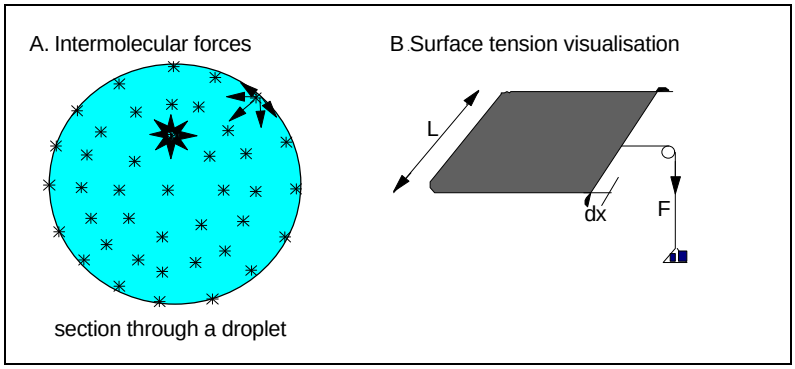

Figure 4. 14: Representation of the intermolecular forces and the surface tension visualisation

A visualisation of the surface tension is realised by considering a soap film in a rectangular metal or glass frame. One side of the rectangle can be moved over distance dx and the force F required for this displacement can be measured as shown in gure 4.14-B. At equilibrium, a force balance gives the relations:

$$g = \frac{F}{2l} \qquad \text{(eq. 4.25)}$$

and

$$F = 2 \cdot g \cdot l \qquad \text{(eq. 4.26)}$$

with:

γ	: surface tension, force per unit length in N/m
l	: length of the rectangle wire in m
F	: force put on the wire in N

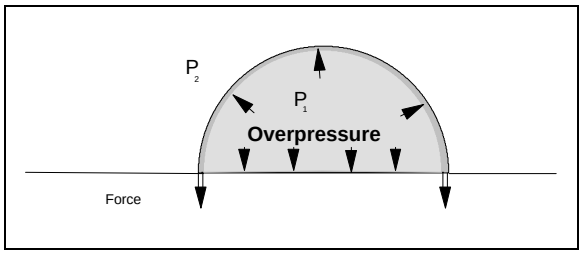

Figure 4.15: Visualisation of the surface tension of a soap bubble.

Soap bubble

Consider a hemispherical soap bubble placed on a flat liquid surface (Fig.4.15). In a state of equilibrium the surface tension acting along the periphery of the circle (2 r) pulls the soap film down. This force has to be balanced by the excess pressure pushing the soap film upwards. In order to have no net force on the liquid plane of the bubble, this upward force must be equal to the force acting downwards: 2 r = r^2 p **(eq. 4.27)**, again resulting in equation 4.25.

4.3.3. WETTABILITY

4.3.3.1. WETTABILITY ON A SMOOTH SURFACE

If a liquid is placed in contact with a solid, the surface of the liquid will tend to contract to its minimum surface area. However there may also be an attractive force between the liquid and the solid. This force is variable, dependent on the affinity of the liquid and the solid (Fig. 4.16).

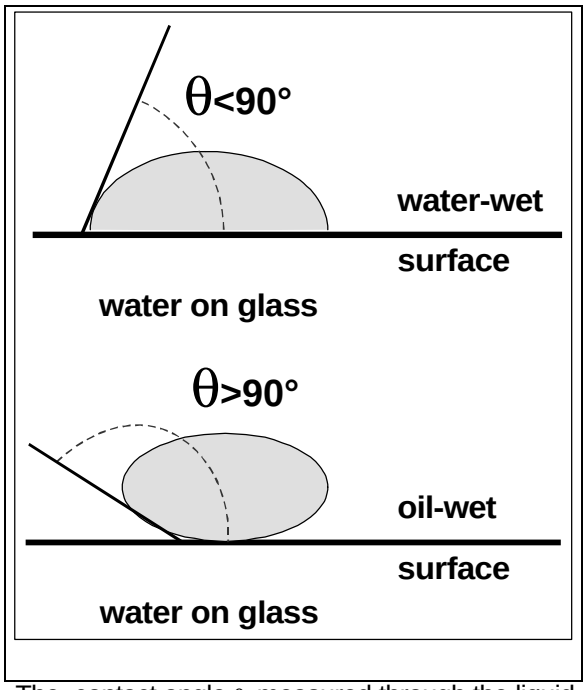

The contact angle θ measured through the liquid indicated by the arcs is called the contact angle. A solid is said to be wet by a liquid if the contact angleis less than 70°. The liquid is intermediate wetting from 70 to 110°,and non-wetting if the angle is greater than 110°. Complete wettting of the solid by the liquid is achieved fo: θ = 0°, and complete non-wetting (theoretically) with θ = 180°.

Figure 4.16: Wettability of water on a glass surface

When, due to production, the oil saturation is reduced to say 25 %, the oil will become the discontinuous phase and restricted to isolated globules surrounded by water. The water phase is then continuous and can still flow, but the oil volume cannot be reduced further by primary production mechanisms, such as pressure depletion and water drive. Injection of chemicals or gas is required to reduce the surface tension between the water and oil and mobilise the oil left behind during the primary production phase.

4.3.3.2. SIGNIFICANCE OF WETTABILITY

The significance of reservoir rock wetting preference can be illustrated with a few examples :

- In water wet rock the affinity between the water and the rock is much larger than the affinity between the rock and the oil. Consequently if both water and oil are present in the pores of the rock in significant quantities, the water will be distributed as a film that tightly clings to the pore surface. In contrast the oil will contract in globules and will be found in the middle of the pores as depicted in the left part of figure 4.17.
- If the affinity between the rock and the oil is larger than the affinity between rock and water the opposite situation will be found. The rock is now covered with an oil film and the water is found in the middle of the pores as shown in the right hand part of figure 4.17.

Most reservoirs are assumed to be water wet. The left-hand picture gives already an indication about the effect of wettability on the fraction of the oil volume that can eventually be produced. If the oil occupied originally say 80 % of the pore volume, it would have formed a continuous phase despite the fact that it is pushed to the middle of the pores by the water that clings to the rock.

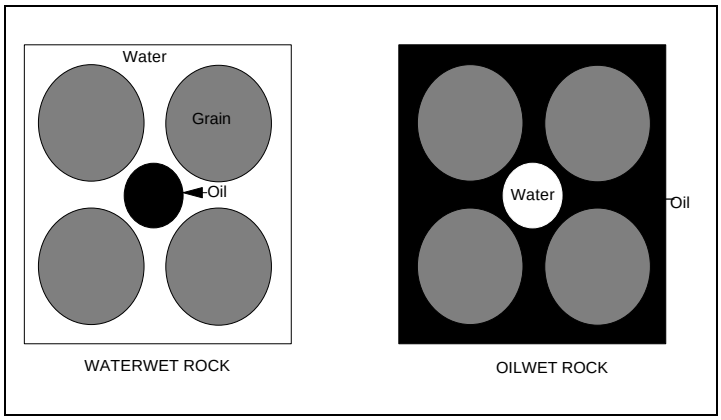

Figure 4.17 Distribution of the water in a water wet and oil wet reservoir.

4.3.4. CAPILLARY PRESSURES IN A TUBE

We have seen that the pressure difference Δp across a curved interface is given by equation 4.27. However the interfacial tension is directed along the interface which makes an angle θ with the wall of the tube. The tension component that lifts the column of water is therefore equal to γ.cos (θ) parallel to the capillary axis. Equation 4.28 is modified to read :

$$\Delta P = P_1 - P_2 = \frac{2 \cdot g \cdot \cos(q)}{r} \qquad \text{(eq.4.28)}$$

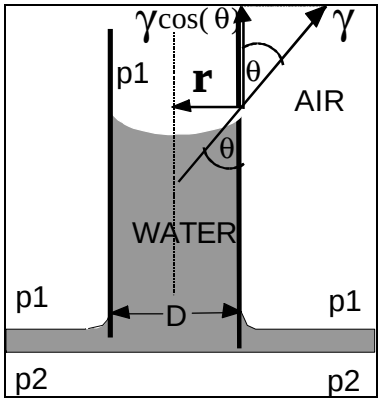

Figure 4. 18: Capillary tube

Equation 4.28 defines the capillary pressure in terms of the radius of the tube. It is this pressure difference which causes the rise of a wetting liquid in a capillary. This can be explained by the affinity of the water for the glass surface of the tube. The water literally creeps up the tube and drags due to its internal cohesion other water molecules upward as well. If the two fluids are air and water, the following relationships are clear:

$$\Delta P = P_c = \left(r_{water} - r_{air}\right) \cdot g \cdot h \qquad \text{(eq.4.29)}$$

where ρ_{air} and ρ_{water} are the densities of respectively air and water; h the liquid rise, g the acceleration of gravity, and P_c the capillary pressure. Equation 4.29 can be rearranged to find the height "h" of the capillary rise:

$$h = \frac{\mathrm{P}}{(r_{water} - r_{\mathrm{air}}).\mathrm{g}} \qquad \text{(eq.4.30)}$$

In combination with equation 4.28 we obtain for this air/water/solid system :

$$h \quad \frac{2g.\quad (q}{\mathrm{r.}\quad (\qquad r_{\mathrm{air}}} \qquad \text{(eq.4.31)}$$

Because surface tension, contact angle and densities are constant for given fluids. It is clear that the height to which the water will rise is inversely proportional to the radius of the tube. If air was replaced by oil similar reasoning leads to the relation :

$$h = \frac{2.g.\cos(q_{o/w})}{\mathrm{r.g.}(r_{water} - r_{\mathrm{oil}})} \qquad \text{(eq.4.32)}$$

It should be noted that the contact angle θ of the water air combination is now replaced by $\theta_{o/w}$, the contact angle of the water - oil system. For a very wide tube (r approaches infinity) both h and P_c will be equal to zero. The water level, which will then be the same inside and outside the tube is called the "**free water level**".

4.3.5. CAPILLARY PRESSURE IN RESERVOIR ROCK

4.3.5.1. CAPILLARY PRESSURE CURVES

Reservoir rock contains numerous pores of different size (radius). If the porous rock shows to be extremely homogeneous and with a constant pore size "r", we could apply equation 4.32 directly to calculate the capillary rise "h", as the interfacial tensions (IFT) and contact angles of various fluid - solid systems are known from laboratory measurements. The data of Table 4.6 are commonly used for

this approximation.

System	θ	cos(θ)	γ (dyne/cm)	γ*cos(θ)
air/fresh water/solid	0	1	72	72
air/saline water/solid	0	1	83	83
oil/water/solid	0	1	35	35
kerosene/brine/solid	0 (30)	1 (0.866)	50 (48)	50 (42)
air/kerosene/solid	0	1	24	24
toluene/brine/solid	0	1	38	38
air/mercury/solid	40 for air	0.766	480	368
Note: γ is the interfacial Tension, 1 dynes/cm = 0.001 N/m or 1 mN/m				

Table 4. 6: Interfacial tensions and contact angles of various fluid/solid systems.

Natural rock has a distribution of pore radii, which we have to take into account. Let us assume we have a rock sample containing pores of only three different sizes: small, medium and large. Since "P_c " and "h" are inversely proportional to the pore radius, the fluid distribution will be as shown in Figure 4.20 for a gas - water - solid system, in which we only show one capillary of each class. The pressure difference between the water and the gas gradients in the height versus pressure cross-plot, at the levels of the three menisci in the capillaries is equal to P_c.

Figure 4.20 shows the same sample 100% water bearing. If the water is displaced by oil we must exceed the capillary pressure for each pore size. Let us assume the values of r to be: 10, 5 and 2.5 μm with a Pc = 1, 2 and 4 psi. If we further assume that the number of pores (straight capillaries) is equal for each size, we can plot the pore volume of each size against the required injection pressure P_c. The value of P_c required for initial displacement is called the initial displacement pressure at the 100% water level. If the sample has a continuous distribution of tubes the left hand side of figure 4.19 evolves into a capillary pressure curve, as shown in figure 4.20 and 4.21.

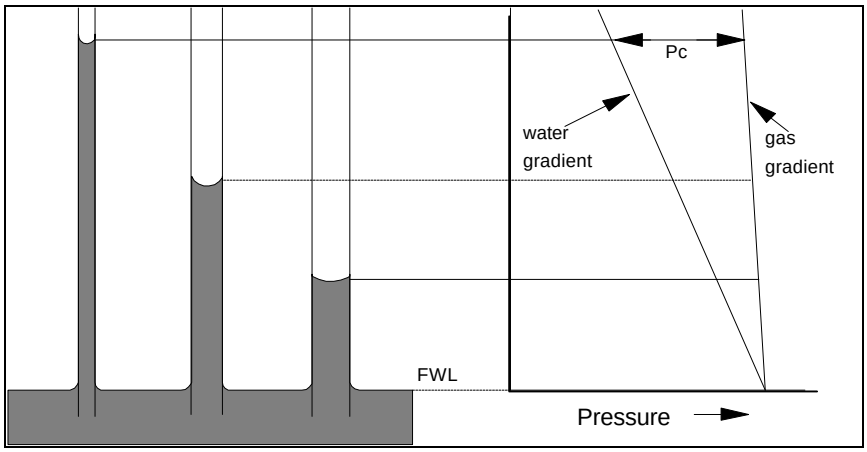

Figure 4. 19: Schematic representation of capillary pressure in reservoir rock.

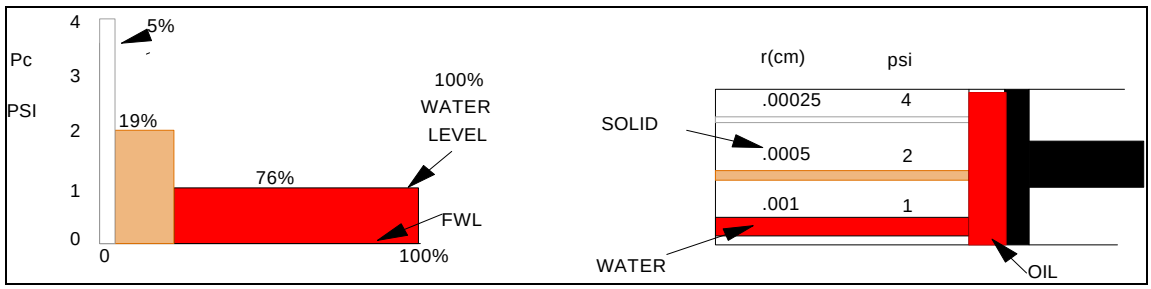

Figure 4. 20: Displacement of water by oil and the corresponding capillary pressure curve.

4.3.5.2. SATURATION LEVEL DEFINITIONS FOR HYDRO-CARBON RESERVOIRS

In water wet rock the following definitions are formulated:

- **Free Water Level (FWL)**
  For a very wide tube (r approaches infinity) both capillary rise and pressure differential will be equal to zero. The water level, which will be the same inside and outside the tube is called the FWL. This is illustrated in the capillary pressure curve of figure 4.21, at the point where S_w=100% and P_c=0.
- **FOL (Free Oil Level)**
  The Free Oil Level can be obtained with reservoir pressures measured with the wireline formation tester. The FOL is located at the transition of the gas bearing to the oil bearing part of the reservoir. For practical purposes it can be considered to be the GOC (Gas Oil Contact) in the reservoir.
- **100% Water Level**
  The 100% Water Level is the level where hydrocarbons start from the bottom up to occupy pore space in a water-wet reservoir. This is not the same level as the FWL because a threshold pressure has to be overcome before hydrocarbons fill the pore space.
- **Oil Water Contact (OWC) or Gas Water Contact (GWC)**
  The definitions that the OWC or GWC are the levels above which respectively water free oil and gas are produced are difficult to verify, because that would involve numerous production tests. For practical reasons the 50% oil or gas saturation levels are often taken instead This is usually accurate for high permeable reservoirs. A second definition is the OWC or GWC are the deepest depths where respectively oil or gas is encountered (similar but not identical to the 100% Water Level), based on the log analysis.
- **Connate water saturation / Irreducible water saturation**
  The connate water saturation refers to the smallest water saturation that can be reached in a water wet reservoir at the top of the oil column. The connate water is immovable and is supposed to form a film on the grains. Increasing the capillary pressure does not decrease the connate water saturation.

In water-wet rock the sequence of the levels from the bottom up is: the FWL, followed by the shallower 100 % Water Level and than at the shallowest depth the OWC or GWC. In oil wet rock the OWC can be located deeper than the FWL. In some cases the reservoir has a mixed wettability: oil wet in the upper part of the oil leg and water wet in the transition zone and in the water leg.

4.3.6. CAPCURVES FROM THEORY TO PRACTICE

4.3.6.1. LABORATORY ANALYSIS OF CAPILLARY PRESSURE CURVES

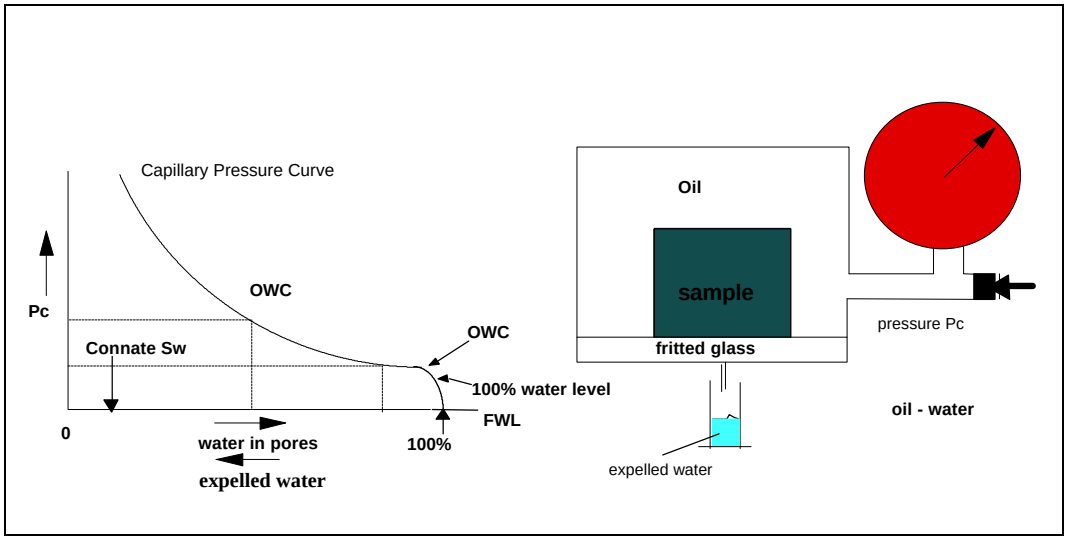

Figure 4. 21: Capillary pressure curve measurement and capillary pressure curve.

Care should be taken to carry out these measurements on representative samples, which cover the various lithologies, permeabilities and porosities present in the reservoir. The samples are cleaned with a hot solvent extraction (mixture of methanol, chloroform and water) to remove the oil. The samples are usually dried at about 105° C for clean reservoir rock, or at 60 C and a relative humidity of 45 % to allow the clay to preserve the clay-bound water. It should be realised that generally the cleaning procedure results in water wet rock. There are various techniques to determine the capillary pressure curve:

- the diaphragm or porous plate technique;
- the centrifuge technique; and
- the air / mercury technique.

Only the porous plate technique will be discussed here. This technique uses a pressure vessel filled with oil in which the water saturated sample is immersed. The pressure in the oil is increased stepwise. At each step the displaced water is measured in a graduated cylinder, as shown in figure 4.21.

A fritted glass disk (porcelain of very low permeability) allows only water to pass. This disk is called a semi-permeable membrane. The capillary pressure curve pertaining to that sample is obtained by plotting the pressure against displaced water as shown on the left hand side of figure 4.21. The water saturation (S_w), plotted on the x-axis, is given as a fraction of the pore volume. The porous plate technique has the advantage that the samples are preserved and can be used for other analyses. The disadvantage is that it is very time consuming because after every pressure step one has to wait till equilibrium is reached and water production stops. The porous plate technique is restricted to rather low pressures up to 12 bar to prevent leakage through the porous plate. When mercury is used instead of oil, and air instead of water, the measurement starts with a dry sample, and can be carried out much quicker. Moreover much higher pressures can be used.

4.3.6.2. EXAMPLES OF CAPILLARY PRESSURE CURVES

Typical capillary pressure curve of two homogeneous sandstones (SST); one with large well sorted grains, the other with small and poorly sorted grains; and a vuggy dolomite are shown in figure 4.22.

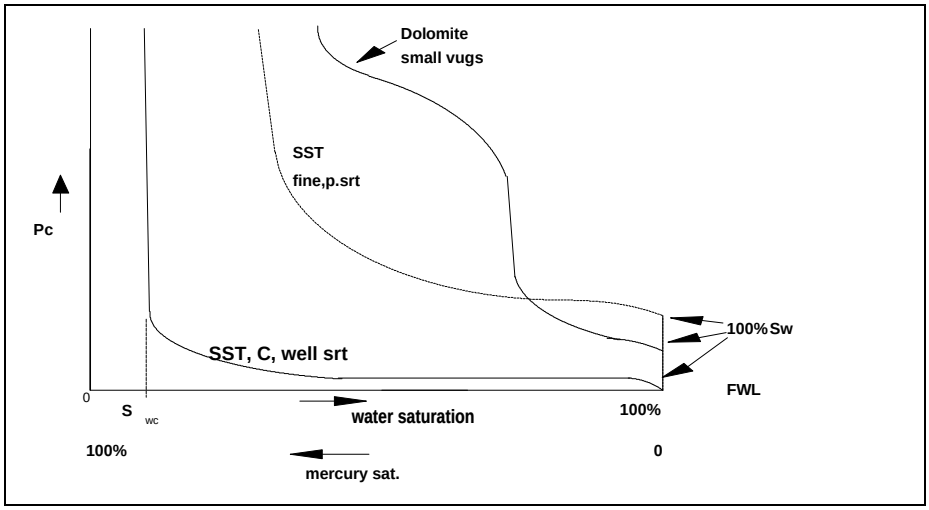

Figure 4. 22: Capillary pressure curves examples

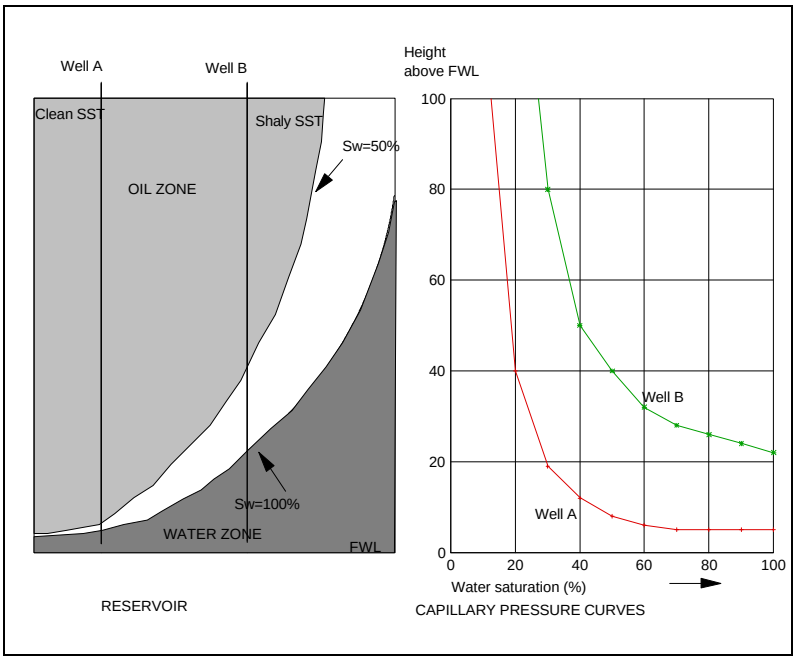

Figure 4. 23: Fluid distribution in a heterogeneous reservoir

4.3.7. CONVERSION FROM LABORATORY TO RESERVOIR CONDITIONS

In order to make use of the measured air/mercury capillary pressure curves, correction for the differences in contact angles and interfacial tensions between the laboratory fluids and reservoir fluids combinations have to be made. Based on equation 4.28 the following conversion is worked out :
Air and mercury filled sample:

$$P_c(Hg/air) = \frac{2.g.\cos(q)}{r} = \frac{2\times 480\times 0.776}{r} \qquad \text{(eq.4.33)}$$

Oil and water filled reservoir:

$$P_c(oil/water) = \frac{2.g.\cos(q)}{r} = \frac{2\times 35\times 1}{r} \qquad \text{(eq.4.34)}$$

Combining eq. 4.33 and 4.34 yields:

$$\frac{P_c(Hg/air \text{ at surface})}{P_c(oil/water.\text{in reservoir})} = \frac{480\times 0.776}{35} = 10.5 \qquad \text{(eq.4.35)}$$

Similarly for a gas - water - solid system we obtain:

$$\frac{P_c(Hg/air \text{ at surface})}{P_c(gas/water.\text{in reservoir})} = \frac{480\times 0.776}{72} = 5.1 \qquad \text{(eq.4.36)}$$

The converted values are often simplified to 10 and 5. This is justified because the inaccuracies in the contact angle and interfacial tension of the fluids is usually large, unless special laboratory equipment is used to measure these parameters separately under reservoir conditions.

To convert the maximum pressure measured on a capillary pressure curve in the laboratory, into an equivalent height above the FWL for reservoir conditions, the following equation is used :

$$h = \frac{g_{res}.\cos(q)_{res}.P_{c\,(\max.lab).}\mathrm{C}}{g_{lab}.\cos(q)_{.lab}.g.\Delta r} \qquad \text{(eq.4.37)}$$

with :

γ_{res} :IFT or inter facial tension of the fluids/solid of the reservoir in mN/m

θ_{res} : contact angle fluid/solid reservoir in degrees

γ_{lab} : IFT of the fluids/solid of the laboratory in mN/m

θ_{lab} : contact angle fluids/solid laboratory in degrees

$P_{c(max.lab)}$: Maximum pressure measured in the laboratory in bar

g : Gravity acceleration in 9.81 m/sec^2

$\Delta\rho$: Density difference reservoir fluids in kg/m^3

C : Constant : 100,000 when using the above units

LABORATORY	γ	θ	cos(θ)	γ*cosθ	P_{cmax} (bar)
air/brine	72	0	1	72	12
kerosene/brine	50	0	1	50	1.4
kerosene/brine	48	30	0.866	42	1.4
air/kerosene	24	0	1	24	5
mercury/air	480	140	0.766	368	4000

Table 4. 7: Input values for laboratory cap. curves used in equation 4.37.

4.4. LABORATORY ANALYSIS OF CAPILLARY PRESSURE CURVES

4.4.1. CAPCURVES: MEASUREMENTS WITH MERCURY

Introduction laboratory analysis of capillary pressure curves with mercury injection

A second method to discuss is the measurement of capillary pressure curves by mercury injection and retraction. The measured data are applicable for:

- the analysis of the response of capillary pressure curves.
- the determination of the pore size distribution.
- to gather attributes of pore geometry.

Subsequent, capillary pressure data, by mercury injection, of water-oil systems are comparable with the strongly water-wet capillary pressure curves obtained by other methods, when they are normalized using Leverett'sj-function. Note that in this case the state of wettability must be considered.

The disadvantages of the mercury injection method are:

- One can drink small amounts of liquid mercury without many problems. However Mercury vapor is toxic and will damage health by hair loss, teeth loss and other nasty illnesses in its syndrome. Hence, strict safety precautions must be followed when using mercury.

- Mercury cannot be safely removed after injection. Thus the remaining core with mercury has to be considered as chemical waste.
- The method is destructive when high pore pressures have to be used. Weak matrix samples can be destroid, which results in inaccurate values for pore sizes.

A mercury injection procedures goes as follows:

1. The core is placed in the sample chamber of the mercury injection equipment (Figure 4.24).
2. The sample chamber is evacuated, and incremental quantities of mercury are injected while the pressure required for injection of each increment is recorded.
3. The incremental pore volumes of mercury injected are plotted as a function of the injection pressure to obtain the injection capillary pressure curve (Figure 4.25).
4. When the volume of mercury injected reaches a limit with respect to pressure increase a mercury withdrawal capillary pressure curve can be obtained by decreasing the pressure in increments and recording the volume of mercury withdrawn (Figure 4.25). A limit will be approached where mercury ceases to be withdrawn as the pressure approaches zero (S_{Wmin}).
5. A third capillary pressure curve is obtained if mercury is re-injected by increasing the pressure incrementally from zero to the maximum pressure at S_{Imax}.

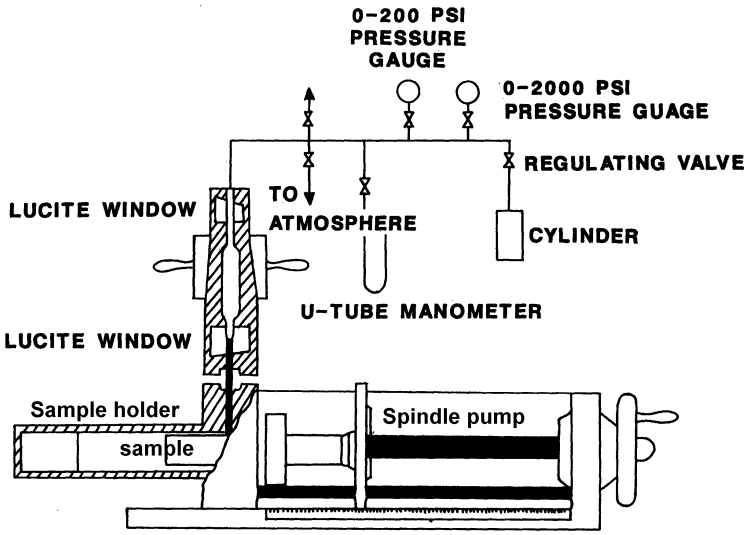

Figure 4. 24: Capillary pressure device for mercury injection

The closed loop of the withdrawal and re-injection is the characteristic capillary pressure hysteresis loop. Mercury is a nonwetting fluid; therefore, the hysteresis loop exhibits a positive pressure for all saturations-that is, the hysteresis loop is above the zero pressure line. In order to transpose mercury injection data to represent water-oil or water air capillary pressure curves, the mercury capillary pressure data are normalized using Leverett'sj-function:

$$J = \frac{P_c\sqrt{\left(\frac{k}{j}\right)}}{s \cdot \cos q} \qquad \text{(eq.4.38)}$$

with;

s_{Hg} = 480 N($I0^{-3}$)/m, q = 140° and k defined in Darcies.

Then capillary pressure transposed from mercury data to represent water-wet, water-oil, or water-air systems ($P_{CW\text{-}O}$ or $P_{CW\text{-}A}$) can be obtained from:

$$\frac{P_{cw-o}}{s_{w-o} \cdot \cos q^\circ} = \frac{P_{cw-a}}{s_{w-a} \cdot \cos q^\circ} = \left(\frac{P_{cHg}}{s_{Hg} \cdot \cos 140^\circ}\right) \cdot \sqrt{\frac{k}{j}} \qquad \text{(eq.4.39)}$$

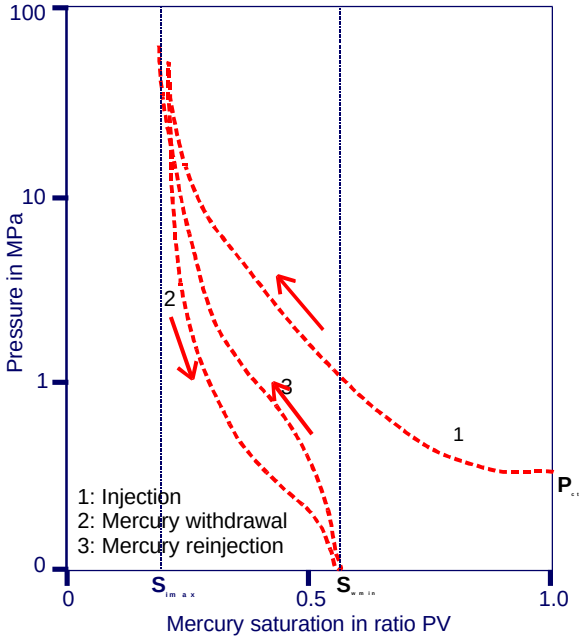

Figure 4. 25: Mercury injection, drainage and reinjection

There is a close correspondence that can be obtained between J-function-normalized mercury capillary pressure curves and curves obtained for water-oil systems using a centrifuge (Figure cap3). As far as as it is accepted practice to consider the contact angle for an airwater system to be equal to zero, one can use this to obtain a relationship between the contact angle and the saturation of water-oil systems as follows:

$$\cos q_{a-w} = 1.0 = \left(\frac{P_{c-aw}}{s_{aw}}\right)\cdot\left(\frac{r}{2}\right) = f\left(S_w\right)$$

(eq.4.40)

In this way an air-displacing water capillary pressure curve is obtained. An oil-displacing water capillary pressure curve is formulated by using :

$$\cos q_{o-w} = \left(\frac{P_{c-ow}}{s_{ow}}\right)\cdot\left(\frac{r}{2}\right) = f\left(S_w\right)$$

(eq.4.41)

The ratio of the capillary pressures at each saturation from S_W = 1.0 to $S_W = S_{iw}$ is obtained, and the contact angle for a water-oil system in a porous medium can then be plotted as a function of the wetting phase saturation. Implicit the next equation shows the assumption that the pore size is the same for a given wetting phase saturation of the two fluids:

$$\cos q_{o-w} = \left(\frac{P_{c-ow}}{s_{ow}}\right)\cdot\left(\frac{P_{c-aw}}{s_{aw}}\right) = f\left(S_w\right)$$

(eq.4.42)

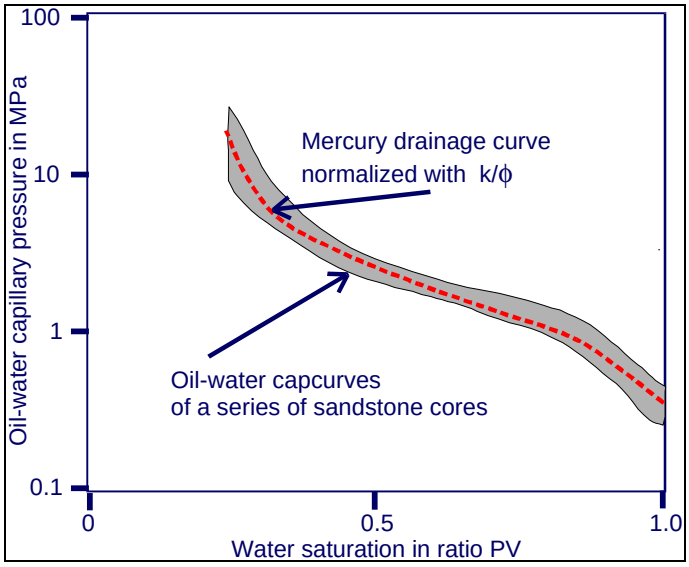

Figure 4. 26: Primary drainage of oil-water versus k/φ normalized mercury

5. ROCK RESISTIVITY, CONDUCTIVITY & AND ELECTRIC POTENTIAL

RESISTIVITY AND CONDUCTIVITY

NATURAL ELECTRIC POTENTIALS

5.1 ROCK RESISTIVITY IN GENERAL

Rock material and rock mass can be classified, for matrix and porosity through its heterogeneity in resistivity. In general a sedimentary rocks shows resistivity by the presence of high conductive and low conductive components. The salinity of water in the pores and the presence or absence of clays and/or shales are important factors in controlling the flow of electric current. Figure 5.1.shows the general relation for a resistance "r" of a material with its ability to impede the flow of electrical current. The resistance is defined as the ratio of the electric field strength and the electric current, or:

$$r = \frac{E}{I} \qquad \text{(eq. 5.1)}$$

With r in Ohm; E in Volt; and I in Ampere. The specific resistance *"R"* is defined as the resistance over a specific volume of matter. Hence, the resistance "r" is multiplied with a surface A and divided by the length L of the specific matter. Specific resistance or resistivity of a substance is defined as *R* or R_O:

$$R = R_o = \frac{E \cdot A}{I \cdot L} \qquad \text{(eq. 5.2)}$$

R is in ohm.m. The conductivity (*C)* is defined as the reciprocal of resistivity, or:

$$C = \frac{1}{R} \qquad \text{with the unity of } (\text{ohm.m})^{-1} \qquad \text{(eq. 5.3)}$$

The unit of conductivity $(\text{ohm.m})^{-1}$ is often replaced by the redefined unit mho/m, or in the metric system S/m (Siemens/m). To avoid very small values, 1 ohm^{-1} is valued as 1000 m.mho (millimho's).

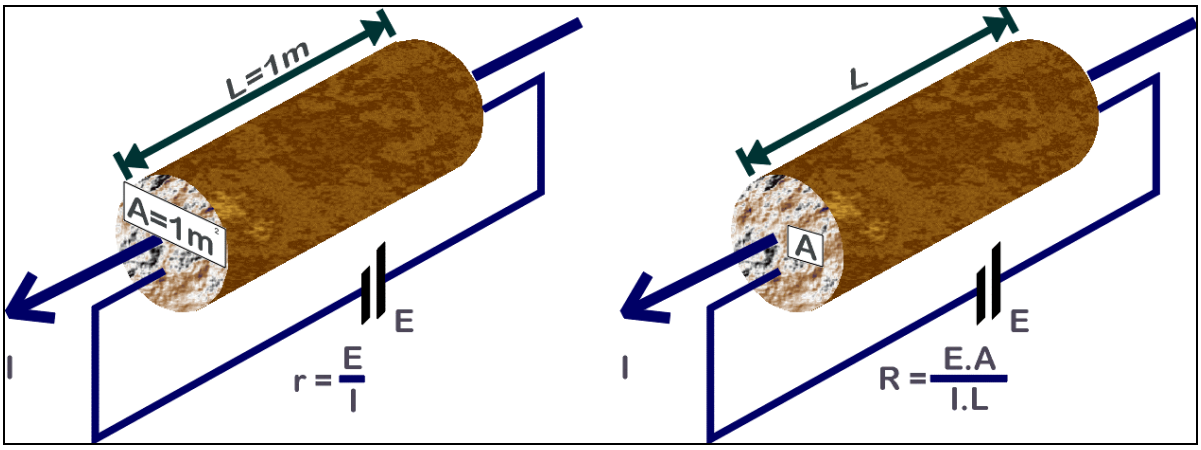

Figure 5. 1: definition of resistance (left) and resistivity (right) of a conducting material.

5.2 RESISTIVITY OF A MULTY COMPONENT SYSTEM

5.2.1 COMPONENTS IN ROCK

Normally a rock, or formation, consist of:

- **Non-conductive components:** like many matrix minerals, such as water-poor silica minerals (quartz, feldspar), carbonates, carbonaceous matter, hydro-carbons and fresh water, and,
- **Conductive components:** such as water bearing silica (shales, clays), ore minerals (magnetite, pyrite, galena as a semiconductor) and brine.

In general the total rock conductivity is controlled by the properties of fluid phase or the pore content or by a multi-component system in which the saturation of the pore space plays an important role. To

characterise the relationship between the components of a rock, or: between the matrix content and the pore content, the generic term **formation resistivity factor** (F or F_R) is brought into being.

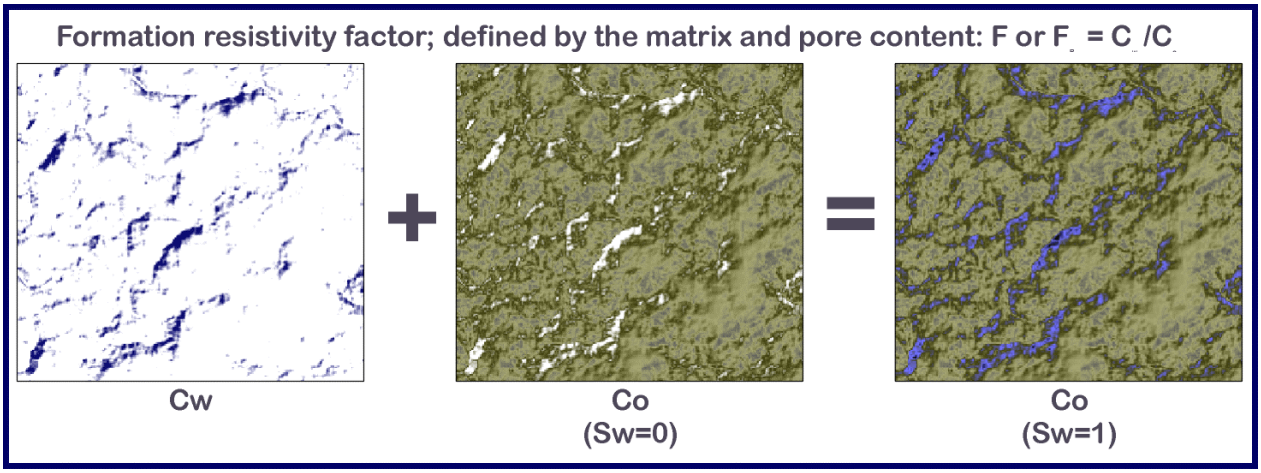

Figure 5. 2: Matrix resistivity and pore resistivity defining the formation factor and total resistivity

5.2.2 THE RELATION BETWEEN F_R AND ROCK POROSITY

When a porous rock sample with porosity j, as shown in figure 5.2, can be exemplified by an equivalent system of n saturated straight capillary tubes and the relationship between the total cross-sectional area (A) of a block with a length L, and the cross-sectional area of n capillary tubes ($A_n = n.\pi.r_c^2$) of length L, then:

$$A_n = jA \qquad \text{(eq. 5.4)}$$

The resistivity of the brine in the capillary pore space is:

$$R_{w.cap} = \frac{E \cdot A_n}{I_{w.cap} \cdot L} \qquad \text{(eq. 5.5)}$$

Now, as shown in figure 5.2 the formation resistivity factor F is the ratio of the resistivities of the matrix and fluid, or the ratio of the equations 5.2 and 5.5:

$$F = F_R = \frac{R_o}{R_{w.cap}} = \frac{A}{A_n} \cdot \frac{I_{w.cap}}{I_o} \qquad \text{(eq. 5.6)}$$

Here $I_{w.cap} = I_o$ since we assumed the n capillaries equal to the porous rock sample. Combining the equations 5.4 and 5.6 gives the basic dependency between the formation resistivity factor and porosity, or:

$$F = F_R = \frac{1}{j} \qquad \text{(eq. 5.7)}$$

If the tubes are replaced by a more natural kind of pore space, the space between a matrix consisting of sand grains, then the formation resistivity factor will change considerably. A porous system consisting of grains simply has no straight capillary tubes. Thus, the tortuosity factor (t), as defined in chapter 4: $t = \left(\frac{L_a}{L}\right)^2$, where; L is the sample length and L_a is the actual length of the flow path, is combined with equation 5.5:

$$R_{w.cap} = \frac{E \cdot j \cdot A_n}{I_{w.cap} \cdot L} \qquad \text{(eq. 5.8)}$$

If the equations 5.2 and 5.8, for respectively R_O and R_W, are divided by equation 5.4, and the assumption of $I_{w.cap} = I_o$ is applied, then the resulting resistivity factor for gives a relation for tortuosity:

$$F_r = \frac{1}{j} \cdot \frac{L_a}{L} = \frac{\sqrt{t}}{j} \qquad \text{(eq. 5.9)}$$

Horizontal or inclined tubes can be compared with a fractured or grain like porous medium, assuming that the total current I_o is the same as the current through the capillaries $I_{w.cap}$. This is possible when a very high resistivity rock is filled with very low resistive water. In that case a capillary tube has to be compared with the current path between the grains. In that specific case the tortuosity (t) shows the essential difference of the textures and the related formation resistivity factors. (Equations 5.7 and 5.9)

5.2.3 RELATION BETWEEN F_R AND MATRIX CEMENTATION/COMPACTION

In the previous sections the matrix minerals were considered to consist of tubes and grain particles. The related pore space is easy to define. However, in nature the grains often are compacted or cemented by various cementing materials, like; silica, carbonates and clay minerals. These cemented grain fabrics usually have lower porosities and, according to equation 5.9, higher resistivity factors, because of the reduction in porosity.

5.2.3.1 HUMBLE AND ARCHIE

From laboratory tests on the formation resistivity factor (F_R) and porosity (ϕ), a relation was found between these two variables. Using the general form of the expression as used in equation 5.7, they show:

$$F = F_R = \frac{1}{j^m} = \frac{R_o}{R_w} = \frac{C_w}{C_o} \qquad \text{; also named the first Archie equation} \qquad \text{(eq. 5.10)}$$

Here m is the cementation factor, which is related to the shape and distribution of pores. For this reason m is also called the lithology exponent. For this relation we can make the following comments, assuming a fixed pore fluid resistivity:

- The total rock resistivity R_O decreases with increasing porosity for the same kind of pore-geometry.
- In this case the pore geometry itself can be considered as a function of the lithology and the texture. Moreover, it characterises how the pores are connected. Hence, pores that are very tortuous or poorly connected do have a higher resistivity than a regular well-connected pore geometry.

A cementation factor can be determined by measuring the formation resistivity factor of several samples and plotting the porosities and the formation resistivity factors on double logarithmic paper. A straight-line relationship (figure 5.3) is often found when equation 5.10 is converted to:

$$\log F = -m \log j \qquad \text{(eq. 5.11)}$$

Now m is the slope. In compacted sandstones and (homogeneous) chalky rocks m has a value of ~2, whereas for highly cemented or compacted silicate-rocks and compact limestones the m increases to values over 3 (table 5.1, 5.2). “m” frequently varies from well to well, due to:

- the lateral heterogeneous character of sediments, even in a formation, and
- variation in burial history in a geological regions.

When m is difficult to determine, a constant “a” is introduced (figure 5.3). “a” depends on all kind of varieties, such as rock type, variation in pore type, quality of the measurement, etc. This adjusted equation, referred to as the Humble formula, also can be used to estimate the formation factor:

$$F = F_R = \frac{a}{j^{m}} \qquad \text{(eq. 5.12)}$$

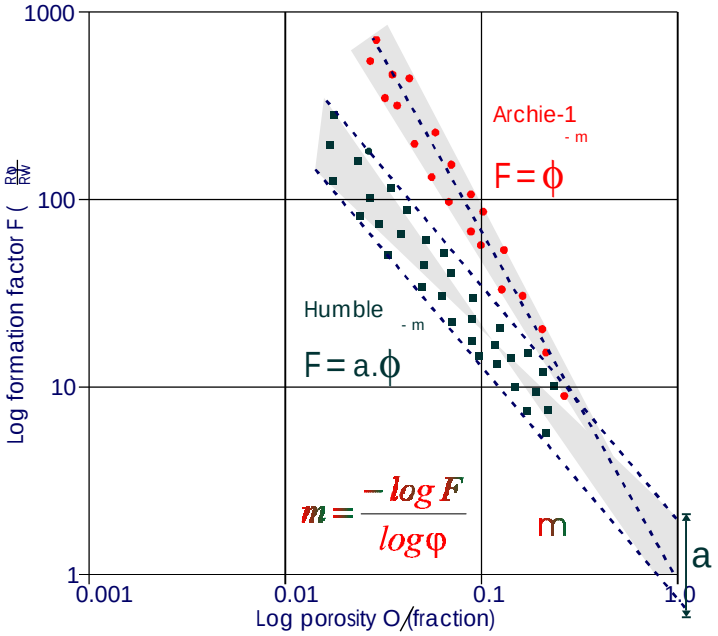

Figure 5. 3: Graphical presentation of the first Archie equation and the revision by Humble.

Again, the best values for both, "a" and "m" are determined by laboratory evaluations. For the siliclastic sediments and the carbonates, the m-values in-situ are higher than under "atmospheric" laboratory conditions.

$$m = \frac{-\log F}{\log j} \qquad \text{(eq. 5.13)}$$

Equation 5.13 shows the effects of compaction on the matrix: less porosity gives less water, and therefore a higher R_O, at a constant R_W.

Consolidation	**atmospheric**	**in-situ**
I BCD, interconnected	2.2	2.4
I BCD, moderate to abundant, poorly interconnected	2.6	2.8
I/II-II, no vugular porosity I/ III-III,	2.0	2.2
I/II-II BC, interconnected I/III-III BCD, moderate, poorer interconnection	2.2	2.4
LIII-II BCD abundant, poorer interconnection I/III-III	2.6	2.8

Table 5. 1: Carbonates Relation of cementation factor (m) and Archie classification.

5.2.3.2 CEMENTATION FACTOR AND SEDIMENT TYPE

After many years of measurements on cores, a wide range of regular values have been found for the cementation exponents of various types of sandstones and carbonates. The tables 5.1 and 5.2 show the atmospheric values and in-situ values for sandstones and carbonates, generally used in log evaluations. The most reliable to validate the above mentioned "m" values is the laboratory analysis of core samples. However this can only be done when cores are available.

- **laboratory measurements performed on plugs cut from cores.**
  For each plug the porosity f and the conductivity C_O of a sample 100% saturated with water of conductivity C_W, is measured. The '*m*' values calculated with equation 5.12 differ slightly from sample to sample even for a very clean homogeneous sand.Therefore they are averaged for the final evaluation.
- **water-bearing reservoirs.**
  When a hydrocarbon column in a reservoir overlies a water leg it is possible to determine the "m" factor from wireline logs alone. The density log, that will be discussed in a coming chapter, provides porosity values, while the rock conductivities C_O. are derived from resistivity logs. The formation water conductivity C_W can be obtained via the spontaneous potential (SP) log (Next topic). The "m" factor can then be calculated using the first Archie equation.

5.2.4 THE RELATION BETWEEN F_R AND THE WATER CONTENT (S_w)

In a hydrocarbon polluted soil, rock formation or an oil and/or gas-bearing zone, pores are filled with highly conductive brine and the hydrocarbons as non-conductive constituents. As shown before, the rock conductivity (C_O) or rock resistivity (R_O) is a function of water saturation S_W. When a part of the water is replaced by hydro-carbons, the true resistivity, R_t, of the porous rock is larger than the resistivity of a rock that is 100 % saturated with brine (R_O), or, equation 5.10 rewritten as:

Consolidation	Atmospheric	in-situ
very unconsolidated sand shallow potable water reservoirs	1.2	1.2
unconsolidated sand	1.4	1.6
unconsolidated to friable sand	1.5	1.7
friable sandstone	1.6	1.8
hard to friable sandstone	1.7	1.9
hard sandstone	1.8	2.0
very hard sandstone	2.0	2.2

Table 5. 2: Sands and sandstone relation of cementation factor (m) and sand consolidation

$$j^{m} \cdot C_w = C_o$$

Water saturation related to the porosity and resistivity index

The total resistivity is much higher and there is less available volume for the flow of electric current. Archie proved experimentally that the resistivity factor F_R of a formation partially saturated with brine could be expressed as:

$$S_w = \left(\frac{R_o}{R_w} \right)^{\frac{1}{n}} = \left(\frac{F_r \cdot R_w}{R_t} \right)^{\frac{1}{n}} \qquad \text{(eq. 5.14)}$$

The ratio which defines the amount of hydro-carbon in the pores, next to water, was named the resistivity index I_R , so:

$$I_R = \frac{R_t}{R_o} = \frac{C_o}{C_t} \qquad \text{(eq. 5.15)}$$

If a porous sample is fully saturated with brine, or S_W=1, then the resistivity index is equal to one. If I_R is greater than one then hydrocarbons are filling a part of the pores. Here the resistivity index is a function of the salinity and the amount of brine. To generalise equation 5.14, for less homogeneous textures, it is combined with Humbles relation (eq. 5.12) to:

$$S_w = \left(\frac{a \cdot R_w}{j^{\,m} \cdot R_t} \right)^{\frac{1}{n}} \qquad \text{(eq. 5.16)}$$

With; R_t as the true resistivity of formation containing hydrocarbons and formation water; R_o as the resistivity of formation when 100% saturated with water; n as the saturation exponent and I_R as the resistivity index.

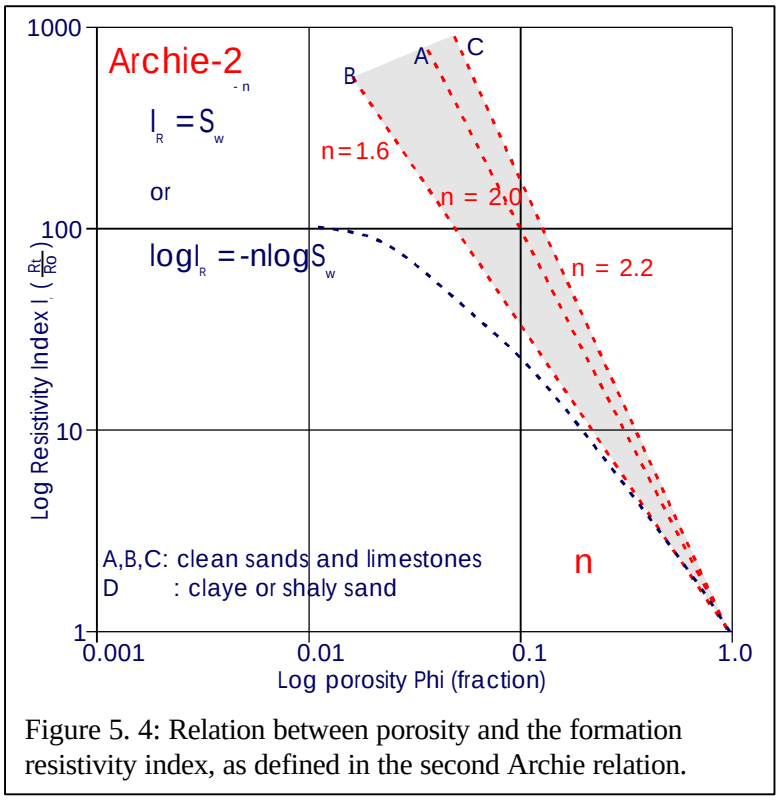

Figure 5. 4: Relation between porosity and the formation resistivity index, as defined in the second Archie relation.

As said before, the relationship between the resistivity index and the water saturation is established by Archie. A properly cleaned and evacuated, sample is saturated with a brine with resistivity R_W and R_O the total resistivity (S_W=1) is measured. The water saturation is decreased stepwise by flushing with oil. After equilibrium is reached at each step, the conductivity R_t is measured again. At each step S_W is calculated from the volume of the expelled water and the porosity. For clean homogenous samples the data points in a double logarithmic plot, usually show a linear trend. The relationship between the ratio of R_O and R_t, the resistivity index I, can be rewritten using the equations 5.14 and 5.15:

$$I_R = \frac{R_t}{R_o} = S_w^{-n} \qquad \text{(eq. 5.17)}$$

Here "n" is the slope of the linear trend in a double logarithmic plot, called the saturation exponent. The majority of the n-values range from 1.6 to 2.4. When core measurements are not available, normally the value n = 2 is accepted to be used. The value of n is influenced by:

- wettability,
- overburden pressure,
- fluid type; brine, oil, fresh water
- heterogeneity of fluid distribution, like tortuosity, and,
- the types and amounts of conductive clays (as already shown in figure 5.4).

The following effects of wettability on the saturation exponent are explained:

1. In homogeneous oil-wet systems with low brine saturations large values for "*n*", of 10 or higher, are possible.
2. If the saturation of the brine is high enough to create a regular thin layer on a grain surface of a porous medium (to build a uninterrupted path for a current flow), then the saturation exponent *n* is basically not subordinate to wettability. This occurs in clean and uniformly water-wet systems. Here

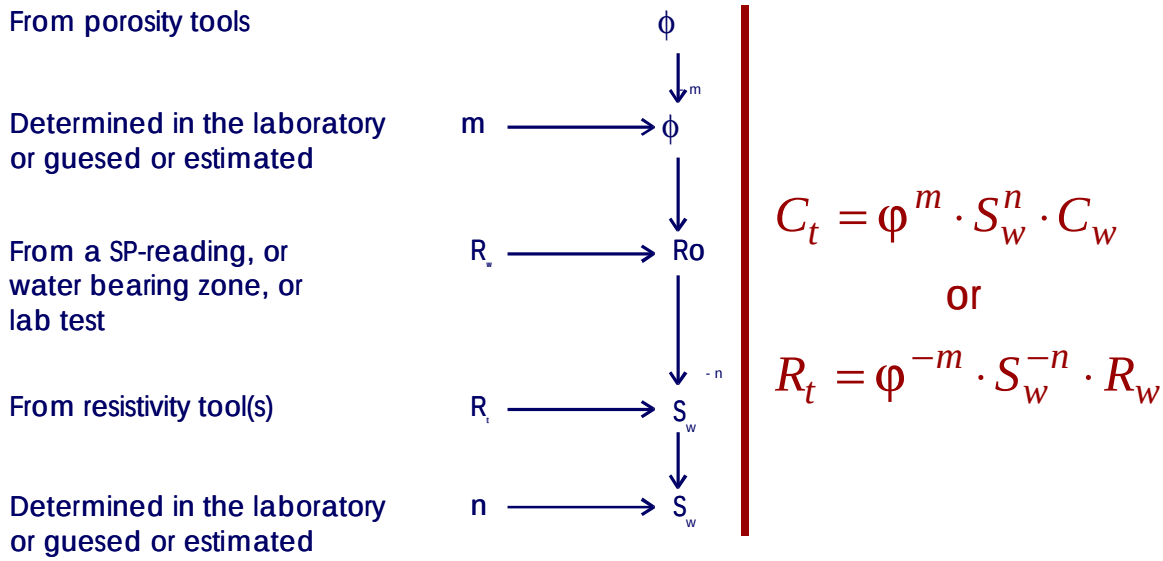

Figure 5. 5: Determination of S_W using the combined Archie equation.

the value of *n* is circa 2. In essence *n* remains constant as S_W is lowered to the irreducible value, S_{wi}.

5.2.5 WATER SATURATION CALCULATIONS USING ARCHIE; LABORATORY AND WILD LIFE

When the equations 5.10 and 5.16 are combined and manipulated, the result will be a general equation in which all resistivity and volumetric parameters are used:

$$C_t = j^m \cdot S_w^n \cdot C_w \quad \text{or} \quad R_t = j^{-m} \cdot S_w^{-n} \cdot R_w \qquad \text{(eq. 5.18)}$$

The five parameters required for S_W are (figure 5.5):

1. the porosity f and conductivity C_t , which are measured with wireline logs.
2. the formation water conductivity C_W , which is determined in a water-bearing zone through sampling or with the spontaneous potential (SP) log.
3. the cementation factor "*m*" and saturation exponent "*n*" preferably from laboratory core analysis.

In general in the calculations leading to the water saturation S_W, each input parameter adds to the overall uncertainty. When either the "n" or "m" exponents are estimated too high, or the porosity f to low, the S_W will be, in all cases, too high.

Till now various resistivity parameters are discussed and used to define the relations between physical and textural aspects of porous rock and its content. The measurements in a well normally are performed in a zone around the drill hole. Normally this area is affected by drilling fluid and therefore named the invaded zone or flushed zone. All direct information on porosity and resistivity, that is gathered in this zone, is detected with fluid mixtures from the drill hole. In the adjacent transition zone the pore fluid

consists of a blend from the borehole fluid and the virgin zone. The codes as shown in figure 5.6 are normally put to use when petrophysical data are evaluated:

di : diameter of the flushed zone, i.e. the zone through which several pore volumes of filtrate circulated, containing a residual hydrocarbon saturation.
Dj : diameter to the virgin or uninvaded zone.
dh : diameter of the borehole
hmc: thickness of the mud cake
h : thickness of the layer
R_w : resistivity of the formation water in the uninvaded pores
R_{mf} : resistivity of the mud filtrate
R_{mc} : resistivity of the mud cake
R_m : resistivity of the mud

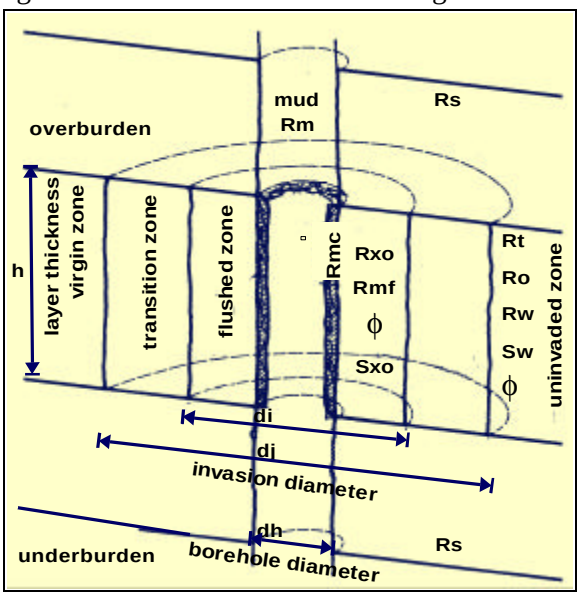

Figure 5. 6: Diagram of the nomenclature in and around a borehole.

Drilling disturbs the equilibrium in the distribution of water and hydrocarbon saturations that is determined by the interaction of gravity and capillary forces in the undisturbed reservoir. As mud filtrate invades permeable formations the conductivity in the invaded zone changes, as discussed in the previous chapters. The shape of this zone is often considered to be cylindrical around the borehole and also assumed to contain water with a conductivity equal to that of the mudfiltrate. The values can be measured on the surface on mud filtrate samples. In relatively impermeable rock, like shales, invasion does not occur. **The flushed zone** is defined as the zone around the borehole where the pores are 100 % filled with mudfiltrate. **The transition zone** contains a mixture of mudfiltrate and original formation fluids. **The virgin zone** only contains original formation water/hydrocarbon saturation. The lateral extent of the flushed zone and the invaded zone are usually not known. Additional conductivity measurements, with different depth of investigation, will therefore be required to locate these zones and compensate for the effect on resistivity measurements, as discussed in the next section.

5.3 RESISTIVITY LOGGING TOOLS

5.3.1 INTRODUCTION AND HISTORICAL DEVELOPMENT

There is a bewildering variation in the design and principles used for resistivity logging. While we usually only want to know one parameter the true resistivity Rt , eleven different resistivity tools will be mentioned in this section. The reason for this avalanche of designs is that the resistivity of the borehole, the mudfiltrate, and adjacent beds all have an effect on the resistivity measured by a tool in the borehole. No single design can fully compensate for all these effects, and a combination of measurements with different tools is required to calculate the illusive R_t

ELECTRIC SONDE: The first resistivity log, an electrical survey (ES) was run in 1927 by Marcel and Conrad Schlumberger. The ES tool contains 3 lead electrodes held together with ropes. One electrode is used to inject current via the borehole in the formation, and the other two are use to measure the potentials generated by this current. Formation resistivity values can only be obtained under favourable conditions, i.e. slim boreholes, relatively high mud resistivity, shallow invasion and thick beds. This simple tool was already successful in detecting layer boundaries and high resistivities indicative for the presence of oil. The first overseas ES log was already run in Brunei (Borneo) in 1929. ES logs although superseded in Western oil and gas logging operations will still be discussed, because similar tools are used for ground-water operations, and a large proportion of well data in older fields consists solely of ES logs

INDUCTION LOGS: Before the second world war many wells were drilled with muds that consisted of locally available clay and water mixtures with a low salinity. These muds were often incompatible with the shales encountered downhole, which led to clay swelling, large wash-outs, and even caving of wells. In the early fifties oil-base muds were developed that had diesel as the continuous phase and therefore significantly reduced clay problems. However these muds did not conduct electric currents and ES tools with electrodes could not be applied anymore. Induction tools were developed for these circumstances, which derived conductivity values of the formation based on the electromagnetic coupling of transmitter and receiving coils in the logging tool via the conductive rock surrounding non-conductive borehole.

LATEROLOGS: In the same period laterolog tools were developed for high salinity drilling muds, applied to drill through salt layers, in which ES tools are virtually short circuited. The laterologs use arrays of electrodes to focus the current emitted by the centre electrode into the formation, and thereby significantly reduce the effect of the mud. Both the induction and laterolog tools are superior to the older ES tools to obtain a reliable value of the true resistivity of the uninvaded formation.

MICRO RESISTIVITY TOOLS: The micro resistivity tools were introduced to provide an accurate assessment of the resistivity of the invaded zone R_{xo}. These tools have in common that the electrodes are very close together and are mounted on a pad that is pushed against the borehole wall to minimise the effect of the borehole fluid.

5.3.2 ELECTRICAL SURVEYS (ES)

5.3.2.1 SHORT NORMAL (SN), LONG NORMAL (LN), AND LATERAL TOOL DESCRIPTION

Wireline logging tools can evidently not measure subsurface parameters without a borehole to accommodate the tools. The presence of the borehole however severely hampers the determination of the formation resistivity due to the conductivity or lack of conductivity (oil base mud) of the borehole itself. If we could place electrodes in the ground without drilling (a typical thought experiment) we could pass an electric current between electrode "A" embedded in an infinite, homogenous isotropic medium and electrode "B" at an infinite distance. The current would then flow radially outward in all directions as shown in figure 5.7. In this case the equi-potential surfaces are spheres with their centres at the current electrode "A". If we would place another electrode "M" near "A", electrode "M" would then lie on the sphere whose radius is the distance AM. If "M" would be connected through a potentiometer to a remote electrode "N", this meter would then indicate the potential at the sphere of radius AM. For a sphere the potential difference between electrode M and electrode N is as follows :

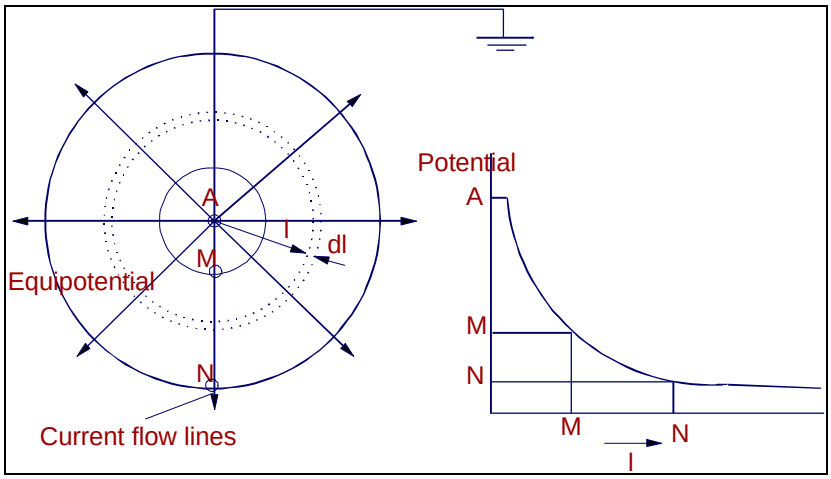

Figure 5. 7: Potential distribution in the radial flow of electricity. (Lynch, 1962)

$$E_m - E_n = \sum_{AM}^{AN} \frac{I.R}{4.p.L^2}.dL = \frac{I.R}{4.p.AM} \qquad \text{(eq. 5.19)}$$

This can be rearranged as :

$$R = \frac{K_n . DE}{I} \qquad \text{(eq. 5.20)}$$

where K_n is a proportionality factor depending on the electrode spacings. If the tool emits a constant current I and the potential difference ΔE is measured, R can then be calculated. The potentials E_m and E_n are measured by electrodes in the borehole. If the borehole resistivity does not deviate too much from the formation resistivity these potentials correspond to similar potentials in the rock formation, as shown in Figure 5.8 at the left. The greater the distance of the two measuring electrodes from the current electrode A, the deeper these equi-potential spheres reach into the formation. In electric logging the long spacing tools are therefore referred to as the deep penetration tools. The price to pay for the deep penetration is the low vertical resolution. The formulation of equation 5.20 demands the postulation of an uniform medium of infinite extend as shown in left hand side of fig.5.8. This condition is rarely encountered in practice. The right hand side of the figure shows the possible distortion of the current pattern that occurs due to the presence of low resistivity layers. The electrode arrangement shown in figure 5.8 is used in the "normal" device. The distance AM is called the spacing. Two spacings are utilised: the "short" normal (AM = 16 inches) and the "long" normal (AM = 64 inches) for shallow and deeper investigation respectively. In actual practice all 4 electrodes are located in the hole. Electrodes B and N are placed at sufficiently great distances from the AM group to ensure a negligible effect on the potential measured between M and N. In the so-called LATERAL device, the M and N electrodes are placed close together compared with their distance from A to M. The spacings is very long (18 ft 8 in) as indicated in figure 5.9. This allows a deep investigation. Consequently the tool has a very poor vertical resolution and a marked asymmetric response. Note, B is the return electrode.

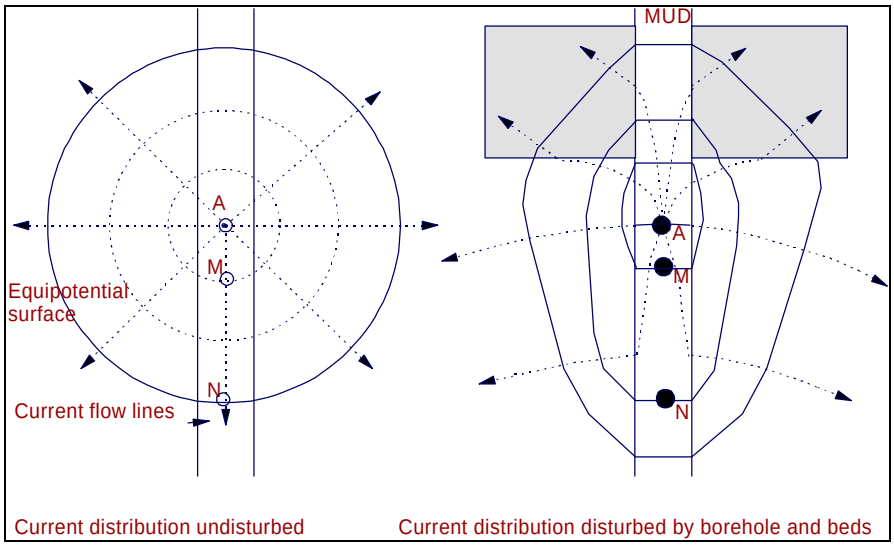

Figure 5. 8: Current distribution with and without a borehole/layer disturbance

5.3.2.2 SN, LN AND LATERAL LOG BEHAVIOUR

The short normal is widely used for geological correlation between wells and provides an fair value of R_{xo}. The long normal and lateral are adapted to supply a reasonable value of R_t in thick beds. Normally homogeneous resistive layers are alternating with low resistivity beds. The tool response in thick resistive beds shows:

- poor bed definition (rounding off) when the bed thickness is smaller than the tool spacings AM
- apparent bed thickness smaller than actual thickness by an amount equal to AM.
- a thin resistive layer is reflected by a depression together with two symmetrical peaks.

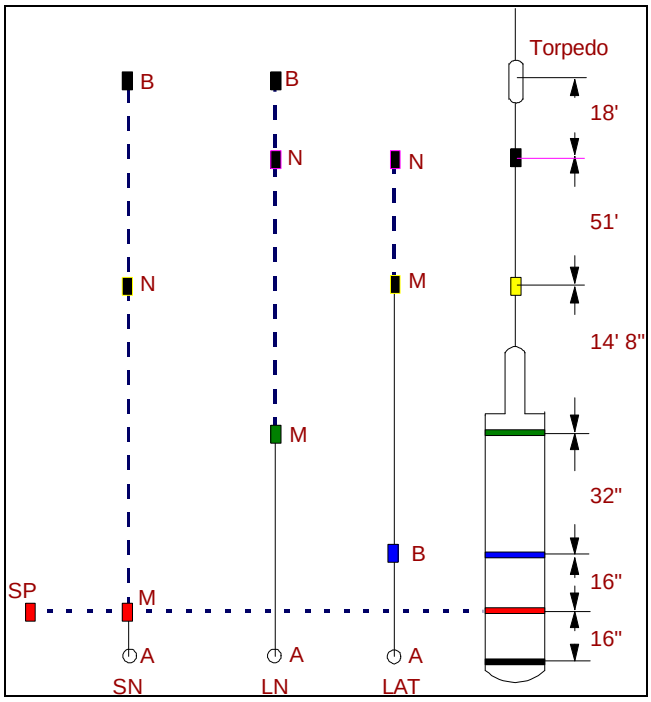

Figure 5.9: The electric sonde with SN, LN and Lateral.

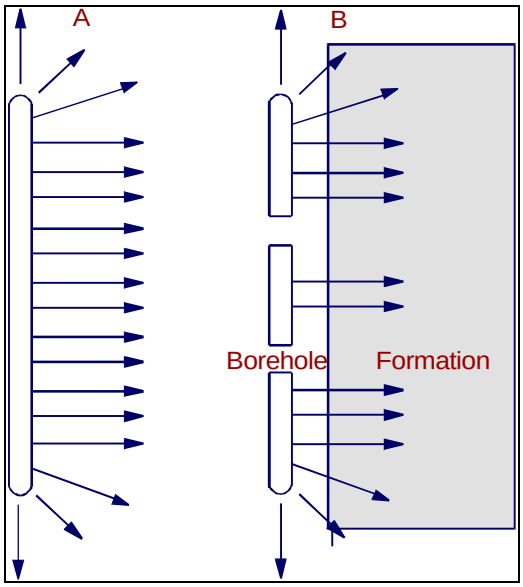

Figure 5.10: Pattern of current flow from a long cylindrical electrode located in a homogeneous medium

5.3.3 LATEROLOG TOOLS (LL3, LL7 & DUAL LATEROLOG)

Logging with laterologs was introduced to cope with salty mud. These muds have a very high conductivity, and consequently the effect of the borehole on resistivity measurements is also very high. The Laterolog technique is therefore complementary to the induction logging method, designed for oil-base mud which has hardly any conductivity at all.

5.3.3.1 LL3

Figure 5.10 shows the principle of the focused current log. On the left a long electrode bar is shown imbedded in a homogeneous medium. The potential is constant all over the bar and the current lines will run horizontal in the middle because current flow lines are perpendicular to equi- potential surfaces. The same principle is applied for the LL3 by using 3 bars as shown at the right in figure 5.10. The centre bar is 1 foot long and the two guard electrodes are 5 feet. By keeping the potentials equal for all three electrodes the current from the middle one is forced horizontally into the formation. This is even true when the bars are surrounded by a layer of mud with a resistivity that is much lower than the resistivity of the formation. The currents of the guards are adjusted to maintain the same potential as the centre electrode, while the potential of the centre electrode is kept at a fixed value. The ratio of the current and the potential of the centre electrode is a good indication of the formation conductivity C_t.

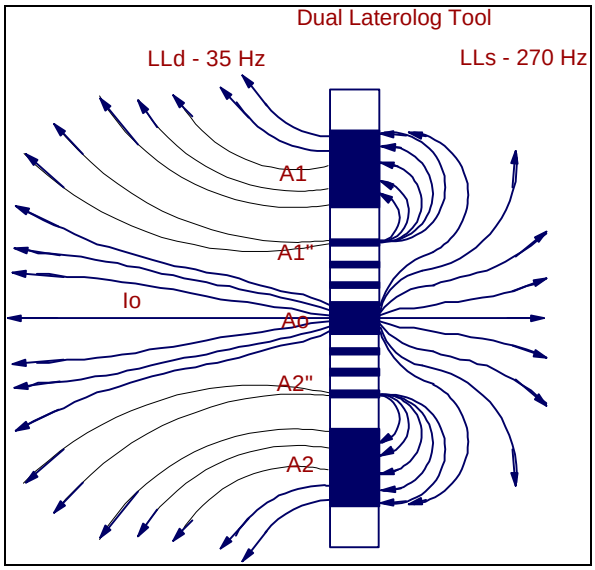

Figure 5. 11: The Dual Laterolog configuration

5.3.3.2 LATEROLOG 7 (LL7)

The laterolog 7 (LL7) is based on the same design as the LL3. In the LL3 the electrodes that carry very high currents (several amperes) are also used to measure potentials. This restricts the dynamic range of the measurements. In the LL7 two separate potential measuring electrode pairs are added, bringing the total to 7. The return electrode is positioned far away from the tool on the logging cable. This lay-out ensures that the current sheet penetrates the invaded zone and improves the measurement of the resistivity of the uninvaded zone.

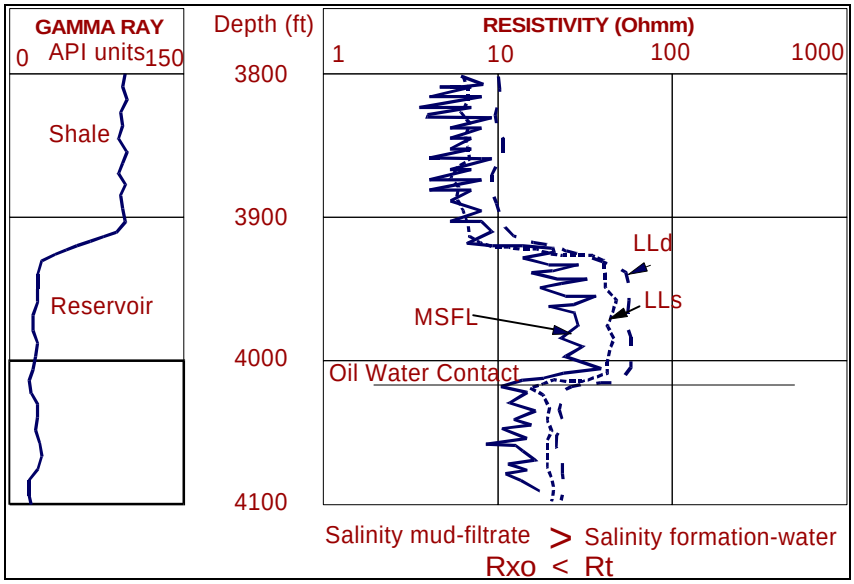

Figure 5. 12: Example of investigation depth of the Dual Laterolog

5.3.3.3 DUAL LATEROLOG

The dual laterolog is a combination of deep (LL_d) and shallow (LL_s) investigation devices. The principles adopted in the LL7 and LL3 have been combined in one tool, which features the 7 electrodes in its centre and 2 large bucket electrodes positioned respectively above and below the series of 7. In the LLd (deep) mode (left of figure 5.11), the surveying current I_o , that flows from the centre electrode, is focused by bucket currents from electrodes A1 and A2 supported by A1" and A2". The four "A" electrodes are all connected in this mode. This arrangement provides strong focusing deep into the formation. In the LL_s (shallow) mode (right-hand part of figure 5.11) the bucking currents flow from A1 to A1" and A2 to A2", reducing the depth of investigation. The electrodes are switched several times per second from one to the other configuration and the two resistivity traces are produced simultaneously. The dual laterolog measurements are often supplemented with a shallow resistivity measurement carried out with electrodes that are mounted in a pad which is pressed against the borehole wall to obtain R_{xo}. In this way three resistivity measurements are obtained simultaneously with different radii of investigation. An example is shown in figure 5.12. This situation is representative for invasion by mudfiltrate with a lower resistivity (higher salinity) than the original formation water. The LL_s is more affected by the invaded zone than the LL_d, while the MSFL reads very shallow in the order of 2-4" and gives a very good approximation of the low resistivity of the invaded zone.

5.3.4 INDUCTION LOGGING

The induction log, originally designed for resistivity recording in wells drilled with non-conductive fluids, has found its widest application in holes drilled with fresh and oil based muds. The sonde contains at least 3 coils, one transmitter and two receiver coils (figure 5.13). The transmitter sends out an alternating current with a frequency of 20 kHz of constant intensity. The alternating magnetic field generated by the primary coil induces secondary ground current loops in the formation. These loops in turn create magnetic fields, which induce currents in the receiver coils. The amplitude of the secondary field is proportional to the conductivity of the formation. The two receiver coils R1 and R2 are wound in opposite directions to compensate the direct coupling between T and R1. Actual logging tools contain 4 to 16 coils, of which the signals are combined to improve the vertical resolution as well as obtain a range of investigation depths (focusing).

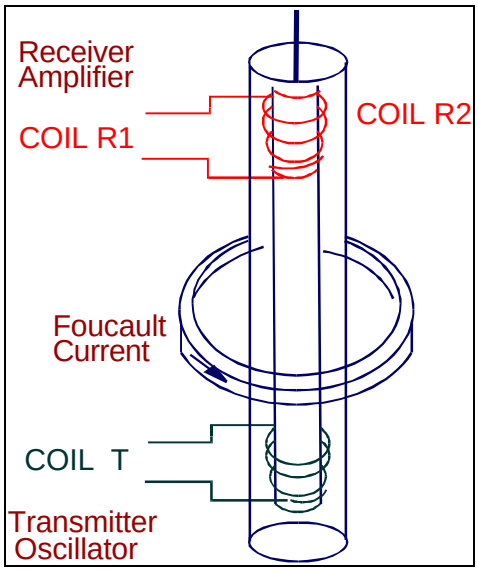

Figure 5. 13: Principle of the Induction Tool

An example of an induction log recording with deep (IL_d) and medium (IL_m) investigation depths is shown in figure 5.14, together with a shallow laterolog (LL_s) resistivity curve, and the spontaneous potential curve that will be discussed in the next chapter. The resistivity logs in figure 5.14 indicate the presence of a hydrocarbon/water contact, here denoted as oil/water contact. The shallow reading laterolog reading LL_s measures a higher resistivity than the induction log medium, which in turn measures higher than the deep induction log. This situation is representative for invasion by mudfiltrate with a higher resistivity (higher salinity) than the original formation water. The LL_s is more affected by the invaded zone than the IL_m, while the IL_d is usually hardly affected by the invaded zone.

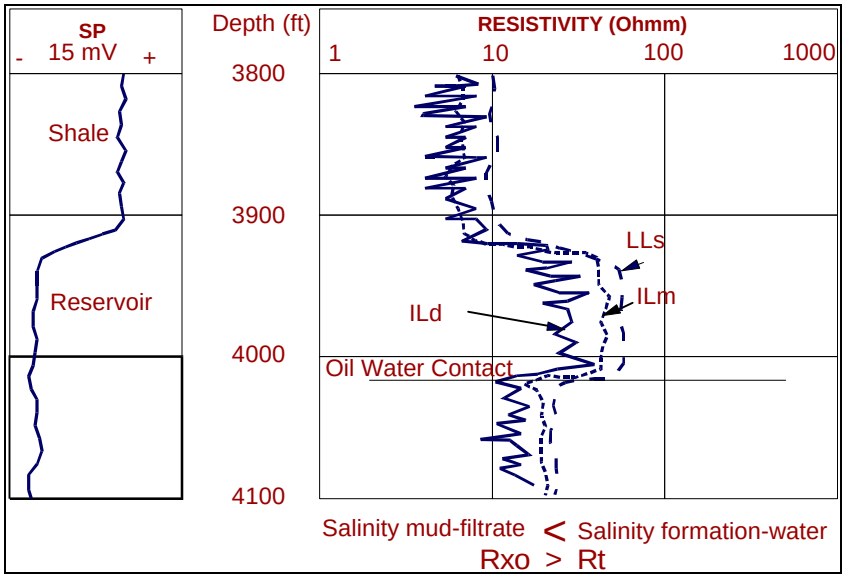

Figure 5. 14: A section recorded by the Dual Induction (DIL) Shallow Laterolog

5.3.5 MICRO-RESISTIVITY DEVICES

These tools are characterised by their short electrode distances of a few inches, which permit very shallow investigation. The micro-resistivity devices provide therefore usually a good approximation of the resistivity R_{xo} of the flushed zone. To avoid that the tools would only read the mud resistivity it is necessary to maintain physical contact between the electrodes and the formation. All tools in this category are therefore equipped with an electrode pad, which is pressed against the borehole wall, and designed to plough through the mud-cake.

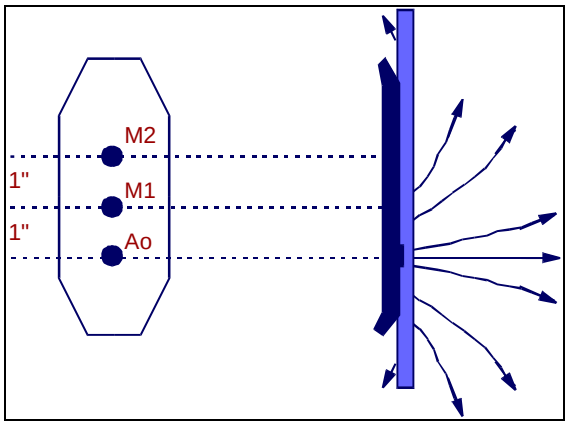

Figure 5. 15: The microlog principle

5.3.5.1 THE MICROLOG (ML)

This tool has 3 small button-shaped electrodes that are embedded in a rubber pad (figure 5.15). The electrodes are placed in a vertical line with a spacing of 1 inch between the successive electrodes. A current of known intensity is emitted from A_o and the potential differences between M_1 and M_2 and between M_2 and a surface electrode is measured. The resulting 2 curves represent a 2 inch normal and 1 inch "inverse" recording. The radius of investigation is smaller for the inverse, which is

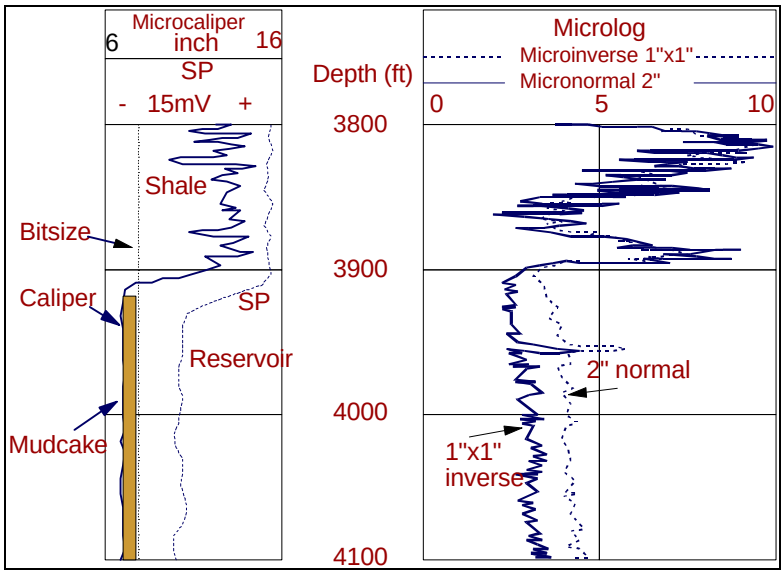

Figure 5.16: A MLC or Microlog Calliper example

therefore strongly affected by the mudcake. The normal curve reads 2 to 3 inch deep and is therefore more affected by the invaded zone.

The mudcake usually has a lower resistivity than the permeable beds, and the "inverse" will therefore read a lower value than the normal. Consequently, the ML detects mudcake by showing a separation between the 2 resistivity traces and thereby delineates the permeable beds. The ML is the best of all micro devices for making "sand counts". In figure 5.16 a section of the ML is shown. The separation of the micro normal and micro-inverse clearly shows the permeable bed delineation. This is confirmed by the separation between the calliper and the nominal bit size, which gives the mudcake thickness.

5.3.5.2 MICRO SPHERICALLY FOCUSED LOG (MSFL)

This device is incorporated in the dual laterolog DLL-R_{xo} tool. Its design is based on the concept that accurate resistivity data can only be obtained when the potential distribution around the current emitting electrode is spherical. This condition has been approximated by an array of concentric electrodes that resembles the Dual Laterolog in cross section as represented in figure 5.17. Note that both contain 9 electrodes. Both, the investigating current I_o and the bucket current I_1 are in this case emitted through centre electrode A_o. The sum of these two currents is adjusted by varying the potential of electrodes A_1 and A_2 in such a way that the measured voltage at M_o is kept equal to a constant reference voltage. I_o is roughly proportional to the conductivity of the slice of the formation that is shaded in figure 5.17. The main advantage of the MSFL over the micro-log is that it is much less affected by the mudcake. Therefore it gives a better estimate of the flushed zone resistivity R_{xo}, which is derived with equation.5.21:

$$R_{xo} = \frac{E_{Mo} - E_{M1}}{I_O} \qquad \text{(eq. 5.21)}$$

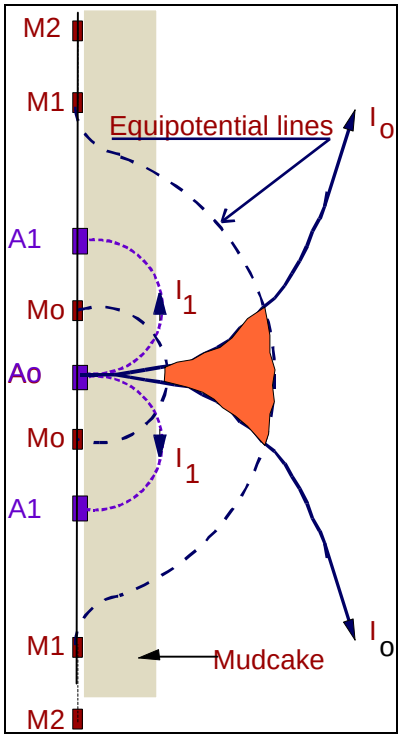

Figure 5. 17: Micro-SFL principle (After Schlumberger)

5.3.6 VERTICAL AND HORIZONTAL RESOLUTION: SUMMARY

In table 5.3 a summary of the depth of investigation of the resistivity tools is given. The values are rounded off in feet. These are only indicative values and it is emphasised that the actual investigation of the resistivity tools is a function of the resistivity of the mud, mudfiltrate, formation water, hydrocarbon content, porosity, borehole size and other parameters, like rock type, etc..

Depth of investigation resistivity tools	**Vertical**	**Horizontal**
(Figures are rounded off in feet)	**(ft)**	**(ft)**
SN (Short Normal)	1.5	1.5
LN (Long Normal)	5	5
Lateral	20	20
ILD Induction deep (6FF40)	6	10
ILD Induction (6FF27)	4	4
ILM Induction medium	5	6
LLD (Laterolog Deep)	2	10
LLS (Laterolog Shallow)	2	2
LL3 (Laterolog 3)	3	4
LL7 (Laterolog 7)	3	4
MLI (Microlog Inverse 1 x 1")	0.2	0.2
MLN (Microlog Normal 2")	0.3	0.3
MLL (Micro-Laterolog)	0.5	0.5
MSFL (Micro-SFL)	1	0.5

Table 5. 3: : Summary of the depth of investigation of the resistivity tools

5.4 NATURAL ELECTRICAL POTENTIAL

5.4.1 ELECTRICAL POTENTIAL AND OCCURRENCE

Electrical exploration involves the search of properties created by electric current flow in the rock, recognised at a surface. Using electrical methods, one can measure natural or artificial potentials, currents and electromagnetic fields in the rock. It is the large difference in electrical conductivity of various rock/mineral types that make the electrical methodologies feasible. Electrical methods that use a natural source are; self-potential, telluric currents/magnetotellurics, audio-frequency magnetic fields and resistivity.

Several electrical properties of rocks and minerals are significant in electrical prospecting. They are natural electrical potentials, electrical conductivity (or the inverse, electrical resistivity) and the dielectric constant. In this chapters we will study the electrical potentials of rocks and minerals. Certain natural or spontaneous potentials phenomena in the subsurface are induced by electrochemical or mechanical activity. Normally the controlling factor is the presence of fluid matter in the sub-surface (fig. 5.18). Potentials are associated with:

- weathering of (sulphide) mineral bodies,
- variation in rock properties (mineral content) at layer contacts,
- bio-electric activity of organic material,
- corrosion,
- thermal and pressure gradient

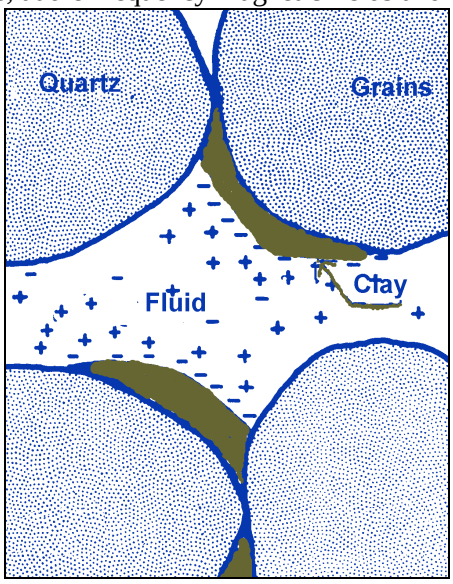

Figure 5.18:Example of charge distribution between minerals

5.4.2 ORIGIN OF ELECTRICAL POTENTIALS

One mechanical mechanism and three chemical mechanisms produce these potentials:

1. **Electrokinetic potential or streaming potential:** This is a well known effect that is shown when a solution of electrical resistivity and viscosity is forced through a capillary or porous medium.
2. **Liquid-junction (or diffusion) potential:** This is due to the difference in mobility of various ions in solutions of different concentrations.
3. **Shale (or Nernst) potential:** When two identical metal electrodes are immersed in a homogeneous solution, there is no potential difference between them. However, if the concentration at the two electrodes varies, then there is a potential difference. This associated diffusion and Nernst potentials are also known as the electrochemical, or static self-potential.
4. **Mineralization potential**. Two different metal electrodes dipped in an aqueous concentration give a potential difference. This electrolytic contact potential and the static self-potential cause large potentials associated with layers and mineral zones. They are known as mineralization potentials. These potentials, usually in zones containing sulphides, graphite and magnetite, are large when compared to the potentials of the preceding sections.
5. Further the magnitude of the static self-potential depends on **temperature**. This thermal effect is resembling to the pressure difference in streaming potential and is of minor importance.
6. **Erratic potentials,** sometimes present, are:
   - Metal corrosion (underground pipes, cables, etc.)
   - Large-scale earth currents induced from the ionosphere, nuclear blasts, thunderstorms
   - Currents of bio-electric origin flowing, for instance, in plant roots are also a source of earth potentials.

Most of the earth potentials discussed above are relatively permanent in time and place.

5.4.3 METHOD OF APPROACH AND APPLICATIONS

In a comprehensive way; for the interpretation of borehole information on groundwater, formation water and minerals, electric currents are propagated in rocks and minerals in three ways:

a) electronic: The first is the normal type of current flow in materials containing free electrons, such as the metals.

b) electrolytic: In an electrolyte the current is carried by ions at a comparatively slow rate.

c) dielectric: Dielectric conduction takes place in poor conductors or insulators, which have very few free carriers or none at all. Under the influence of an external varying electric field, the atomic electrons are displaced slightly with respect to their nuclei; this slight relative separation of negative.

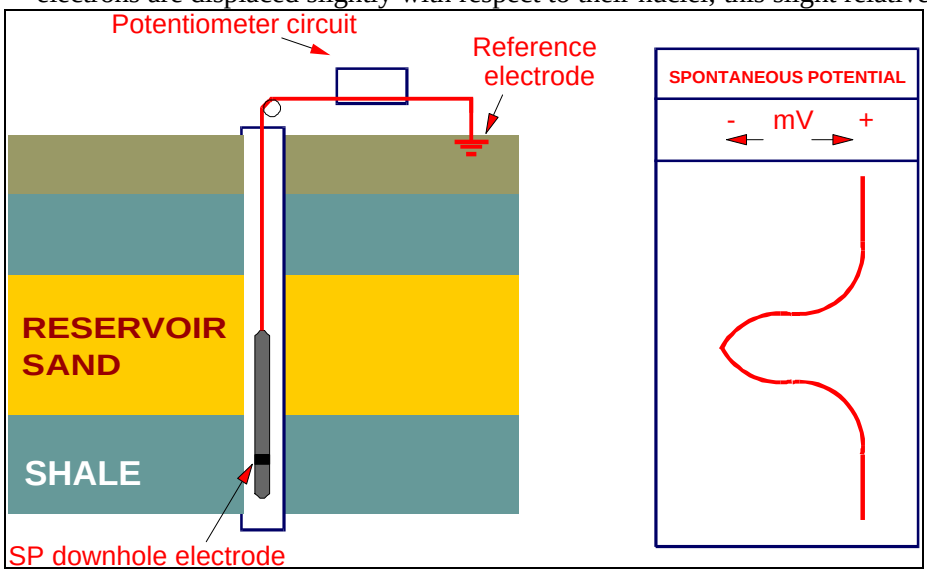

Figure 5.19: Sketch of a spontaneous potential measurement in a drill hole

The spontaneous potential (or SP) curve reflects the potential difference between a movable electrode in the borehole and a fixed reference electrode at the surface as depicted in figure 5.19. In the shale zone the SP readings are usually fairly constant and tend to follow a straight line, called the **shale base line**. In the sandy zone or in permeable formations the SP shows deviations from the shale base line to one or more **sand line** levels. Depending on the relative salinity of the formation water and the mudfiltrate, the deflection may be to the left or the right of the shale base line. The SP effect is produced by two components : the electro-chemical and the electro-kinetic potentials.

The main applications for SP-measurements are:

- Groundwater control
- Determination of formation water resistivity
- Determination of the environment of deposition
  - Evaluation of lithologies such as shale and coal
  - Determination of the shale content of a layer
- Detection of permeable beds and their boundaries
- Well to well correlation

5.5 THE ELECTROCHEMICAL COMPONENT

The electro-chemical component *Ec* consists of the Liquid junction potential (*Ej*) and the membrane potential (*Em*). These potentials create a current that flows at the shale - reservoir interface. When a reference electrode is moved across this interface a potential difference is measured.

The mud-weight is usually higher than the formation fluid pressure. This produces an over-pressure at the face of the reservoir exposed by the borehole and causes mudfiltrate to invade the reservoir.

Thereafter a mudcake is formed and the fluid invasion slows down. An invasion profile as shown in Figure 5.20.b. is formed. In this case the mudcake separates a high saline formation water and a low salinity mudfiltrate.

5.5.1 LIQUID JUNCTION POTENTIAL

The liquid junction potential Ej is created at the interface between the invaded and the uncontaminated zone, due to a salinity difference between mud filtrate and formation water. Since the negative Cl^- ions, assuming a NaCl solution, have a greater mobility than the positive Na^+-ions, the net result is a flow of negative charges, of Cl^- ions, from the more concentrated solution to the less concentrated solution. This mechanism, driven by the conductivity difference the mudfiltrate and formation water, is further explained in figure 5.20.c.

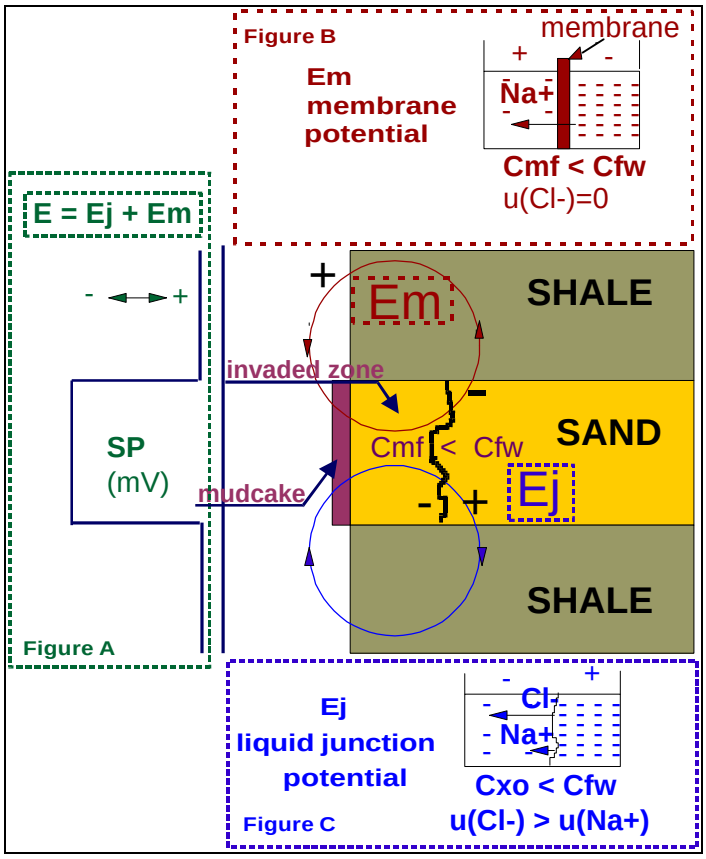

Figure 5. 20: Scheme of potentials measured with the SP.

5.5.2 MEMBRANE POTENTIAL

Figure 5.20.b shows that the membrane potential "Em" is functioning across the shale, between the uncontaminated zone in the reservoir and the mud in the borehole. Shales can act as membranes, which means that they are permeable for one type of ion and a barrier for other types. This property is called ionic perm-selectivity. Its result is that the shale-membrane can preferentially prevent the movement of negative ions. Shales are cation exchangers; they are electro-negative and therefore repel anions. In most instances the shales are 100% effective and therefore repel all the chlorine ions. The positive sodium ions move toward the lower salinity mud in the borehole and the chlorine ions cannot follow this movement. As a result a positive potential is generated toward the low concentration NaCl solution.

Considering that at the interface shale / reservoir a current is created by the Ej and Em potentials which act in series. Ej has a positive value toward the uncontaminated zone containing formation water. In contrast Em is positive toward the mud in the borehole, which has the lower NaCl concentration.

The magnitude of both the liquid junction potential and the membrane potential depends on the difference in ion concentration of the mud (filtrate) and the uncontaminated formation water. Both they can be expressed as :

$$E = k.log\frac{Con_w}{Con_{mf}} \qquad \text{(eq. 5.22)}$$

Here Con_W and Con_{MF} are the ion concentrations in respectively the formation water and the mudfiltrate that produce the Ej and Em potentials. Con_W and Con_{MF} are inversely proportional to respectively the resistivity *Rw* of the formation water and *Rmf* the resistivity of the mudfiltrate. The constant *k* is

different for the *Ej* and the *Em* potential but the equivalence of the relations allows the combination into one effective potential E:

$$E = E_j + E_m = (-71).log\frac{R_{mf}}{R_{wf}} \qquad \text{(eq.5.23)}$$

With *E* expressed in mV, and the factor (-71) as the combination of the "*k*" constants. Normally the resistivity of the mudfiltrate *Rmf* is measured at the wellsite at room temperature. The SP measures the potential *E* at borehole temperature and the *Rmf* should therefore be corrected for this temperature difference. Using equation 6.2 and the measured values for *E* and *Rmf*, the resistivity of the uncontaminated water in the formation *Rw* can be calculated. From the value of *Rw* the formation water salinity can be derived taking into account the reservoir temperature.

5.6 ELECTROKINETIC COMPONENT

In the foregoing the "streaming potential" caused by the movement of the mudfiltrate through the mudcake has been ignored. Like the shale layers, the mudcake acts also as a membrane that hinders the movement of the negative ions. A potential difference "*Ek*" is thereby generated, and the SP has to be corrected for this electrokinetic component. The value of *Ek* can be obtained from laboratory experiments with various muds that are in common use. For modern muds that seal the formation very effectively the streaming potential *Ek* can often be ignored.

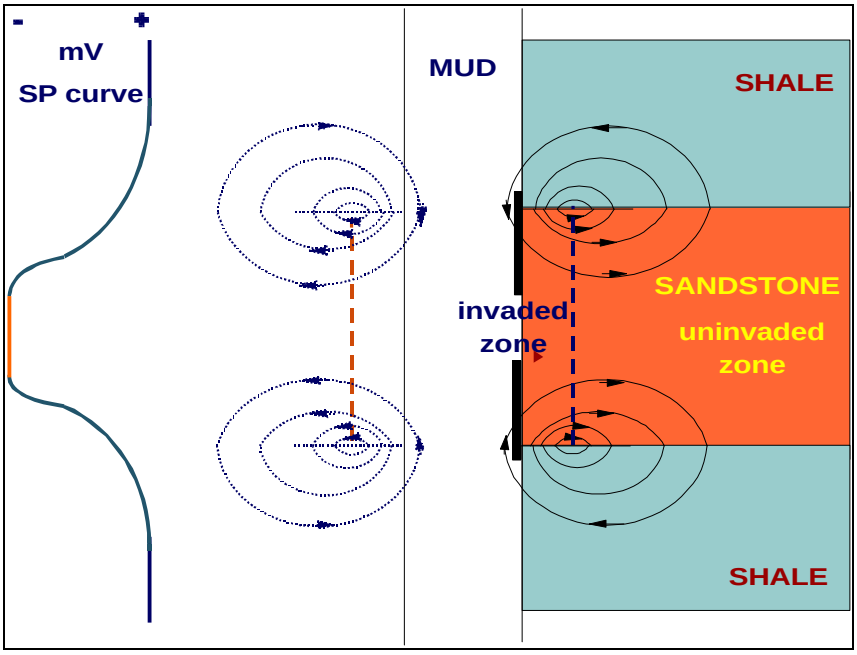

Figure 5. 21: Currents created in the mud, invaded zone, shale and sandstone, by the *Ej* , *Em*, and *Ek*.

5.7 THE COMBINATION OF SP COMPONENTS

The combined junction- , kinetic-, streaming- and membrane potentials, create a current through the shale/reservoir interface, as illustrated in figure 5.21. The currents created by this series of potentials flow through 5 different media, each with its own resistivity:

1. the borehole filled with mud (*Rm*),
2. the mudcake (*Rmc*),
3. the invaded zone filled with mudfiltrate (*Rxo*),
4. virgin zone filled with uncontaminated fluids (*Rt*),
5. the surrounding shales (*Rsh*).

In each medium the potential along a line of current flow (*I*) drops in proportion to the resistance that is encountered.

$$E_{total} = I \cdot R_m + I \cdot R_{mc} + I \cdot R_{xo} + I \cdot R_t + I \cdot R_{sh} \qquad \text{(eq.5.24)}$$

Hence, the driving force behind the potential (E_{total}) can be expressed as :

$$E_{total} = E_m + E_j + E_{kmc} + E_{ksh} \qquad \text{(eq. 5.25)}$$

As mentioned in the previous section the streaming potentials E_{kmc} over the mudcake and E_{ksh} through the shale are often ignored. The SP often is used to estimate the groundwater or formation water salinity in exploration wells in which no production has taken place, and formation water samples have not been analysed.

Clay	Density (g/cm^3)	Hydrogen (%)	Average Q_{CEC} (meq/g)
Kaolinite $Al_4(Si_4O_{10})(OH)_8$	2.69	1.5	0.03
Illite $K_{1-1.5}Al_4(Si_{6.5-7.0}\ Al_{1-1.5}O_{20})(OH)_4$	2.76	0.5	0.20
Montmorillonite $(½Ca,Na)_{0.7}(Al,Mg,Fe)_4(Si,Al_8O_{20})(OH)_4$	2.33	0.5	1.0
Chlorite $(Mg,Al,Fe)_{12}(Si,Al)_8O_{20}(OH)_{16}$	2.77	1.2	0.0

Table 5. 4: Clay properties that contribute to changes in the spontaneous potential of shaly sediments.

5.8 SHALE VOLUME CALCULATION

The presence of shale in the reservoir suppresses the SP. The shale volume can be calculated from the SP as follows :

$$V_{sh} = \frac{PSP - SSP}{SSP} \qquad \text{(eq. 6.5)}$$

with,

Vsh : the shale volume as fraction of the bulk volume in %

PSP : the SP log reading of a shaly reservoir as a deflection from the shale base line corrected for environmental effects such as mud resistivity Rm,. The SP electrode only measures a potential deflection while travelling uphole ($SP = I \times Rm$).

SSP : the SP log reading in a clean reservoir as the deflection from the shale base line corrected for environmental effects. The SSP can be obtained by taking the SP reading in the thickest and cleanest reservoir.

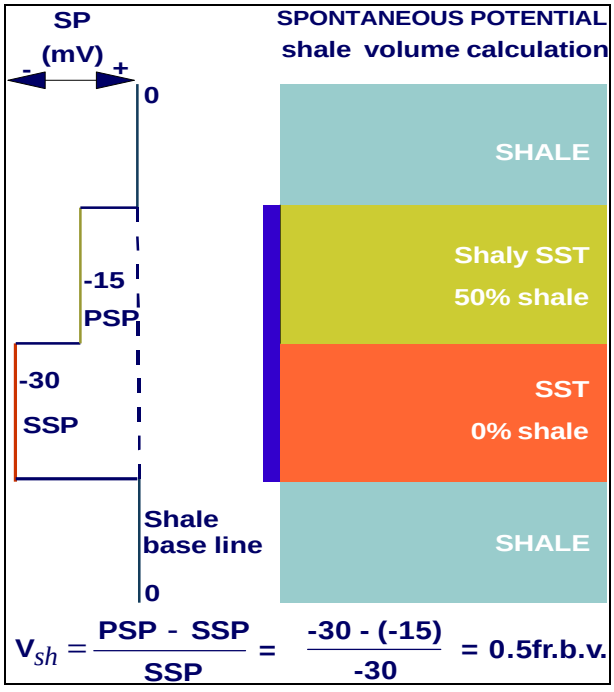

Figure 5.22: Shale volume calculation example using the SP

5.9 GEOLOGICAL INFORMATION

The environment of deposition is often indicated by the log shape. Examples for a channel sand, barrier bar, beach sand and deltaic section are shown in the figures 6.6 a-d. As shown, the grain size plays an important role. At low energy sedimentary environments a higher amount of clays can be deposited. As shown, the contribution of clays in the sub-surface and related formation water content, also gives an extra contribution to the E_{ksh}.

As shown in figure 5.23, shale content determines the shape of the SP-curve. For this reason many

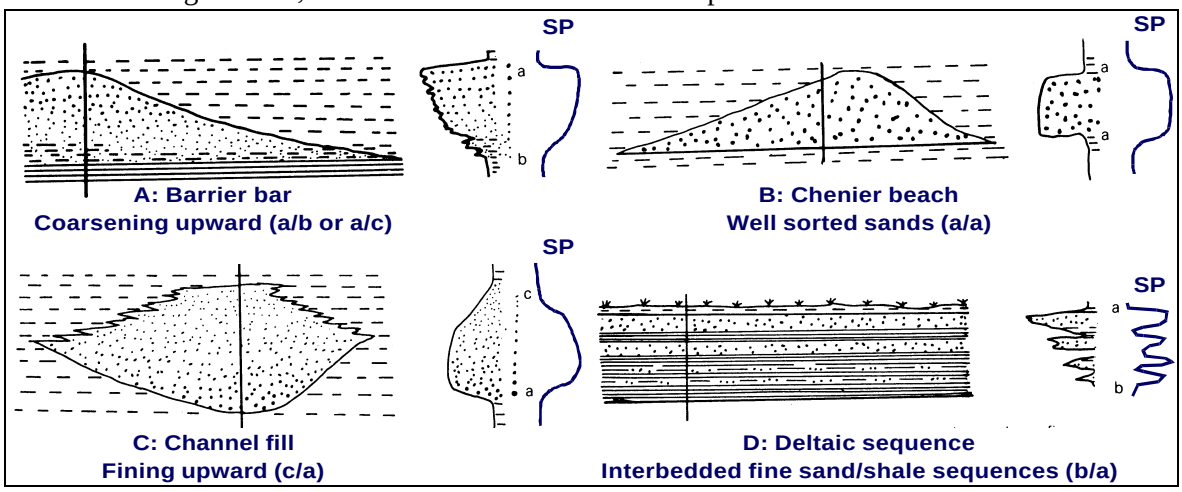

Figure 5. 23: Typical geometries of SP-curves for sandstone environments (revised after Tizzard et al., Bull. Can. Petr. Geol., 1975)

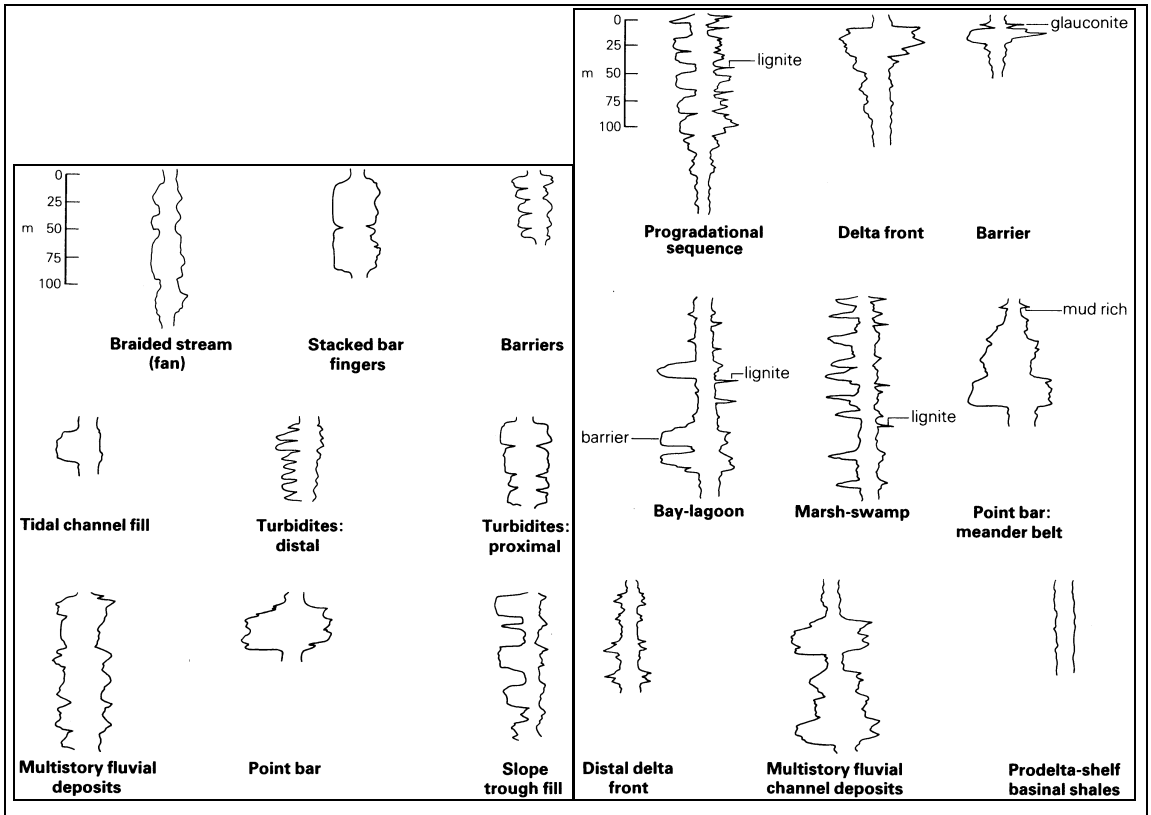

Figure 5. 24:Schematic representations of SP/Resistivity log patterns: The left group shows sand rich depositions; note the blocky appearance. The right group shows the variety of sand/shale depositional environments. (revised after Gracia, AAPG bull., 1981)

sedimentary environments are characterised on their SP-shape. During a log-analysis and correlation session, all wells in a certain geological area, can be correlated, in order to define the lateral continuity of shales, sands and other rock types. The figures 5.24 and 5.25 show various type curves for both, SP and resistivity logs.

5.10 THE EFFECT OF THE SHALINESS - Q_v

As shown, the SP is very sensitive to the presence of shale or clay in permeable formations, in which only the electrochemical contribution is affected. As already shown in figure 5.18 and 5.25, clay or phyllosilicates, do have highly reactive surface exchanging ions, such as Ca, Mg, K, Na, etc., which create an additional conductivity. This conductivity is expressed as the "Cation Exchange Capacity", or CEC, which can be defined as:
The amount of positive ion substitution that occurs per unit weight of dry rock. This expression is valued in units milli-equivalents per one hundred grams of dry rock; meg./100 g. In equations CEC is expressed as "Q_V", which is defined as the cation-exchange capacity per unit pore volume; meq/l.

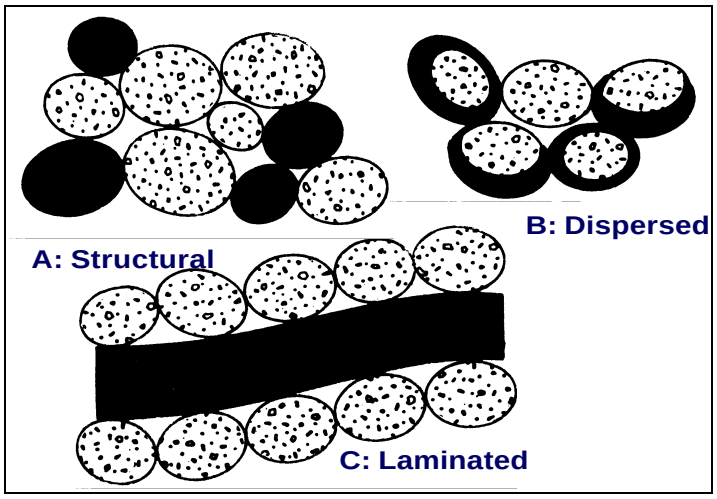

Figure 5. 25: Three types of clay distribution in a permeous sand aggregate.

The Q_V of a pure shale is considered to be equal to 1. In the Shell laboratories, Q_V, the "Cation Exchange Capacity" was determined for a series of shales in relation to their water salinity (C_{NaCl}). The example in figure 5.27, shows such a relation

Three methods are valid for measuring the Cation Exchange Capacity:

1. **Conductivity measurements** at multiple fluid salinities. The method is non-destructive and described in the next section, that discuss the Waxman-Smits equation.
2. **The wet chemistry technique**: The method is destructive because the sample is grinded. Via a titration technique with ammonium acetate the number of positive exchange ions are established. The CEC increases for the same sample when the grinded particles become smaller. Therefore one has to be careful with this method.
3. **The membrane Potential**: The method is non-destructive by measuring the membrane-potential on a sample. Than the Q_V can be calculated.

The most reliable method is considered to be the conductivity method. Another method of obtaining the Q_V of a reservoir is solving the water-bearing equation in a water-bearing zone when the other parameters are known by other means.

5.11 A WATER SATURATION EQUATION: PRACTICE

The effect of clay is that it reduces the resistivity and consequently the derived hydrocarbon saturation calculated with Archie is too low. There are two types of saturation equations that can correct for the extra conductivity caused by the shale. The shale volume and cation exchange capacity method. Here we discuss the latter.

5.11.1 CEC BY WAXMAN-SMITS

The first CEC-method was developed by Waxman and Smits (1968). Their equation relates the electrical conductivity of a shaly sand to the water conductivity and the cation exchange capacity per unit pore volume of the rock, Q_V. The method is assumed to be independent of the clay distribution.

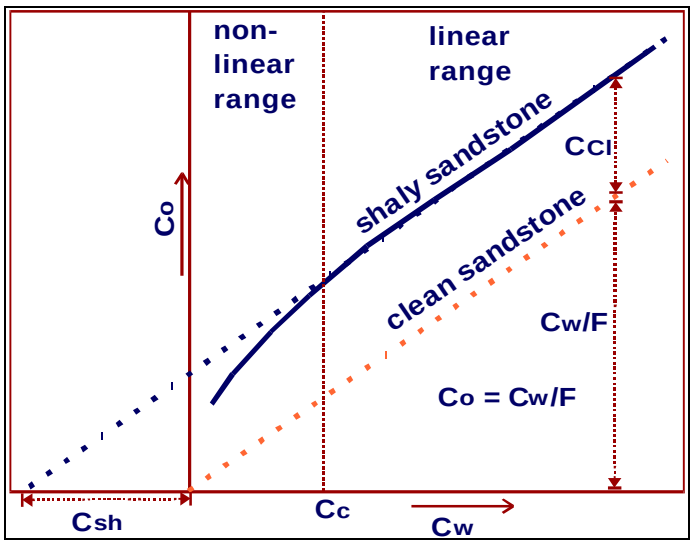

Figure 5.26: Relation between clean sand, clay content, formation conductivity and water conductivity.

5.11.2 WATER BEARING RESERVOIRS

The conductivity of the shaly water bearing sand is expressed by the equation:

$$C_0 = \frac{1}{F^*}\left(C_w + C_e\right) \qquad \text{(eq. 5.27)}$$

where:

*F** : formation factor corrected for shale
Co : conductivity of 100% water-bearing reservoir, mmho/m
Cw : conductivity of the formation water, mmho/m
Ce : conductivity of the clay fraction, mmho/m

If *Co* and *Cw* are measured in the laboratory, then *F** and *Ce* can be obtained (figure 5.26) through:

$$Ce = B \times Qv \qquad \text{(eq. 5.28)}$$

with B as the equivalent conductance of the counter-ions as a function of the solution conductivity "*Cw*" in Ohm^{-1} cm^3 meq^{-1}. The *Ce* is obtained from conductivity measurements. It is plotted versus *Qv*, which is obtained from titration techniques, for a large number of samples. The slope is more or less linear. The original article suggests that the distribution of the clays is a mixture of each type that is available. Therefore B is assumed to be independent of type, distribution and/or amount of clay in the sample. In some areas locally valid relationships between *Qv* and the total porosity have been found from laboratory data. This allows the assessment of the *Qv* distribution throughout the reservoir column based on porosity log data. The usual values of *Qv* in shaly sands range from 0.01 to 2 meq cm^{-3}.

Empirical relationships between *B* and *Rw* have been established at various temperatures. It was found that at temperatures in between 50 and 200 °C (or 120-390 °F), the product of *Rw.B* is not dependent on temperature. Therefore it can be represented as a function of water salinity alone. For temperatures ranging from 120-390 °F, the empirical relation is:

$$B \times R_w = 13.5 \times Sal^{-0.70} \qquad \text{(eq. 5.29)}$$

With; S_{al} as the salinity in g/l NaCl equiv., and; *Rw* as the formation resistivity in Ohm.m. For temperature of about 80 °F (or surface conditions), the empirical relation changes to:

$$B \times R_w = 6 \times Sal^{-0.64} \qquad \text{(eq. 5.30)}$$

5.11.3 HYDROCARBON BEARING RESERVOIRS

In hydro-carbon bearing formations the exchange ions associated with the clay become more concentrated in the remaining pore water. This concentration, *Qv'*, is related to *Qv* and *Sw*, according to the equation:

$$Q_V' = \frac{Q_V}{} \qquad \text{(eq. 5.31)}$$

Using the equations 6.6 to 6.10 and combining them with the Archie equation gives:

$$_t = \ _t^+ \ ^* \times S_{wt}^{+n*} \quad C \left(+ \frac{\times B \quad Qv}{} \right) \qquad \text{(eq. 5.32)}$$

where:

Ct : log reading of conductivity (mmho/m) corrected for borehole, bed thickness and invasion.

f_t : total porosity, fraction of bulk volume

*m** : cementation factor corrected for shale effect

Sw :water saturation, fraction of pore volume

*n** : saturation exponent corrected for shale effect

Cw : formation water conductivity

Rw : formation water resistivity

Qv : cation-exchange capacity per unit pore volume, meq/ml.

Csh : shale conductivity, mmho/m

This equation is not a simple linear function and has to be solved by iteration. If *n** has not been established from core measurements, a value of 1.8 may be used for shallow and 2.0 for deeper sands (say below 6000 ft). Juhasz developed in 1981 the normalised Qv method as showed in equation 6.12:

$$C_t = f_t^{+m*} \times S_{wt}^{+n*} \times C_w \left(1 + \frac{Qvn}{Swt} \left[\frac{Ccw}{Cw} - 1 \right] \right)$$

(eq. 5.33),

where: *Qvn* = *Qv*/*Qvsh*

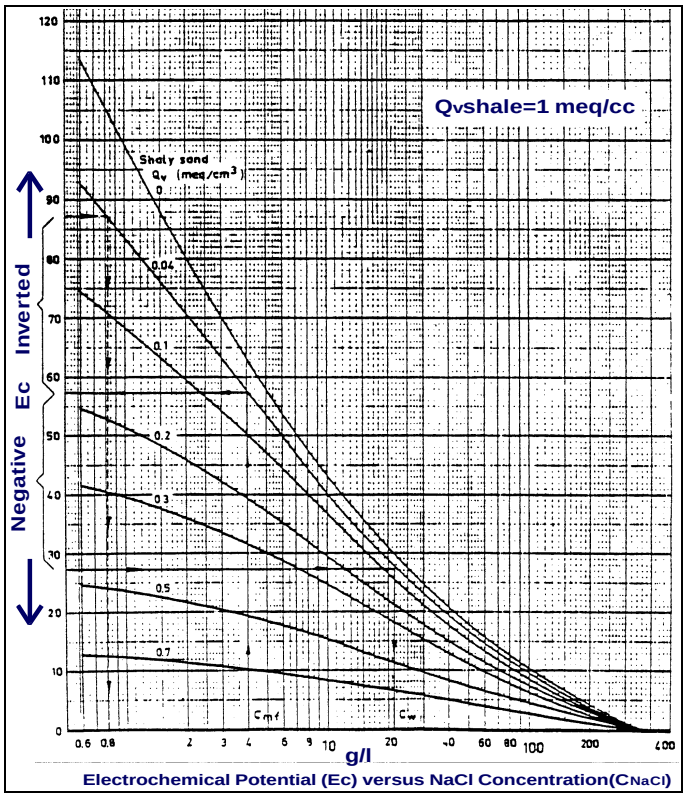

27: Example of the effects of fluid salinity on the

6. ROCK NUCLEAR BEHAVIOUR & APPLICATIONS

6.1 GENERAL INTRODUCTION

6.2. NATURAL RADIOACTIVITY

- 6.2.1. Introduction
- 6.2.2. Radioactivity of Rocks
- 6.2.3. Gamma-ray detectors

6.3. THE GAMMA-GAMMA OR DENSITY APPLICATION

- 6.3.1. Introduction
- 6.3.2. Interaction of gamma-rays and atoms
  - 6.3.2.1. Compton scattering
  - 6.3.2.2. Photo-electric effect
  - 6.3.2.3. Pair Production
- 6.3.3. Density of the sedimentary rock
- 6.3.4. Photo-electric effect of the reservoir
- 6.3.5. Explanation of tools, environmental qualities and log readings
  - 6.3.5.1. Density tool configuration
  - 6.3.5.2. Mudcake compensation
  - 6.3.5.3. Density log characteristics
  - 6.3.5.4. Calibration
- 6.3.6. Applications of density logging tools

6.4. NEUTRON LOGS

6.1 GENERAL INTRODUCTION

Each element in the periodic table of elements has its own number of electrons, protons, neutrons and mass. As already discussed in chapter 3, the use of an electron charge on one spot gives a reflection product which consist of various wavelengths, with various amplitudes and (if needed) under various reflection angles. These factors can be used to identify specific elements or minerals (X.R.D., X.R.F., and Microprobe). In addition many elements are isotopes with specific decay times and related natural radiation or natural radioactivity. These properties can be measured with borehole- instruments, which can be divided into:

- a passive group groups that measures the **natural radioactivity,** usually by means of recording the gamma-rays that are emitted by elements in the formation, and,
- an active group, that contain both a radioactive source and detectors, and measures the **induced radioactivity** by means of a radioactive source. This source emits neutrons or gamma rays that penetrate the borehole and the surrounding formation.

In contradiction to electric logs, which are described in the previous chapter, the radioactivity or nuclear logs can be used through well casing.

Three types of radioactivity borehole-measurement apparatuses are normally used in combination:

1. **The gamma-ray application.**
   It is used to distinguish argillaceous rocks from non-argillaceous rocks. The first group shows to be more radioactive. Nevertheless, feldspathic sandstones, which are originally from igneous rock (high K-content in granite, gneiss, etc.), can be highly radioactive when compared to neighbouring shales. Consequently in clastic basins with much feldspathic sandstones the usefulness of the gamma-ray curve is reduced.
2. **The gamma-gamma, or density application.**
   It is used for rock porosity determination. A high-velocity gamma radiation source is pushed at a borehole wall and the rays are emitted into the formation. The amount of backscattering of the gamma radiation created by collisions with the mineral electrons, is measured. This measurement is directly related to the electron density and by that to the true bulk density. Further it is inversely related to the porosity.
3. **The neutron application.**
   Neutrons are able to follow the abundance of hydrogen nuclei in fluids, or, the higher the content, the lower the reading. All solutions in and around a borehole accommodate hydrogen, which "consumes" neutrons. For that reason porous rocks give low counts. Neutron logging shows variations in carbonate porosities. Accordingly they are logged by compensated neutron-density logs. Differences between water, oil, and mud filtrate cannot be distinguished by neutron detection, because of the corresponding percentage of hydrogen nuclei. Conversely dry gas shows very high neutron readings; there are hardly any hydrogen nuclei in the gas phase when compared to the liquid phase.

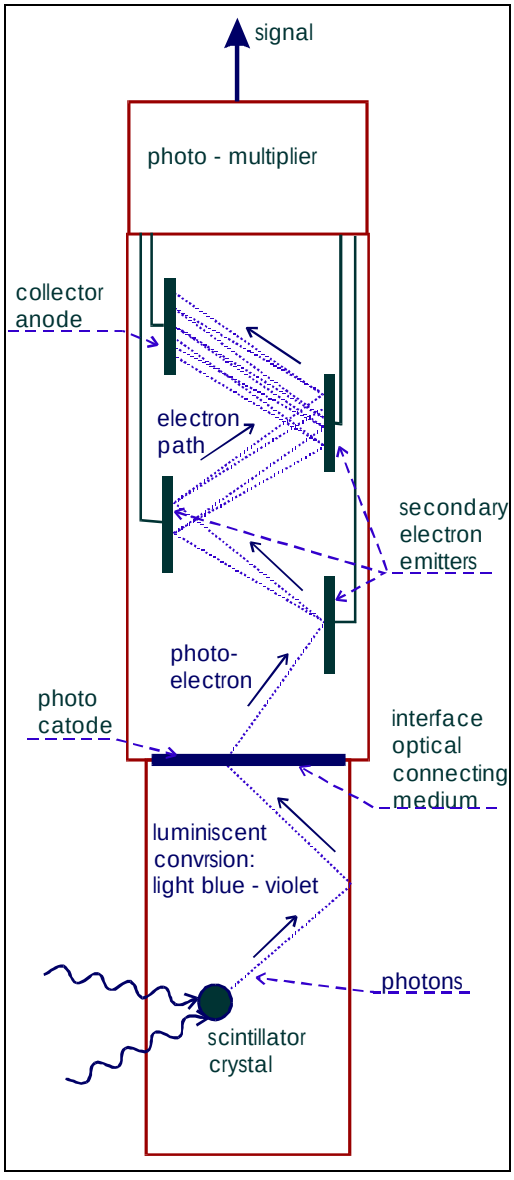

Figure 6. 1: Schematic view of a scintillator and photo-multiplier tube: The basic principle for gamma-ray detection

In this chapter the principles of electron/neutron emission and registration are explained in relation to rock properties and tools for application. The methods are used in:

- Groundwater detection,
- Oil/gas exploration,
- Coal exploration
- Civil Engineering purposes (in other tool modifications; dredging, tunnelling, foundations, etc.)

6.2 NATURAL RADIOACTIVITY

6.2.1 INTRODUCTION

This section deals exclusively with natural radioactivity. Radioactivity is associated with the structure of the elements. An element contains protons and neutrons in its nucleus and electrons in one or more orbits. Its unique number of protons (Z) identifies each element. The majority of the elements consist of a mixture of two or more isotopes. Isotopes have the same number of protons but a different number of neutrons. Many isotopes are not stable and emit alpha, beta and/or gamma radiation, in order to permute to stable isotopes. Since beta- and alpha particles have a very limited penetration depth, often less than one cm in dense or heavy materials, the gamma-radiation is recorded with logging equipment in wells. Gamma rays, or photons, have a considerable penetration depth and even allow recording of natural gamma-radiation emitted by rocks through a steel casing.

6.2.2 RADIOACTIVITY OF ROCKS

Unstable elements of significant abundance that contribute to the natural gamma-radiation are:

- U-Ra : uranium-radium elements and their unstable daughter series of elements
- Th : thorium series
- K40 : potassium - 40 isotope.

The U-Ra and Th isotope series expose a wide range of energies, whereas Potassium - 40 radiates gamma rays with one single radiation energy (1.46 MeV). The radiation intensity (photons per gram per second) is shown in table 6.1

Radiation intensity photons/g.s	**Isotope series**
26000	U - RA
12000	Th
3	K^{40}

Table 6. 1: Radiation intensity of the main isotopes.

The basic constituents of igneous rocks are:

- quartz, with a low degree of radioactivity
- feldspars and mica's, with K^{40} and sometimes U-Ra and Th

During rock weathering, sedimentological transport and diagenesis, feldspars decompose at a relatively rapid rate into clay minerals. Here radioactive-elements are trapped in the new minerals and the related rock structure. The Potassium content (0.02 vol.% of K^{40}-isotope) amounts to about 0.3% of ordinary clays (Table 6.2). As clay minerals are the principle constituents of shales, these are generally radioactive as well. Sometimes, in some shales, as much as 0.01 vol.% of U-Ra or Th is found. However, like most rules in

Lithology type	**Average Radioactivity in Radium Equivalent per Gram x 10^{-12}.**
Sand	4.1
Shaly and silty sand	7.1
Siltstone	10.3
Sandy shale	11.0
Shale	20.3
Black & grayish black shale	26.1
Calcareous sand	8.5
Limestone	3.8
Dolomite	3.1
Granite wash	6.9

Table 6. 2: Gamma-ray activities of sedimentary rock, from various sources.

geosciences, the previous mentioned general statements are hard and fast as well. Very good reservoir sands in some parts of the North Sea contain (Caledonian) mica, which contains a significant amount of radioactive potassium. They have a gamma-radiation level as high as the surrounding shales.

6.2.3 GAMMA-RAY DETECTORS

In the first measuring instruments Geiger-Müller tubes were used to detect gamma rays. These tubes have the disadvantages that the count-rates are low and that the output is not proportional to the energy of the individually detected gamma photons. Since the sixties scintillation counters are used to measure radioactivity in boreholes. These counters are based on the physical phenomenon that gamma rays, which interact with the crystal lattice, can produce secondary radiation, even in the visible light (florescence). The principle is depicted in figure 6.1. The most widely used material is Ta activated sodium iodide NaI. Other materials such a BGO (bismuth-germanium-oxide) and GSO (Gadolinium oxy-ortho-silicate) gain in popularity due to their higher density, and therefore more efficient conversion of gamma rays to scintillation.

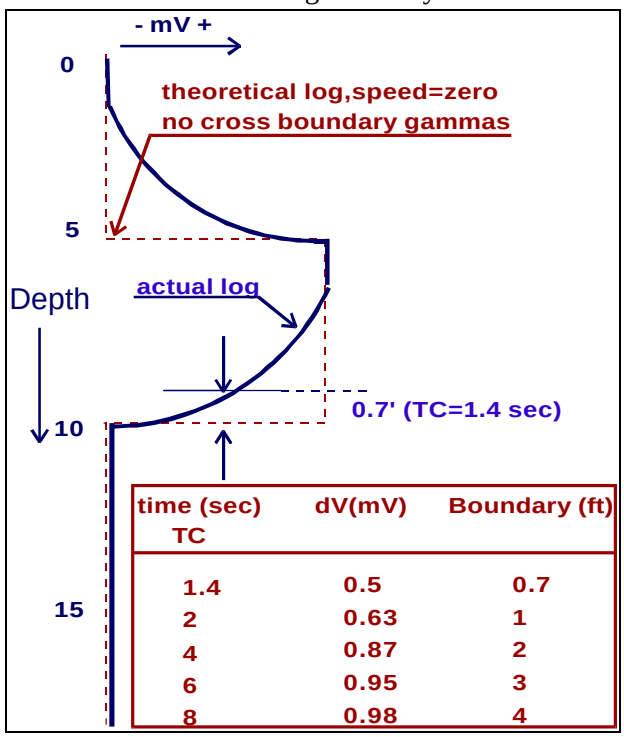

Figure 6. 2: Example of a boundary displacement gamma ray reading

The crystals are coated with a reflecting layer and the light quanta will therefore eventually hit the photo-cathode of a photo-multiplier where they dislodge one or more electrons. These electrons are in turn accelerated by a cascade circuit of electrodes, where each subsequent electrode has a higher voltage, and dislodge more electrons at each stage. This multiplication process leads to an avalanche of electrons that produce a measurable electric pulse at the last anode of the tube. An attractive feature of this technique is that the pulse height is proportional to the energy of the original gamma-photon.

Radioactive emissions are random phenomena, which vary in time and create statistical fluctuations of a gamma-ray log. In order to minimise the fluctuations, averaging is applied. In the past this was accomplished by an simple resistivity-capacitor (R-C) circuit, nowadays the averaging is carried out digitally from an analogue to a digital (A-D) conversion. A time-averaging constant TC is applied to smooth the gamma-log. The faster the tool moves through the hole the less gamma's will be counted per depth unit, and the longer time averaging period has to be to smooth out the statistical fluctuations. A theoretical example (figure 6.2) shows, for a logging speed of 1800 ft/hr and a time-averaging constant TC = 2 sec, that the time lag produces an apparent boundary displacement of about 1 foot. The averaging procedure causes a time lag on the log boundaries which increases with logging speed and TC as demonstrated in the table placed in figure 6.2. The selection of the TC is a practical compromise of logging speed and log quality (see table 6.3). The normally used standards are a speed of 1800 ft/hr and a TC of 2 sec. The

Logging speed (ft/hr)	3600	1800	1800	900
Time constant, (sec)	5	5	2	4
Statistical variations	low	low	fair	low
Travel during TC, ft	5	2.5	1	1
Thin bed definition	poor	poor	good	good

Table 6. 3: Logging speed versus log quality for the GR

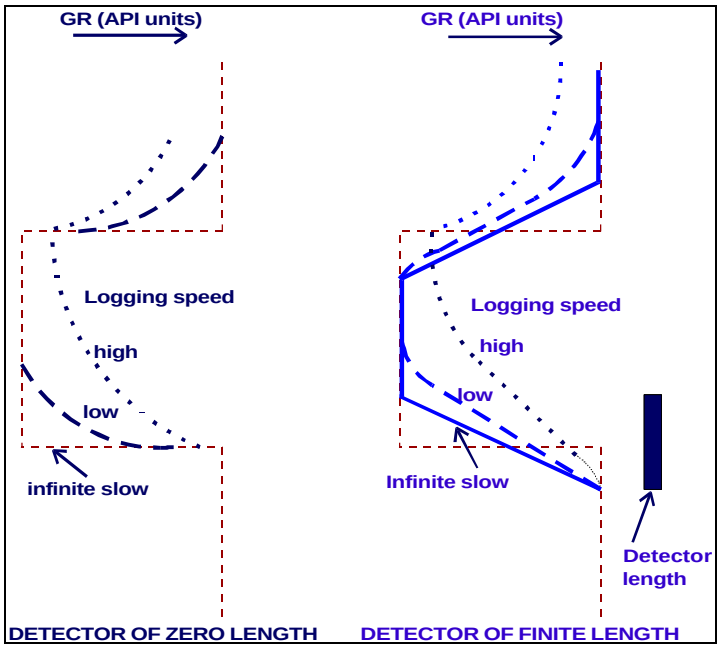

Figure 6. 3: Effects of detector length and logging speed on the shape of the gamma ray log.

parameters listed in the last column of table 6.3. can be used over short intervals for a good bed or an explicit layer definition. It is customary to maintain the product of logging speed (ft/sec) and TC (sec) at one foot. Figure 6.3 shows the GR log shapes as a function of logging speed for a fixed TC of 2 sec.

The investigation volume of the Gamma Ray tool has the shape of a sphere around the detector. The depth of investigation is determined by:

- The rock density and mud density which attenuate the gamma-rays
- The natural gamma ray energy
- The detector length; 4", 8", and occasionally 12”

An approximate value for the vertical resolution is 2 feet. The depth of investigation is about 1 foot. In figure 7.3 the effect of the detector size on the vertical resolution is explicated.

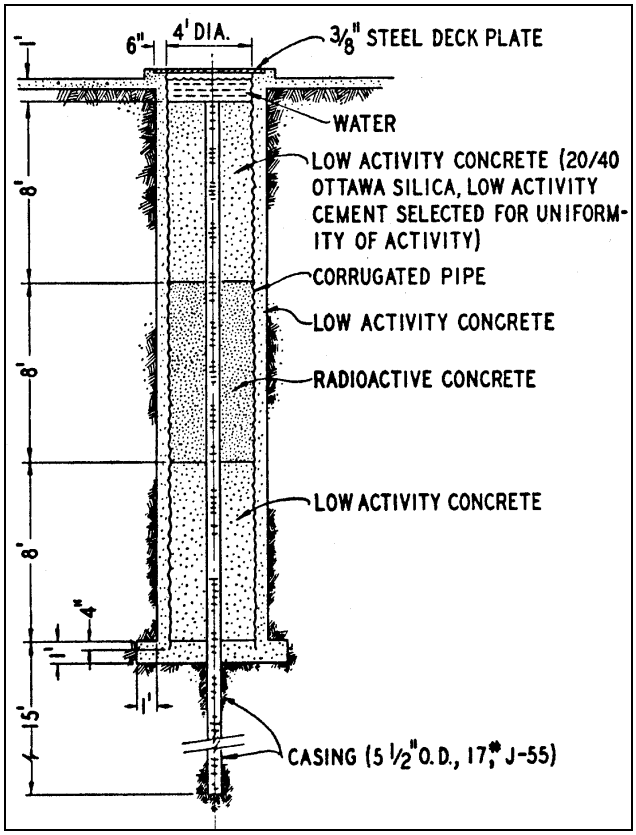

Figure 6. 4: Schematic view of the gamma ray log calibration pit.

6.2.4 CALIBRATION

The unit of gamma-ray intensity is defined by a standard calibration procedure carried out in the test pit of the University of Houston Texas (figure 7.4). The API Gamma Ray unit is 1/200 of the difference in log deflection between the two zones of different Gamma Ray intensity. In the test pit a combination of radioactive concrete with 13 ppm U, 24 ppm Th, 4% K (mica), and a layer with very low radioactive concrete is used to define this unusual API “unit”. For calibration at the well site, to check the API reading, one uses a small radioactive source placed at a fixed distance from the detector.

6.2.5 THE CALCULATION OF SHALE VOLUMES

The more or less linear behaviour of the natural gamma ray increase with the increase of clay or shale, by the presence of potassium, gives the opportunity to calculate the shale/clay-content in K-feldspar free sands. With the natural gamma ray log readings the shale volume V_{sh} can be calculated as follows:

$$V_{sh} = \frac{GR - GR_{min}}{GR_{sh} - GR_{min}} \qquad \text{(eq. 6.1)}$$

With; GR as the actual log reading corrected for environmental influences; Gr_{min} as the gamma ray reading in a clean (with no shale) interval, and; GR_{sh} as the gamma ray reading in a 100 % shale interval

An example is given in figure 6.5. This linear relation between V_{sh} and GR reading usually gives a pessimistic (too high) shale volume.

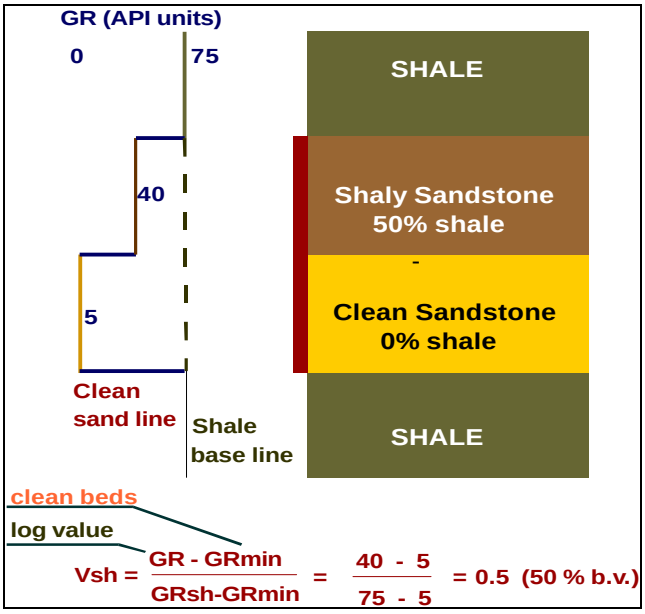

Figure 6. 5: Example of a shale volume calculation, using a clean sand and the shale base line.

6.2.6 INTERPRETATION OF ENVIRONMENT

As shown with the SP-readings, a consistency in mineral content gives the opportunity to translate a series of log readings to a rock type or even a sedimentary environment. Moreover, with various log readings it is also possible to make correlations between wells, or in one well through time. Figure 6.6 shows the log readings of various examples of sediment types and related sedimentary environments. furthermore it shows parallel the differences between gamma ray readings and neutron readings.

6.2.7 APPLICATIONS OF THE NATURAL GAMMA-RAY LOG (GR)

The main applications of the GR in lithology determination are:

- obtaining information on clay typing and shale volume estimates
- delineating reservoir rock (sand / shale separation)
- determination of the ash content of coal seams
- well-to-well correlation of GR logs to recognise layer (dis-)continuities
- depth correlation of different logging runs carried out:
  - ➔ in one well,
  - ➔ through a casing,
  - ➔ as a correlation between production logs,
  - ➔ for perforating guns,
  - ➔ for formation testers, and,
  - ➔ for open hole logs.
- the indication of environment of deposition and its lateral extension (comparable with SP log applications).
- detection of radioactive evaporates - sylvite (KCl)

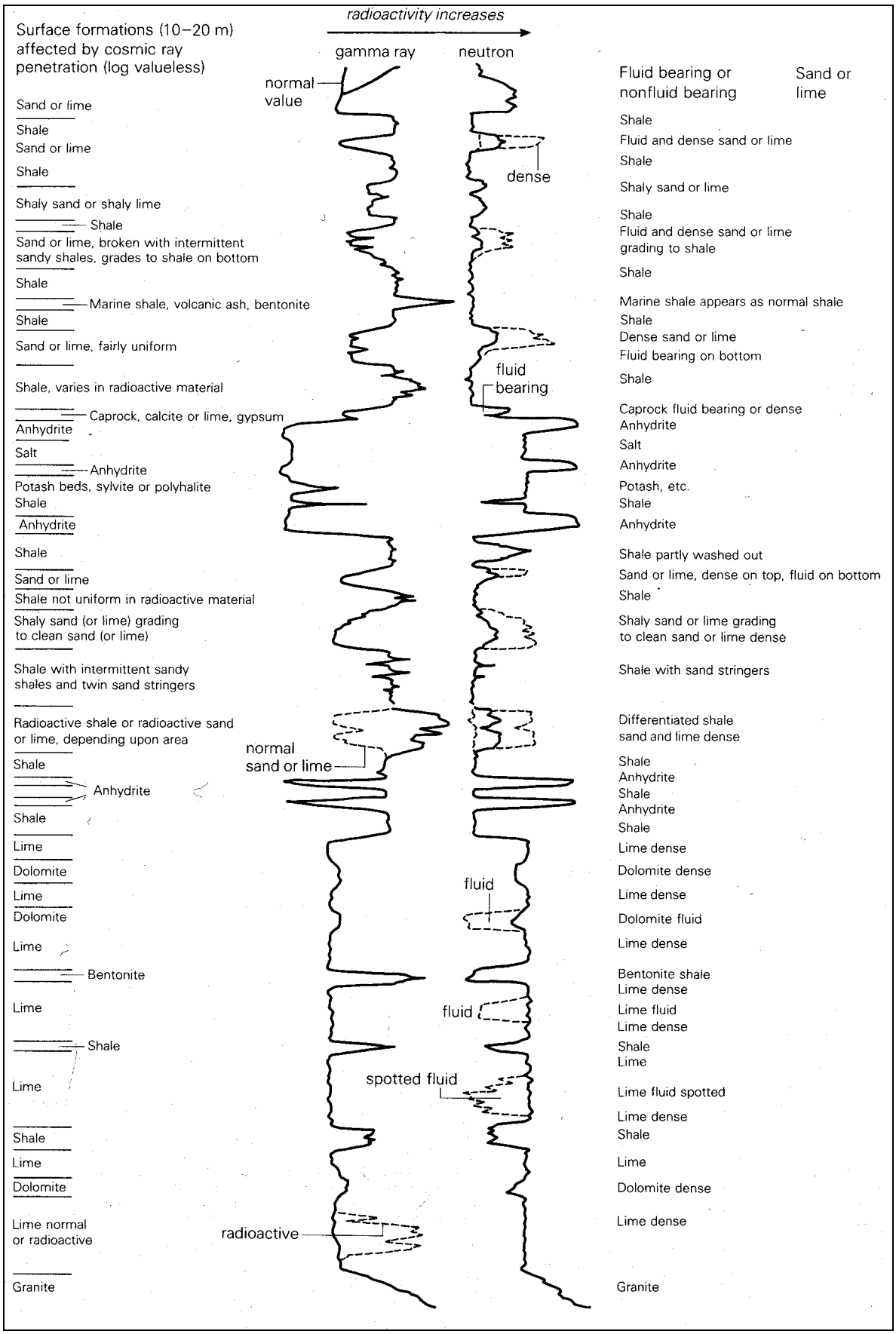

Figure 6.6: Gamma-ray and gamma-gamma log readings. Examples from various sedimentary environments

6.3 THE GAMMA-GAMMA, OR DENSITY APPLICATION.

6.3.1 INTRODUCTION

In contrast to the gamma ray, which only contains a passive detector, the density tool contains a chemical gamma-ray source, consisting of the isotopes Caesium 137 or Cobalt 60, and two ore more gamma-ray detectors. The density tool is therefore called an induced gamma or gamma-gamma tool. The induced gamma rays are scattered by the rock and only a few reach one of the gamma-ray detectors in the tool (figure 6.7). The basic principle shows that a higher density of the rock material will attenuate more of the gamma rays and less will reach the detectors. The use of the gamma-gamma tool for density measurements is based on this attenuation phenomenon.

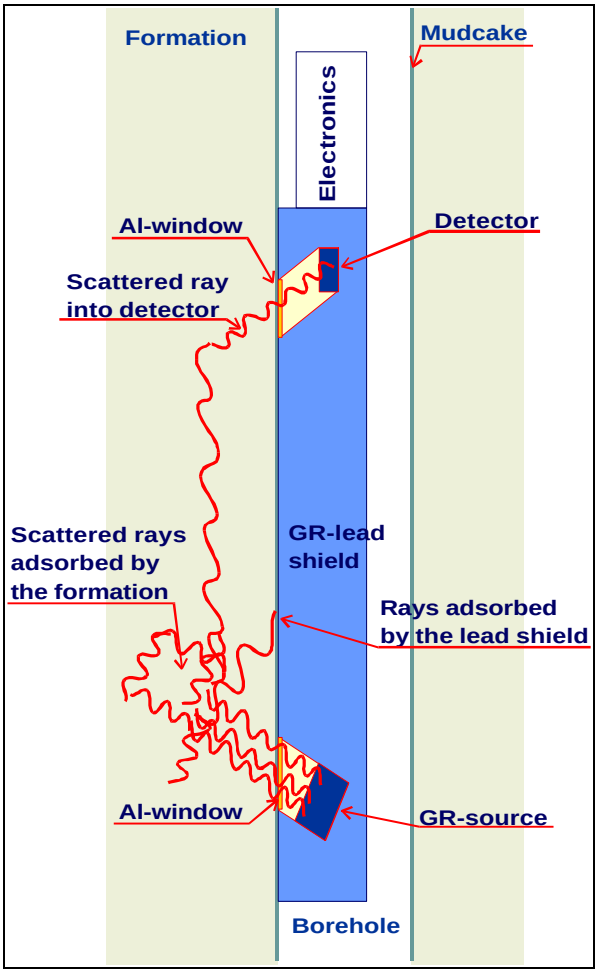

Figure 6.7: A sketch of a single gamma-gamma density tool

6.3.2 INTERACTION OF GAMMA-RAYS AND ATOMS

There are 3 ways for an atom to interact with gamma rays as depicted in figure 6.8:
1: Compton scattering
2: Photoelectric effect
3: Pair production

6.3.2.1 COMPTON SCATTERING

The high-energy gamma rays emitted by the source collide with the electrons in the formation. At each collision the photon loses some of its energy to an electron, which can be ejected from its orbit. The scattered gamma ray has less energy than the gamma ray that caused the collision, and the energy level of the scattered gamma ray is strongly dependent on the collision angle. When the number of gamma rays is recorded as a function of their energy in a frequency vs. energy diagram an energy spectrum is obtained. The energy spectrum of the scattered gammas is the well-known Compton continuum.

6.3.2.2 PHOTO-ELECTRIC EFFECT

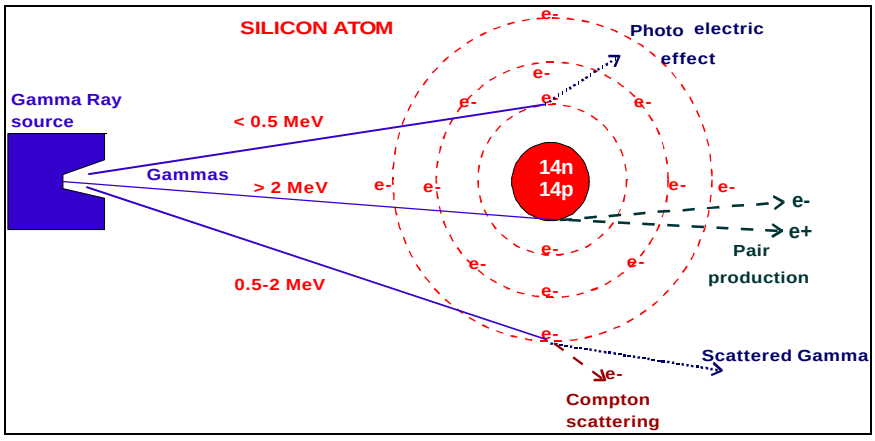

Figure 6. 8: Various interactions between gamma rays and the Si atom

After several collisions the gamma rays that result have lower energies (< 0.5 MeV). Below this energy level, the photoelectric effect becomes predominant. Then the gamma rays can interact with the electrons of the inner bands. The gamma energy is used to push an electron into a higher band. If the electron falls back to the original band gamma

rays are emitted with energies characteristic for the atomic number.

6.3.2.3 PAIR PRODUCTION

In this process the high energy photon (>2 MeV) looses all it's energy and the gamma-ray is converted into an electron and a positron. The positron combines almost immediately with another electron and two gamma rays each with an energy of 1.04 MeV are emitted in opposite directions. The density tools use sources that emit gamma rays with energies below 2 MeV, hence pair production will not be further discussed in the context of gamma-gamma logging.

When a beam of gamma-rays with initial intensity I_0 is scattered by a slab of material with thickness "x" resulting in an intensity I at the other side of the slab, the following relation is valid :

$$I = I_0.e^{-m.x} \qquad \text{(eq. 6.2)}$$

or

$$ln\frac{I}{I_0} = -m.x \qquad \text{(eq. 6.3)}$$

In other words, the logarithm of the ratio of intensities of the attenuated and the original beams is proportional to a) the slab thickness and b) a proportionality factor m. Here m is defined as the mass absorption coefficient. In figure 6.9 the mass absorption coefficient, expressed in cm^2/g, is plotted against the energy of the gamma rays. The lines indicate the probability that one of the three interactions described above will occur as a function of the gamma-ray energy.

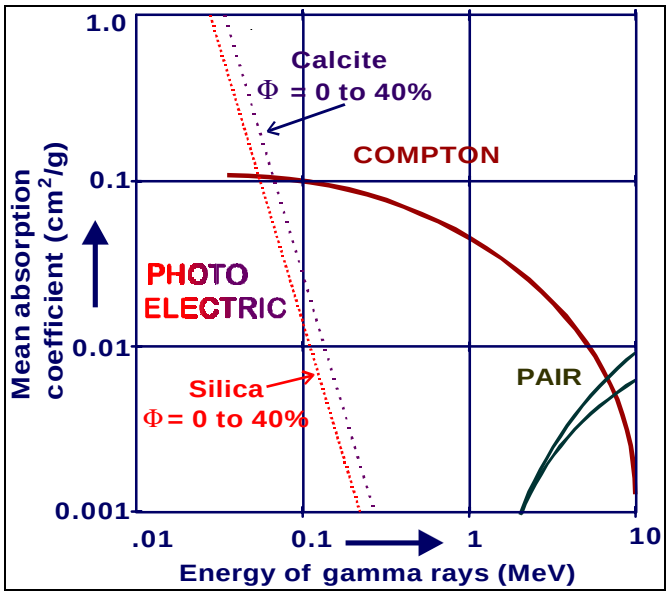

Figure 6. 9: Gamma ray mass absorption coefficient over the energy range of interest. (Revised after Tittman and Wahl, 1965)

6.3.3 DENSITY OF THE SEDIMENTARY ROCK

At the distance of some 20 - 30 cm between source and detector the gamma rays usually scatter two to three times before some of them reach the detector. The number of collisions between the electrons and gamma's is directly related to the number of electrons in the formation. A low count is indicative for a high number of electrons and thus for a high-density formation. In essence, the response of the density tool is determined by the electron density ρ_e that is related to the bulk density as follows:

$$r_e = \frac{N.Z.r_b}{A} \qquad \text{(eq. 6.4)}$$

with:

r_e : electron density in number per volume unit

N : Avogadro's number as $6.03 * 10^{23}$ atoms per gram atom

Z : atomic number or number of protons, which is dimensionless

r_b : as the bulk density, in $g.cm^{-3}$

A : as the atomic weight, which is related to number of protons and neutrons

The bulk density depends on the density of the rock material, porosity and the densities of the different phases of oil, gas and water that are present in the pore space. For most formation substances the

factor 2 (Z/A) is very close to unity (for hydrogen close to 2), as demonstrated in Table 6.4. The resulting apparent bulk density ρ_a, as seen by the tool, is related to the electron density ρ_e:

$$r_a = 1.07.r_e - 0.188 \qquad \text{(Eq. 6.5)}$$

For liquid filled sandstone, limestone and dolomite the tool that is reading ρ_a is practically identical to the actual density ρ_b, as shown in table 6.5. Corrections are required e.g. in anhydrite, sylvite, halite and also in gas bearing formations. For a number of minerals the chemical and other physical characteristics are also given.

Element	A	Z	2 Z/A
H	1.008	1	1.9841
C	12.011	6	.9991
O	16.000	8	1.0000
Na	22.99	11	.9569
Mg	24.32	12	.9868
Al	26.98	13	.9637
Si	28.09	14	.9968
S	32.07	16	.9978
Cl	35.46	17	.9588
K	39.10	19	.9719
Ca	40.08	20	.9980

Table 6. 4: 2Z /A values for various elements

6.3.4 PHOTO-ELECTRIC EFFECT OF THE RESERVOIR

Compound	Formula	Actual	2SUM(Z's)	Electron	Apparent
		density ρ_b	molar weight	density ρ_e	density (tool) ρ_a
Quartz	SiO_2	2.654	0.9985	2.650	2.648
Calcite	$CaCO_3$	2.710	0.9991	2.708	2.710
Dolomite	$CaCO_3$, $MgCO_3$	2.870	0.9977	2.863	2.876
Anhydrite	$CaSO_4$	2.960	0.9990	2.957	2.977
Anth. coal		1.4-1.8	1.030	1.442-1.852	1.355-1.796
Bitum. coal		1.2-1.5	1.060	1.272-1.590	1.173-1.514
Fresh water	H_2O	1.000	1.1101	1.110	1.00
Salt water	200.000 ppm	1.146	1.0797	1.237	1.135
"Oil"	n(CH_4)	0.850	1.1407	0.970	0.850
Methane	CH_4	ρ_{met}	1.247	1.247 ρ_{met}	1.335 ρ_{met}-0.188
"Gas"	$C_{1.1}$ $H_{4.2}$	ρ_g	1.238	1.238 ρ_g	1.325 ρ_g -0.188
In which ρ_{meth}, and ρ_g are the density of methane and composite gas respectively.					

Table 6. 5: Values related to the density tool (After Serra, 1984)

The photoelectric effect P_e curve is an index of the effective photoelectric absorption cross section of the formation. The unit of the photoelectric absorption cross section *t* is in barns (10^{-24} cm^2) per atom. As mentioned in the introduction the gamma rays of the photoelectric effect are produced when electrons in the inner bands return to their original state. The energy of these gamma rays is therefore dependent on the binding forces of electrons in the inner bands and strongly dependent on the atomic number *Z*:

$$t = K.Z^{4.6} \qquad \text{(Eq. 6.6)}$$

t : Photoelectric absorption cross section in barns per atom
Z : atomic number
K : a "relative" constant

The coefficient *K* varies with the energy level of the incident gamma rays. Dividing *t* by Z and calibrating the P_e log such that *K* is arbitrarily taken as $E^{-3.6}$, gives:

$$P_e = (Z/10)^{3.6} \qquad \text{(Eq. 6.7)}$$

Where, P_e is again the effective photoelectric absorption cross section, but now expressed in barns/electron.

To obtain a parameter that is proportional with the volume fractions of the formation constituents P_e is multiplied with the electron density. This yields the effective photoelectric absorption cross section index per unit volume $U=P_e.r_e$. Then the relative volumes of the rock and pore components can describe the formation:

$$U = \phi .U_{fl} + (1-\phi).U_{ma} \qquad \text{(eq. 6.8)}$$

The effective photoelectric absorption cross section per unit volume "U" is, as demonstrated by the equations 6.7 and 6.8, strongly dependent on the atomic number and therefore an excellent lithology indicator.

6.3.5 EXPLANATION OF TOOLS, ENVIRONMENTAL QUALITIES AND LOG READINGS

6.3.5.1 DENSITY TOOL CONFIGURATION

In order to minimise the influence of the mud column the tool features two or more gamma-ray detectors. A configuration with two detectors at approximately 8 and 16 inches from the source is shown in figure 6.10. Both the detectors and the source are mounted on a skid and shielded from the borehole. The skid, which has a plough-shaped leading edge to remove part of the mudcake, is pressed firmly against the wall by means of an eccentring arm. The two detectors are necessary to account for remaining mudcake or mud interposed between the skid and the formation. The litho-density tool (LDT) offers a combination of the density and the photoelectric absorption P_e measurements.

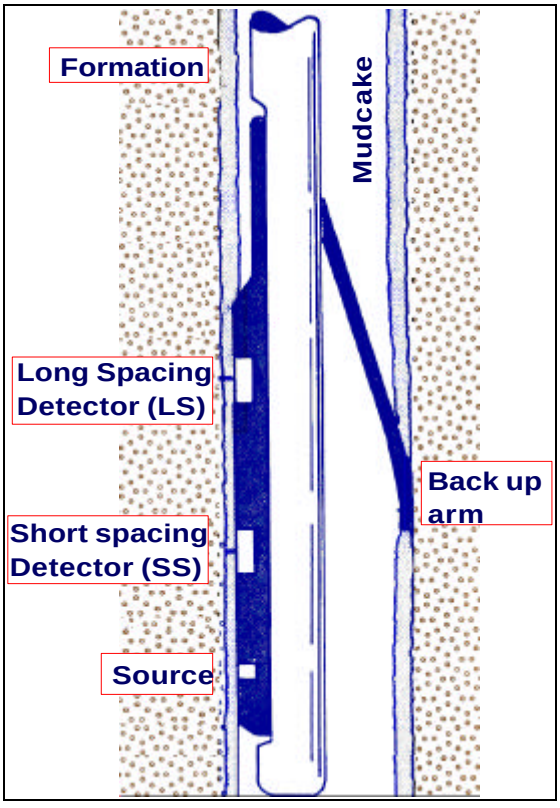

Figure 6. 10: Dual-spacing formation density log (revised after Schlumberger)

6.3.5.2 MUDCAKE COMPENSATION

Although the source and detectors are pressed against the borehole wall, there are small washouts and irregularities called hole rugosity that will affect the gamma-ray attenuation. Moreover, normally there is a thin layer of mudcake between the skid and the borehole wall. Since the two detectors have a different depths of investigation due to their short (SS) and long (LS) spacing from the source, the wash-outs and mudcake have a different effect on the SS and LS detector responses. By combination of the two responses the effect of the mudcake and small washouts can be compensated. This method is called the "spine- and ribs correction", and has been automated and incorporated in the surface computer. The density readings displayed on the log shown in figure 6.11, have already been compensated with the correction $\Delta\rho_b$. This is the difference between the densities provided by the LS and SS detectors.

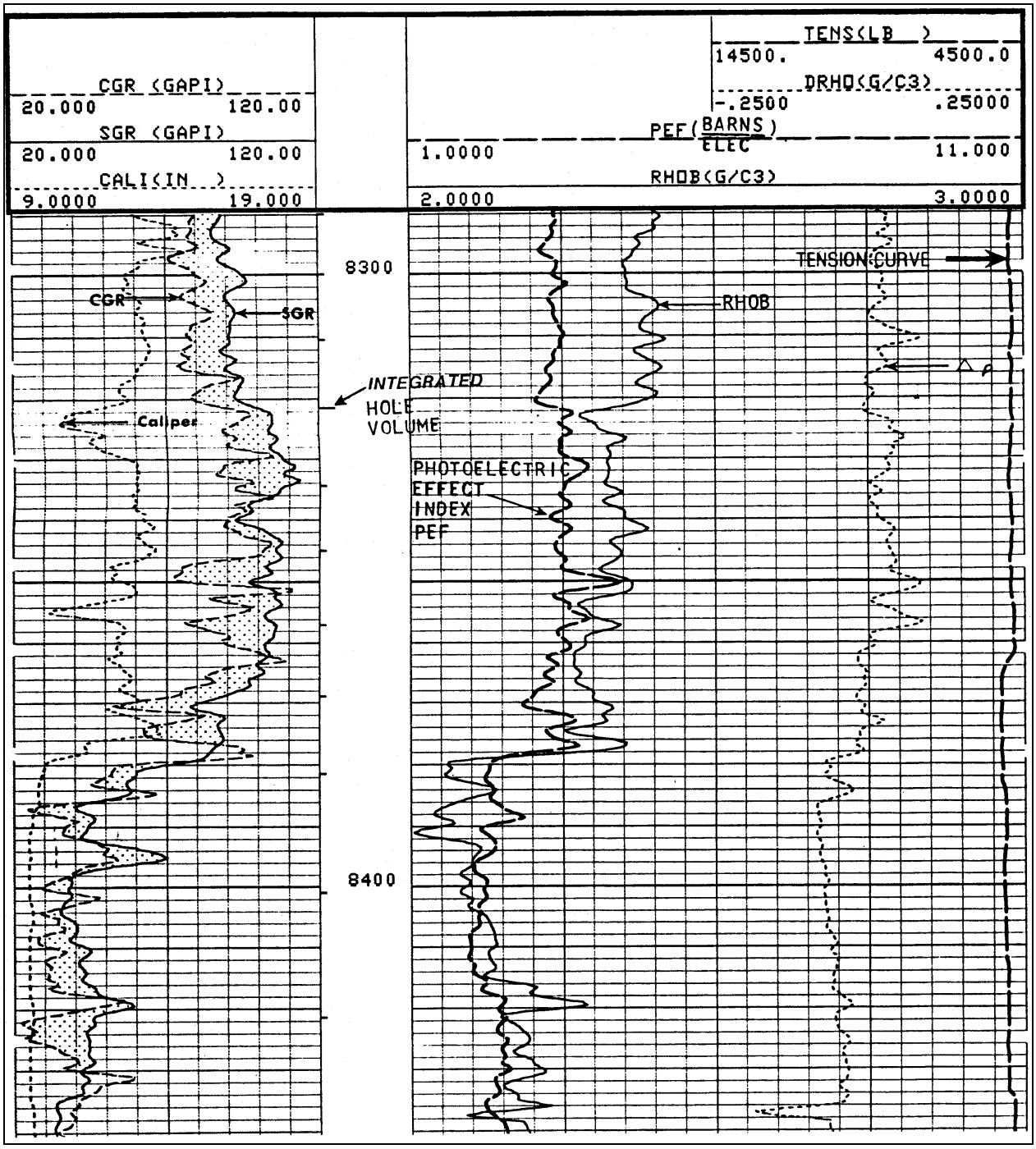

Figure 6. 11: An example of a litho-density log as can be expected from Schlumberger.

6.3.5.3 DENSITY LOG CHARACTERISTICS

The actual density measurement and the P_e photoelectric effect curve are usually recorded in tracks 2 and 3 of the log as shown in figure 6.6. The first track is customarily reserved for the natural gamma curve together with the calliper of the density tool (extension of back-up arm shown in figure 6.10). The horizontal depth of investigation is quite shallow; approximately 6 inches. Accordingly, in many permeable formations the log only measures in the flushed zone. The vertical resolution of the tool is about 1 ft.

6.3.5.4 CALIBRATION

The **primary calibration standards** for the density tools are laboratory fresh-water-filled limestone formations of the test pit at the Houston University discussed in the previous section (figure 6.4). The **secondary standards** are large aluminium and sulphur blocks into which the sonde is inserted in the field workshop of the logging contractor. With the blocks two different thicknesses of artificial mudcake are used to check the automatic mudcake correction. At the well site a radioactive test jig produces a signal of known intensity in order to check the detector response. Normally the best checks are:

- comparison of repeat section with the original log curve
- calibration in typical pure deposits like anhydrite with a density of 2.98 g/cc.

6.3.6 APPLICATIONS OF DENSITY LOGS

The Formation Density log has several practical applications:

- porosity calculation
- acoustic impedance determination; the density combined with the sonic travel times gives the acoustic impedance. This is important for calibration of seismic signals
- identification of various evaporites
- gas detection in reservoirs

The P_e curve is a good lithology indicator. The influence on the P_e of the reservoir porosity and fluid content, including gas, is insignificant.

6.4 NEUTRON LOGS

6.4.1 INTRODUCTION

Neutron tools were the first logging instruments that used radioactive sources to determine the porosity of the formation. After the later introduction of the gamma-gamma density tool, the neutron log was used to correct the density porosity readings for the effects of shale and gas. The neutron tool response is dominated by the amount of hydrogen atoms present in the formation (figure 6.12). If the rock material contains little hydrogen (thus no high shale contents) and the fluid in the pore space is either oil or water (thus the hydrogen index = 1), then the neutron log response is a good measure for the porosity. For the assessment of porosity in gas bearing formations and shaly members or formations, a combination of the neutron tool and density tool is often required. The big advantage of neutrons, i.e. to travel through steel casing and cement, gives the opportunity to acquire porosity information and hydrocarbon saturations in cased holes[1].

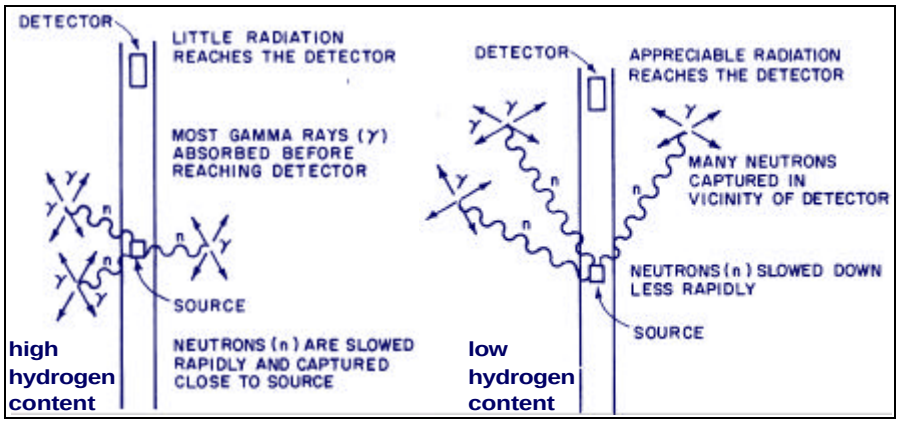

Figure 6. 12: The relation between hydrogen content and count rate at the detector. Left; a high content, right; a low content

[1] This section is restricted to open hole applications.

6.4.2 THEORETICAL BACKGROUND

6.4.2.1 BASIC CONCEPT

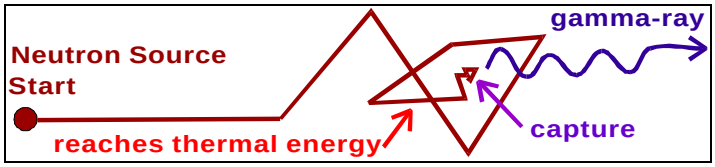

Figure 6. 13: Emission, travelling and collisions of a neutron in a formation

The electrically neutral neutrons have a mass, which is practically identical to that of hydrogen atoms. The neutrons that are emitted from a neutron source have a high energy of several MeV. After the emission they collide with the nuclei of the borehole fluid and formation materials. With each collision the neutrons loose some of their energy (figures 6.13 & 6.14). The largest loss of energy occurs when the neutron collides with a hydrogen atom. Therefore the slowing down of the neutrons largely depends on the amount of hydrogen in the formation. The first free path length is the longest successive path length-decrease until the neutrons reach thermal velocities with a thermal energy of about 0.025 eV. At this energy level the neutrons are in thermal equilibrium with the other nuclei in the rock formation. Sooner or later the neutrons are captured with the emission of a capture gamma ray. The amount of energy lost at each collision depends on the relative mass of the target nucleus, and the scattering cross section. In other words, it depends on the probability for collision of a neutron with a nucleus (fig. 6.14). The principles of the neutron tools are summarised as follows :

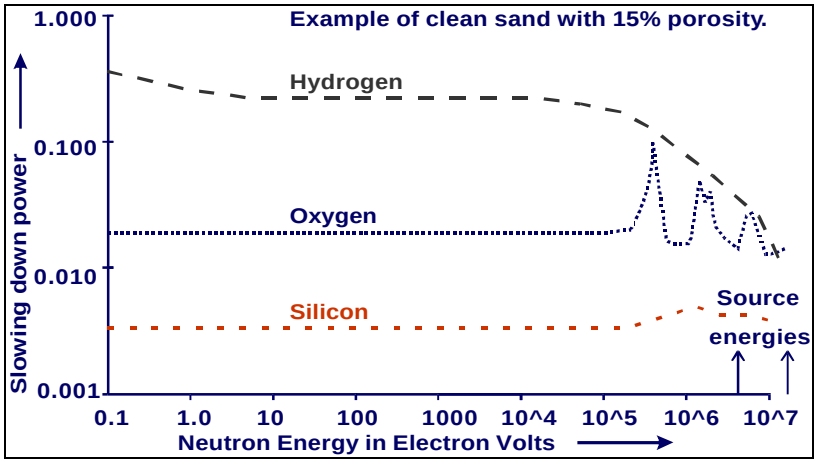

Figure 6. 14: Slowing down power of H, O, Si for different neutron energies

- a neutron source emits a continuous flux of high energy neutrons
- collisions with formation nuclei reduce the neutron energy
- at thermal energy level (ca 0.025 eV.) neutrons are captured
- neutron capture results in an emission of gamma rays
- the detector measures the slowed down neutrons and/or emitted gamma rays

Energy loss is greatest when neutrons collide with hydrogen atoms. Figure 6.15 illustrates the slowing-down process. Depending on the type of tool, either the so-called capture gamma rays, the epithemal or the thermal neutrons that reach a detector are counted.

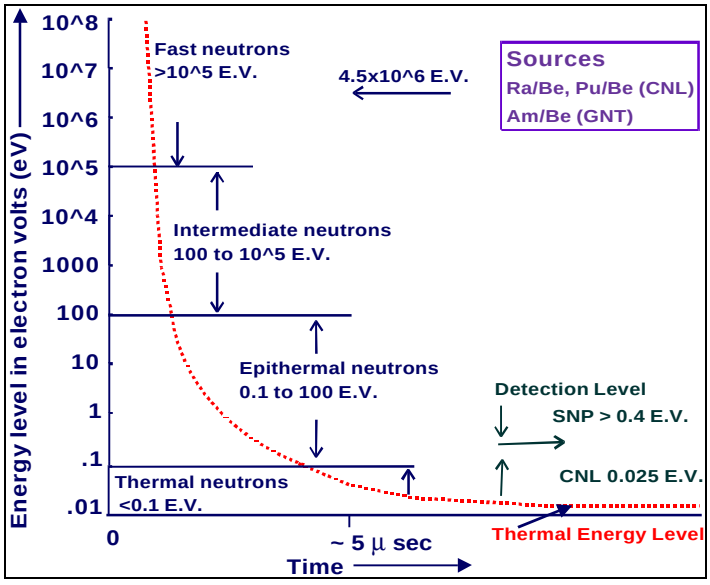

Figure 6. 15: Neutrons energy level versus time, showing decay after leaving the source.

6.4.2.2 HYDROGEN INDEX

The H-concentration has been defined in terms of a Hydrogen Index (HI), which is proportional to the quantity of H atoms per unit volume. The hydrogen index of fresh water at surface conditions is taken as the unity.

$$HI = \frac{number\ of\ H\ atoms}{(volume\ ).(number\ of\ H\ atoms\ in\ 1\ cc\ H_2O)} \qquad \text{(eq. 6.9)}$$

- For a paraffinic oil (nCH_2) we find $HI_{(oil)} = 1.29.r_{(oil)}$. If the in situ density of this oil is 0.78 g/cc, its hydrogen index is equal to that of water which has, as mentioned by definition, a value 1.
- For methane (CH_4) the hydrogen index depends strongly on the gas pressure. A typical value for HI_{CH4} at 100 bar is 0.225.

Since the zone of investigation of the neutron tool is often confined to the flushed zone, the porosity derived from the Neutron log (ϕ_n) is related to the true porosity (ϕ) by the equation (figure 6.16):

$$j_n = j.(HI_{mf}.S_{xo} + HI_{hc}.(1 - S_{xo})) \qquad \text{(eq. 6.10)}$$

In the above quoted case of the paraffinic oil with a density of 0.78 g/cc density we find $f_n = f$
In the case of CH_4 with in-situ density 0.1 g/cc and flushed zone water saturation S_{xo} of 0.7 we find :

$$j_n = j.(1*0.7 + 0.225\ *\ 0.3) = 0.77 * j \qquad \text{(eq. 6.11)}$$

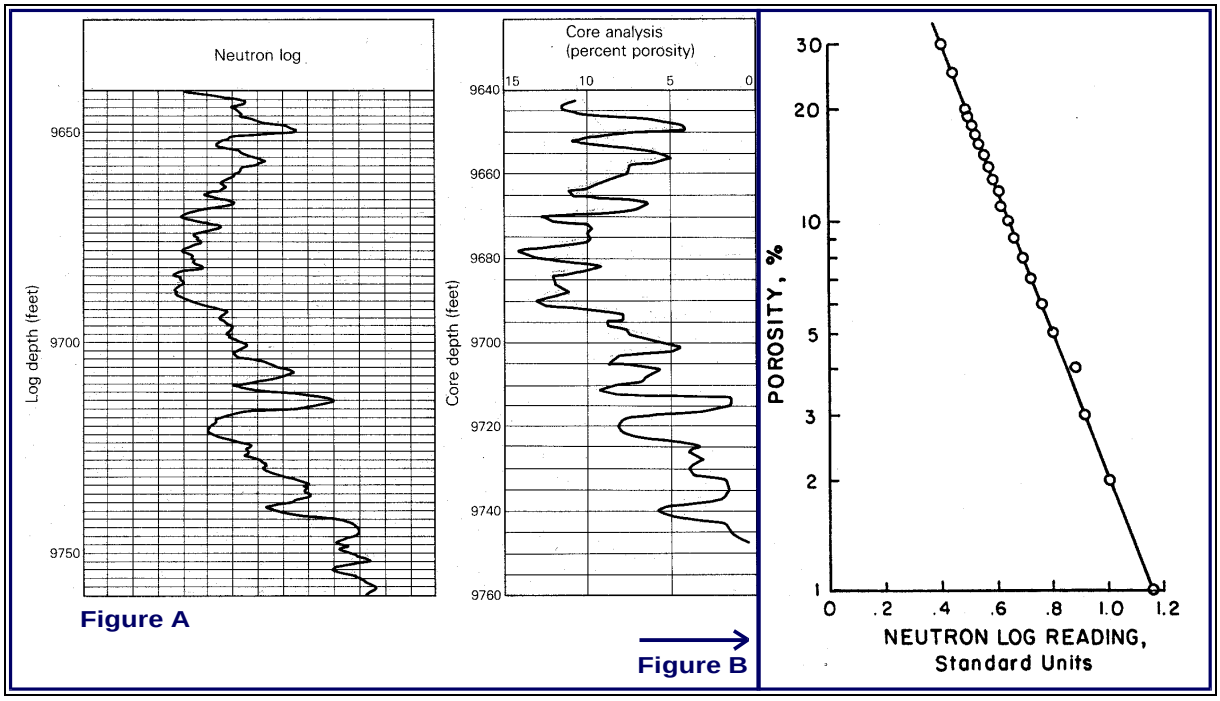

Figure 6. 16: Porosity/neutron log reading correlation. A: Neutron logs readings correlated with laboratory porosities, B: Neutron logs readings versus porosities.

6.4.3 TECHNICAL ASPECTS AND VARIETY IN NEUTRON TOOLS

6.4.3.1 PRINCIPALS AND TECHNICAL HISTORY

The neutron tools that pick up capture gamma rays are equipped with NaI-detectors. These detectors are also used in the natural gamma-ray tool and the density tool. If the neutron tool detects neutrons HeF-tubes, based on the same principles as Geiger Müller tubes, are applied. Epi-thermal neutrons are preferentially detected by shielding the HeF-detectors from thermal neutrons with a thin boron layer on the outside of the detector. The evolution of neutron tools is as follows :

GNT : 1950's - responds to capture gamma rays and thermal neutrons (Am-Be source).
SNP : 1960's - responds mainly to epi-neutrons with energy level > 0.4 eV, detector shielded.
CNL-C: 1970's - responds to thermal neutrons, capture gammas are recorded.
CNL-G: 1980's- contained two sets of two thermal and epi-thermal neutron detectors.
APS : 1990's- has an array of one thermal and two pairs of epi-thermal neutron detectors.

6.4.3.2 CHEMICAL SOURCES

The chemical neutron sources usually consist of a mixture of beryllium (Be) and an alpha emitting radioactive element Radium (Ra), Plutonium (Pu), or Americium (Am). In the mentioned tools the following natural radioactivity reactions take place:

1. Radium decays to Radon and Helium:

$$_{88}Ra^{226} \text{ ---> } _{86}Rn^{222} + _{2}He^{4} \qquad \text{(eq. 6.12)}$$

2. The alpha particles from Helium (He) bombards the Beryllium target and both neutrons and gamma rays are produced:

$$_{4}Be^{9} + _{2}He^{4} \text{ ---> } _{6}C^{12} + _{o}n^{1} + \text{gamma rays.} \qquad \text{(eq. 6.13)}$$

3. Within a few microseconds the neutrons are slowed down to the thermal energy level, as shown in the figure 6.13 and 6.15. After that they normally are captured by H- or Cl-nuclei in a process that can take up 1000 μs. The capturing nucleus becomes exited and emits gamma rays, e.g.:

$$_{1}H^{1} + _{o}n^{1} \text{ ---> } _{1}H^{2} + \text{gamma rays} \qquad \text{(eq. 6.14)}$$

The detectors are located at distances less than 1 feet and 2 feet from the source. The detector distances in the neutron tools[2] are chosen in such a way that the neutron density around the detector is low when the hydrogen content of the formation is high. In other words the hydrogen atoms in the formation act as a shield to keep the neutrons away from the detectors. **Thus,** the count rate of neutrons or gamma rays produced by thermal neutron capture is therefore *LOW* in *HIGH* porosity rocks that contain oil or water. When dealing with a low porous rock the neutrons can penetrate deeper into the formation and the count-rate around the detector will be higher. If gas, which has a very low hydrogen content, is present, then the neutrons will penetrate deeper and the count rate will be higher compared to a water or oil filled rock with the same porosity and matrix composition. Gas will give the erroneous impression that a low porosity formation is logged.

Another source type is the *accelerator (minitron) neutron source*. This non-chemical source will be discussed in the section of the accelerator porosity sonde (section 6.4.3.5).

[2] with the exception of the accelerator porosity sonde **(**APS)

6.4.3.3 SIDE-WALL NEUTRON POROSITY TOOL (SNP)

The SNP tool is designed for operation in the open hole. The source and the "one" detector are placed in a skid, 16 inches away from each other, using a configuration that resembles the density tool.

- The detector is shielded from thermal neutrons with a boron compound.
- The skid is applied to the borehole wall to minimise borehole and mudcake effects.
- The advantages of the SNP tool are that the log can be recorded simultaneously with the density log, and that the log is much less sensitive for shale because it detects epi-thermal neutrons instead of capture gamma rays.
- The disadvantage is the use of only one detector that prevents correction of remaining mudcake and borehole effects.

The tool was very successful in combination with the density tool in detecting gas. It was withdrawn due to its low logging speeds that were necessary due to the low epi-thermal neutron count rate.

6.4.3.4 COMPENSATED NEUTRON LOG (CNL)

The CNL tool from Schlumberger, and equivalent models from other logging contractors, is the most widely used neutron-logging tool at the early 90's. As shown in figure 6.17, the **CNL-C** version is equipped with 2 detectors, which are sensitive to thermal neutrons.

- The detectors are located at 15 and 25 inches from the source. The far detector has a larger volume than the near one in order to maintain adequate count rates.
- The tool measures the rate at which the thermal neutron population decreases from the near to the far detector.
- A very strong neutron source (16 Curie) reduces statistical variations and permits longer spacings. This in turn increases the zone of investigation.
- Furthermore, the effect of borehole is reduced as shown in the figure. The tool can be run in cased and open liquid filled holes.
- A large bow-spring ensures eccentring of the tool and optimum contact with the borehole wall.

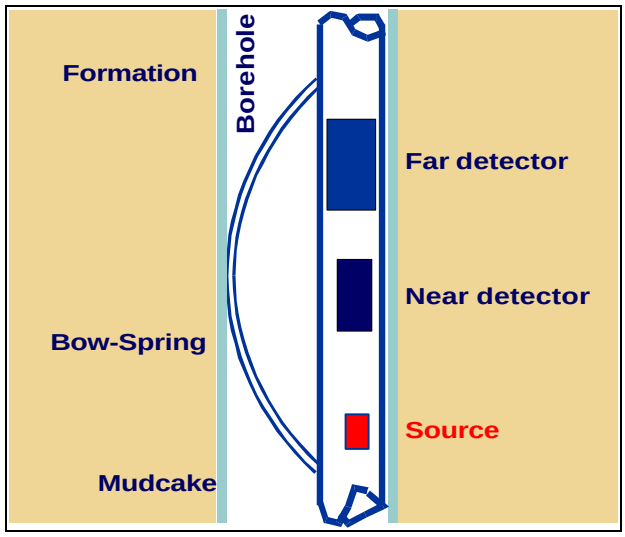

Figure 6. 17: The CNL tool

The **CNL-G** version has two epi-thermal detectors in addition to the thermal detectors at the other side and closer to the source. Due too the low epi-thermal count rates, which led to low logging speeds, this tool is (except for special low speed operations) also out of use,.

6.4.3.5 ACCELERATOR POROSITY SONDE (APS)

In contrast with all foregoing neutron tools this instrument has an *accelerator (minitron) neutron source*, instead of a chemical source. The accelerator porosity sonde (APS) was partly developed to comply with stricter environmental and safety regulations, which are expected to be enforced in the near future. However the use of a pulsed neutron source, which has a very high output, also enabled the design of a tool that contains detectors at three different spacings. This construction produced a stable epi-thermal neutron, which can be run at logging speeds compatible with the density tool. The tool combines the responses of the various detectors to compensate for lithology and matrix density effects.

6.4.4 CALIBRATION

The primary standard for calibration is again a shallow hole at the University of Houston, called the API "neutron pit" (figure 6.4). For the out-of-date gamma-neutron GNT tool the response of the neutron tools in the 19 % porosity and water filled limestone was arbitrarily defined as 1000 API units. The primary standard of calibration for SNP, CNL, and APS tools is performed in limestone, sandstone and dolomite formations of high purity and accurately known porosity. The departure of the sandstone and dolomite calibrations from the reference limestone calibration is presented on charts provided by the contractor.

The wellsite calibration is carried out by means of an U-shaped polyethylene block with a two-position block, providing two different count rates, equivalent to 11 vol.% and 22 vol.% limestone porosity. The CNL is calibrated in the workshop in a calibrating tank. A calibrated test source is used at the wellsite. The repeat section recorded at the bottom of the hole is the best check for a reliable and repeatable log. Further checks can be made in a formation with a known lithology such as anhydrite and halite intervals (the theoretical CNL reading of 0 vol.% pore volume).

6.4.5 APPLICATIONS FOR NEUTRON TOOLS

The open hole neutron porosity logs have a multitude of applications:

- porosity determination usually in combination with the density tool
- gas detection usually combination with the density tool, but also with a sonic tool
- shale volume determination in combination with the density tool
- lithology indication again in combination with the density log
- Revised neutron tools are nowadays also in use to identify the type and extension of river/lake sediments for the controlled optimisation of dredging speed and control of mud/sand dumping sites.

CHAPTER 7:
ROCK ACOUSTICAL AND RELATED MECHANICAL BEHAVIOUR

7.1 GENERAL INTRODUCTION

The velocity of a pulse through a solid or fluid medium is understood to be an important method to understand the composition of rocks. The behaviour of the pulse is, among other things, depending on the mechanical behaviour of rocks. The propagation of acoustic waves through rock and in the borehole results into the following rock mechanics related physical properties that are measured for characterisation:

- the shear wave velocity,
- the shear wave attenuation,
- the compressional wave velocity,
- the compressional wave attenuation, and,
- the amplitudes of the reflected waves.

The sonic or acoustic log was developed in the 1950's to provide a detailed record of acoustic velocities along the well trajectory. If interval travel times and the depth intervals corresponding to the travel times are recorded a velocity depth profile can be constructed. This profile can be used to convert seismic events, recorded in two-way travel times, to images that can be plotted as function of depth. Soon it became apparent that the sonic travel times can also be used for other purposes such as:

- porosity estimation,
- lithology assessment together with density & neutron tools,
- gas detection, and most important of all,
- to evaluate together with the density tool mechanical properties of the rock.
- cement-bond property-measurements and fractured-zone identification, which are based on measurements of wave attenuation. Also, the assessment of reflected-wave amplitudes is applied to locate vugs and fractures, in order to evaluate fracture orientations and to inspect casings.

Hence, acoustic logging in open holes (uncased boreholes) consists mainly of acoustical velocity measurement. This measurement, usually called a sonic log, is a record of the time, *Dt*, which is required for an acoustic wave, in order to travel a given distance through the formation that surrounds a borehole. This parameter is named the acoustic transit time, which is generally defined in microseconds per foot. Velocity, *v*, and transit time, *Dt*, are related by:

$$Dt = \frac{10^6}{v} \quad , \qquad \text{(eq. 7.1)}$$

where; *Dt is* in μsec/ft and *v* is in ft/sec.

7.2 BASIC CONCEPT

The fundamental idea is based on the combined use of a transmitter and one or more receivers that sent specific wave types and receive converted waves. These waves or pulses have been sent to a body with a known length and a specific density and texture.

At the source the following wave-types are sent in a pulse:

- *compressional or longitudinal waves*:
  They can be considered as a series of zones of compression and dilatation that move in the direction of the propagation. These compressional waves move through both solids and fluids.
- *shear wave or transverse waves:*
  They consist of a series of vibrations motions perpendicular to the direction of movement. They are moving through solid media. In rigid matter the motion of the particles perpendicular to the wave propagation be accommodated. For that reason, the shear wave only is present in solids, because of its shear strength.

So, acoustic velocity of rock depends on the elastic properties. In the coming sections we discuss the relation between rock strength and pulses through a rock *in "the basic concepts of elasticity and elastic wave propagation in (porous) media"*. And so the parameters that influence acoustic velocity and related equations are also explained.

7.2.1 RIGIDITY OF ROCK

Rigidity, or stress and strain, or elasticity of rock, concerns to the connection between the external forces on a body and the resulting change in size and shape. Force is described by force per unit area, or stress.

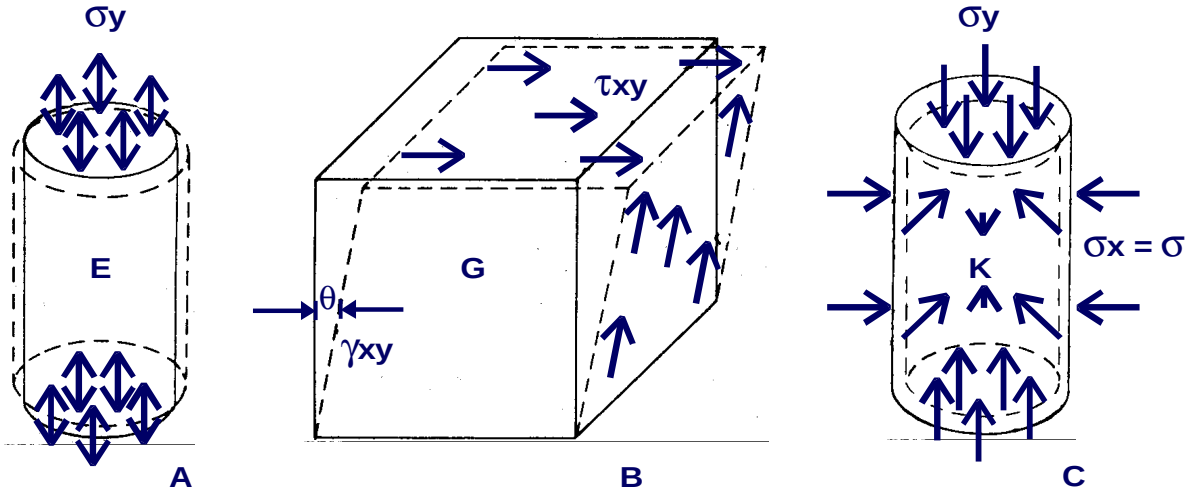

Figure 7. 1: Loading geometries to define elastic moduli. A: Young's modulus or Poisson's ratio, B: Shear modulus, C: Bulk modulus.

7.2.1.1 STRESS-STRAIN RELATIONS

- A force applied perpendicularly to a cylinder of length *L* and diameter *d* and away from or to the body on which it acts results in respectively a tensile stress or a compressive stress that causes a change of Δ*L* (figure 7.1a).
- With a tangential force applied, then it is referred to as a shear stress (fig.7.1b). Note that a shear stress causes deformation by displacement with no volume change.
- Stress induced deformation and displacements are strains.
- Strains derived by compressive and tensile stresses are named longitudinal strains, e_l, and transverse strains, e_t .

$$e_l = \frac{DL}{L}; and \cdot, e_t = \frac{DD}{d} \qquad \text{(eq. 7.2, eq. 7.3)}$$

with; *L* and *d* as the respective length and diameter of the cylinder and *DL*, *Dd* the respective displacements. The shear stress result is named the shear strain, e_s, (figure 7.1b), which is defined by:

$$e_s = \frac{DL}{L} = tanq \qquad \text{(eq. 7.4)}$$

Here θ is the deformation angle, and $e_s \approx \theta$, when the strain is small.

The elastic constants are the elastic properties of a matter and defined for strains within the elastic limit[1], as follows:

Young's modulus (*E*); (Figure 7.1a)
the Young's modulus is the ratio of tensile or compressive stress to the corresponding strain:

$$E = \frac{F \cdot L}{A \cdot DL} \qquad \text{(eq. 7.5)}$$

With an *E* for most rocks, ranging from 10^{10} to 10^{11} Pa. The Young's modulus is closely related to the Poisson's ratio.

Poisson's ratio, (*m*); (Figure 7.1a)
The Poisson's ratio is the explication of the geometric change of shape under stress and it is defined as the ratio of transverse to longitudinal strains:

$$m = \frac{e_t}{e_l}, \qquad \text{(eq. 7.6)}$$

where, in the case of a cylinder, μ is expressed as:

$$E = \frac{F \cdot L}{A \cdot D L} \qquad \text{(eq. 7.7)}$$

In general, for rocks, the Poisson's ratios are in between 0.05 and 0.40, with an average for sedimentary rocks of about 0.25.

Shear modulus, (*G*); (Figure 7.1b)
The shear modulus describes the ratio of shear stress to shear strain:

$$G = \frac{F}{A \cdot q \cdot}, \qquad \text{(eq. 7.8)}$$

with a G of about 0.3 to 1.5 times E, for a major part of the rocks.

Bulk modulus, (*K*); (Figure 7.1c)
The bulk modulus is a magnitude of the stress/strain ratio when a body is exposed to uniform compressive stress. The stress or, in this case, pressure, *p*, is related to volume change, *DV*, by:

$$K = \frac{p \cdot V}{DV \cdot}, \qquad \text{(eq. 7.9)}$$

Note that the bulk modulus is the reciprocal of the compressibility.

The previous discussed elastic constants; *E, m, G, K,* are dependent of each other parameters, because they can be expressed in the terms of two others. The most frequently applied relationships are:

$$G = \frac{E}{[2(1+m)]}, \qquad \text{(eq. 7.10)}$$

and;

$$K = \frac{E}{[3(1-2m)]} \qquad \text{(eq. 7.11)}$$

[1] With elasticity the body returns to its original condition if the force causing the strain is removed

7.2.1.2 ELASTIC BODIES AND WAVE PROPAGATION

If an elastic body is imposed by an abrupt stress or pressure, and by that immediately compacted, then in the region with high compaction the particles of the grain frame will distribute, away from the point of impact (figure 7.2). In a wave-like form they are transmitted through the body by a series of compressions and compression releases. This wave propagation is expressed by the following equations:

$$s = A_0 \cos 2p\left[f_t - (x/l)\right], \qquad \text{(eq. 7.12)}$$

and

$G = \frac{E}{[2(1+m)]}$, and , $f=1/t$

(eq. 7.13 and 14)

With:

- s as the stress at any time t, at a distance x within an elastic wave,
- A_o as the amplitude of the stress at the source,
- l as the wavelength, or the distance between a maximum compression and dilatation (or rarefaction) at any time, t as the period, or the time interval between successive maximum compressions or dilatations,
- f the frequency of compression and dilatation cycles and v *the* velocity of propagation.

Absorption is weakening of elastic waves, so the wave amplitude, A, at a distance x from the source is:

$$A = A_0 \cdot e^{-ax} \qquad \text{(eq. 7.15)}$$

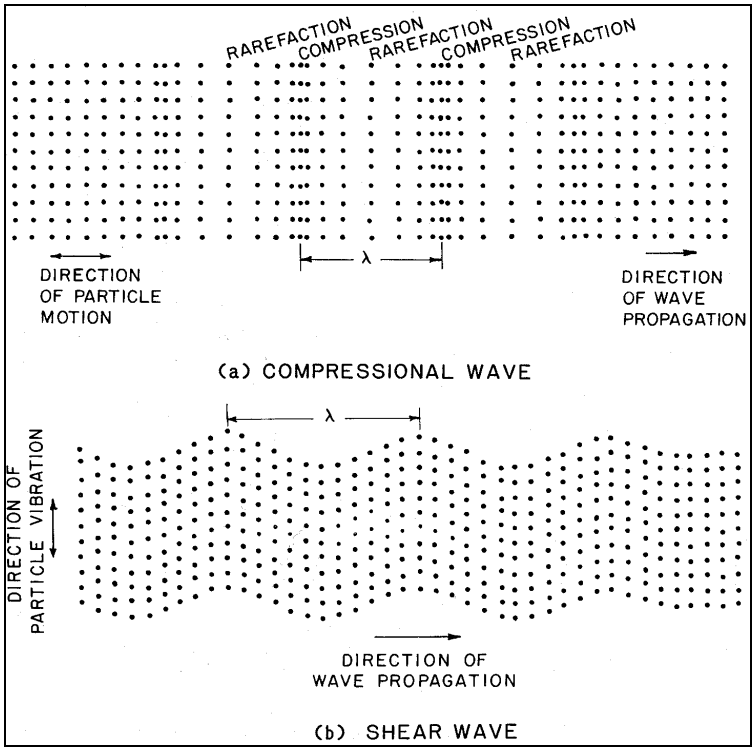

Figure 7. 2: Visualisation of a compressional wave and a shear wave.

Where a is the absorption coefficient, which depends on the rock properties through which the wave is propagating. When this weakening or attenuation effects are included in equation 7.12, then:

$$s = A_0 \cdot e^{-ax} \cdot \cos 2p\left[f_t - (x/l)\right], \qquad \text{(eq. 7.16)}$$

Elastic waves can be grouped as body waves and boundary waves. Body waves propagate in unbounded media. Boundary waves arise at the presence of boundaries like a borehole wall (fluid/rock interface). The two main types of body waves are compressional and shear waves.

ACOUSTIC COMPRESSIONAL VELOCITIES AND TRANSIT TIMES IN ROCK MATRICES OF INTEREST IN WELL LOGGING

Material	v_p (ft/sec)	Δt (μsec/ft)
Sandstone	18,000 to 19,500	55.5 to 51.0
Limestone	21,000 to 23,000	47.6 to 43.5
Dolomite	23,000	43.5
Anhydrite	20,000	50
Shale	5,900 to 17,000	170 to 60
Salt	15,000	66.7

Table 7. 1 Examples of acoustic properties

With the compressional- or longitudinal- or P (primary)- waves, the particle movement is in the direction of wave propagation. Here the velocity of compression propagation, v_p, depends on the elastic properties of the rock and can be derived from the equation of motion:

$$v_p = \left[(K + 4/3)G/p\right]^{1/2} = \left\{\frac{(E/r)(1-m)}{(1-2m)(1+m)}\right\}^{1/2}, \qquad \text{(eq. 7.17, 7.18)}$$

With $\boldsymbol{r}$ as the density of the medium.

In the shear- or transverse- or S (secondary)- waves, the particle motion is perpendicular to the direction of wave propagation and can be derived from the equation of motion as:

$$v_s = (G/r)^{1/2} = \left[\frac{E/r}{2(1+m)}\right]^{1/2} \qquad \text{(eq. 7.19, 7.20)}$$

For shear waves the medium needs to have shear strength, in other words: shear waves only travel through solid material. The compression- and shear wave velocities can be compared with the equations 7.17 to 7.20, in:

$$\frac{v_p}{v_s} = \left[(4/3) + (K/G)\right]^{1/2} = \left\{\frac{2(1-m)}{(1-2m)}\right\}^{1/2} \qquad \text{(eq. 7.21, 7.22)}$$

Always is in force: $G > 0$ and $K > 0$, so $v_p > v_s$, and because $0 < m < 0.4$, as stated before;

$$v_p > \sqrt{2v_s}\,, \qquad \text{(eq. 7.23)}$$

or converted to the transit time, Dt;

$$Dt_s > \sqrt{2Dt_p}\,, \qquad \text{(eq. 7.24)}$$

with Dt_P and Dt_S as the transit times of the primary and secondary waves. The equations 7.23 and 7.24 show that in under elastic conditions shear waves propagate slower than compressional waves.

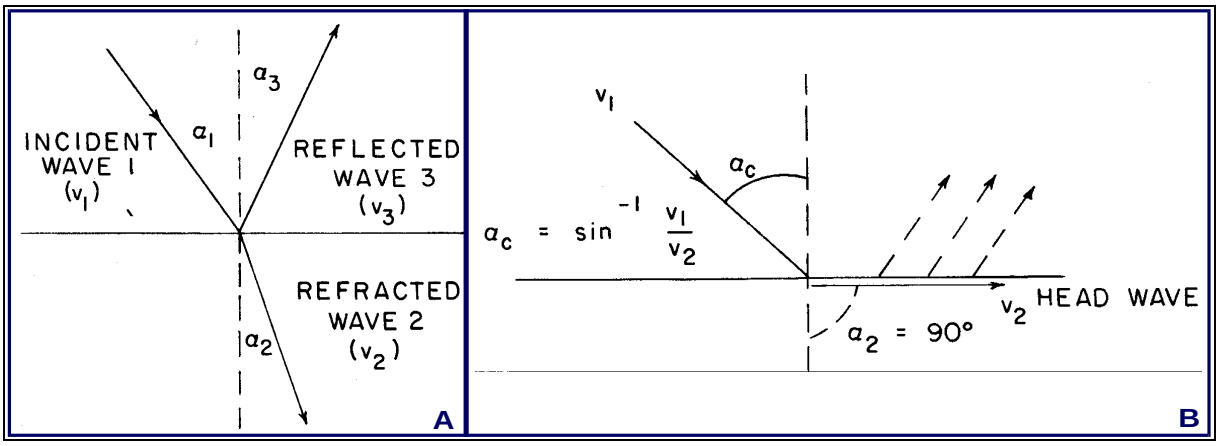

Figure 7. 3.A: Refraction and reflection of elastic waves at the interface of two different substances. B: Head wave created by a wave incident at a critical angle of reaction.

7.2.1.3 THE REFRACTION AND REFLECTION OF ELASTIC WAVES.

Elastic waves encounter phenomena like reflection, diffraction, refraction and interference. Refraction and reflection occur when a wave meets an interface between two substances with different elastic properties. Then a part of the energy of the incident wave is reflected and a part is refracted. The incident wave can be converted into other types of vibrations upon reflection or refraction. This phenomenon is called mode conversion. Figure 7.3a explains the geometry of the rays along which the acoustic waves propagate:

1. A wave with velocity v_1 has an incident at an angle a_1 on a plane boundary separating two media of different elastic characteristics.
2. A wave with velocity v_2 is refracted into the second medium at an angle a_2.
3. A third wave with velocity v_3 is reflected back into the first medium at an angle a_3.

The different velocities $v_{1,2,3}$ are specific for the media and the wave types and when translated to Snell's law:

$$\frac{\sin a_1}{v_1} = \frac{\sin a_{21}}{v_2} = \frac{\sin a_3}{v_3}, \qquad \text{(eq. 7.25)}$$

If the reflected and incident wave are of the same type, then $v_1 = v_3$ and by that $a_1 = a_3$. Further, the angle of refraction a_2 is always different from a_1, since v_1 is different from v_2. In addition the angle a_2 is expressed as:

$$\sin a_2 = \left(\frac{v_1}{v_2}\right) \sin a_1 \qquad \text{(eq. 7.26)}$$

when:

$$\sin a_1 = \left(\frac{v_1}{v_2}\right) = \sin a_C \qquad \text{(eq. 7.27)}$$

As illustrated in figure 7.3b, $\sin a_2 = 1$ and $a_2 = 90°$ and the angle a_C is the critical angle of refraction. This critical refracted wave travels along the interface at a velocity V_2 and is named the **head wave**. It generates energy back into the first medium as it travels along the boundary. Note, that if the incident angle is greater than the critical angle, then no refraction will occur and the wave is totally reflected.

A compressional wave which is travelling in environment 1 or medium 1, at a velocity v_{P1} will generate a compressional head wave in environment 2 if its angle of incidence is critical. This critical angle, "a_{PC} " is defined according to equation 7.27:

$$\sin a_{pc} = \left(\frac{v_{p1}}{v_{2p}}\right) \qquad \text{(eq. 7.28)}$$

A compressional wave that is going through environment 1 or medium 1 will create a shear head wave if its angle of incidence is critical. This critical angle, "a_{SC} ", is also defined according to equation 7.27, as:

$$\sin a_{sc} = \left(\frac{v_{p1}}{v_{s2}}\right) \qquad \text{(eq. 7.29)}$$

When the equations 3.28 and 3.29 are combined, then the result will be:

$$\frac{\sin a_{sc}}{\sin a_{pc}} = \left(\frac{v_{p2}}{v_{s2}}\right) \qquad \text{(eq. 7.30)}$$

As shown in figure 7.4 and already stated, v_{P2} is always greater than v_{S2}, so; $a_{SC} > a_{PC}$

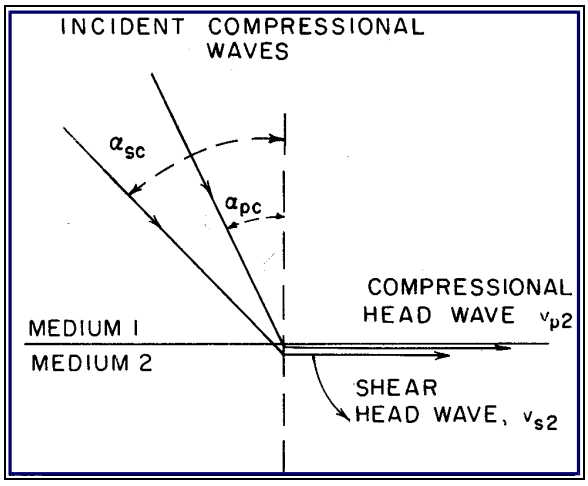

Figure 7. 4: Compressional and shear head waves due to compressional waves at critical refraction angles a_{P2} and a_{SC}.

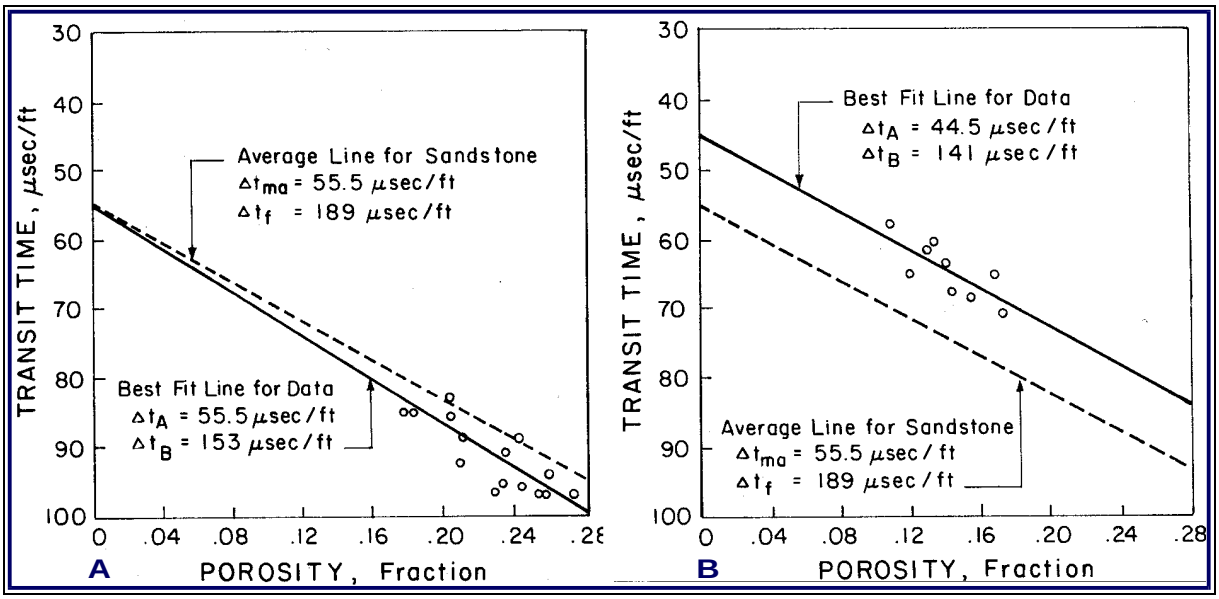

Figure 7. 5: The transit time as a function of porosity for a dense packed sand (A) and a more friable sand (B)

7.2.1.4 ASPECTS OF THE TRANSIT TIME - POROSITY RELATIONSHIP

As shown in figure 7.5a,b, normally there is a good correlation between rock porosity and the acoustic interval travel time. The time-average equation or Wyllie-equation is often used in log analysis. The model of an ideal medium, consists of a layered system of parallel slices alternating a solid and a liquid which is crossed by a wave path perpendicular to the solid/fluid interfaces. Here, the total travel time is equal to the sum of the signal's travel time through the pore-fluid and through the rock-solid fraction. The equation is simply written as:

summed travel time = travel time in liquid fraction + travel time in matrix fraction, **or:**

$$\frac{1}{v_b} = \frac{f}{v_f} = \frac{1-f}{v_{ma}} \qquad \text{(eq. 7.31)}$$

or,

$$Dt = Dt_f f + Dt_{ma}(1-f) \qquad \text{(eq. 7.32),}$$

with,

$v_{b,f,ma}$ as the respective bulk-, fluid- and matrix-velocities, and

$t_{f,ma}$ as the fluid- and matrix- transit times. Now the porosity can be described as a function of transit times, or:

$$f = \frac{(Dt - Dt_{ma})}{(Dt_f - Dt_{ma})} \qquad \text{(eq. 7.33)}$$

This time-average model shows just a part of the truth. It suggests that only rock matrix and fluid properties influence wave velocity. The effects of the mechanical properties, or previous mentioned moduli, are neglected. However, this perception of porosity vs. travel-times is applicable in friable or

A

ACOUSTIC COMPRESSIONAL VELOCITIES AND TRANSIT TIMES IN ROCK MATRICES OF INTEREST IN WELL LOGGING

Material	v_p (ft/sec)	Δt (μsec/ft)
Sandstone	18,000 to 19,500	55.5 to 51.0
Limestone	21,000 to 23,000	47.6 to 43.5
Dolomite	23,000	43.5
Anhydrite	20,000	50
Shale	5,900 to 17,000	170 to 60
Salt	15,000	66.7

B

ACOUSTIC COMPRESSIONAL VELOCITIES AND TRANSIT TIMES FOR FLUIDS OF INTEREST IN WELL LOGGING

Fluid	v_p (ft/sec)	Δt (μsec/ft)
Water		
200 kppm, 15 psia	5,540	180.5
150 kppm, 15 psia	5,375	186.0
100 kppm, 15 psia	5,200	192.3
Pure	4,380	207.0
Drilling mud (26°C)	4,870	205.3
Drilling-mud cake (26°C)	4,980	200.8
Oil	4,200	238.0
Methane (15 psia)	1,600	626.0
Air (15 psia)	1,088	919.0
Ethane ($\rho = 0.00125$ g/cm^3)	1,010	989.6
Carbon dioxide ($\rho = 0.0019776$ g/cm^3)	850	1,176.5

Table 7. 2 a,b: Material and fluid velocities and transit times for common media in and around a borehole

loose sandstones and carbonates.

The tables 7.2a,b give an indication of velocities and transit times of various minerals and fluids. Note the correlation between density and velocity.

7.3 THE PRACTICAL METHOD OF APPROACH

As shown in figure 7.6, a magnetostrictive alloy or piezoelectric crystal with a resonance frequency between 5 to 20 kHz is used as material for the transducers. The transmitter sends out pulses with an oscillatory wave-form that generate different wave types :

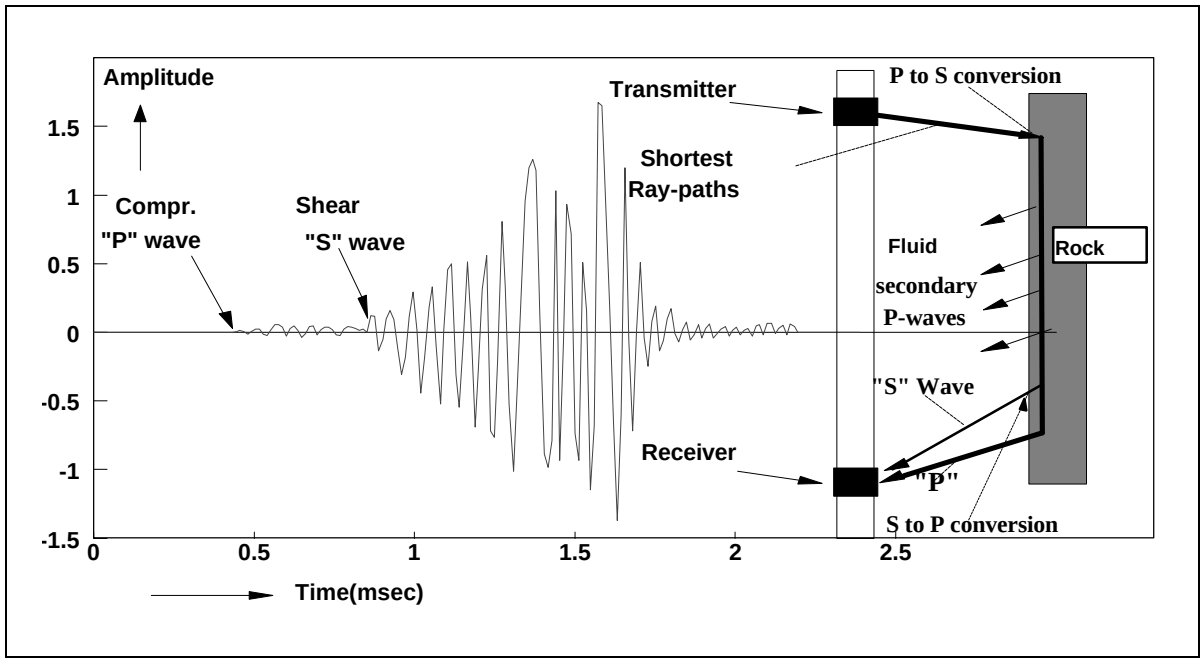

Figure 7. 6: Acoustic pulse recording in a borehole

1. ***The compressional (P) wave***, which is generated by the transmitter in the borehole fluid, will travel in all directions till it hits the borehole wall. At the borehole wall the P-wave will continue in the rock as a fast P-wave, but some of the P-wave energy at the wall will be converted to a shear (S) wave in the rock. Although both waves will expand in all directions from the point of impact only the path along the wall, or the wave of interest, is drawn. The wave travelling along the borehole wall will continuously produce compressional waves back into borehole as indicated by the small arrows. However the velocity of the wave front in the formation will out run the P waves created in the borehole because the P-wave velocity of the formation is higher than velocity of the borehole fluid. The P wave that travels the shortest distance through the mud will be the first one to arrive at the receiver.
2. ***The shear (S) wave,*** that is front travelling along the borehole wall. It will also create secondary P waves in the fluid, because a fluid can only sustain compression waves and has no shear strength. Along the borehole wall a continuous conversion of S back into P waves is the result. The shortest P and S wave paths will not be identical, due to the refraction of the waves on the borehole wall. The slow S wave will according to the law of Snellius refract less to the normal than the fast P wave.

Note: As shown in figure 7.6, the “P” wave, which represents the converted “S” wave, will arrive later than the leading “P” which represents the “P” wave of the formation.

The receiver is triggered by the arrival of the fastest wave (compressional), which is called the "first arrival". About ten pulses are transmitted per second. The measured parameter is the reciprocal velocity, or “travel time, ΔT”, which is expressed in microseconds per foot (equation 7.1). The velocity

of the compressional wave depends on the elastic properties of the rock matrix and the fluids in the pore space. The measured travel time is therefore a function of:

- the rock matrix,
- the fluid type, and,
- the porosity.

7.3.1 THE ACOUSTIC TOOL DESCRIPTION

The early tools included only one transmitter and one receiver (figure 7.7a) embedded in a sonde body consisting of rubber (low velocity and high sonic attenuation). The sound pulse travels through the mud (A) at relatively low velocity. The compressional wave is refracted at the formation face and passes through the formation with formation velocity (B). The last lag (C) is again through the mud. The measured travel time is therefore too long due to the passage through the mud. Besides, the physical length of B is not constant since changes in velocity alter the refraction angle. Later versions, as shown in figure 7.7b, incorporated one transmitter and two receivers, a few feet apart, to cancel the above problems. This system measures in effect only the time required to travel interval D, assuming intervals C and E take the same travel times. In that case distance D, which is the distance that the P waves travelled in the formation, is equal to the spacing R1 - R2. The only serious shortcoming of this system is that distance C is not equal to E, when the tool is tilted in the hole or when the hole size changes over short intervals (figure 7.7c). Later versions of the sonic tool like the Borehole Compensated tool (BHC) incorporated two transmitters and four receivers (figure 7.7d). The transmitters are pulsed alternately and ΔT values are obtained from alternate pairs of receivers as indicated. The two ΔT values are averaged to cancel differences in the C and E distances due too tool tilt. The tool consists of a slotted metal body housing, which ensures that the sonic wave travelling through the tool has to follow a labyrinth like path and arrives later than the wave that travels through the formation, and even the direct wave through the mud.

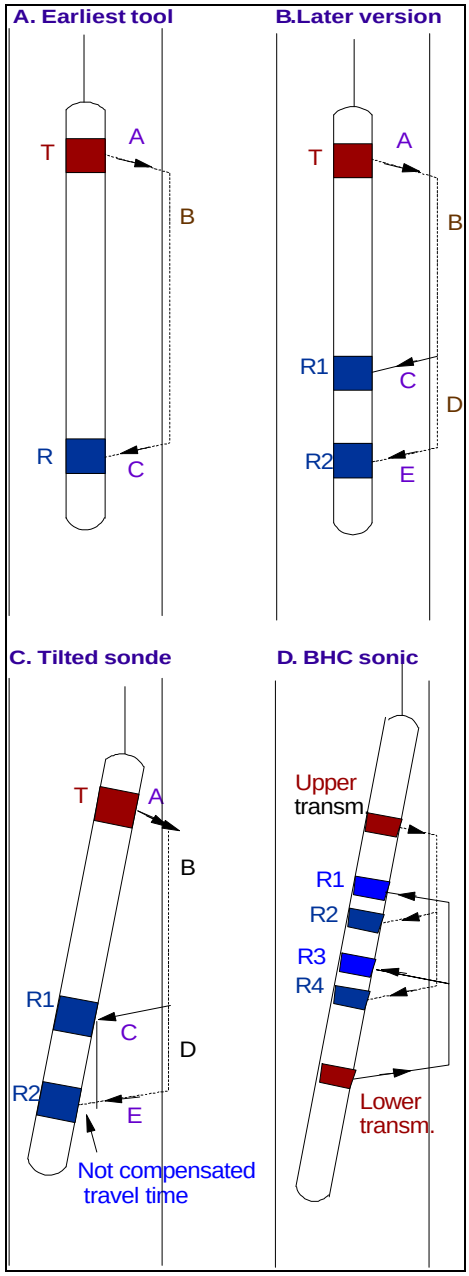

Figure 7.7: A) and B) Older sonic tool versions. C) a tilted sonic tool and D) the borehole compensated tool.

7.3.2 LIMITATIONS OF ACOUSTIC LOGGING

The conventional tools that measure travel times contain a threshold circuit, which triggers when the received signal passes beyond a pre-set threshold. The limitations of the conventional tools are all associated with either this trigger mechanism, the shape of the waveform that is detected or the tool calibration.

- **NOISE**
  Noise can be generated mechanically or by stray electric signals that are picked up by the receiver electronics. If this noise exceeds the trigger level A (figure 7.8) before the arrival of the P wave which travelled through the formation, the receiver circuit will be triggered prematurely and the time

measurement will be erroneously small. To limit this possibility all receiver circuits are switched off for 120 microseconds after transmitter firing. The far receiver is the most sensitive due too longer "open" periods and the larger attenuation of the acoustic wave for longer spacings. Noise spikes are usually intermittent and lead to much smaller travel times over very short intervals. The log readings around these noise induced short travel times can usually be trusted. Editing out noise peaks is very important for seismic applications where a cumulative travel time that is too short will lead too horizons that are located too deep in the seismic section where two way travel times are converted to depth.

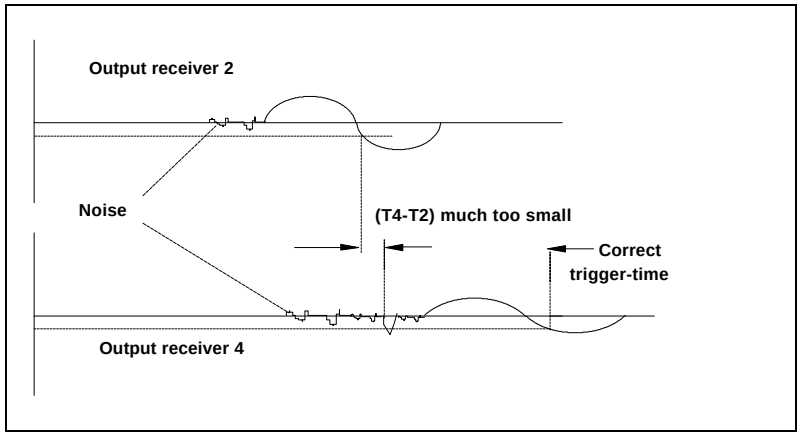

Figure 7. 8: Noise spikes.(Thomas, 1978)

ΔT STRETCH

The second and third cycles of the wave-form are usually of progressively larger amplitude. It was already mentioned above and depicted in figure 7.6, that the signal arriving at the far receiver is usually weaker. As the trigger level is constant for both receivers, triggering at the far receiver can occur too late, causing ΔT to be slightly too large. This phenomenon is shown in figure 7.9, and is called "ΔT stretch".

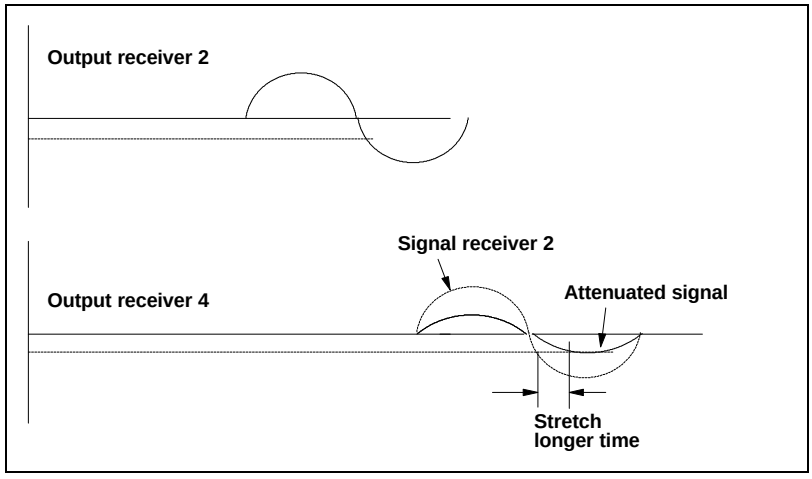

Figure 7. 9: Sonic stretch (Goetz,Dupal)

- **CYCLE SKIPPING**

Worse than ΔT stretch is the occurrence of triggering at the second or even third cycle (figure 7.10). Cycle skipping leads to a marked sudden shift to a higher ΔT value and later to a similar abrupt shift back to the correct value.

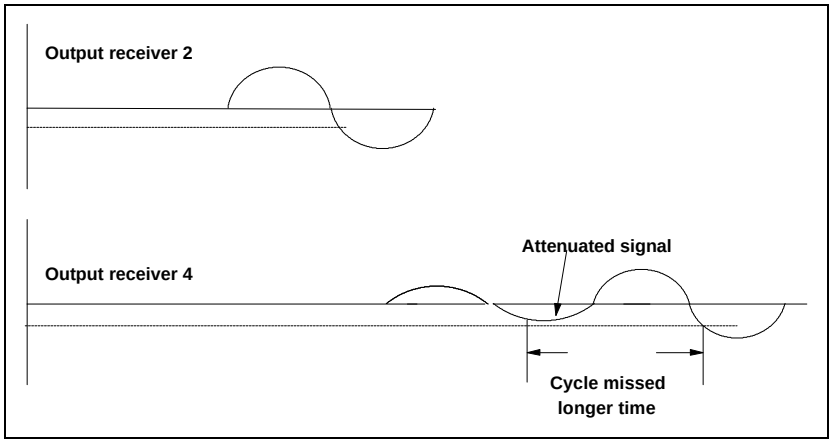

Figure 7.10: Cycle skipping (Goetz, Dupal)

- **CALIBRATION**

Even when the tool is triggering properly, we require proof that the recorded ΔT is correct. A true calibration shows the response of the complete tool to a standard environment. An excellent check is the recorded transit time in casing which should show the typical value of 57 s/ft for steel. The transit time of pure

anhydrite, which is a common deposit in carbonate areas, is also a good benchmark and should read 48 s/ft. As with all logs a repeat section of at least 200 ft should be recorded, which should overlay within a few μ sec with the main log run over the total objective interval.

- **PHYSICAL LIMITATIONS**

A graph of transmitter-receiver (TR) distance against the time to travel from T to R (figure 7.11) shows that the fastest sound path is through the mud at spacings less than a critical spacing "X_C". For larger spacings, the wave path that takes the shortest time to travel, is the one that passes through the formation.

The formation velocity v_1 is measured only when the spacing X_1 is larger than X_C. However assuming that the tool is centred in the hole $X_{C\ increases}$ with increasing hole diameter D (larger mud-path X_M), or decreasing formation velocity v_1 (slope $1/v_1$ becomes steeper, and X_C will be larger). A spacing TR1 of 3 feet is usually sufficient to avoid these problems.

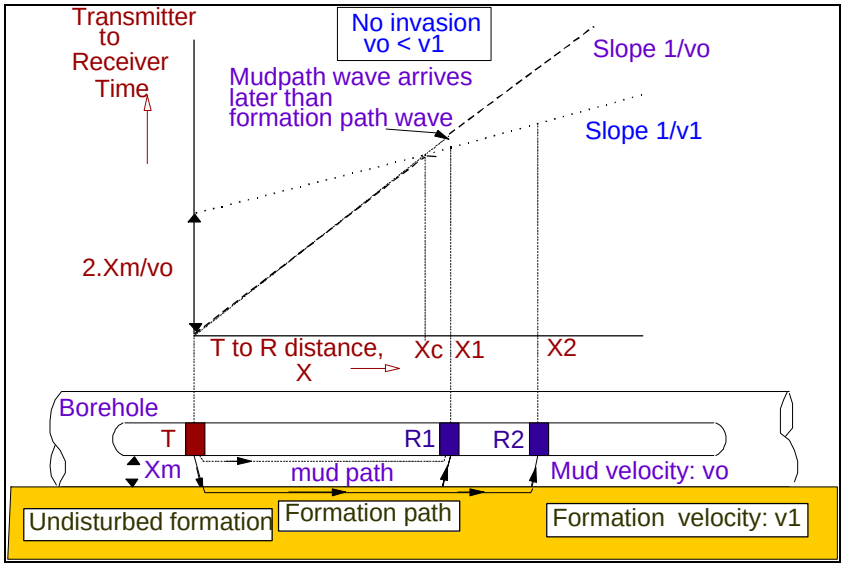

Figure 7. 11: Effect of TR spacing, no altered zone

An "altered" zone around the borehole can exist where the formation has sucked up mud-filtrate. The result will be a lower sonic velocity. Examples are soft hydroscopic clays. This low velocity zone can be circumvented in the same way as the low velocity mud layer by increasing the spacing between transmitter and receiver. However due to the smaller difference between the altered zone velocity and the undisturbed zone velocity the spacing has to increase substantially before the wave, that travels through the high velocity undisturbed zone, out-runs the wave through the low velocity altered zone. The distance X_C even under these adverse conditions is seldom more than 10 feet, hence sonde spacings with this length usually produces accurate readings, whereas the BHC would give too high ΔT readings. When the velocity of the shear wave is lower than the compressional velocity of the mud it is physically impossible for the shear wave to leave the formation. The shear wave should, according to Snellius law for $v_{mud} > v_{forrmation}$, be refracted away from the normal. However, the wave that travels along the borehole has already an angle of 90° with the normal. Hence, no shear wave will produce a secondary compressional wave in the borehole, and detection of the shear wave velocity with this conventional tool is not possible. The critical shear velocity can be calculated with:

$$\frac{\sin(j_{formation})}{\sin(j_{mud})} = \frac{V_{mud}}{V_{formation}} \qquad \text{(eq. 7.34)}$$

in which the $\sin(j_{formation}) = 1$

7.3.3 RECENT TOOLS

Since the mid-eighties new tools became available that were designed to overcome most of the limitations that were discussed in this section.

- **Array Sonic Tool**
  This tool uses two transmitters and up to eight receivers **t**o record the wave trains at 8 source to detector spacings. The 8 wave trains are "stacked" using a process that has some resemblance with cross-correlation. The process is called semblance processing and the maxim in a move-out versus acoustic power plot yield the wave velocities of the Shear and Compressional waves. The effects of cycle skipping, stretch, and noise are removed by the semblance-processing scheme.

- **Digital Sonic Imager**
  It uses not only monopole transmitters and receivers, but also two crossed pairs of dipole transducers that generate and receive preferentially shear waves. This tool can record shear waves even in formations where the shear velocity is less than the mud velocity.

These more advanced tools will be discussed in more detail in the third year's Petrophysical course for Petroleum Engineers and Geophysicists.

7.4 APPLICATIONS OF ACOUSTIC LOGS

The Acoustic logging tools have a wide range of applications:

- Porosity determination in consolidated formations
- Mechanical properties in combination with the density log
- Acoustic impedance determination in combination with the density log
- Velocity depth profiles for seismic calibration
- Lithology indications from the ratio of compressional velocity over shear velocity
- Horizontal and lateral monitoring of drillings for civil engineering purposes, i.e. Tunnel boring and horizontal drilling for gas-/oil-/water-/electrical-/emergency-piping.

CHAPTER 8:
SYNOPSIS OF PHYSICAL PROPERTIES OF ROCK & COMBINED APPLICATIONS

8.1.General introduction

8.2. Resistivity logs

8.2.1. Applications:

8.2.2. Operating principle

8.3. SP (Spontaneous Potential)

8.3.1. Applications

8.3.2. Operating principle

8.3.3. Interpretation principle

8.3.4. Limitations

8.4. GR (Gamma Ray)

8.4.1. Applications

8.4.2. Operating principle

8.4.3. Interpretation principle

8.4.4. Limitations

8.5. BHC (Borehole Compensated Sonic Log)

8.5.1. Applications

8.5.2. Operating principle

8.5.3. Interpretation principle

8.5.4. Limitations

8.5.5. Accuracy

8.6.density tools

8.6.1. Applications

8.6.2. Operating principle

8.6.3. Interpretation principle

8.1 GENERAL INTRODUCTION

In this chapter the physical properties and applications of the chapters 3 to 6 are resumed and combined with each other. The most important logging tools, with their lateral resolution and vertical resolution, are related to equations for rock/pore/fluid-interpretations and rock/pore/fluid-interactions. Although, the chapters 1 and 2 are as much important as the others are, they are not resumed because of their diversity in subjects. They are treated as a part of the practical work in the Dietz Laboratory.

8.2 RESISTIVITY LOGS

8.2.1 APPLICATIONS:

Resistivity measurements of the:

- uninvaded zone (R_t),
- flushed zone (R_{xo}),
- mudcake (R_{mc})
- mud (R_m)

Combination of the first two gives an "apparent" diameter of invasion: d_I

8.2.2 OPERATING PRINCIPLE

ELECTRICAL SONDE	(-) Normal tools do not read far into the formation (-) Strongly affected by adjacent beds			
Tool	Short Normal		Long Normal	Lateral
Spacing	16 inch		64 inch	18ft-8inch
INDUCTION LOGS	(+) Measure deep into the formation (-) Vertical resolution deep induction tools only 5 ft (+) Operate reliable in resistive muds (-) Conventional tools not accurate at high resistivities			
Tool	IES	IES	ISF	DIL
Spacing	40 inch	28 inch	40 inch	40 inch
Combination	6FF40	6FF28	6FF40	6FF40
	SN	SN	SFL	Ilm
	SP	SP	SP	SP
			Sonic	LL8
LATEROLOGS	(+) Measure deep into the formation (+/-) Vertical resolution limited to 3 ft (+) Operate reliable in salt saturated muds (+) DLL can be combined with micro-resistivity tool (-) Does not operate reliable in resistive muds			
Tool	LL3	LL7	LL9	DLL
Spacing	1 ft	3 ft	2 ft	2 ft
MICRO RESISTIVITY TOOLS	(+) Reading confined to first few inches (+) Very good vertical definition ~ 6" ML The best tool for thin/permeable bed definition MLL MSFL MCFL excellent vertical definition 2" (combined with new high resolution density tool from Schlumberger)			

Table 8_1: Resistivity tools and their spatial characteristics. Advantages (+); Limitation (-)

8.3 SP (SPONTANEOUS POTENTIAL)

8.3.1 APPLICATIONS

- Correlation between logs run in different wells, and between logging runs in the same well with different tool combinations, which both contain an SP module
- Shale volume content
- Bed boundaries
- Reservoir versus non reservoir (shale)
- Formation water resistivity
- Environment of deposition

8.3.2 OPERATING PRINCIPLE

The spontaneous potential in the reservoir is measured using only one electrode at the tool and a reference electrode at the surface. The chemical and kinetic potentials create a current across the bed boundary between reservoir and clay causing a potential drop in the mud at the boundary.

8.3.3 INTERPRETATION PRINCIPLE

- The PSP (Pseudo Static Potential) of the reservoir is a relative measure towards the shale base line.
- The PSP is corrected with the appropriate charts and converted into the SSP (Static Spontaneous Potential).
- The kinetic potential of mudcake (E_{kmc}) and shale (E_{ksh}) can be estimated and subtracted from the SSP.
- The resulting effective chemical potential can be used to obtain the formation water resistivity in water-bearing zones.
- The chemical potential consists of the membrane (E_m) and liquid junction (E_j) potentials.

$$E_{total} = E_m + E_j + E_{kmc} + E_{ksh} \qquad \text{(Eq. 8.1)}$$

$$V_{sh} = \frac{PSP - SSP}{SSP} \qquad \text{(Eq. 8.2)}$$

8.3.4 LIMITATIONS

- Poor SP response in salt water based mud.
- A salinity contrast between mudfiltrate and formation water is needed.
- In non-conducting mud the SP can not be recorded.
- In Hydrocarbon bearing zones the SP is suppressed.

The vertical and horizontal resolutions depend on the formation and borehole characteristics.

- Vertical resolution: 3 ft
- Depth of investigation: variable from 3 - 10 ft depending on invasion profile

8.4 GR (GAMMA RAY)

8.4.1 APPLICATIONS

- Correlation of logs carried out with different logging tools and in different wells
- Shale volume content
- Evaporites (Potassium salts)
- Uranium prospecting
- Cased hole correlation - depth control
- Bed boundaries
- Environment of deposition

8.4.2 OPERATING PRINCIPLE

A scintillation crystal coupled to a photo-multiplier in the logging tool measures the natural radiation intensity. The tool also records through the casing. If the gamma rays are sorted by energy the contributions of Uranium, Potassium and Thorium can be separated and recorded as volume fractions.

8.4.3 INTERPRETATION PRINCIPLE

With the GR the shale volume can be calculated as follows:

$$V_{sh} = \frac{GR - GR_{min}}{GR_{sh} - GR_{min}} \qquad \text{(Eq. 8.3)}$$

where: GR = log reading corrected for environmental influences
GR_{min} = GR reading in clean (non-shale) intervals
GR_{sh} = GR reading opposite a shale interval

This linear equation gives the highest shale volume. Other non-linear equations can be used resulting in lower shale volumes depending on the age of the rock.

8.4.4 LIMITATIONS

- Logging speed (ft/sec) x time constant (sec) = 1
- Radioactive minerals in reservoir rock influences interpretation e.g. arkosic sands, micaceous sands.

Depending on speed and time constant the resolution is:

- Vertical resolution : 2 ft
- Depth of investigation: 1-2 ft depending on the density of the formation and the presence of a casing.

8.5 BHC (BOREHOLE COMPENSATED SONIC LOG)

8.5.1 APPLICATIONS

- Porosity
- Velocity (seismic)
- Lithology (in combination with other porosity tools)
- Mechanical Properties in combination with the density tool
- Correlation
- Compaction

8.5.2 OPERATING PRINCIPLE

An upper and a lower transmitter emit acoustic pulses with a frequency of 5-20 kHz, depending on tool-type. These wavetrains travel through the mud and formation and reach 2 receivers spaced 2 ft apart. The wavetrains are recorded as a function of time. The difference in first arrival times of the receivers is used to calculate the velocity. By taking the difference the formation velocity is compensated for borehole effects and tool tilt.

8.6 INTERPRETATION PRINCIPLE

$$j = \frac{DT - DT_{fl}}{DT_{ma} - DT_{fl}} \qquad \text{(Eq. 8.4)}$$

Where ϕ = porosity, fraction bulk volume.
ΔT = transit time of the log [or slowness in $\mu s/m$ $\{10^6$/velocity (m/s)$\{$]
ΔT_{ma} = transit time of the matrix
ΔT_{fl} = transit time of the fluid

For unconsolidated sands the above equation usually produces too high porosities, which have too be corrected for compaction.

8.6.1 LIMITATIONS

- Cycle skipping (gas, fractures, and borehole) causes too long travel times.
- Noise spikes generally causes too short travel times
- Stretch generally causes too long travel times.
- Shale effect causes generally too long travel times.
- Unconsolidated sands need a compaction factor correction
- In gas zones travel times are commonly unreliable
- Sonic can not be run in boreholes without liquid

8.6.2 ACCURACY

- Vertical resolution : 2 ft
- Depth of investigation : few inches

8.7 DENSITY TOOLS

8.7.1 APPLICATIONS

- Porosity
- Density
- Impedance together with the sonic velocity for seismic applications
- Lithology (in combination with other porosity tools)
- Gas detection (in combination with the neutron tool)

8.7.2 OPERATING PRINCIPLE

A radioactive source (Caesium 137) emits medium energy gamma rays into the formation. The GR are counted within the energy band where Compton scattering is dominant. The Compton scattering is a function of the formation density. An automatic mudcake correction is obtained by using both the long and short spacing detectors. The correction is already incorporated in the log reading. Measured property: electron density.

8.7.3 INTERPRETATION PRINCIPLE

$$j = \frac{r_{ma} - r_b}{r_{ma} - r_{fl}} \qquad \text{(Eq. 8.5)}$$

H.C.bearing zones:

$$r_{fl} = S_{xo} . r_{mf} + (1 - S_{xo}) . r_{hc} \qquad \text{(Eq. 8.6)}$$

Where,

ρ_b	=	bulk density, g/cc
f	=	porosity, fr.b.v. (fraction of bulk volume)
ρ_{ma}	=	matrix density, g/cc
ρ_{fl}	=	fluid density, g/cc
ρ_{hc}	=	hydrocarbon density, g/cc
ρ_{mf}	=	mudfiltrate density, g/cc
S_{xo}	=	mudfiltrate saturation, fr.p.v. (fraction of pore volume)

8.7.4 LIMITATIONS

- gas correction needed in gas-bearing zones
- borehole correction needed above 9''
- caliper cuts into the mudcake

- Vertical resolution : 2 ft
- Depth of investigation : 0.5 ft

8.8 PHOTO - ELECTRIC EFFECT

8.8.1 APPLICATIONS

- Lithology (hardly effected by fluid, porosity)
- Fracture detection when using barite mud.

8.8.2 OPERATING PRINCIPLE

A radioactive source (caesium 137) emits medium energy gamma rays into the formation. The GR are counted within the energy band where Compton scattering and the photoelectric effect are dominant. The long-spacing detector detects both and the short-spacing detects only the Compton scattering. The ratio of long/short spacing measurement results in the photoelectric absorption cross section. Since the latter is strongly dependent on the atomic number a good indication of the lithology is obtained.
Standard configuration: GR, CNL and LDT.

Measured property: effective photoelectric absorption cross section

8.8.3 INTERPRETATION PRINCIPLE

$$U = P_e . r_e \qquad \text{(Eq. 8.7)}$$

Where,

P_e units	=	barns/electron
r_e units	=	electrons/volume
U	=	the effective photoelectric absorption cross section index per unit volume barns per unit volume.

The parameter U allows adding up the cross sections of the various components of a formation. The relative volumes of the components can then describe the formation:

$$U = j . U_{fl} + (1 - j) . U_{ma} \qquad \text{(Eq. 8.8)}$$

8.8.4 LIMITATIONS

Barite mud influences the P_e curve heavily. P_e of Ba is about a factor 30 higher than of the other minerals. The experience is that, above 12 1b/gal mud in combination with rugose holes, the presence of barite is detrimental to the P_e measurement. The novel back-scatter density tool from Schlumberger is less affected by these restrictions.

8.8.5 ACCURACY

- Vertical resolution : 1 ft
- Depth of investigation : 0.5 ft

8.9 NEUTRON TOOLS

8.9.1 APPLICATIONS

- Porosity
- Lithology (in combination with other porosity tools)
- Gas detection (in combination with the density tool)

8.9.2 OPERATING PRINCIPLE

A Pu-Be source emits at steady state about $4x10^7$ neutrons/sec. into the formation. The neutrons are slowed down to a thermal level as a function of the hydrogen content. In water or oil bearing zones this results in the porosity being measured. A long-spacing and short spacing detector measure the neutrons at thermal energy level. The combination of both detectors results in a borehole correction and cement correction in cased holes. Standard configuration: GR, CNL and LDT. Measured property: Hydrogen content.

8.9.3 INTERPRETATION PRINCIPLE

- Hydrogen Index of fluid is obtained by normalising the Hydrogen content of the fluid by that of water.
- Water (HI_{water} = 1) contained in a pure limestone results in a direct porosity reading of the neutron log.

- Lithology correction

$$\phi_n = \phi . HI_{water} \qquad \text{(Eq. 8.9)}$$

- Hydrogen Index correction

$$\phi_n = \phi .(HI_{mf} . S_{xo} + HI_{hc} .(1 - S_{xo})) \qquad \text{(Eq. 8.10)}$$

- HI_{hc} can be expressed in HI_{gas} or HI_{oil}:

methane	$HI_{gas} = 2.25 \times \rho gas$	e.g.	ρ_{gas} = 0.1 g/cc; HI_{gas} = 0.225
oil	$HI_{oil} = 1.29 \times \rho oil$	e.g.	ρ_{oil} = .78 g/cc; HI_{oil} = 1

where: ϕ_n - tool porosity (LST units) ϕ - true porosity
HI_w - Hydrogen index water HI_{gas} - Hydrogen index gas
HI_{oil} - Hydrogen index oil HI_{mf} - Hydrogen index mudfiltrate
S_{xo} - flushed zone sat., fr.p.v. ρ_{oil} - oil density, g/cc

8.9.4 LIMITATIONS

- Strong lithology effect
- Strong gas effect results in too low neutron porosity
- Clay gives too high neutron porosity because the Hydrogen Index of clay is high

8.9.5 ACCURACY

- Vertical resolution : 2 ft
- Depth of investigation : 1 ft

CHAPTER 9A:
EVALUATION OF MINERALS, FLUIDS AND IN-SITU ENVIRONMENTS: OIL & GAS

9A.1 GENERAL INTRODUCTION

In this chapter the evaluation of wireline logs for oil and gas reservoirs, coal, groundwater and ores, will be discussed. As mentioned in the general introduction impressive progress was made during the last decade in the interpretation of geophysical measurements, which were made at the surface. Direct coal, ore, hydrocarbon or groundwater indicators can frequently be derived from surface seismic, provided accurate well data over the area of interest is available for calibration. For exploration and appraisal activities direct physical contact with the prospective layers is even now required to resolve the question whether profitable occurrences are present. In Chapter 3, committed to various methods of formation evaluation, the analysis of drill cuttings and cores was discussed. These methods are common for the four petrophysical application areas covered in these lectures:

- hydrocarbons,
- coal,
- groundwater, and
- minerals and/or mechanical properties.

This section 9A will concentrate on the analysis of wireline logs to determine the hydrocarbon reservoir parameters as listed in table 9A.1.

9A.2 EVALUATIONS FOR OIL AND GAS

Wells have to be drilled to penetrate (profitable) oil and gas layers, to get direct physical evidence from drill cuttings, hydrocarbon in the mud, core samples, and production tests, or indirectly from wireline logging measurements. Table 9A.1 lists the reservoir parameters that have to be deduced from the data based on cores, logs, cutting descriptions, and production & wireline tests.

LOCATE:	Reservoir non-reservoir
DETECT:	fluid content water/oil/gas
EVALUATE:	lithology porosity permeability capillary properties mechanical strength salinity of the water original hydrocarbon saturation movable hydrocarbons residual hydrocarbons % oil / gas / water gross / net thickness reservoir pressure

Table 9A. 1: Objectives of a petrophysical interpretation

9A.2.1 RESERVOIR DELINEATION

For a sedimentary layer to be a potential reservoir it should have both porosity (storage capacity) and permeability (fluid flow capacity). When core samples are not (yet) available only a combination of several different wireline-logging measurements can give a good indication whether both conditions are fulfilled. For conventional evaluations the following tools are used to distinguish reservoirs:

- the natural gamma radiation tool (GR),
- the spontaneous potential tool (SP), and
- a combination of micro-resistivity readings to prove invasion of mud-filtrate.

The principles of these tools were discussed in Chapters 5, 6, 7 and 8.

9A.2.2 NATURAL GAMMA RADIATION (GR)

Shale, clays, and silts usually have no reservoir potential due to their very low permeability (μD range). Nature has been kind because these sediments, as a rule, accumulate much more natural radioactive minerals (uranium U, thorium Th, and potassium K isotopes) than clean porous sand, limestone, and dolomite layers, in which the majority of producable hydrocarbons are stored.

Separating layers with a high natural radiation level from layers with a low level is usually the first step in log analysis. In this way shale layers and potential reservoir layers are recognised.

An example of this division is shown in Figure 6.6. for a sand/shale sequence. The separation between the GR log deflection in a clean sand and in a 100% shale interval can be used to estimate the shale content in the shaly sand layers as discussed in the chapters 6 and 8.

Sometimes the presence of mica, which has a high natural gamma-radiation, can mask the presence of reservoir sands with a high oil production potential. The use of spectral gamma-ray logs that can separate the contributions of U, Th, and K, in combination with the photoelectric absorption coefficient P_e, is applied to recognise the occurrence of these minerals. This method will be discussed in the second part (third year petroleum engineering & geophysics) of this lecture series.

9A.2.3 SPONTANEOUS POTENTIAL (SP)

The physical phenomena that underlie the functioning of this tool were discussed in Chapter 5. The difference of salinity between the water in the pores of the reservoir and the salinity of the mud on the one hand and the membrane potential between shales and the porous reservoir on the other hand, produce a combined electrical potential difference in the mud that can be measured with an SP tool. The potential only occurs when ions can move from the mud into the pores, which implies that porosity and a minimum permeability must exist before the spontaneous potential can be detected.

Various examples of the detection of permeable layers and related sedimentary environments are shown in chapter 5. The SP signal is most prominent for fresh water based mud and on-shore wells when a good return of the current to the surface electrode is ensured. It is not surprising that the better SP logs were recorded in the past when both conditions were fulfilled. The SP is one of the few measurements that did not improve in time and senior petrophysicists (prof. M. Peeters) can become very nostalgic about the good old days in the jungle when SP interpretations and human relations were much easier. I prefer nostalgia on an ore body in Lapland (K-H. Wolf).

9A.2.4 MICRO-RESISTIVITY TOOLS (MLL)

This tool was originally designed to record the resistivity of the invaded zone with two depths of investigation. In its most simple form it had one current and two voltage measuring electrodes with electrodes spacings of approximately 1" as shown in chapter 5. The resistivity measured with the proximate pair of electrodes (micro-normal curve) proved to be much lower than the resistivity measured with the outlying pair (micro-inverse curve) when permeable reservoir sand is present. This came initially as a surprise but could be explained readily by the presence of the high conductive mudcake, which consists often for more than 50% of mud-filtrate. This mudcake affects the shallow measuring pair much more than the deeper measuring pair of electrodes.

Obviously mudcakes can only be deposited when a layer is permeable. The borehole wall then acts as a filter that sieve the solid mud particles from the mud when it invades the reservoir. The separation between the two micro-resistivity curves is therefore an excellent indicator of the presence of a permeable layer. The indication is digital, which means that it only shows the presence or absence of permeability, but does not quantify this parameter. The separation method has the highest vertical resolution of the three reservoir delineation methods discussed in this chapter.

9A.2.5 NET OVER GROSS (N/G)

The reservoir layer thicknesses derived from the SP, GR, MLL or a combination of these tools are added to arrive at the net reservoir thickness "N" contained in the total reservoir depth interval "G", which was surveyed by the logs. The division N/G gives the net over gross ratio.

9A.2.6 POROSITY DETERMINATION

When the porous rock contains only *one fluid*, and *one homogeneous matrix mineral combination*, a "one to one" relation can be established between the porosity and the log readings of the three porosity tools.

9A.2.6.1 DENSITY LOG

For a clean formation of matrix density r_{ma} containing a fluid with density r_{fl}, the bulk density as measured by the log r_b can be expressed as a linear relationship between matrix and fluid points.

$$r_b = (1-j).r_{ma} + j.r_{fl} \qquad \text{(eq. 9A.1)}$$

Rearranged to:

$$j = \frac{r_{ma} - r_b}{r_{ma} - r_{fl}} \qquad \text{(eq. 9A.2)}$$

When the pores contain a mixture of mudfiltrate and hydrocarbons, r_{fl} is calculated as follows :

$$r_{fl} = S_{xo}.r_{mf} + (1 - S_{xo}).r_{hc} \qquad \text{(eq. 9A.3)}$$

where;

r_b	=	bulk density, g/cc
f	=	porosity, fr.b.v.(fraction of bulk volume)
r_{ma}	=	matrix density, g/cc
r_{fl}	=	fluid density, g/cc
r_{hc}	=	hydrocarbon density, g/cc
r_{mf}	=	mudfiltrate density, g/cc
S_{xo}	=	mudfiltrate saturation, fr.p.v. (fraction of pore volume)

The volume fraction of mudfiltrate in the pore space in the flushed zone is usually much larger than that of the hydrocarbons. The hydrocarbon effect is therefore usually small, unless light oil or gas is present. This is further discussed in section 9A.2.7 on the gas effect. In figure 9A.1 the core porosity is plotted versus the bulk density. Extrapolation of the regression line to the intersect with the density axis provides the apparent matrix value, r_{ma}.

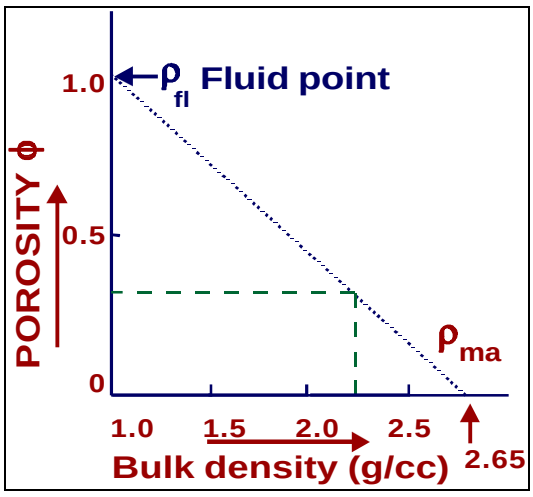

Figure 9A. 1: Core porosity versus bulk density, r_b

9A.2.6.2 SONIC LOG

The sonic instruments described in chapter 7 measure the acoustic travel time. For the relation between the travel time of the compressional wave and porosity Wyllie proposed a relation that is equivalent to the relation used for the density log. Transit times increase linearly with porosity according to the Wyllie equation :

$$DT = j.DT_{fl} + (1-j).DT_{ma} \qquad \text{(eq. 9A.4)}$$

or

$$j = \frac{DT - DT_{ma}}{DT_{fl} - DT_{ma}} \qquad \text{(eq. 9A.5)}$$

where;

ϕ : porosity, fraction of the bulk volume (fr.b.v);

ΔT **:** transit time of the log [or slowness in μs/ft]. Here the slowness is defined as the reciprocal of the velocity **(1/velocity)**;

ΔT_{ma}**:** transit time of the matrix;

ΔT_{fl} **:** transit time of the fluid.

This relationship is displayed in figure 9A.2. Here the porosity versus transit time is exposed for ΔT_{fl}=189 μs/ft. **Note:** The latter value is valid for fresh water or fresh mud filtrate. In the case of unconsolidated (uncompacted) sands the above "Wyllie" equation may give porosity values which are too high. Lack of consolidation is indicated when adjacent shales exhibit ΔT values greater than 100 μs/ft. An empirical correction factor, B_{cp} (refer figure 9A.4), is then applied to the Wyllie equation. B_{cp} is about equal to the reading in shale in μs/ft divided by 100.

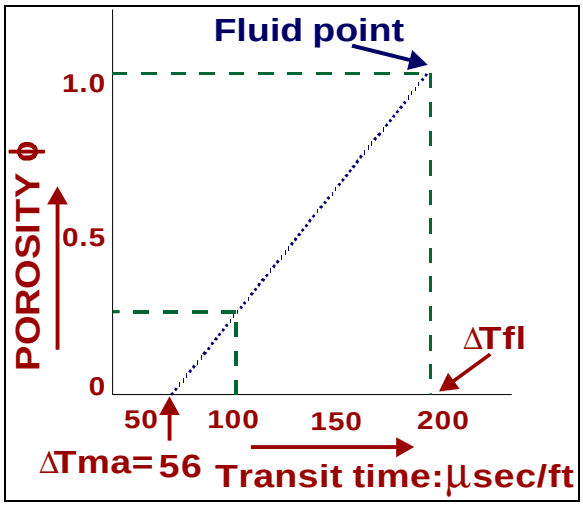

Figure 9A. 2: Graphics display of the Wyllie equation.

The most accurate method to calibrate log porosities obtained with the sonic tool is to compare them with core porosities. Here a good core recovery and a good depth correlation are necessities.

9A.2.6.3 NEUTRON LOGS

The porosity indication provided by the neutron tools is based on the Hydrogen index HI and was discussed in chapter 7. Since the zone of investigation of the neutron tool is often confined to the flushed zone, the porosity derived from the Neutron log (ϕ_n) is related to the true porosity (ϕ) by:

$$\phi_n = \phi .(HI_{mf} .S_{xo} + HI_{hc} .(1 - S_{xo})), \qquad \text{(eq. 9A.4)}$$

in which HI_{xo} ,HI_{mf}, are the hydrogen indices of respectively the residual hydrocarbons in the pores, and the mudfiltrate.

9A.2.7 GAS EFFECT

The presence of gas can be recognised and assessed with the readings of a neutron log and a gamma-gamma or density log

9A.2.7.1 NEUTRON LOG

The gas-effect can be spit into two parts the HYDROGEN effect and the EXCAVATION effect. In these lectures only the hydrogen effect will be discussed. The neutron porosity (ϕ_n) is related to the true porosity (ϕ) according to equation 9A.4. The hydrogen index of natural gas (CH_4) for a gas-bearing reservoir at 8000 ft and 200°F is approximately 0.33, and evidently much less than the value "1" which is valid for oil or water. If we

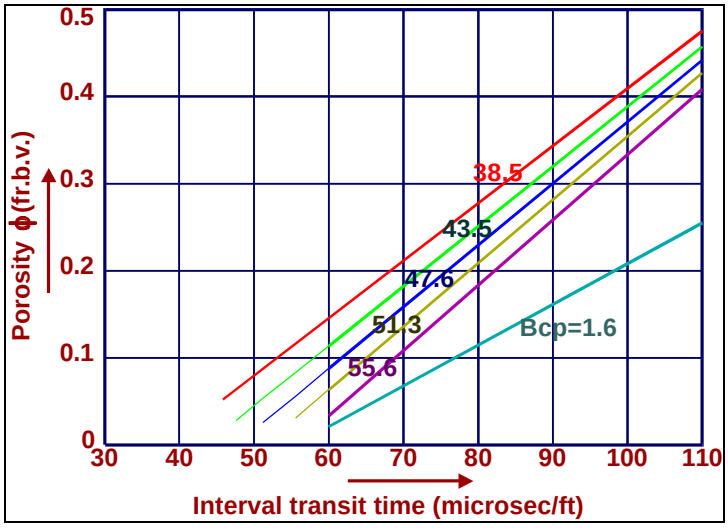

Figure 9A. 3: Graphics presentation of the Wyllie equation

assume a formation with a porosity ϕ of 33 % and water saturation S_{xo} in the invaded zone of 70 %, the neutron log reading for this situation is:

$\phi_n = 0.33.[1 \times 0.7 + 0.33 \times 0.3] = 0.26$.

Additionally, when the matrix has no effect we would expect the tool to read 0.33 (33 %) if the pores are filled for 100% with water. The depression due to the presence of gas is therefore 7 % b.v.

9A.2.7.2 DENSITY LOG

The resulting *apparent bulk density*, "ρ_a", as seen by the tool, is related to the *electron density* "ρ_e":

$$r_a = 1.07.r_e - 0.188 \qquad \text{(eq. 9A.5)}$$

For liquid filled sandstone, limestone and dolomite the tool reading ρ_a is practically identical to ρ_b. Corrections are required e.g. in anhydrite, sylvite, halite and also in gas bearing formations. For a number of minerals the characteristics were given in tables in chapter 6. The value of ρ_e is the product of 1.238 and the gas density, which is the actual in situ density for CH_4. In practice we assume the gas composition ("natural" gas) to be 90% CH_4 and 10% C_2H_6, and find $\rho_e = 1.238\rho_{gas}$.

Example I:

At a reservoir depth of 8000 ft, with a pressure gradient of 0.44 psi/ft, we find a pressure of 3500 psi. Assuming a temperature of 200°F we find for ρ_{gas} 0.15 g/cc. Hence, ρ_a (gas) = 1.07 x 1.238 x 0.15 - 0.188 = +0.01 g/cc.

Note: *that r_a for gas, as seen by the density tool, is much lower than the actual r_{gas}*. The effect of gas on the density log, assuming that the investigation depth is shallower than the invasion depth, can be quantified as follows, :

- Mudfiltrate only : $\rho_b = (1 - \phi) \times \rho_{ma} + \phi \times \rho_{mf}$
- Residual gas : $\rho_b = (1 - \phi) \times \rho_{ma} + \phi \times S_{xo} \times \rho_{mf} + \phi \times (1 - S_{xo}) \times \rho_{agas}$

When the density is not corrected for gas the porosity calculated with eq. 14.2 would be too high :

Example II:

$\rho_b = 2.11$; $\rho_{ma} = 2.65$; and $\rho_{mf} = 1.0$ all in g/cc

With no gas present ($S_{xo}=1$): $\phi = 0.33$

With $S_{xo}=0.70$, and $\rho_{agas} = +0.01$ we find $\rho_b = 2.01$ g/cc. Using this value to back calculate the porosity with a fluid density of ρ_{fl} of 1 g/cc we find $\phi = 0.39$

The apparent porosity is therefore 6 % too high.

For the same example the neutron tool reads 7 % lower porosity i.e. 26 instead of 33 %. **This results in 13 porosity units separation for the porosities derived from density and neutron logs.** Since the gas effects on the density and neutron porosity log readings have opposite direction a large separation is quite common as shown in chapter 7. This negative separation is a very strong gas indicator.

9A.2.8 LITHOLOGY

Lithology determination, i.e. the qualitative mineral content of specific layers already can be done with one single log. For example the SP and GR readings give shale/sand distributions. In addition the shape of the readings give information about the environment of deposition. The accuracy of lithology determination and even quantification of mineral content are possible when two or more (multi) log readings are used.

9A.2.8.1 SINGLE LOG

Many combinations of porosity values and lithology types are possible when only one log is available (figure 9A.4). When it is known from cuttings, cores or other information that only one mineral is present it is no problem to calculate one unique porosity value in a water-bearing reservoir. The neutron log can be corrected for lithology using a correction chart. For example a neutron log reading of 13 apparent limestone (LST) porosity units converts to 17 % in a sandstone (SST) reservoir and 6% in a dolomite (DOL) reservoir.

It is possible in some reservoirs to obtain the lithology from the acoustic log alone. The ratio of shear transit time (ΔT_S) over compressional transit time (ΔT_C) gives a good indication of lithology provided that shale and gas effects are corrected for. The following values can be useful in the absence of a combination of neutron and density log :

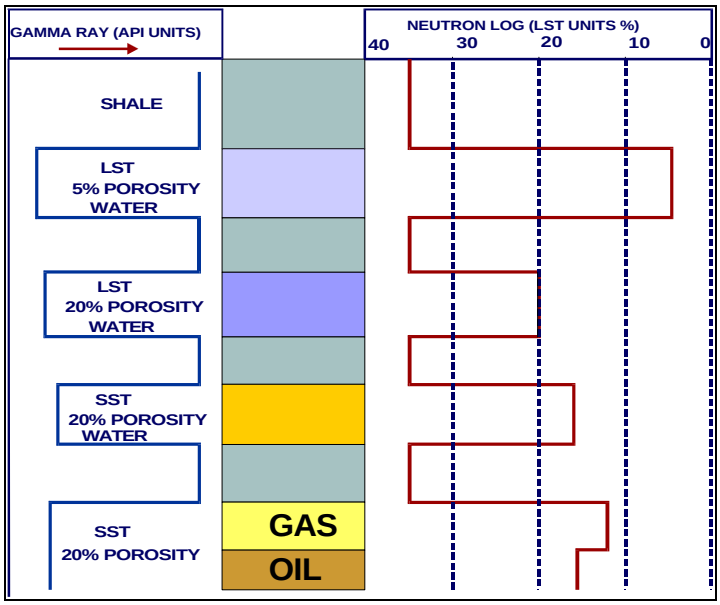

Figure 9A. 4: Lithology and hydrocarbon effects on the neutron

Lithology	$\Delta T_S/\Delta T_C$
Sandstone	1.6
Dolomite	1.8
Limestone	1.9

9A.2.8.2 TWO LOGS / POROSITY CROSS-PLOT

Lithology assessment is often based on a combination of two porosity logs, usually the density and the neutron log. The data from the porosity logs are plotted on a chart the so-called cross-plot. An example for a water bearing formation is shown in figure 9A.5.

If the formation consists of one single lithology, the data points of a water bearing formation fall on the appropriate lithology curve. If the lithology is a mixture of 2 components, e.g. calcite (limestone) and dolomite, the points fall in between 2 lithology curves. This permits identification of the lithologies and determination of their volumetric proportions. Moreover the porosity can be estimated more accurately based on the lithology mix. An example is given by point A in Figure 14.9A. The density log reads ρ_b = 2.48 g/cc and the neutron log ϕ_n = 19 p.u. on the limestone (LST) porosity scale used on the x-axis. This point most likely represents a carbonate interval containing 34% dolomite and

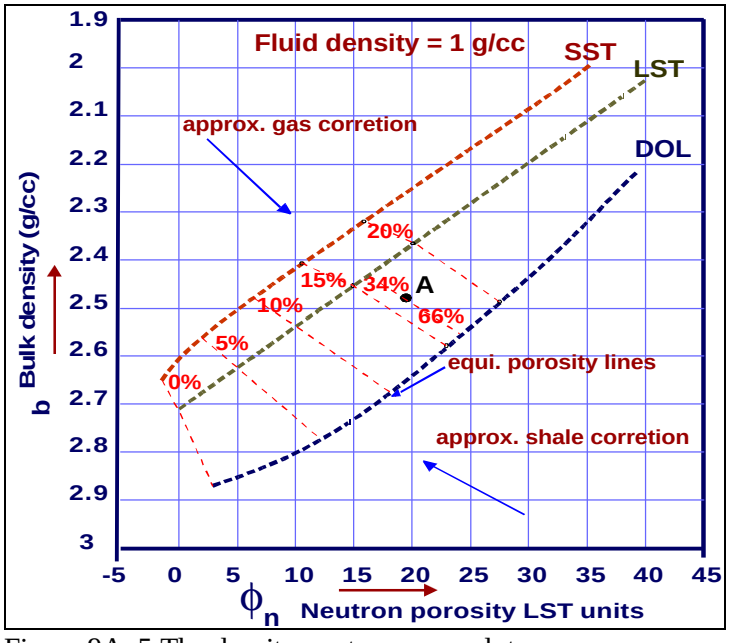

Figure 9A. 5:The density-neutron cross-plot.

66% limestone. The porosity is found by interpolation to be 16 %. Keeping mind that :

- The position of the top point on the chart could also be interpreted to represent a sandstone-dolomite mixture. Additional information is therefore required to make an unique interpretation.
- The presence of shale and/or hydrocarbons especially gas often requires large corrections to the log readings before the lithological interpretation sketched above can be applied with confidence.

Cross-plots of neutron vs. sonic log readings and density vs. sonic are also infrequently used for simultaneous lithology and porosity determination.

9A.2.8.3 SHALY SANDS

In the chapters 5 and 6 the calculation of estimates for the shale volume from respectively the spontaneous potential SP and the gamma-ray log GR were discussed. If the reservoir rock contains a mixture of sand and shale the neutron-density cross-plot can also be used for shale volume calculations. For shaly sands the concept *effective* porosity ϕ_e is defined as :

$$j_e = 1 - V_{sa} - V_{sh} \qquad \text{(eq. 9A.6)}$$

In which V_{sa} is the sandstone matrix volume and V_{sh} the shale volume. This model is the basis of the so-called neutron-density cross-plot (figure 9A.5,6), commonly used to assess ϕ_e and V_{sh} in a shaly formation, whereby the following equations apply:

$$r_b = (1 - j_e - V_{sh}).r_{ma} + j_e.r_{mf} + V_{sh}.r_{sh} \qquad \text{(eq. 9A.7)}$$

$$j_n = j_e + V_{sh}.j_{nsh} \qquad \text{(eq. 9A.8)}$$

The method is graphically illustrated in figure 9A.6, for water bearing shaly sand. A triangle is constructed from the clean matrix point (ϕ_n=0; ρ_{ma}=2.65), the 100 % fluid point of water (ϕ_n =100%; ρ_{fl} = 1.0) and the 100% shale point (ϕ_{nsh} and ρ_{sh}), the latter values are derived from a nearby shale layer. The fluid and shale points are converted to porosities, or; ϕ_{fl} =1, ϕ_{sh}=0.5. The linear effective porosity scale is indicated on the line 100% matrix to 100% water, and also on the 100% shale to 100% water line. Near horizontal lines with the same effective porosity values are drawn between the matrix and shale sides of the triangle. The linear V_{sh} scale is indicated on the matrix-shale side as well as in the shale-water side. Lines with the same V_{sh} values are also drawn. Each data pair (ϕ_n , ϕ_b) entered in this chart produces a value of effective porosity and shale volume fraction.

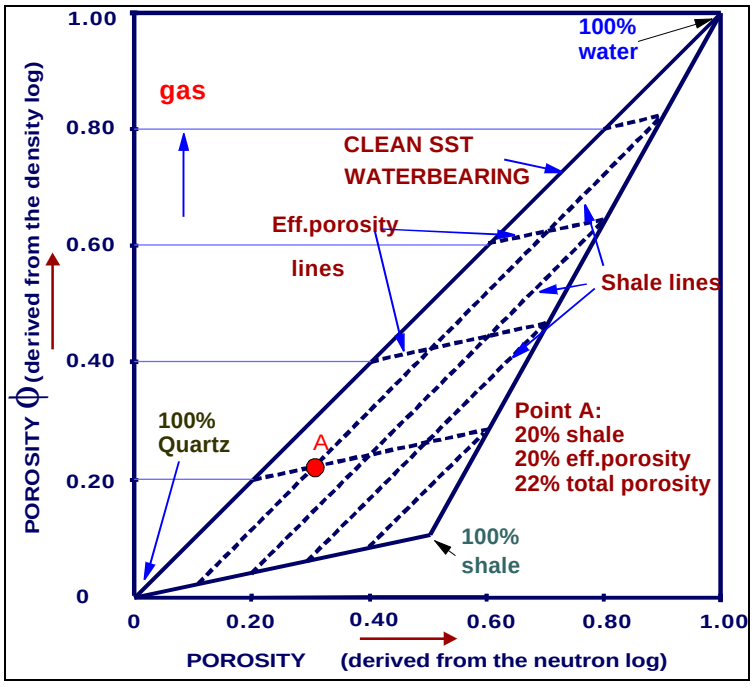

Figure 9A.6: Shale volume and porosity lines in Density-Neutron cross-plot

9A.2.8.4 MULTIPLE MINERAL LOG EVALUATIONS

The unknown matrix volumes and porosities of mixtures of two minerals in a reservoir can be solved with simple matrix algebra. This is possible when the tool responses can be simplified to a set of linear

equations. The response of a tool to a mixture of minerals and water is assumed to be the response of the tool to 100% of these minerals multiplied by the volume fractions of the individual minerals. For the density and neutron tool combination three equations can be written accordingly :

- $\rho_b = V_{ma1} . \rho_{ma1} + V_{ma2} . \rho_{ma2} + \phi . \rho_{fl}$ (eq.9A.9)
- $\phi_n = V_{ma1} . \phi_{nma1} + V_{ma2} . \phi_{nma2} + \phi . c$ (eq.9A.10)
- $1 = V_{ma1} + V_{ma2} + \phi$ (eq. 9A.11)

where:			dimension
ρ_b	=	bulk density reading log,	g/cc
ϕ_n	=	Neutron bulk reading log, porosity units	%
V_{ma1}	=	Volume matrix mineral 1, fr.b.v.	%
V_{ma2}	=	Volume matrix mineral 2, fr.b.v.	%
ρ_{ma1}	=	matrix density of 100% volume of mineral 1,	g/cc
ρ_{ma2}	=	matrix density of 100% volume of mineral 2,	g/cc
ϕ	=	porosity, fraction of bulk volume%	
ρ_{fl}	=	fluid density, gr/cc	
ρ_{fl}	=	neutron response of 100% fluid, porosity units	%

The known variables, which are based on the log readings, are ρ_b and ϕ_n. The fluid properties are normally based on the mudfiltrate. The mudfiltrate density can be measured on the surface, and the neutron response can be estimated e.g. 1 for 100% fluid. From cuttings the mineral composition is well estimated, so mineral matrix densities can be made. Normally are used; quartz 2.65 g/cc, dolomite 2.87 g/cc and limestone 2.71 g/cc. The unknowns are the matrix volumes V_{ma1}, V_{ma2} and porosity ϕ.
Then three equations with three unknowns can be solved. With the three porosity tools and the photo-electric absorption coefficient P_e many combinations can be made to obtain three equations with three unknowns. The equation for a Sonic - Pe combination is as follows:

- $\Delta T = V_{ma1} . \Delta T_{ma1} + V_{ma2} . \Delta T_{ma2} + \phi . \Delta T_{fl}$ (eq. 9A.12)
- $P_{eb} . \rho_b = V_{ma1} . U_{ma1} + V_{ma2} . U_{ma2} + \phi . U_{fl}$ (eq. 9A.13)

Where :			dimension
ΔT	=	sonic log reading,	µs/ft
ΔT_{ma1}	=	sonic log reading 100% matrix mineral 1,	µs/ft
V_{ma2}	=	sonic log reading 100% matrix mineral 2,	µs/ft
ΔT_{fl}	=	sonic log reading 100% fluid,	µs/ft
P_{eb}	=	photoelectric absorption cross section of the formation	barns (1 barn = 10^{-24} /atom)
ρ_b	=	bulk density formation, g/cc	
U_{ma1}	=	volumetric eff. photoelectric abs. index of mineral 1,	barns/vol
		$U = P_{eb} . \rho_b$ in which ρ_e stands for the electron density	
U_{ma2}	=	volumetric eff. photo electric abs. index of mineral 2,	barns/vol
U_{fl}	=	volumetric eff. photo electric abs. index of fluid,	barns/vol

The logical extension of this evaluation scheme is the incorporation of more log readings from other tools. However incorporating more equations can lead to an over-determined system, with more equations than unknowns. Computer programmes have been constructed based on least squares algorithms that solve sets of tool response equations for porosity, mineral & shale volume fractions, taking into account the error bars of the measurements, and the constraints of the equations by means of weight factors. These evaluation methods will be discussed in the third year lectures.

9A.2.9 SATURATION DETERMINATION FROM LOGS

In chapter 5 the Archie equations were discussed :

$$C_t = F^m . S_w^n . C_w \qquad \text{(eq. 9A.14)}$$

The cementation factor m and saturation exponent n, are usually estimated to be 2 due to the absence of core analyses. If information on the consolidation of the reservoir rock is available, the m,n-lithology tables in chapter 5 can be used to refine this estimate. The conductivity C_t and the porosity ϕ are measured with well logs, while the formation water conductivity C_w is obtained from the analysis of produced water samples or can be derived from the SP log. For the latter an accurate analysis of a representative mud-filtrate sample is required to estimate the mud-filtrate conductivity C_{mf}.

$$E = (-71).log \frac{C_w}{C_{mf}} \qquad \text{(eq. 9A.15)}$$

If the reservoir extends into a water zone (S_w =1) equation 9A.15 can be rearranged as :

$$C_w = C_t / f^m, \qquad \text{(eq. 9A.16)}$$

In this way a reliable estimate of the formation water conductivity C_w is obtained. An additional advantage of deriving C_w from a water-bearing zone is that errors in estimating the cementation factor "m" and C_w are partly compensated.

Remember that the effect of the clay conductivity in shaly sands can have a large disturbing effect on the determination of water saturations with the Archie and the Humble equations.

9A.2.10 FLUID CONTACTS

Knowledge on the in-situ present fluids is essential to identify:

- the reservoir fluid type,
- the spatial characteristics in the reservoir (vertical presence),
- reservoir flow characteristics
- fluid transport characteristics in the production well.

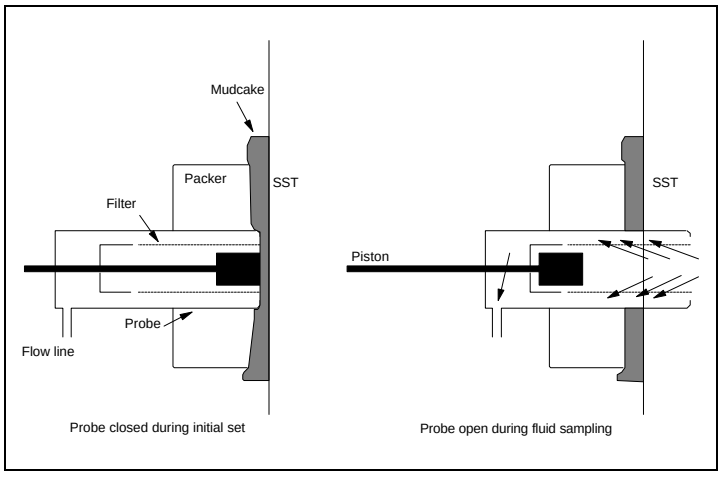

Figure 9A. 7: Operation of the RFT tester probe (After Schlumberger)

9A.2.10.1 WIRELINE FORMATION TESTING

Wireline logs can give indirect indications on the fluid type that occupies the pore space, however the acquisition of physical samples is often required to solve unclear wireline log interpretations. Moreover, when the reservoir layer, which is penetrated by the well, contains only a part of the total oil column, pressure data are required to identify the oil water contact. In the sixties the formation tester was introduced, which consisted of a sample chamber and a pad in which a shaped charge was embedded. The pad was pressed (set) against the borehole wall and the perforating charge was then used to establish communication between the reservoir and the sample chamber via a flow line. In the seventies a nozzle that could be extended through the mudcake into the reservoir replaced the perforating charge. An example of this tool type is the repeatable formation tester or "RFT" of which

the principle is depicted in figure 9A.7. In contrast with its predecessor, the RFT is limited to measuring formation pressure and to retrieving formation samples in open holes only. The flow-line that connects the nozzle or probe to the chamber contains a number of valves that allow multiple settings of the tool and collection of several formation fluid samples. At each setting the pressure of the reservoir fluid can be measured with a strain gauge or a quartz high-resolution pressure gauge.

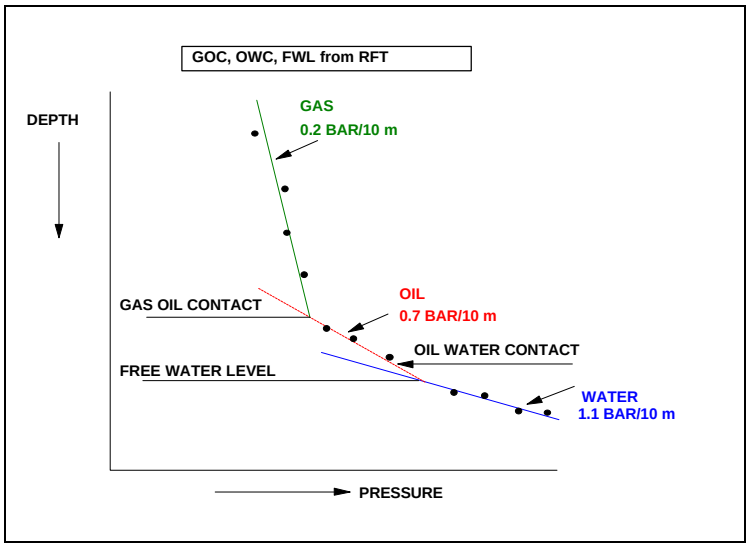

Figure 9A. 8: Fluid contacts that can be obtained with fluid pressure measurements.

In the eighties the modular formation tester or "MDT" was introduced. It has two or three sampling probes and measures vertical permeabilities based on the propagation of a pressure sink from one probe to the other positioned higher up in the hole. Running a GR or a SP with the wireline test tool can control the accuracy of the setting of the test tools at a certain depth. Correlation of these GR or SP logs with open hole SP or GR curves gives the desired depth control.

The reservoir pressure measurements plotted against the depth will produce a gradient that is very steep for gas, much flatter for oil, and has the smallest angle for water. The pressure measurements are used to detect gas/water, gas/oil or oil/water contacts based on the recorded fluid gradient (figure 9A.8).

9A.2.10.2 LOG SATURATION PROFILES AND CAPILLARY PRESSURE CURVES

The water saturations derived from resistivity logs give accurate information on the saturations of individual layers. However, they are surprisingly unreliable in isolation to determine the hydrocarbon water contacts. This is due to the very gradual transition from some 85% water to 100% water saturation that occurs in most reservoirs. Moreover, the free water level (FWL), defined as the level where the capillary pressure is zero, can be several meters lower than the depth where the logs give 100% water saturation (chapter 4, capillarity)

If capillary pressure curves, measured on core samples, are available, then a direct comparison between water saturations, derived from logs and from capillary pressure curves, can be made. An example is shown in figure 9A.9. If the saturation profiles of the two data sources are depth matched a more reliable estimate of the free water level (FWL) can be made even when the log derived saturation profile does not extend to the water table.

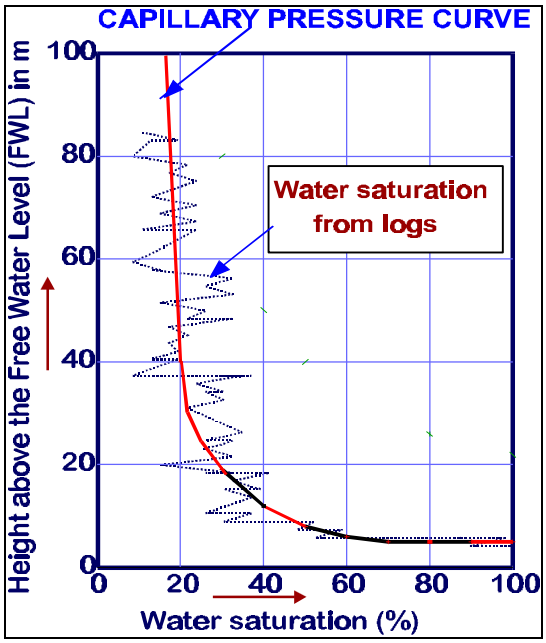

Figure 9A. 9: Comparison log-derived and cap-curve derived saturation profiles

9A.2.11 HYDROCARBON RESERVES VOLUME ESTIMATION

The Hydrocarbon-Initially-In-Place is the product of bulk reservoir volume, net/gross ratio, effective bulk porosity, initial hydrocarbon saturation, and hydrocarbon formation volume factor :

$$HCIIP = V_b.N/G.\phi .S_{hc}.\frac{1}{B_o}, \qquad \text{(eq. 9A.17)}$$

where			dimension:
HCIIP	=	Hydrocarbon-Initially-In-Place	m^3
V_b	=	Gross Rock Bulk volume	m^3
N/G	=	Net over Gross ratio	d.l.
ϕ	=	Porosity, fraction of bulk volume	fraction
S_{hc}	=	initial Hydrocarbon Saturation, fraction of pore volume	fraction
B_o	=	Initial hydrocarbon Formation Volume Factor	d.l.

The B_o factor converts the volume of oil under reservoir pressure and temperature conditions to the conditions on the surface. The B_o factor comprises the shrinkage and gas expansion. The recoverable reserves are defined as :

$$recoverable\ reserves = HCIIP\ .\ RF \qquad \text{(eq. 9A.18)}$$

The Recovery Factor RF indicates what fraction of the original oil volume that is present in the reservoir, is eventually expected to be brought to the surface. RF can vary from more than 50% for a reservoir with a very strong natural water drive, to less than 10% for tight carbonate reservoirs with very little natural drive energy. With enhanced oil recovery in the form of water injection, gas injection, polymer or CO_2 flooding, the RF factors can be increased very significantly.

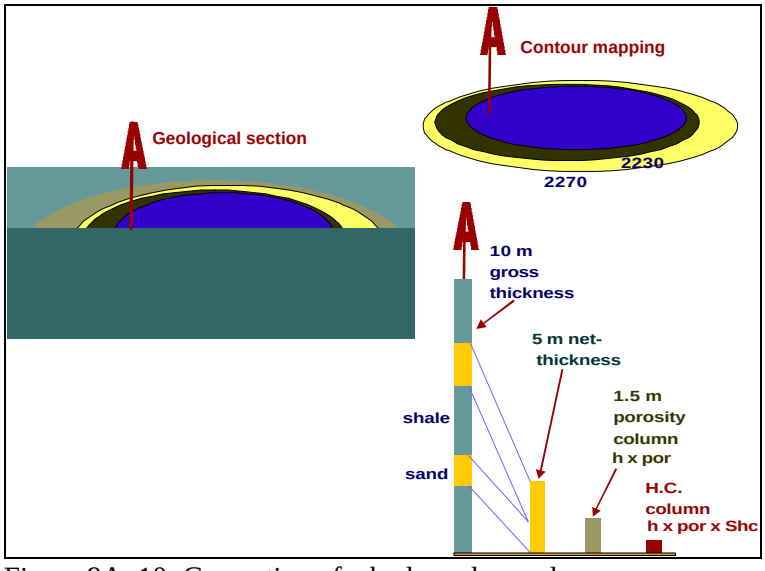

Figure 9A. 10: Generation of a hydrocarbon column

The product h. Φ. S_{hc} , in which "h" is the net reservoir thickness, and "S_{hc}" is the hydrocarbon saturation, is called the hydrocarbon column. The generation of this column is shown in figure 9A.10 and it is further discussed in the following example.

Example:
The interval consists of shales alternated with oil-bearing sandstones. The sandstones have an average porosity of 30 % and an average oil saturation of 67 %. The **gross** interval of 10 m in our example refers to the total interval including non-reservoir sections. The net interval refers to the cumulative reservoir thickness and amounts to 5 m. Compressing the 5 m net reservoir with an average porosity of 30 % results in 3.5 m of massive (0 % porosity) rock and a 1.5 m **porosity column** (with 100 % porosity). The porosity column is filled for of 67 % with oil which is equivalent to 0.67x1.5 = 1 m **oil column** and a 0.5 m water column.